INFORMATION TO USERS

This manuscript has been reproduced from the microfilm master. UMI films the text directly from the original or copy submitted. Thus, some thesis and dissertation copies are in typewriter face, while others may be from any type of computer printer.

The quality of this reproduction is dependent upon the quality of the copy submitted. Broken or indistinct print, colored or poor quality illustrations and photographs, print bleedthrough, substandard margins, and improper alignment can adversely affect reproduction.

In the unlikely event that the author did not send UMI a complete manuscript and there are missing pages, these will be noted. Also, if unauthorized copyright material had to be removed, a note will indicate the deletion.

Oversize materials (e.g., maps, drawings, charts) are reproduced by sectioning the original, beginning at the upper left-hand corner and continuing from left to right in equal sections with small overlaps.

ProQuest Information and Learning
300 North Zeeb Road, Ann Arbor, MI 48106-1346 USA
800-521-0600

HYDRATION AND COORDINATION AT IONISED NITROGEN CENTRES

by

L. H. Laliberte

A thesis submitted in partial fulfillment of the requirements for the degree of

Doctor of Philosophy

in the

Department of Chemistry
University of Ottawa
Ottawa, Canada

August, 1969

B. E. Conway
Professor of Chemistry
Research Supervisor

L. H. Laliberte
Ph.D. Candidate

PREFACE

The study of the properties of aqueous solutions formed one of the first areas of investigation in physical chemistry. Early workers were concerned about the nature of the substances in solution and once the significance of dissociation of salts was understood, rapid advances were made. It was also recognised that electrolyte solutions behaved in a quite non-ideal manner because of the charged nature of the solute salts when dissociated in solution. The Debye-Hückel theory, in the early twenties, formulated the problem of long-range ion-ion interactions and this treatment led to many important advances, particularly in the area of ionic conductance and the thermodynamics of aqueous electrolyte solutions.

Renewed interest in recent years in solution thermodynamics has been stimulated in part by studies of the structure of water. This most common of solvents has turned out to be extremely complex insofar as structural aspects of its behaviour are concerned. The properties of non-polar ionic solutes, particularly in aqueous solutions, have also been the subject of numerous investigations in the last fifteen years. These compounds are not only of intrinsic interest but are also important as models for the study of biologically active molecules such as proteins, enzymes and their substrates.

One of the ways of investigating the specific nature of ion-solvent interaction is by determining the partial molar volume of salts in solution. The partial molar volume of an ion is comprised of two main contributions: its intrinsic volume plus the negative (electrostriction) or positive volume change it brings about in the solvent. It is this latter term which contains information about the type and magnitude of the ion-solvent interactions. Correspondingly, the variation of the partial molar volume as a function of concentration is determined limitingly by the ion-ion interactions and at high concentrations also by changes of ion-solvent interaction. Aspects of the latter effect form an important part of the present study. The effects of pressure and temperature on the partial molar volumes have also been examined since the compressibility and expansivity also reflect the state of the water in the vicinity of the ion.

Because water is such a unique solvent it is very difficult to determine explicitly the effect of various properties of water such as its dielectric constant and hydrogen bonding behaviour, on the thermodynamic properties of salt solutions. The usual recourse of investigating different solvents such as alcohols often produces further ambiguous results since the large changes in the nature of the solvent often completely change the character of the hydration. The studies reported here on H_2O solutions have been complemented by work on D_2O. This provides the opportunity of introducing a slight perturbation into the structure of water and of examining the resultant effects on the partial molar thermodynamic properties of the solute.

The principal part of the original work described in this thesis is experimental in nature and is concerned with the precise determination of partial molar volumes, compressibilities and expansibilities of ionisable nitrogen containing salts exhibiting a varying degree of coordination at the N centre. A more detailed summary of the original contributions is given in the section "Contributions to Original Research".

Some of the work described in this thesis has been published and the remaining portions are being prepared for publication, as indicated in the following list of papers:

1) Hydration and Coordination at Ionised Charged Nitrogen Centres, B.E. Conway and L.H. Laliberte, Hydrogen Bonded Solvent Systems, Eds. A.K. Covington and P. Jones, Taylor Francis Ltd., London, 1968 (paper prepared in honour of Professor W.F.K. Wynne-Jones on the occasion of his retirement).

2) H_2O-D_2O Isotope Effect in Partial Molal Volumes of Alkali Metal and Tetraalkylammonium Salts, B.E. Conway and L.H. Laliberte, J. Phys. Chem. 72, 4317 (1968).

ACKNOWLEDGMENTS

The author wishes to express his thanks to Professor B. E. Conway, under whose direction and supervision this work was done. Professor Conway was always willing to give freely of his time to discuss problems which arose in the design of experiments and in the preparation of the manuscript. The author also wishes to thank Dr. J. Lawrence for his help in building the mechanical assembly for the ultrasonic measurements and for stimulating discussions.

Grateful acknowledgment is also made to the University of Ottawa, Department of Chemistry, for the use of its research facilities, the National Research Council (Canada) for support of this work and for the award of a scholarship (1966-1969) to the author. The help of the support staff of the Chemistry and Physics Department of the University of Ottawa, together with the workshop staff of the Division of Pure Chemistry, National Research Council is also gratefully acknowledged.

TABLE OF CONTENTS

Page No.

CHAPTER IV

Page No.

LIST OF FIGURES

Page No.

Page No.

Page No.

LIST OF TABLES

ABSTRACT

The apparent molar volumes, ϕ_v, of a series of tetra-n-alkylammonium bromides have been measured down to high dilutions by means of a modified Stokes and Hepler dilution dilatometer and at higher concentrations with a differential buoyancy balance. Despite conflicting indications in earlier literature, the present measurements have shown that the limiting law slope for the apparent molar volume is approached at sufficiently high dilutions. Measurements of the apparent molar volume and the apparent molar adiabatic compressibility have also been carried out on a series of substituted pyridinium and piperidinium salts. The effects associated with indirect and direct blocking at the N^+ centre were observed with these two series of salts and allowed comparisons to be made with the results of measurements carried out on a series of alkylammonium salts where direct blocking of the charge centre arises.

The partial molar volume and adiabatic compressibility of aqueous solutions of neutral pyridine and piperidine bases were also investigated. The apparent molar volume of these solutes showed pronounced maxima and minima when evaluated as a function of concentration. Some measurements of ϕ_v in D_2O solutions for the same solutes also showed a similar type of concentration dependence.

The apparent molar volume of a series of 1:1 inorganic electrolytes and tetra-n-alkylammonium bromides were measured in D_2O solutions at 25°C as a function of concentration. It was found that some salts had a larger partial molar volume in D_2O than in H_2O while the reverse was the case for other salts. The sign of the solvent isotope effect in the partial molar volumes, $\Delta\bar{V}^{o}_{D_2O\text{-}H_2O}$, was interpreted in terms of the structure-making and structure-breaking ability of the ions in the water solvent.

The temperature dependence of the apparent molar volume of a series of inorganic and tetra-n-alkylammonium salts was also determined in H_2O and D_2O from 25°C down to the freezing point of the two solvents. With the exception of NaF and Me_4NBr, all of the other salts examined had identical partial molar expansibilities in D_2O and H_2O.

An extrapolation procedure, analogous to the one proposed by Conway and Verrall, has been developed for obtaining the individual ionic contributions to $\phi^{o}_{K(S)}$. An examination of the implicit assumptions made in such extrapolations has been made and is presented in this thesis. The difference between the partial molar volume of the bromide ion in H_2O and D_2O has been determined, thus establishing an absolute scale of ionic partial molar volumes in D_2O.

The partial molar volume and apparent molar adiabatic compressibility changes resulting from ionisation of a series of pyridinium and piperidinium salts have also been determined. The sign and magnitude of these changes have been interpreted in terms of the hydration and coordination at the charged centres and also in terms of the interactions between the neutral base and water.

CHAPTER I

INTRODUCTION

1. Interest in Organic Ions

(i) General

The study of the behaviour of charged and neutral solutes in aqueous and non-aqueous solvents has played a central role in the development of physical chemistry. The early work in this field which was initiated nearly 100 years ago was concerned with the nature of the species in solution. Once it had been established that ions existed freely in solution and originated either directly from ions in the crystal lattice, i.e. NaCl, or from the reaction of potential electrolytes e.g. HCl, CH_3COOH, with the solvent, the question of their properties could be examined in detail. The success of the Debye-Hückel theory in the early 1920's stimulated a great deal of research into the behaviour of electrolytes at low concentrations. Their theory, however, dealt only with long range interactions between ions and neglected solute-solvent and short range solute-solute interactions. At the present time, nearly 50 years since the original Debye-Hückel theory was presented, there is still no equivalent à priori theory for concentrated electrolyte solutions or for the limiting thermodynamic

behaviour of very dilute solutions of non-electrolytes, although a general theory of interchange energy has been given for binary mixtures by Van Laar (1894) and Hildebrand (1931). Quantities such as the excess volume of mixing can now be predicted in the 0.1 to 0.9 mole fraction region (1). Extensions of the Debye-Hückel theory have, however, been made to take into account the cut-off in the space charge distribution because of the finite size of the ions, but the upper concentration limit for this improved theory is still about 0.01 molar, and has been placed as low as 0.001 m (6).

It was perhaps unfortunate that aqueous solutions were studied first, since water has turned out to be the most complex solvent in our environment. The three-dimensional structure of the solvent arising from the ability of water to hydrogen bond, together with the electrically anisotropic nature of the molecule make the description of ion-solvent interactions very complex. Attempts to describe these using a continuum or structureless model for the solvent were initiated by Born (2), and similar approaches have been employed for many years by other workers. A more promising approach to the theoretical treatment of hydration was developed by Bernal and Fowler (3), based on a molecular model. This type of model is rather more involved than the continuum theories but at present seems to present the only realistic picture of hydration (4, 5). Bernal and Fowler (3) were the first to direct attention to structural aspects of solvation in relation to the structure of the solvent itself. The latter question will, however, be reviewed later in this chapter.

The solvation of ions and neutral molecules plays an important role in fields as divergent as biochemistry, colloid chemistry, electrochemistry and solution kinetics. With the increasing importance of molecular biology in recent years, and the discovery by Frank and Evans in 1945 of hydrophobic hydration (7), the study of organic salts in aqueous solution has become recently of great interest and importance.

(ii) Structural Effects in Ionisation Reactions

Since water is the universal biological medium, the study of enzymes, proteins and biological processes at the molecular level requires an understanding of the solvation of these macromolecules. The catalytic activity of enzymes is due in part to the conformation which they can adopt in solution, and this in turn is determined by the interactions of the polar and non-polar groups of the molecule with water. Since many of these biologically important molecules contain large non-polar groups as well as ionised centres, it is important for it to be understood what sort of interactions take place when these groups are placed in a highly polar solvent such as water. The study of simpler organic ions provides basic information on model compounds and the principles elucidated can then be related to situations encountered with more complex cases arising in biological systems.

The role of the solvent in determining the ionisation behaviour of organic acids and bases probably encompasses most of the relevant questions in the field of ionics. For example, in a typical proton transfer reaction of the type

$$BH^+ + H_2O \rightleftharpoons B + H_3O^+$$

the value of the equilibrium constant K, or the free energy change ΔG^o, will depend on the difference between the free energy of solvation of the products and reactants. Interactions of BH^+ and B with water will depend on the structure of the organic ions and molecules including the nature of their substituent groups.

One of the earliest attempts to take into account the role of the solvent in an acid-base equilibrium of the type shown above, was made by Wynne-Jones (8) in 1933. Using an electrostatic model based on the Born equation, he showed how a change in the dielectric constant of the solvent would affect the strength of the acid. The over-simplification involved in such a treatment was demonstrated by Everett and Wynne-Jones (9) in 1938 when they studied the ionisation behaviour of substituted methylammonium ions in water. Predictions of ΔS^o and ΔC_p^o made on the basis of a Born treatment were completely reversed, because in the Born theory a very important part of the hydration energy had been neglected. It was found that the hydrophobic interaction of the neutral base with the water solvent was one of the major contributing factors in determining the free energy change.

In the above discussion, we have alluded to a rather special type of hydration which occurs when non-polar groups interact with water. It will be one of the purposes of this thesis to try and define more closely the nature of this special solute-solvent interaction. In order to understand the unique solvation behaviour of ions and molecules in water it is necessary to examine the structure of the solvent, then with an admittedly limited picture of water we shall proceed to an interpretation of the solvation behaviour of some electrolytes and non-electrolytes.

2. Structure of Water: Models

(i) General

In general, liquids are more difficult to define than either solids or gases, and in a number of ways exhibit certain characteristics which are reminiscent of both depending whether the temperature is near to the boiling point or the freezing point of the liquid. Within the broad class of liquids there are other divisions, such as metallic, non-polar, and polar liquids. Water falls into the last category; it is a polar liquid, but a rather special one since H_2O molecules have the ability to hydrogen bond into three-dimensional networks and it is this unique property of individual H_2O molecules that gives rise to many of the special properties of liquid water. The study of liquids can be approached from two directions; liquids can be considered as condensed gases, or in the other extreme can be looked at as disordered solids. The ability of water molecules to hydrogen bond in three dimensions has favoured an approach to consideration of its liquid structure in terms of models based on a disordered solid state.

(ii) Structure of Ice

The question of the structure of ice is initially relevant and has been reviewed by Owston (10). The most common form of ice is ice I, i.e. the hexagonal form. In this modification, the oxygen atoms lie in layers, with each layer consisting of a network of open, puckered, hexagonal rings. Each oxygen is surrounded by four hydrogen atoms, two at 0.96 Å and two others at 1.80 Å. This structure has been confirmed recently by neutron diffraction experiments on D_2O ice (11).

Bernal and Fowler (3) had proposed a regular arrangement for the hydrogen atoms, realising that the most probable structure would be one of the irregular ones "crystalline only in the positions of its molecules but glass like in their orientation" (3). This has since been confirmed by measurements of the residual entropy (12). Apart from ice I, there are at least nine high-pressure forms of ice. Thus, even in its solid form, water presents some formidable problems with respect to structure elucidation.

(iii) Early Theories on Water Structure

Most theories on water structure must explain several unusual physical properties, e.g. the density of the liquid goes through a maximum at 4°C and is higher than that of the solid, even though the nearest-neighbour distance has increased from 2.76 Å in ice to 2.9 Å in water. Similar and even more marked effects arise in D_2O.

Two of the oldest theories about liquid water were those proposed by Rowland in 1880 and by Röntgen in 1892, who already visualised (cf. Bernal and Fowler, 3) water as a "mixed solution of ice and steam that varies in proportion with temperature", a concept that is not far removed from those commonly accepted today. The early X-ray work of Stewart (13), which showed that there was definitely short range order in liquid water, provided the basis for the first quantitative theory of water structure by Bernal and Fowler (3).

The latter authors proposed that water consisted of a mixture of two forms which could be represented in terms of the structures of ices I and I(c). A change in temperature was regarded as producing a shift in the relative amounts of these species. Their model

explained the density maximum at 3.86°C, but did not reproduce exactly the radial distribution function for water (13), particularly as a function of temperature (14). Although "mixture" models seem to be accepted in principle today, the model of Bernal and Fowler (3) which involved a mixture of two "solid" forms implied too much structure in the liquid.

(iv) Modern Theories of Water Structure

More recent X-ray work (15) over a wide range of temperatures (4° →200°C) has produced diffraction patterns with much higher resolution than those obtained in previous studies. This work showed that the first peak in the radial distribution function remained pronounced up to the highest temperatures studied, while the beginning of the continuum region changed from 10 Å at 4°C to 6 Å at 200°C, reflecting the loss of long-range structure with increasing temperature. It was found (15) that the best fit to the X-ray diffraction data was given by an anisotropically expanded ice-I lattice, surrounded by other molecules at randomly distributed distances, with occupancy of the structural cavities in the lattice being permitted. These workers were careful to point out that agreement of the predictions from the model with the X-ray data was a necessary but not sufficient proof of the correctness of the model. The importance of accurate X-ray data such as that presented in ref. (15) is that it allows models to be discounted which do not conform to the R. D. F. Thus the Pauling (16) clathrate type model was examined (15) but rejected on the basis of the X-ray data.

A detailed examination of all of the theories on water structure presented in the last 25 years will not be attempted here; rather, after a brief examination of some of the representative models, an attempt will be made to point out their relevance in the light of the

experimental evidence that is now available. Generally the models can be classified into two main groups: first, those that treat water in terms of a "continuum" of structures and secondly those that regard the liquid as a mixture of a small number of distinguishable states. All of these models have been extensively reviewed in the recent literature (17 - 23).

(a) Mixture models:

The model considered by Forslind in 1952 (24) was similar to that recently proposed by Narten, Danford and Levy (15). Forslind considered that liquid water retained an expanded ice-I form with some water molecules occupying interstitial positions. Samoilov (19, 25) had proposed a model similar to this earlier. Further work with a model based on an expanded ice-like framework has been carried out by Gurikov (26-29).

The work of Everett and Wynne-Jones on the ionisation of alkylammonium ions (9), which was referred to earlier, and another important analysis of Frank and Evans (7) on the thermodynamics of dissolution of inert gases in water, showed that these non-polar solutes had a rather special effect on the properties of water. It was found (7), for example, that the (standard) loss of entropy upon dissolving 2 moles of argon in water at 25°C was -60.4 e.u. which is more negative than the loss of entropy associated with the dissolution of 1 mole of KCl (-51.2 e.u.). Since this loss of entropy could not be due to electrostriction in the case of the argon, it indicated that a new effect was operating on the solvent and somehow restricting its molecular motions. It was also found that this effect

was reduced as the temperature was increased. The above observations led Frank and Evans to propose that a region of increased "crystallinity" was formed around the solute and that this region, which they also likened to microscopic icebergs, was susceptible to melting as the temperature was raised and thus accounted for anomalously high partial molar heat capacities, e.g. as found in the ionisation studies of Everett and Wynne-Jones (9).

In 1957, Frank and Wen (30) proposed a new theory for the structure of water which encompassed the results of Frank and Evans (7), and some heat capacity data on large non-polar organic salts (30) which had anomalously high partial molar heat capacities. Frank and Wen postulated that the formation of hydrogen bonds in water was a cooperative process which led to the formation of highly hydrogen bonded regions, in a dynamic equilibrium, which they called "flickering clusters". They estimated the mean lifetime of a cluster to be 10^{-10} - 10^{-11} sec at room temperature. They also suggested that non-polar solutes would stabilise these clusters, and this was supported by observed (31) longer dielectric relaxation times for water/non-polar solute solutions.

Based on the model proposed above, Némethy and Scheraga (32) formulated, on a semi-empirical basis, a detailed statistical-thermodynamical model of water. They considered a system with five discrete, equally spaced energy levels which represented 0, 1, 2, 3 and 4-fold H-bonded water molecules. Using a semi-empirical value for the hydrogen bond energy, and known infra-red and Raman frequencies for various modes in liquid water,

they calculated the relative amounts of the variously bonded species. Marchi and Eyring (33) applied the so-called "theory of significant structures" to the case of water and calculated the fraction of bound water molecules at various temperatures. Vand and Senior (34) developed a qualitative theory based on the same principles as those involved in the Némethy and Scheraga model but introduced the idea of energy bands for the H-bonding instead of discrete energy levels. They also imposed certain topological restrictions on the clusters. Their calculated thermodynamic properties of water are in excellent agreement with experiment.

In a recent paper, Levine and Perram (35) have pointed out that the combinatorial factor used in the statistical mechanical treatments of previous models (32 - 34) counted the number of ways of distributing the molecules, whereas the number of arrangements of the hydrogen bonds subject to a given value of the energy of a particular distribution of hydrogen bonds should have been considered. They found that the number of "monomeric" water molecules deduced in their calculations was much smaller than that calculated by Némethy and Scheraga.

Other mixture models have also been proposed (36 - 38), but will not be discussed here.

(b) Continuum models

A different type of model for water structure was proposed in 1951 by Pople (40). He considered that hydrogen bonds remained essentially intact with increasing temperature, but were capable of being distorted or bent. This view conflicts with that of Frank and Wen (30) who implied an "all or nothing" character to hydrogen bonds in their theory, i.e. bent states were not considered. This seems unrealistic since bent states may be shown still to be "bonding" up to a certain angle and bent H-bonds are encountered in some intramolecular interactions (39). The high proportion of "broken" hydrogen bonds predicted by the various mixture theories do not seem to be reconcilable with the high value of 4 - 6 Kcals normally quoted for the hydrogen bond energy (but see 35). Pople's model does not lend itself easily to calculation of thermodynamic properties but some success was nevertheless achieved using this model. Levine's (35) treatment is a hybrid one since it allows the hydrogen bond in the cluster to bend to a certain degree and then "break", i.e. there is no longer an attractive potential energy. Unfortunately the model of Levine has not yet been developed to the point where thermodynamic functions can be calculated.

3. Structure of Water: Spectroscopic Evidence

(i) General

The models presented above are still far from being able to provide an à priori treatment of water structure. In all of the theories there are adjustable empirical parameters which render the value of the significance of the final agreement of calculated properties with experiment doubtful. As we shall see in this section, the basic postulates made in the treatments of the mixture models, i.e. that there are bonded and unbonded water molecules in the liquid, are not universally accepted. Frank (41) has pointed out that the major problem in the discussion of water structure is the difficulty in finding experimental evidence which requires either the acceptance or the rejection of any given model. Since the treatments based on mixture models rest on the premise that there are bonded and unbonded water molecules in a dynamic equilibrium and that a molecule is considered bound if it participates in a particular hydrogen bond for 10^{-10} - 10^{-11} sec, then the logical course would be to try and identify experimentally these two species. This should be possible with infra-red and Raman spectroscopy since these methods view the structure on a 10^{-13} - 10^{-14} sec. time scale.

(ii) Infra-red and Raman Spectra

Buijs and Choppin (42) studied the near infra-red spectrum of water as a function of temperature and found three peaks at 8620 cm^{-1}, 8330 cm^{-1} and 8000 cm^{-1}, the intensities of which were temperature dependent. They assigned these bands by comparison with the spectrum of water vapour to sums and multiples of the fundamental vibrations of water. The temperature dependence of the bands was interpreted as reflecting the changing concentrations of 0, 1, and 2-fold hydrogen-bonded species. Hornig (43) objected to the assignments made by Buijs and Choppin, and pointed out that other bands could equally well be assigned to the region they studied. Walrafen (44) examined the effect of temperature on the low frequency Raman spectrum of H_2O and D_2O. The intensity variation of the 175 cm^{-1} band was interpreted in terms of an equilibrium involving bound and unbound water molecules. The enthalpy of the process of breaking one hydrogen bond was estimated as +3.1 Kcals/mole. Luck (45 - 47) also interpreted his infra-red studies of water in terms of clusters of bound water molecules and a fraction of "spectroscopically" free OH groups. Stevenson (48) examined the vacuum ultraviolet spectrum of water in CCl_4 and CH_3Cl from which he determined the absorption position of monomeric water. By comparison with the spectrum of pure water, he concluded that the "free" water concentration in pure water was $< 1\%$. The fact that the "monomeric" water in a non-aqueous solvent is in a very different environment from the unbound water normally visualised in mixture models places some doubt on the value of Stevenson's conclusions and in particular on the upper limit of 1% for the fraction of unbound water quoted above.

Falk and Ford (49) reviewed the whole question of the determination of the fraction of bound and unbound species in water by means of infra-red or Raman spectroscopy. They pointed out that the values of the fractions of unbound water obtained by various workers ranged from 0.1% (48) to 60% (50) ! A recent paper by Boettger, Harders and Luck (51) has shown that a unique solution is not obtained in the calculation which many authors have used (42, 52, 53) to determine the fraction of bound and unbound species of water in solution, and in fact these workers calculated other sets of solutions from the same data.

If liquid water consists of a mixture of molecules with broken and unbroken H-bonds, then every OH stretching band (either a fundamental or an overtone) should exhibit two sub-bands. Also the frequency corresponding to a "free" OH should be higher than that of a bonded OH group (49), and the relative intensities of these bands should be temperature dependent. The situation is complicated by the fact that υ_1 , υ_3 and $2\upsilon_2$ lie close together and for overtones and combination bands the situation is more confused by the presence of overlapping bands and band clusters. Further, since the water molecule is subject to an asymmetric field its symmetry is lowered; this results in υ_1 and υ_3 being no longer purely symmetric and asymmetric stretching modes, and allows both modes to enter into Fermi resonance with $2\upsilon_2$, the first overtone of the bending mode. The situation in the overtones is even more complex. Finally, intermolecular coupling would tend to broaden and distort all band shapes.

By studing solutions of HOD in H_2O or D_2O, some of the above-mentioned difficulties can be circumvented. Because of the different symmetry of HOD compared with that of H_2O or D_2O, intermolecular coupling does not occur, and also the fundamental vibrational modes are more widely separated.

The infra-red spectra of dilute HOD solutions were measured (49) from 0^o to 130^oC, and the three fundamental bands showed a single maximum having a nearly Gaussian contour, with a complete absence of shoulders. The two stretching bands υ_1 and υ_3 moved to higher frequencies with increasing temperature, while the bending mode υ_2 shifted to lower frequencies. It was concluded that the infra-red spectra fully supported a continuum model and were incompatible with the existence of discrete molecular species in water (mixture model). Their conclusions agreed with the conclusions of Wall and Hornig (54) based on Raman studies on HOD. Franck and Roth (55) measured the OD stretching vibrations of HOD in H_2O from 30^o to 400^oC and from 50 to 4000 bars. They found only one intense absorption maximum with a simple shape at all temperatures and at all densities above 0.1 g/cm^3. The complete absence of shoulders was interpreted again as support for the continuum model.

Walrafen (56) reported further Raman studies of water in the 152 - 175 cm^{-1} region and revised his earlier estimate of the enthalpy of the hydrogen bond energy (in liquid water) from 3.1 to 2.8 Kcals/mole. Hartman (57) also examined the infra-red spectra of the OH bands of HOD over a range of temperatures, and interpreted the shift in the maximum in terms of bonded and unbonded species.

Further Raman studies on H_2O were reported more recently by Walrafen (58). He showed that the contour heights at fixed frequencies exhibited two types of behaviour as a function of temperature: from 3100 to 3400 cm^{-1}, the contour heights decreased with temperature, while from 3500 to 3600 cm^{-1} they increased with temperature. It was also found that the family of curves exhibited an isosbestic point with changing temperature. Four Gaussian contours could be fitted under the curve, two of them above the isosbestic point at 3535 and 3620 cm^{-1} and two others below the isosbestic point at 3247 and 3435 cm^{-1}. The objection that the "free" OH band exhibited too low a frequency compared to that of a free OH in the vapour state was countered by pointing out that the "unbonded" water in the liquid state was still being subjected to intense short range forces. Further evidence for the position of the band associated with the non-bonded species was provided (59) by the presence of two well resolved bands at 3545 and 3650 cm^{-1} in the infra-red spectrum of water at 374°C, and the absence of bands normally associated with the bound water. Support for the isosbestic frequency has been provided by Worley and Klotz (60), who found an isosbestic frequency at 6812 cm^{-1} which, when substracted from twice the Raman value obtained by Walrafen (58), leaves a reasonable anharmonicity of 108 cm^{-1}. In addition, they obtained an enthalpy of formation of -2.4 Kcals/mole for the hydrogen bond. Walrafen has suggested (58) that the slight band asymmetry observed by Wall and Hornig (54) and Falk and Ford (49) would under computer analysis reveal at least two Gaussian contours.

In a further study by Walrafen (61), Raman spectra of the OD stretching region of HOD in H_2O were reported. A definite shoulder at 2645 cm^{-1} was present on the band which had a peak at 2525 cm^{-1}. A preliminary report on the effect of pressure on the Raman intensities indicated that the fraction of "unbonded" water increased by ca. 10% per K bar, which would indicate a volume change of ca. -7 ml/mole upon breaking a hydrogen bond.

Ford and Falk (62) have compared the OH and OD profiles of the υ_3 and υ_1 bands of ice-I with the profiles which they obtained with liquid HOD solutions (49). The major difference between the bands in water and ice was the wide distribution of frequencies about the peak value. Whereas 90% of the range of vibrational energies in ice lie within 1 Kcal of the peak value, the corresponding value for the liquid is only 10 - 20%. The presence of a fraction of weakly interacting molecules in the liquid was thought to account for the observed magnitudes of the viscosity and self-diffusion constant for liquid water.

Luck (63) discussed the question of the presence of shoulders on band contours and pointed out that two overlapping bands with the same extinction coefficient would give rise to only one band if

$$\Delta\upsilon < 0.85\,\Delta\upsilon_{1/2}$$

where $\Delta\upsilon$ is the separation between the bands and $\Delta\upsilon_{1/2}$ is the half band width. Frank (41) pointed out that two Gaussian contours separated by 100 cm^{-1} and with half widths of 130 cm^{-1} would give rise to a contour which on visual inspection looks like a single Gaussian profile. If the two component bands are slightly more separated, the resultant band will show a shoulder. The two state model need not produce a sharp isosbestic point, since if the band for bonded species became broader with increasing temperature, then a pseudo or diffuse isosbestic point would be observed.

It can therefore be concluded that the absence of two separate and distinct peaks in the OH stretching region is not sufficient evidence for the rejection of the two-state model, while the recent evidence, particularly with respect to the fundamental vibration region, provides strong evidence for the validity of the mixture model.

Very recently Deryaguin (64 - 68) has reported that water condensed into quartz capillaries under certain conditions, exhibits very anomalous properties. This anomalous water is reported to have a density of 1.2 - 1.3 g/cm^3, fifteen times the viscosity of normal H_2O, and 1.5 times the thermal expansion coefficient. A molecular weight of ca. 72 (i.e. $4H_2O$) and a boiling point $> 200^oC$ have also been reported. An interpretation of these data in terms of a four molecule cluster has been recently proposed (69). It was surmised that the clean quartz surface catalysed the formation of the cluster which when formed was very stable. Since these results are still quite controversial, we will reserve comment on them. They have been included, however, in this discussion for completeness and to underline the fact that even now the problem of water structure may be much more complex than we suspect.

4. Structural Effects in Solution and the Hydration of Ions

(i) General

We have examined the various models used to describe the solvent and, by means of a discussion of the X-ray (15) and spectral work on pure water, an assessment of the correctness of these models has been given. The study of solutes, particularly ions, dissolved in water has provided a great deal of insight into the behaviour of the solvent. It has been possible to look at the changes of the properties of the solvent brought about by ions in solution, and from an understanding of these changes infer structural aspects of the ion-solvent interaction.

A wide range of physical measurements can, of course, be made on solutions. We shall now briefly review some of the methods which are currently being used in the study of ionic solutions.

(ii) Experimental Methods Used

The study of changes in the bulk properties of water brought about by the presence of solutes has provided a considerable amount of information about electrolyte solutions. Changes in viscosity (70), dielectric constant and relaxation time (31), temperature of maximum density (71 - 74), self-diffusion coefficients for ions and water in ionic solutions (75) and ultrasound absorption (76) have all been interpreted in terms of water-solute interactions. X-ray diffraction, N.M.R., infrared and Raman spectroscopy have also been used extensively. These methods are often limited, for reasons of sensitivity, to the concentration region above 1 molar and, as such, caution must be exercised in interpreting the results in terms simply of ion-solvent effects.

(a) X-ray diffraction

X-ray diffraction studies of electrolyte solutions should yield mean ion to water distances and time average coordination numbers. The method involves a comparison between the radial distribution function (R. D. F.) of a solution and that of pure water or a suitable reference solution. The method is restricted to concentrations greater than 2 molar, and has been used to estimate ionic radii in concentrated solutions where ion-pairing is known to occur.

(b) Infra-red and Raman spectroscopy

The basis for studying infra-red and Raman spectra of liquid water was discussed earlier in this chapter in connection with the question of water structure. The concept of "structural temperature" of an electrolyte solution was one of the first results of spectral studies on solutions (3). Worley and Klotz (60) used the concept and found that (n-Bu)$_4$NBr at concentrations below 2 molar decreased the structural temperature of water by 3 to 6°C. Bunzl (77) examined the frequency shifts of the 0.9μ band to determine the effects of salt concentration and temperature on the structure of water. His results showed that Bu_4NBr and Pr_4NBr were net structure makers while Et_4NBr showed no effect and Me_4NBr acted as a structure breaker*.

---

* The term structure maker has been applied to ions which have an effect on the solvent which is analogous to lowering its temperature (see also Section (iii) (c) of this chapter).
The term structure breaker has been used to describe ions which cause a breakdown of the water structure to a more random state analogous to that produced by an increase in temperature of the solvent (see also Section (iii) (b) of this chapter).

Anions will affect the OH stretching frequencies of the water molecule by virtue of their interaction with the hydrogen atoms, while cations in electrostatically interacting with the oxygen of H_2O will affect the bending mode (υ_2). The half width of the υ_2 band has been found to reflect the degree of hydrophilic hydration of the cations (70). Low frequency Raman studies (44, 56, 78) have provided information on the librational behaviour of water in the presence of ions. The librational bands show only a slight temperature dependence in the presence of ions in contrast to the marked temperature dependence in the case of pure water, indicating the strength of the ion-water interactions. The intermolecular O-H---O stretching band (175 cm^{-1}) was examined by Walrafen (44) in the presence of alkali halides and it was found that the band decreased in intensity in the presence of Br^- more so than with Cl^-. This result was interpreted in terms of the ability of the Br^- ion to break hydrogen bonds in the solvent. Studies of the infra-red OH-stretching vibrations (57) of water in the presence of tetraalkylammonium (TAA) salts and sodium carboxylates have also been made.

The carboxylates produced a shift to lower frequencies, presumably because of the OH interaction with the $-CO_2^-$ group. The R_4NX salts produced a shift to higher frequencies but this may be due to the pronounced effects of anions and also to the high ($>$ 1 molar) concentrations used. Near-infra-red spectra have also been used and the results obtained (a) confirm the structure-breaking character; (b) establish sequence of the halide ions (42, 60) with regard to the magnitude of the effects they produce, and (c) indicate the order-promoting character of OH^- and F^-. For cations, which have much less effect on the stretching modes

of water, the agreement on the order of effectiveness of the structure-breaking in a series of ions is not as definite. Near-infra-red studies (60) seem to provide more information regarding the effects of ions on water than does the study of the fundamental stretching modes, and seem to provide support for the present concepts of structural effects of ions in solution.

(c) N.M.R. studies

The study of the magnetic resonance and the relaxation time of the solvent, i.e. with ^{1}H or ^{17}O, can provide a useful probe for the effects of ions in solution. The resonant frequency of a nucleus depends on the electron distribution around it and, under the influence of a strong field, e.g. at an ion, the electron cloud will be distorted and the chemical shift will be changed. As shown by Hindman (79) the proton shielding constant could be separated into seven terms, some of which could not be evaluated. The method is restricted to solutions of concentration > 0.5 molar and because of rapid exchange of water molecules in the solvation sheath of the ion, only one resonance peak is normally observed. Hindman (80) has described the possible contributions to ion-induced proton shifts in terms of the following effects:

(1) High-field shifts due to breaking of hydrogen bonds in the hydrophobic hydration process with additional bond breakage in the structure-broken region;

(2) Low-field shifts due to enhancement of local structure of the solvent by relatively non-polar ions, distortion of the electron distribution around protons of neighbouring water molecules and non-electrostatic interactions between cations and the oxygen of the coordinated water molecules.

Other explanations involving steric distortion of the water lattice (81) and hydrogen bonding of water molecules to anions (57) have been proposed.

The n.m.r. spectrum is affected mostly by anions, the shift for F^- being in the same direction as that associated with decrease of temperature (lower fields), while shifts for Cl^-, Br^- and I^- are to higher fields (57, 80, 82). These findings are in accord with the usual picture of hydration which will be described later. For cations the situation is more confused since K^+ shifts the resonance frequency to higher fields than do either Cs^+ or Rb^+ (80). A correction to the shift due to hydrogen bond breakage (82) resulted in a cation-independent chemical shift which was proportional to anion size and thought to be related to the anion polarisabilities.

Upfield shifts have been observed with large non-polar salts (83 and 85). These shifts correspond to the behaviour observed if the temperature of the pure solvent is raised and thus conflict with the conclusions of the i.r. and Raman studies. These results have been attributed (a) to the fact that the type of structure which is locally formed might be different from that present in cold water; (b) to increased covalency of the H- bonds, and (c) to the important fact that the experimental data were obtained at relatively high concentrations where some structure-making ions are thought to become structure-breakers.

Engel and Hertz (86) have studied the longitudinal relaxation rate ($\frac{1}{T_1}$) of water in ionic solutions. The reorientation time of the water molecule (cf. Samoilov [19]) was taken as an indication of the type of hydration in which the ions were involved. A salt was considered to be a structure-breaker if the rotational freedom of the water was greater than

that in pure water, and the converse of this criterion defined structure-making solutes. The relaxation time results seem to provide a criterion for distinguishing between the various types of hydration and are easier to interpret than the chemical shift data.

(iii) Models of Hydration

Throughout the discussion of structural effects in aqueous solutions, we have made reference to various "types" of hydration, i.e. hydrophilic, structure-breaking and hydrophobic. The current models of ionic hydration have already been reviewed (70, 23). Having examined the evidence for structure in the pure solvent itself and in solutions, we are now in a position to describe more fully these special interactions between solutes and water.

(a) Hydrophilic hydration

Historically, the first type of hydration that was recognised was of the electrostatic polarisation or hydrophilic type. If an ion with a high surface charge density is placed in solution, the strong electric field at the periphery of the ion (viz. $> 10^7$ V/cm) may immobilize a certain number of water molecules. The hydration sheath thus formed will move with the ion in solution*. Hydrophilic hydration has also been referred to as hydration of the first kind (87) or near hydration (19). There is general agreement amongst workers in the field that ions such as Li^+, F^-, Na^+ and divalent alkaline earth cations are involved in hydrophilic hydration.

---

*

In point of fact, there is usually a dynamic equilibrium of solvent between the solvate sheath and the solvent but in the time-average, solvent is transported with the ion.

(b) "Negative" hydration

With the exception of the three ions mentioned above, all other simple univalent ions display various degrees of what is called structure breaking, or negative hydration (19). The following observations characterise the behaviour of these ions: they have negative B viscosity coefficients in the Jones-Dole relation (88); the reorientation time of a water molecule in their vicinity is shorter than that in pure water (86); the apparent Stokes radii are smaller than the crystal radii (89); positive contributions to the structural temperature of the solvent are exhibited in i.r. and Raman studies, and self-diffusion coefficients of water in the ionic solutions are greater than that of pure water (90). These facts indicated that the water in the vicinity of ions such as K^+, Cl^-, Br^-, I^-, etc. had greater freedom of movement than it had in the pure solvent.

The explanation for this phenomenon was proposed independently by Frank and Evans (7) and by Gurney (91). It was suggested that the competing influence of the field of the ion and the tendency of the water to remain in the normal (bulk) state, led to an intermediate region of relatively greater disorder. Frank and Wen (30) suggested three concentric regions around an ion: an inner shell of hydrophilic hydration, a middle shell of structure-broken water and an outer shell of water still slightly polarised by the ion. An ion would be a structure-breaker if the middle shell region predominated over the inner shell. Horne and Birkett (92) have interposed a structure enhanced region between the electrostricted inner layer and the structure-broken layer. Samoilov (19), Gurney (91) and Engel and Hertz (86)

considered that the structure-broken region extends up to the "surface" of the ion. Engel and Hertz (86) have proposed a model for structure-breaking which involves a cooperative motion of the water molecules around the ion. Since the activation energy for translational and rotational diffusive motions in pure water is of the order of 4 Kcals/mole, in order for structure-breaking to occur, an alternate pathway is needed with a lower activation energy. In their model the hypothetical charging of a rare gas atom to a singly charged ion was considered; the particle was regarded as being embedded in a structural arrangement of water corresponding to hydrophobic hydration. Consideration of the configurational part of the free energy led them to the conclusion that the charging process up to ± 1 electron charge had the effect of making the energies of the configurations rather similar in magnitude. In other words, the low energy barrier which they showed to exist between configurations leads to what has normally been called the structure-broken region.

Experimental evidence for a structure-broken region extending up to the "surface" of the ion was thought to be found in the fact that the molecular motions of water molecules in the immediate vicinity of the I^- ion did not become slower as the concentration of KI was increased to 6 molar. At such a high concentration all of the water would be involved in hydration of the ions, as may be readily seen by calculating the number of water molecules available per ion.

(c) Hydrophobic hydration

Throughout the discussion presented so far, we have implied that there are also ions which increase the degree of structure in water. This type of effect was recognised early on in connection with the behaviour of neutral solutes (9) and in ionisation of bases, but Frank and Evans (7) were the first to use the term "iceberg" explicitly in connection with this structural enhancement. Their findings that rare gas atoms caused this effect on the water structure have now led workers to consider this as the normal state of water in the vicinity of most non-polar solutes (86). Frank and Wen (30) proposed that even ions with non-polar side chains would stabilise the flickering clusters envisaged in their model of water. Nemethy and Scheraga (32) used their quantitative model of water structure to compute the increase in the number of hydrogen bonds near a structure-making ion or molecule. The exact structure of the icelike region around non-polar solutes is still open to discussion; it may be truly icelike, clathratelike or nontetrahedrally hydrogen bonded (87). The following section in this chapter will deal with the special structural effects brought about by R_4NX salts and the question of hydrophobic hydration, a matter investigated further in part of the experimental work described in this thesis.

5. Structural Effects in Solution and the Behaviour of Tetraalkylammonium Salts

The tetra-n-alkylammonium salts (TAA salts) provide almost ideal model ions for studying ion-solvent interactions; consequently, a large number of studies reporting the physico-chemical behaviour of solutions of these salts have been made in the recent years. A brief review of these results will be given here since the interpretation of results obtained in the present work, to be reported below, on this system, must be made in the light of the current knowledge about aqueous solutions of these salts.

In postulating the flickering cluster concept of water structure, Frank and Wen (30) reported unusually high positive heat capacities for n-Bu_4NBr. These results were interpreted in terms of stabilisation of water structures near the tetrabutylammonium ion, and these structures were considered more difficult to "melt" than an equivalent volume of ordinarily structured water in the pure liquid.

N.m.r. studies by Hertz and Spalthoff (84) showed an upfield shift of the water protons in TAA salt solutions. The difficulties involved in interpreting chemical shifts in terms of solvent structural changes have already been discussed above and, for the moment, seem to preclude any definite conclusions being made. Hertz and Zeidler (93) studied the proton relaxation of water in aqueous R_4NX solutions. They found that the presence of alkyl groups increased the relaxation time to two to three times that found in pure water. From a study of the temperature dependence of the relaxation

time , they showed that the activation energy was increased for relaxation in the vicinity of the large, non-polar ions. The viscosity B coefficients were measured as a function of temperature for the TAA salts (94) in H_2O, D_2O and methanol solutions. It was found that the B values for Me_4NX increased with temperature while the values for Et_4NX to Bu_4NX had an increasingly negative temperature dependence indicative of increased structure around the ions. This behaviour was not, however, observed with methanolic solutions, thus indicating that the structural effects were associated specifically with water. The results obtained with D_2O solutions showed a trend toward greater structure in D_2O solutions than in H_2O solutions but the differences between the results for the two solvents were on the limit of experimental significance. In a recent review, the effect of solvent structure on ionic mobilities and viscosity B coefficients (95) has been fully discussed.

Conductance measurements, because of their high sensitivity, can be made down to very low concentrations and the data obtained can be analysed extensively with the available conductance equations. Evans and Kay (96) reported conductance measurements at 25° C and 10° C on aqueous solutions of R_4NX salts. They found abnormal behaviour with increasing anion size which was attributed to association as the cation and anion became larger. Analysis of the data in terms of the conductance equations indicated that association was only significant in the case of Pr_4NI and Bu_4NI. Levien (97) analysed her conductance data by using the crystallographic radii for $\overset{o}{a}$, the distance of closest approach, and found association in

the cases of Me_4NB_r and Me_4NI. Notwithstanding the fact that the radius of an ion in solution is probably different from that in the crystal, giving $\overset{o}{a}$ such a strict physical meaning may not be justified. It was concluded (96) that the relative decrease in ionic mobility of these large ions was due to water structure enhancement about the alkyl chains. An examination of the Walden products for the TAA ions in aqueous and non-aqueous solutions (98) has shown that the effective sizes of $Pr_4N^+ \rightarrow Am_4N^+$ cations are greater in water than in non-aqueous solvents, and this conclusion is consistent with the incipient clathrate model for these ions. The temperature dependence of the Walden product in water indicates that Me_4N^+ (which exhibits a negative temperature dependence similar to that for large alkali halides) is a structure-breaker, while Et_4N^+ shows little temperature dependence and is on the borderline between being a structure-maker or structure-breaker. The larger TAA ions show positive $\partial(\lambda_o\eta)/\partial T$ indicating that the thermal destruction of the structure around the ion permits it to move anomalously fast, i.e. at a rate greater than that expected simply on the basis of the decrease of η with temperature. An earlier study of the conductance behaviour of the TAA salts in D_2O (99) had shown that the concentration dependence was nearly the same as that in H_2O. Association of Bu_4NI was found to occur to the same extent as in H_2O. This observation conflicts with the structure enforced ion pairing model proposed by Diamond (100), since D_2O with its greater degree of structure should tend to cause more association. The ratio of the Walden product in D_2O and H_2O (99) thus provided a means

of distinguishing structure-makers from structure-breakers. It has also been shown (101) that the substitution of a hydroxyl group for a terminal methyl group in the Pr_4N^+ ion, results in the disappearance of the anomalous values of mobility and viscosity B coefficient which have been associated with structure promotion. A conductance study of the alkyl sulphonium iodides in aqueous and non-aqueous solvents (102) indicated that cation-anion association was not significant in aqueous solution except for the case of Bu_3SI; the case of Bu_4NI was similar. This result was taken as further evidence that association did not occur in the lower members of the TAA salt series since the trialkylsulphonium salts with their exposed positive charge would be expected to associate (electrostatically) to a greater extent than the R_4NX salts. The R_3SX salts also have the structure-enhancing characteristics of the R_4NX salts, as evidenced by the temperature dependence of their Walden products. The pressure dependence of the conductivity of TAA salt solutions has been measured up to 4 K bars (103). Little pressure dehydration was reported and the behaviour of the Br^- and I^- series was complex, going through a maximum in the relative conductance K_p/K_{atm} (measured at pressure P and at 1 atmosphere) for $\underline{n}$-Pr_4NBr and Et_4NI, while the values of this ratio for the chlorides varied in a regular manner. Pressure induced salting-in was proposed to explain the results.

Extensive studies of the activity coefficients of the TAA salts have been carried out (104, 105). It was found that $\gamma_{\pm}$ decreased with increasing size of the anion, increased with cation size in the fluoride series and decreased with cation size in the iodide series, the inversion occurring between the chlorides and bromides. The large variation in $\gamma_{\pm}$, [i.e. the fluorides exhibit the highest $\gamma_{\pm}$ values of any 1:1 electrolyte at 25°C (104)] and the inversion in the order has been interpreted in terms of the structural effects of these ions. Structure-promoted ion pairing (100), association (97, 106), and micelle formation (105) have all been proposed as explanations for the concentration dependence of the behaviour of the bromides and iodides. Frank (107, 108) has proposed structural salting-in of Bu_4N^+ to explain the deviation from the Debye-Hückel law. Ultrasonic absorption studies of Bu_4NBr solutions by Atkinson, Garnsey and Tait (109) have shown that all three proposed causes for deviations from the limiting law can be accommodated to the data. They estimated values of the equilibrium constant for association [3.9], ion pair dimerisation [2.9] and for cation-cation pairing [3]. The inversion in $\gamma_{\pm}$ observed with the fluorides (104) has been attributed to the incompatibility of the structure-making tendencies of the fluoride (hydrophilic) and TAA ions (hydrophobic effect) which leads to a structural salting-out effect. The substitution of terminal methyl groups by hydroxyl groups (110) diminishes the activity coefficient and in fact $(EtOH)_4NF$, which is similar in size to n-Pr_4NF, behaves almost like KF. Similar studies (111) have also been made on the chlorides and bromides.

Studies of the enthalpy and entropy of dilution (112-114) of the TAA salts have shown that these two quantities are much more sensitive to structural changes than are the free energies. For a given halide, the order of the heat involved was $Bu_4N^+ > Pr_4N^+ > Et_4N^+ > Me_4N^+$ and for a given TAA ion the order was $F^- > Cl^- > Br^- > I^-$. The entropies decrease with decreasing size of the cation, but the entropies of n-Pr_4N^+ (Br^-, Cl^- and I^-) are practically identical, as are those of n-Bu_4NCl and n-Bu_4NBr. This suggests that the structure-promoting ability of these salts, as reflected in the entropy, overshadows the differences due to the sizes of the co-anions. The behaviour of the heats has been interpreted in terms of structural salting-in (114).

Partial molar adiabatic compressibility* studies of the TAA salts have also been reported by Conway and Verrall (115) from this laboratory. The behaviour of $\phi^{\circ}_{K(S)}$ which increases from NH_4^+ to $(CH_3)_4N^+$ and then decreases from $(CH_3)_4N^+$ to Bu_4N^+, exemplifies the transition from a structure-breaking NH_4^+ ion to the borderline Me_4N^+ - Et_4N^+ cases, then to the structure-making n-Bu_4N^+ ion.

The partial molar volume behaviour of the TAA salts has also been the object of extensive studies. These salts exhibit marked deviations from the Debye-Hückel limiting law at quite low concentrations and such deviations have been interpreted in terms of ion pairing and dimerisation of ion pairs (116), of cation-cation interactions (117-119), and also in terms of solute-solvent size ratio (120). Some of the above interpretations have been questioned (121). New work on the partial molar volumes and expansivities of the TAA salts in H_2O and D_2O is the subject of part of the original work reported later

* The partial molar adiabatic compressibility described by $\phi_{K(S)}$ or $\phi^{\circ}_{K(S)}$ for the infinite dilution value is defined by equation II.17.

in this thesis, so that a detailed discussion of the previous work on this topic will be reserved for the following section of this chapter and for the Discussion chapter.

In conclusion, it is evident from the extensive studies of the physico-chemical properties of aqueous solutions of the TAA salts, that a new type of hydration is operating which is connected with the special ability of water to form three-dimensional hydrogen bonded networks. The question of the exact molecular configurations involved is still a hotly debated topic.

6. Previous Work on Special Topics Examined in the Present Research

(i) Partial Molar Volume of Salts in H_2O and D_2O

Gilkerson and Steward (122) and Wen and Saito (123) have studied the TAA bromide series down to 0.1 molar. Dilatometric studies down to 0.002 molar (124, 125) have shown that the partial molar volume data for Me_4NBr and Bu_4NBr salts exhibit the Debye-Hückel limiting slope at sufficiently low concentrations. Conway and Verrall (120, 126) measured the partial molar volume of the TAA chloride, bromide and iodide series at 25°C down to 0.01 molar using a differential buoyancy balance technique. Franks (127) studied the Br^- series at 5° and 25°C down to slightly lower concentrations using a magnetic float densitometer. Wirth (116) has measured the partial molar volumes of the TAA bromide series using a dilatometer. It has also been shown that substitution of an OH for a terminal methyl group in a TAA salt removes the anomalous concentration dependence of the partial molar volumes (110).

The temperature dependence of the partial molar volume of the TAA iodides (128) and chlorides (129) in aqueous solution has also been studied. Partial molar volume studies on the TAA salts have also been made in methanol (130) and in mixed solvents (131). The alkylammonium series RNH_3Br was also studied (132) where R was varied from H to n-octyl-, and it was shown that micelle formation resulted in a rapid rise of ϕ_v. Volume measurements on $[Bu_3N\text{-}(CH_2)_8\text{-}NBu_3]Br_2$ (133), a bolaform salt, have been made and used as a model for study of cation-cation pairing.

Some partial molar volumes of alkali halides in D_2O (134) have been reported. Volume studies as a function of temperature on 1:1 and 1:2 electrolytes (135-138) have also recently been reported. Very precise partial molar volume measurements at 25°C on alkali halide salts have indicated changes in slope which have been interpreted in terms of structural transitions in the solvent (139).

(ii) Partial Molar Volume of Nonelectrolytes in H_2O

The partial molar volumes of the normal alcohols have been measured and the P. V. T. relations have been extensively reviewed (140). Similar measurements at high dilutions, and as a function of temperature, on the isomeric butanols were reported by Franks and Smith (141). The temperature of maximum density (T. M. D.), and its variation with solute concentration, has been used with aqueous alcohol and amine solutions (73, 74) to detect the presence of structuring in water.

(iii) Partial Molar Adiabatic Compressibilities

Conway and Verrall (115) reported $\phi^{o}_{K(S)}$ data for the tetraalkylammonium iodides and bromides, and also for the alkylammonium chlorides. Work at higher concentrations on alkali halides and TAA salts in H_2O and alcohol solutions was reported by Allam and Lee (142). Their data were analysed in terms of hydration numbers of the various salts. Aqueous solutions of the alkali halides have been examined down to high dilutions (143,144) and, in some cases, the partial molar isothermal compressibilities have been calculated from the specific heat and expansivity data.

7. Aims of the Present Work

The general aims of the work described in this thesis were to achieve a better understanding of steric aspects of solute-solvent interactions, and in particular, the behaviour of ions containing non-polar groups in aqueous solution. Through the use of precise experimental determinations of the partial molar volume, partial molar compressibility and partial molar expansibility at high dilutions, information regarding the nature of ion-solvent interactions and their dependence on the structure of the solute and of the solvent could be obtained.

The concentration dependence of the partial molar volume of the tetraalkylammonium salts has been extensively studied (120, 122-125) and has been shown to reflect the complex and non-ideal nature of the ion-solvent interactions involved, which persist even at relatively low concentrations. In the present work, it was also our aim to establish, through precise dilatometric measurements at high dilutions, the conditions under which the partial molar volumes of these salts approached the limiting law behaviour, and thus to establish the magnitude and possibly the origin of the non-ideal behaviour.

A partial molar volume and expansibility study in D_2O was also undertaken since a comparison between the thermodynamic behaviour of solutes in H_2O and D_2O should be expected to provide information concerning the effects of small perturbations of the properties of the aqueous medium on ionic hydration. The advantage of using D_2O as a solvent is that it provides a slight modification in

structure with respect to that of ordinary water but does not fundamentally change the character of the hydration. Differences in the behaviour and magnitude of the measured thermodynamic properties in H_2O and D_2O will be interpreted in terms of the nature of the hydration and of the properties of the two solvents.

Previous studies in this laboratory (152) on the effects of the coordination of charged nitrogen centres on the hydration of cations have dealt with direct coordinatinn at the nitrogen centre, e.g. in the case of TAA salts and alkylammonium ions (132). The study of a series of pyridinium salts provides the opportunity of indirectly blocking the hydration at the charged centre by placing substituent alkyl groups adjacent to the nitrogen atom, but on the ring. Thus, a series of pyridinium, piperidinium and alkylammonium salts have been studied with regard to their partial molar volume and compressibility behaviour since a combination of the two types of data will yield information about the state of the water in the vicinity of these ions; such information would not be available from isolated measurements of either property.

The question of the determination of individual ionic partial molar properties is important in the study of electrolytes since most models which have been employed as a basis for calculation of thermodynamic solvation properties of necessity deal only with a single ion. The evaluation of such individual ionic contributions to the measured value for the whole salt is also of great importance in assessing the specificity of effects of ions on solvent

structure and in relation to the structure of the ions themselves. There is no purely thermodynamic method of separating a measured thermodynamic property for a salt into its ionic components, but various schemes have been proposed to effect this division. The individual partial molar volumes were determined by a method developed in this laboratory by Conway and Verrall (126) using an extrapolation procedure. In the present work, a similar extrapolation procedure has been developed to separate the partial molar compressibility into its ionic components.

Finally, the effect of solvation in the ionisation behaviour of the substituted pyridines and piperidines will be considered, as reflected in the volume and compressibility changes which occur upon ionisation of these substances in aqueous solutions. Such information requires knowledge of the volume and compressibility behaviour of the neutral bases and their conjugate protonated ions as well as that of the co-anion X^- present in the solution, or that of the acid H^+X^- employed in the ionisation reaction. These quantities can be usefully related to the heats and standard entropies of ionisation in relation to the solvent structural effects attendant upon protonation.

CHAPTER II

FORMULATION OF PARTIAL MOLAR VOLUMES, COMPRESSIBILITIES AND EXPANSIBILITIES

1. Partial Molar Volumes

An extensive property, X, of a system can be expressed as a function of its temperature, pressure and composition, i.e.

$$X = f(T, P, N_i \ldots .) \qquad \text{II.1}$$

In particular, for a two component system, any change in X at constant temperature and pressure is given by:

$$dX = \left(\frac{\partial X}{\partial N_i}\right)_{T, P. N_2} dN_1 + \left(\frac{\partial X}{\partial N_1}\right)_{T, P, N_2} dN_1 \qquad \text{II.2}$$

If X is the total volume of the system, then the partial differential coefficients of X with respect to N are called the partial molar volumes, i.e.

$$\left(\frac{\partial V}{\partial N_i}\right)_{T, P, N_j} = \bar{V}_i \qquad \text{II.3}$$

Equation II.2 can be integrated to give:

$$V = n_2\bar{V}_2 + n_1\bar{V}_1 \qquad \text{II.4}$$

where n_1 and n_2 refer to the solvent and solute, respectively. If n_2 moles of solute are added to a large volume of solvent and the partial molar volume of the solvent is taken as its infinite dilution

value $\bar{V}_1^o$, then a quantity known as the apparent molar volume ϕ_v can be defined:

$$\phi_v = \frac{V - n_1 \bar{V}_1^o}{n_2} \qquad \text{II. 5}$$

The apparent molar volume of the solute can be obtained from the density of the solution. If the concentration of the solute is given in molality (m), then the apparent molal volume is given by:

$$\phi_v = \frac{1000}{m d d_o} (d_o - d) + \frac{M_2}{d} \qquad \text{II. 6}$$

whereas concentrations in molarities (c) yield the apparent molar volume through the following equation:

$$\phi_v = \frac{1000}{c\, d_o} (d_o - d) + \frac{M_2}{d_o} \qquad \text{II. 7}$$

where d and d_o are the densities in g. ml^{-1} of the solution and solvent, respectively, and M_2 is the molecular weight of the solute. The molal and molar volumes are numerically identical in the concentration range that we have investigated.

Differentiating eq. II. 5 with respect to n_2 at constant n_1 gives the partial molar volume $\bar{V}_2$ of the solute:

$$\bar{V}_2 = \left(\frac{\partial V}{\partial n_2}\right)_{n_1} = \phi_v + n_2 \left(\frac{\partial \phi_v}{\partial n_2}\right)_{n_1} \qquad \text{II. 8}$$

and since for 1:1 electrolytes $(\frac{\partial \phi_v}{\partial c^{1/2}})$ should be a constant at sufficiently high dilution, equation II.8 can be written:

$$\bar{V}_2 = \phi_v + \left[\frac{1000 - c\phi_v}{2000 + c^{3/2}(\frac{\partial \phi_v}{\partial c^{1/2}})}\right] c^{1/2} \left(\frac{\partial \phi_v}{\partial c^{1/2}}\right) \qquad \text{II.10}$$

2. Partial Molar Compressibilities

The apparent molar compressibility of the solute in a two-component system is defined as:

$$-\phi_K = \left(\frac{\partial \phi_v}{\partial P}\right)_T \qquad \text{II.13}$$

Therefore differentiating eq. II.5 with respect to pressure at constant temperature ϕ_K is obtained as

$$-\phi_K = \frac{-V\beta + n_1 \bar{V}_1^o \beta_o}{n_2} \qquad \text{II.14}$$

where

$$\beta = -\frac{1}{V}\left(\frac{\partial V}{\partial P}\right)_T \quad \text{and} \quad \beta_o = -\frac{1}{\bar{V}_1^o}\left(\frac{\partial \bar{V}_1^o}{\partial P}\right)_T$$

The apparent molar compressibility may be calculated from compressibility and density data using the following equation:

$$\phi_K = \frac{1000}{c}(\beta - \beta_o) + \beta_o \phi_v \qquad \text{II.15}$$

Accurate coefficients of compressibility at atmospheric pressure and as $c \rightarrow 0$ are difficult to obtain from isothermal P-V relationships. An alternative method involves the measurement of the adiabatic compressibilities by measuring the velocity of sound waves through a solution. An acoustic or pressure wave travelling through a solution produces a rapid compression which, unlike a static compression, does not allow sufficient time for any heat flow to or from the system. Therefore the compression process is adiabatic. It can be shown (145) that the velocity of propagation of such a pressure wave is related to the adiabatic compressibility β_s and the density d of the solution through the following equation:

$$U^2 = \frac{1}{\beta_s d} \qquad \text{II.16}$$

The apparent molar adiabatic compressibility is given by

$$\phi_{K(S)} = \frac{1000}{c}(\beta_s^o - \beta_s) + \beta_s^o \phi_v \qquad \text{II.17}$$

The adiabatic and isothermal compressibilities are related through the ratio of the heat capacities C_p and C_v of the solution at constant pressure and volume, respectively:

$$\beta_s = (\frac{C_v}{C_p})\beta \qquad \text{II.18}$$

Because C_v and C_p data were not available for these solutions, the adiabatic compressibilities have been directly used in the present work. It has been shown for KCl and NaCl that the difference between ϕ_K^o and $\phi_{K(S)}^o$ amounts to less than 10% (143).

3. Partial Molal Expansivities

The apparent molal expansivity is given by

$$\phi_E = \left(\frac{\partial \phi_v}{\partial T}\right)_P \qquad \text{II.19}$$

Although ϕ_E may be calculated from an equation analogous to eq. II.17, where β_s has been replaced by α the coefficient of thermal expansion of the solution, the measurement of α requires the measurement of d as a function of temperature. Therefore ϕ_E is usually calculated directly from the ϕ_v versus T data.

CHAPTER III

EXPERIMENTAL

1. Partial Molal Volumes

The determination of partial molar volumes requires the density of solutions to be measured with considerable precision as a function of concentration. An examination of the various methods available for determination of densities has been given in (146). Certain factors such as the concentration range under study, the volatility of the solvent, the temperature and the reactivity of the solvent or solute toward O_2 or CO_2 will determine the choice of a suitable method for measuring the density.

Various methods based on the use of magnetically balanced floats, both differentially with two floats (147,148), or with a single float (149,137,127) have yielded excellent results and are particularly well suited for volatile systems. For operation at high temperatures and high pressures, Ellis (135) has used a dilatometric method. The hydrostatic balance method of Kohlraush (150), based on the Archimedian principle, was shown by Wirth (151) to give a high degree of accuracy when used differentially. This method was employed for part of the work presented here. The magnetically operated float and the hydrostatic balance can yield densities that are

accurate to 1 - 3 x 10^{-6} g/ml. The accuracy is determined in part by the size of the floats so that Vaslow (139), using a 250 ml float, attained an accuracy of ± 5 x 10^{-7} g/ml. Under such conditions, however, precision of temperature control becomes a limiting factor. The methods discussed above will give satisfactory partial molar volumes down to a concentration of 0.01 molar. In order to examine the density behaviour of solutions below this concentration, a dilatometer has been developed by Hepler et al (124), which can be used down to 0.002 molar. In the present work, an improved version of the Stokes dilatometer has been used to examine the density of solutions down to very high dilutions.

(i) Apparatus used and Calibration Procedure

(a) Hydrostatic balance

A photograph of the differential buoyancy balance is shown in Fig. 1. A schematic diagram showing the principal parts of the apparatus appears in Fig. 2. The apparatus is similar to that described in a previous thesis by Verrall (152) so that only the modifications made will be pointed out. The balance used was an Oertling model HO3, modified for under pan weighing on both the front and back pans. The vessels containing the solution and the solvent were made of 48 mm i.d. pyrex tubing and were mounted beneath the balance in plexiglass holders. Separate mounts were used for each vessel to permit independent alignment under the balance and thus prevent the floats from sticking to the walls of the vessel. The vessels were also provided with plexiglass covers having small holes for the

Figure 1. Photograph of Differential Buoyancy Balance.

Figure 2. Differential Buoyancy Balance.

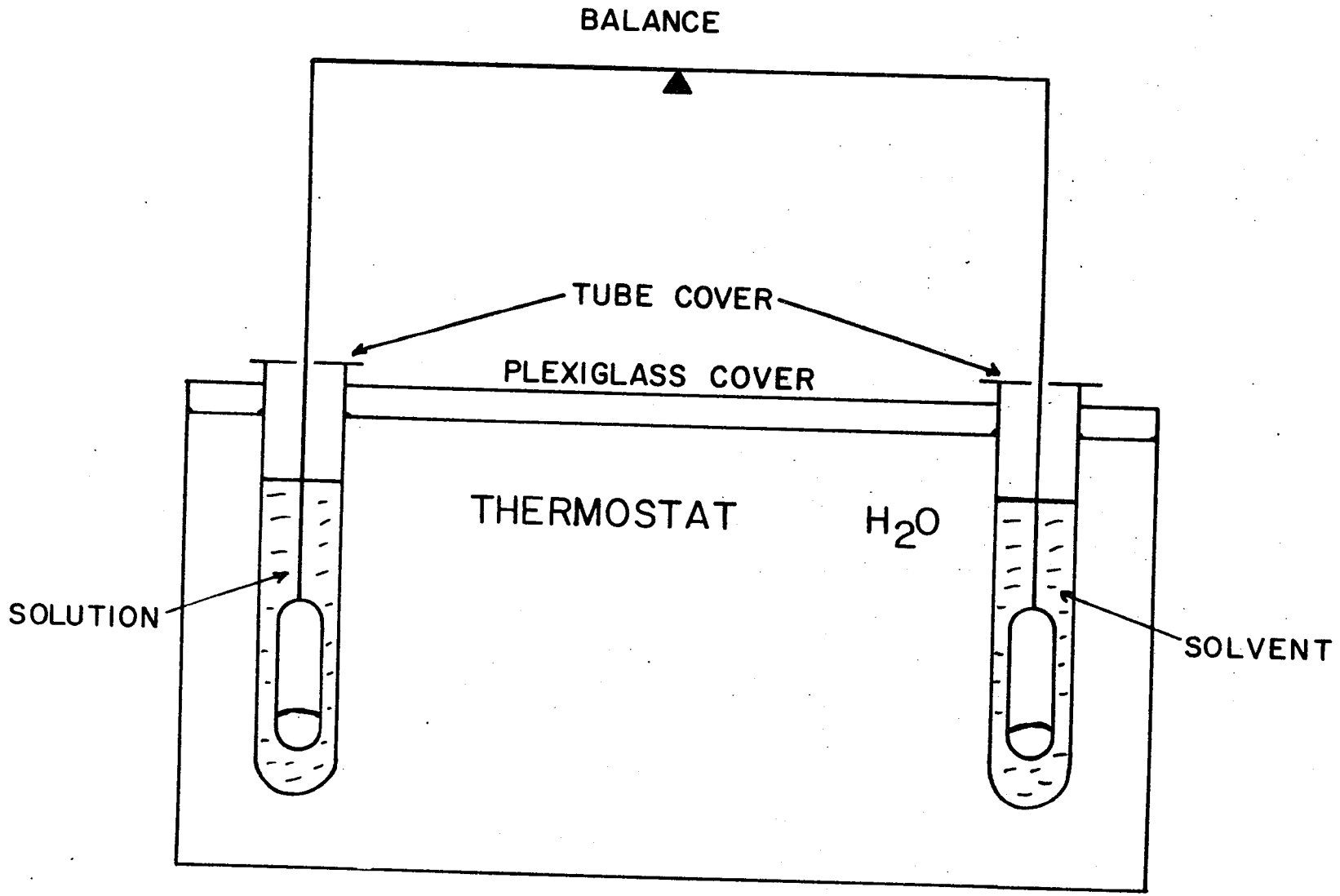
BALANCE
TUBE COVER
PLEXIGLASS COVER
THERMOSTAT
H_2O
SOLUTION
SOLVENT

support wires. The floats were cylindrically shaped, had a volume of about 120 ml and were partly filled with mercury to give them an apparent density of about 1.12. They were suspended in the vessels by means of 0.002" diameter tungsten wires, which were connected to gold plated chains attached to the balance pans. The tungsten wires were soaked in water when not in use to ensure uniform wetting and thus minimize surface tension effects.

All measurements were made in a 150 litre, well lagged water thermostat provided with an annular window and heated by means of a partially immersed electric bulb. The bath was located in a room where the temperature was controlled to better than $1^{\circ}C$. The thermostat was maintained at a temperature of $25.00 \pm 0.01^{\circ}C$ measured on a large mercury in glass thermometer, calibrated by the National Research Council of Canada, having a 12 inch scale for a range of $6^{\circ}C$. A uniform temperature was maintained by means of an effective stirrer situated deep in the bath. The density measurements were reproducible to 3 in the sixth decimal place and the absolute accuracy was checked with test runs on KCl solutions. The values obtained agreed to within 0.1% of the published data (139).

Figure 3. Schematic Diagram of Dilution Dilatometer.

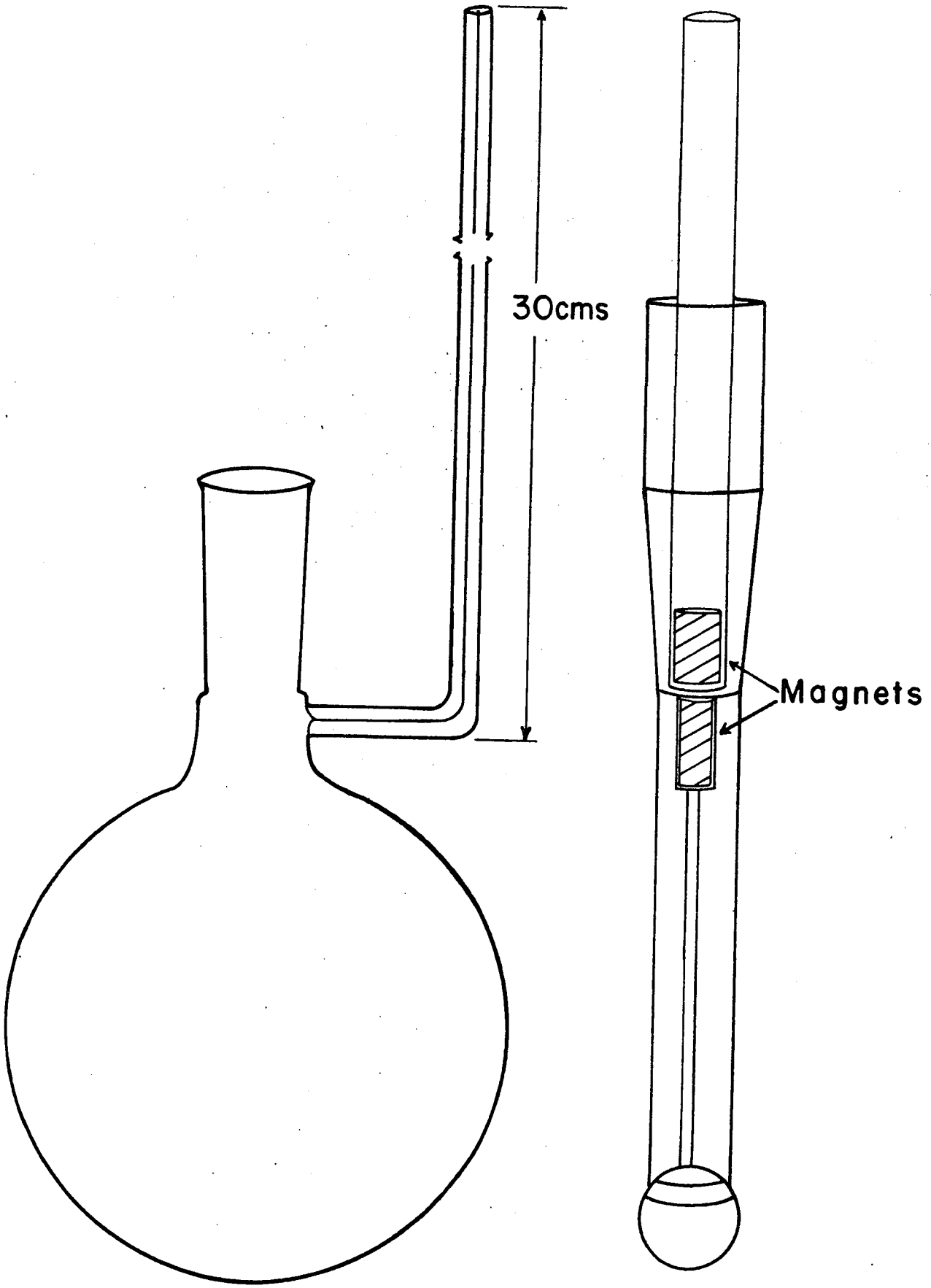

DILATOMETER

(b) Dilution dilatometer

The dilatometer used was based on the instrument developed by Hepler et al (124) and various modifications were made which, it was felt, simplify the operation and improve the reliability considerably. A schematic diagram of the dilatometer is shown in Fig. 3. The dilatometer was made of pyrex glass and had a volume of about 500 ml. The magnetically operated capsule had a volume of about 10 ml. which was known to 0.001 ml since this volume together with the initial concentration of solution in the capsule determined the number of moles of solute that would be diluted. The total volume of the instrument did not need to be known so accurately since only the final concentration, after dilution, has to be determined. The capillary had a radius of ca. 0.05 cm and its exact value was determined by weighing threads of mercury of known length.

The system for control of temperature of the dilatometer required some careful development since the dilatometer was in effect a water thermometer. A well lagged water thermostat of about 50 litres capacity was used. This thermostat was placed in a thermostated enclosure in which the temperature was maintained at $24.5 \pm 0.1^{\circ}C$. The bath was heated by means of continuously operating, low energy heater together with a partially immersed electric bulb which was controlled by a mercury-toluene thermoregulator through an electronic relay. This arrangement, combined with an effective stirrer situated in the centre of the bath, provided a temperature stability of $\pm 0.001^{\circ}C$. All measurements with the dilution dilatometer were carried out at $25.000 \pm 0.001^{\circ}C$.

The absolute accuracy of the apparent molar volumes obtained were checked by performing some measurements on KCl solutions and the values determined agreed to within 0.1% of the data of Vaslow (139). It was not found necessary to correct for the change in volume due to the change of hydrostatic head as the liquid in the capillary moved up or down.

(c) Dilatometer for expansivity measurements

Four dilatometers were also constructed to measure the change in partial molar volume with temperature. These were simply round bottom flasks fitted with a 24/40 joint and stopper. A capillary of ca. 2 mm. diameter and 30 cm. in length was glass blown to the neck of the flask and the dilatometer was annealed at 560°C for 1 hour to relieve any strains caused by the glassblowing which might cause the volume to change with time. With these dilatometers, the change in density with temperature was measured directly. The radius of the capillary was determined by weighing threads of mercury of known length. The volume of the dilatometer at 25.00°C was determined by weighing it empty, then filled with water; appropriate buoyancy corrections were made. The volume of the dilatometer was determined as a function of temperature by measuring the apparent density of water as a function of temperature and from the data on H_2O compiled by Kell (153); the "true" volume of the dilatometer was evaluated as a function of temperature. Other corrections, such as the change in volume due to the change in hydrostatic head and the fact that 0.4% of the solution was at room temperature by virtue of being in the part of the capillary that was not immersed in the thermostat, were absorbed into this volume correction.

The same water thermostat as that used for the dilution dilatometer was employed in these experiments. To lower the temperature of the bath, an antifreeze mixture at -5°C was pumped from a holding tank through a 30 ft. copper coil which was wound around the inside of the bath. The flow of coolant through the coil was regulated so that the heat gain of the bath was just overcome by the cooling provided by the coil. The temperature was then maintained at the desired level by the electric bulb/mercury-toluene system previously described. This sytem gave a temperature that was stable to ± 0.002°C down to 1°C. The temperature was measured with a series of calibrated Beckman thermometers.

In the case of the dilution dilatometer and the four expansivity dilatometers discussed above, the volume changes were measured by means of a cathetometer by observing the change in level of the liquid in the capillaries, as measured from a fiducial mark.

(ii) Method of Measurement

(a) Hydrostatic balance

Two slightly different procedures have been used in measurements conducted with the hydrostatic balance. In the work on the series of pyridinium salts the procedure discussed in detail by Verrall (152) was used. Each solution was made up volumetrically in a calibrated flask at 25°C, the salts being weighed out by difference. The solution was then pre-thermostated at 25.5°C prior to use.

In order to measure the density difference between the solvent and the test solution, solvent was placed in both test vessels up to a certain mark. A "zero" reading (wt_o) was then taken with solvent in both vessels. Subsequently one of the vessels was removed and the solvent was replaced by the same volume of solution, thus ensuring that the same length of support wire was immersed. A second reading (wt) was then taken after allowing 20 min. for thermal equilibrium to be reached and after ensuring that no air bubbles were adhering to the surface of the bulb. The difference in density was then given by

$$\Delta d = \frac{wt - wt_o}{V_B} \qquad \text{III.1}$$

where V_B is the volume of the bulb in the test vessel.

The vessels were kept stoppered during the thermal equilibration and while the measurement was being taken, a plexiglass cover with a hole ca. 5 mm. in diameter was placed over the top of the vessel. As discussed by Verrall (152), the final reading was always approached with the bulb in the test vessel descending. To verify that the bulb was not adhering to the sides of the test vessel a weight of 10 mg. could be momentarily dialed off the balance, displacing the test bulb in an upward direction. It was then allowed to redescend again to its equilibrium position. Using this procedure, wt and wt_o readings were reproducible to ± 0.1 mg.

A second slightly modified procedure was also employed, in particular for the work in D_2O. This modification was in the preparation of the test solutions. The solvent was degassed on a water pump at 40°C for one hour, then a weighed amount of solvent was placed in the test vessel which also contained a small teflon covered magnetic stirring bar. The zero reading was taken as before, then the vessel was removed and placed in a second water thermostat at 25.5°C. A quantity of salt was weighed into the vessel by difference and the resulting solution was stirred for 10 min. by means of a magnetic stirrer located under the bath. Using degassed solvent, no bubbles remained on the bulb or the walls of the vessel after 10 min. of stirring. The stoppered vessel containing the test solution was then replaced in the main bath for the wt reading. Other solutions of progressively higher concentration (molalities) were prepared by adding more salt in the manner described above. Loss of solvent by evaporation over a typical run of 1 - 2 days was minimised by keeping the vessel stoppered at all times except during the actual weight measurement when it was covered in the manner described above.

This procedure which was used in the D_2O work did not allow any significant contamination of the D_2O by water vapour. This was checked by determination of the difference of density between H_2O and D_2O. The advantage of this second procedure is the reduction in the amount of salt (0.15 moles) needed for a run and also the 10 to 20-fold reduction in the amount of solvent used; these considerations become significant with non-aqueous solvents and when expensive salts are used.

(b) Dilution dilatometer

This instrument does not measure the density of the solution directly, but rather it yields the difference in apparent molar volume between a more concentrated starting solution and the final diluted solution at lower concentration. As was shown in (124), from the definition of apparent molar volume,

$$\phi_v = \frac{V - n_1 \bar{V}_1^o}{n_2} \qquad \text{III. 2}$$

where V = total volume of the solution, $\bar{V}_1^o$ = molar volume of pure solvent, n_1, n_2 = number of moles of solvent and solute, respectively.

If a small volume v of concentrated solution is mixed isothermally with a large volume v' of solvent, where $v \approx 60v'$, the change in volume upon mixing is Δv and V, the final volume is then:

$$V = v + v' + \Delta v \qquad \text{III. 3}$$

Further, if $\phi_{v(init)}$ is the apparent molar volume of the salt in the initial, more concentrated solution and $\phi_{v(fin)}$ is the apparent molar volume of the salt in the final diluted solution, then using III. 2 and III. 3 it can be shown that:

$$\phi_{v(fin)} = \phi_{v(init)} + \frac{\Delta v}{n_2} \qquad \text{III. 4}$$

Since the initial concentration is between 0.1 and 0.5 molar, $\phi_{v(init)}$ can be measured with the hydrostatic balance to ± 0.01 ml.

All solvents used were degassed as described previously. The concentrated solution was pre-thermostated at 25°C prior to filling the capsule, in order to prevent leakage of the concentrated solution into the dilution section of the apparatus during thermal equilibration. Particular care was taken in filling the capsule and inserting the magnetically held stopper, that no air bubbles were present. The outside of the capsule was then carefully rinsed and inserted into the top of the filled dilution vessel, forcing the excess solvent out of the capillary. The whole assembly was then placed in the water thermostat and the solvent in the dilution vessel was stirred with the magnetic stirrer for two hours. That thermal equilibrium had been established was shown by the stability of the height of liquid in the capillary. The solution in the capsule was then diluted by removing the magnet which held the magnetic stopper, and allowing the solutions to mix.

After one hour, the final stable reading of the height of the liquid in the capillary was taken and thus the volume change on mixing (Δv) was determined. The number of moles of solute that was diluted was determined by the initial concentration and the known volume of the capsule. The change of volume ΔV in the capillary could be measured with an accuracy of $\pm 1 \times 10^{-4}$ ml.

(c) Expansivity measurements in the dilatometers

This apparatus described in an earlier section measures directly the density of a solution as a function of temperature. It is essentially a "thermometer". Since the density of the solutions which were being studied were known accurately at 25°C from the hydrostatic balance measurements, only the change in density with temperature had to be determined, i.e. ϕ_v had to be evaluated as a function of temperature.

Since $$d_o = \frac{M}{V_o} \qquad \text{III. 5}$$

where d_o is the density of the solution, V_o is the volume of the solution and of the dilatometer, and M is the mass of solution, all at 25°C, at a temperature T°C, the following relation applies:

$$d = \frac{M}{V_T - \Delta V} \qquad \text{III. 6}$$

where d is the density of the solution at the temperature T, V_T is the volume of the dilatometer, and ΔV is, in this case, the change in volume of the solution upon cooling.

From equations III. 5 and III. 6, the following expression for the change in density of the solution with temperature can be obtained:

$$\Delta d = d - d_o = \frac{d_o(V_o - V_T + \Delta V)}{(V_T - \Delta V)} \qquad \text{III. 7}$$

The experiment was performed by filling the dilatometer with a solution of known density and placing it in the water thermostat. The level of the solution in the capillary was measured relative to a fixed mark on the capillary. The measurement determined V_o, the

volume of the solution at 25°C. The temperature of the bath was then lowered by about 3°C and the change in level of the liquid in the capillary was noted, which, together with the known radius of the capillary enabled ΔV to be calculated. The volume of the dilatometer (V_T) as a function of temperature had been determined as described previously.

This procedure was followed down to 1° for H_2O solutions and 3°C for D_2O solutions. The solvent densities at various temperatures were taken from (153) and the apparent molal volumes were calculated in the usual way.

2. Compressibilities

(i) General

The method used to measure the velocity of sound in solution was a differential one first described by Carstensen (154) and is based on the following principle.

Two transducers are mounted as described in the following section so that one is located in the solvent (H_2O) while the other is placed in the solution under study. The separation between the two transducers is adjusted with a micrometer screw so that there is an integral number of wavelengths between them. If the physical separation of the transducers is d, and the path length in water is z,

$$n = \frac{z}{\lambda_w} + \frac{d - z}{\lambda_x} \qquad \text{III.8}$$

where λ_w and λ_x are the wavelengths in water and the test solution, respectively. The distance d between the transducers is kept constant and the transducer assembly is moved along the axis of the test vessel a distance Δz until the acoustical path length has increased to n + 1, where n is the number of acoustical wavelengths between the two transducers.

$$n + 1 = \frac{z + \Delta z}{\lambda_w} + \frac{d - z - \Delta z}{\lambda_x} \qquad \text{III.9}$$

where $\lambda_x > \lambda_w$.

Subtracting equation III.8 from III.9, the following expression is obtained for the difference in wavelength between solvent and solution:

$$\Delta\lambda = \frac{\lambda_w^2}{\Delta z - \lambda_w} \qquad \text{III.10}$$

Introducing velocities instead of wavelengths, and the frequency f,

$$\Delta U = U_x - U_w = \frac{U_w^2}{f\Delta z - U_w} \qquad \text{III.11}$$

The main source of errors in the measurement of ΔU occurs in the determination of Δz. For the lowest concentrations studied (ca. 0.02 molar), only one 360° phase shift can be measured but, with the higher concentrations, up to 30 360° phase shifts can be observed.

(ii) Apparatus used and Method of Measurement

A photograph of the differential ultrasonic velocity apparatus is shown in Fig. 4. It consisted of two main parts:

1. the electronic components, shown diagrammatically in Fig. 5;
2. the test vessel and mechanical assembly shown in Fig. 6.

The electronic components have been described in detail elsewhere (152). They consisted of a radio-frequency generator producing a 10 MHz signal which was modulated in the form of pulses. Part of this pulsed signal was admitted to the test vessel through a piezo-electric transducer and subsequently transmitted to a detector and mixer circuit where it was added to a reference signal

Figure 4. Photograph of the apparatus for differential measurement of the velocity of sound.

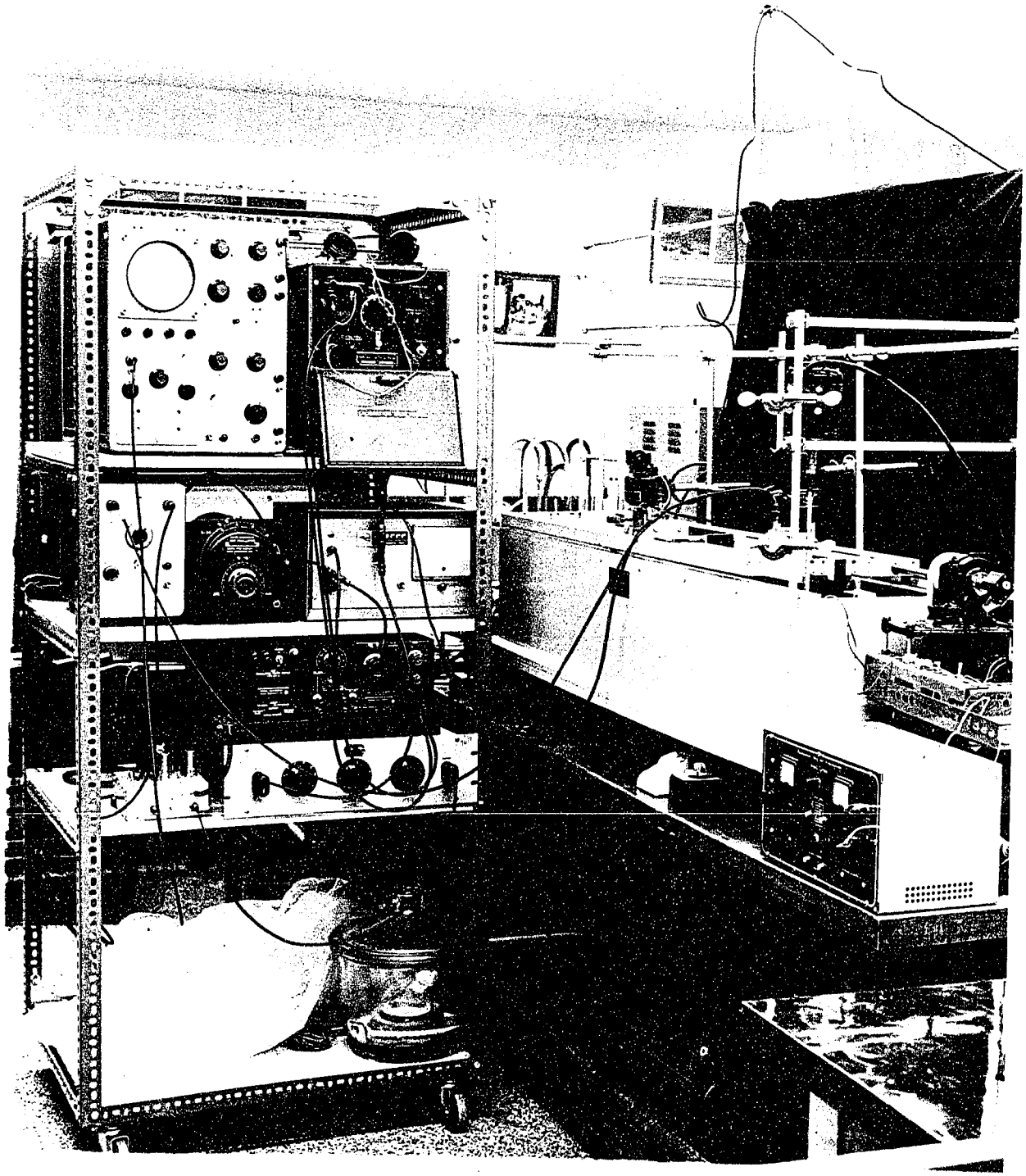

Figure 5. Diagrammatic representation of electronic components

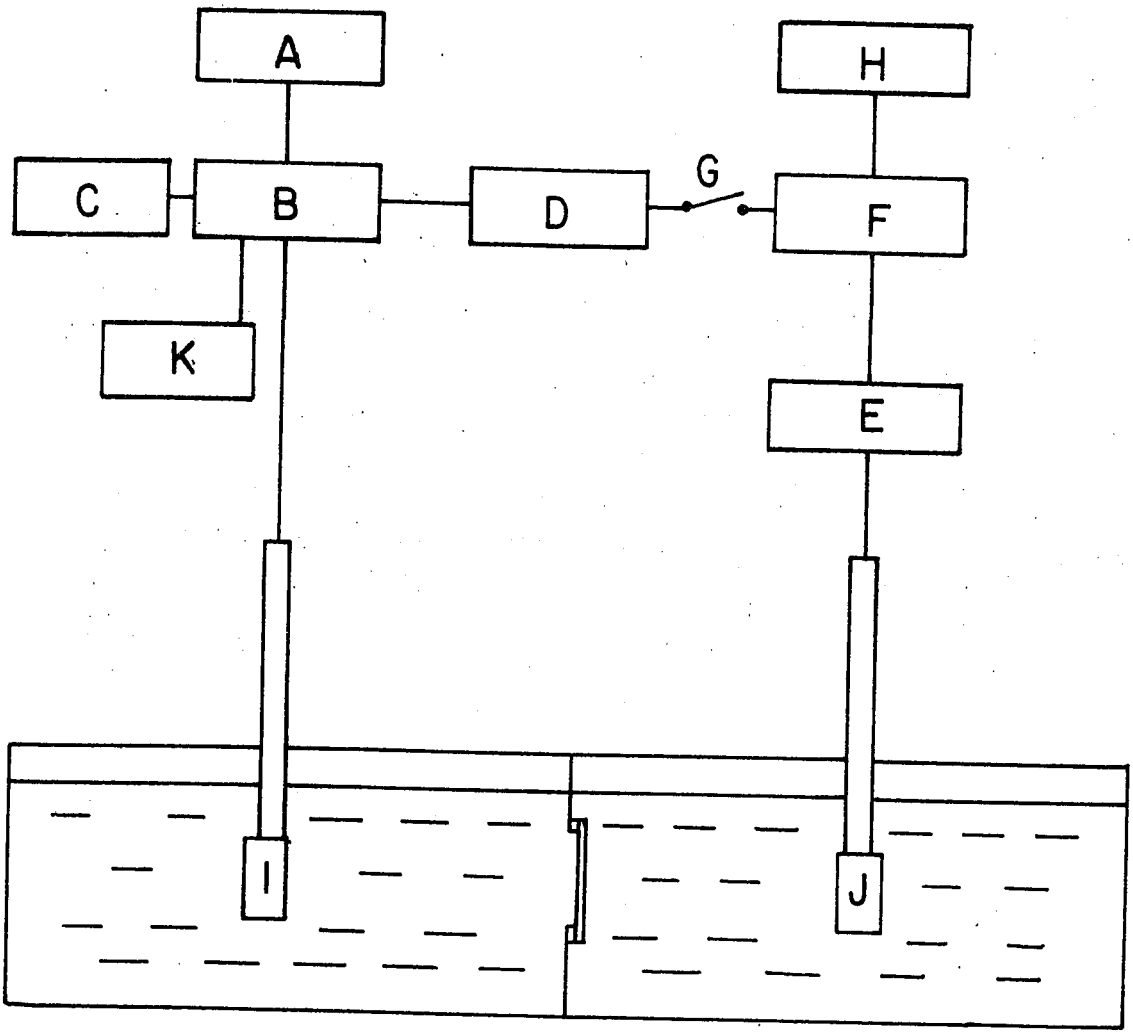

KEY

A - R.F. Oscillator
B - Pulse Modulator
C - Pulse Generator
D - Decade Attenuator
E - Broad Band Amplifier
F - Tuned Amplifier and Mixing Circuit
G - Phase Comparison
H - Oscilloscope
I - Source Transducer
J - Receiver Transducer
K - Frequency Meter

Figure 6. Schematic representation of mechanical assembly used in differential velocity measurements, and details on the test vessel used.

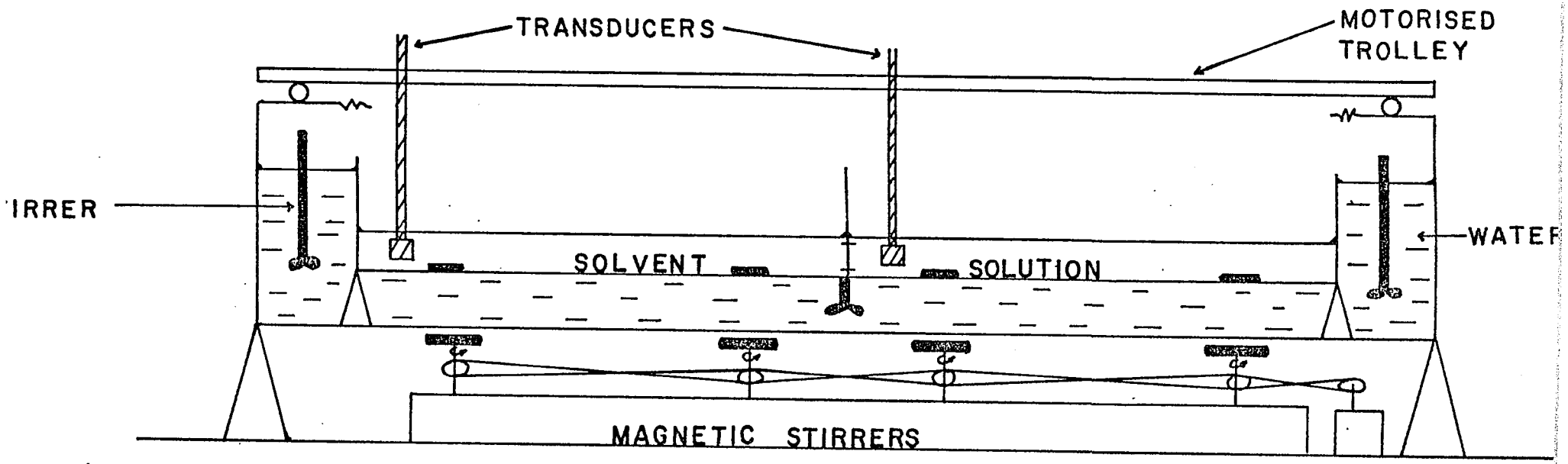

DETAILS OF TEST VESSEL

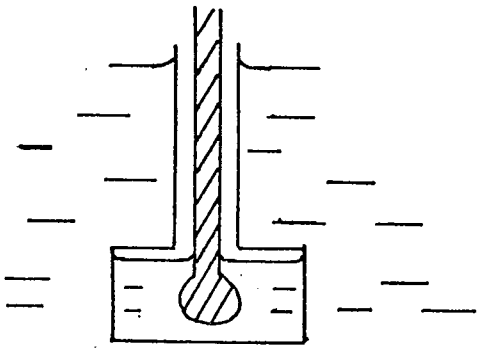

END VIEW

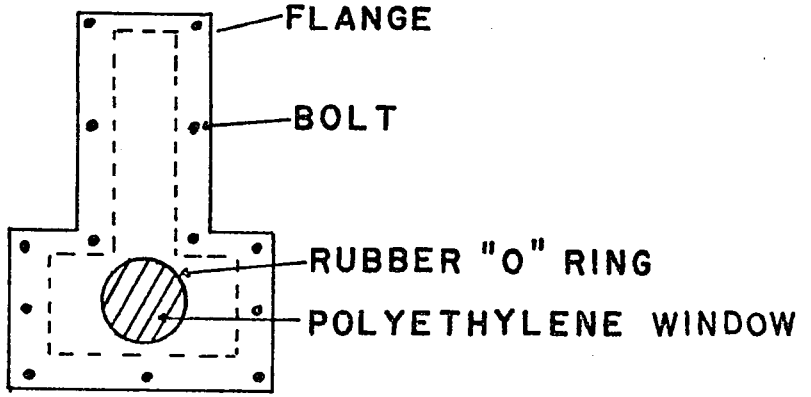

CENTRAL END SECTION

which had come directly from the pulse modulator. The resulting signal was amplified and displayed on an oscilloscope. This circuitry enabled the determination to be made of the extent to which the signal which had passed through the test vessel was in phase or out of phase with the reference signal.

The test vessel and the mechanical assembly were also described in (152). However, certain improvements were made to this system and will be described below.

A new apparatus was constructed using the same design as that described previously (152) but the ultrasonic path length was twice that used in the older system. The test vessel was of a different design and is shown diagrammatically in Fig. 6. It was made of 0.5 mm No. 304 stainless steel and consisted of two identical sections. The sides and bottom of the vessel were made from one sheet of material, and the extreme ends of each half were blocked with stainless steel plates which were soldered into place. The seams were covered with RTV 11 General Electric silicon rubber. The other end of both halves was fitted with a 1" flange and a 2" diameter 'O' ring. A polyethylene sheet was placed between the rubber 'O' rings and the two halves of the test vessel were joined and held in place with 14 bolts placed around the flange.

As was seen, the accuracy with which the difference in the velocity of sound between solvent and solution can be determined depends on the measurement of the distance that the transducers must be moved at constant separation in order for the signal to undergo a 360^{o} phase shift. With a longer test vessel, it is possible to go through

more maxima and minima and thus determine the length of one 360° phase shift more accurately. Also, since the distance that the transducers must be moved to increase the differential acoustical path length in the solution and solvent by one wave length increases as the concentration decreases, this new assembly permits differences in velocity to be measured down to lower solute concentrations. It was possible to measure a difference in velocity between solvent and solution as low as 1 m/sec.

The second modification that was made was in the temperature control system. One of the main advantages of the differential method of velocity measurement is in the temperature control requirements. For a direct interferometric measurement, the temperature must be controlled to ± .001°C if the velocity is to be measured to ± .01 m/sec. With the differential method, a fluctuation in the temperature will introduce an error which is dependent on the temperature coefficient of the velocity difference between solvent and solution. Therefore a temperature control of ± .01°C suffices for our ΔU measurements to be stable to ± .01 m/sec. It was, however, very important to maintain a constant temperature over the entire length of the test vessel (100 cms.).

A 45 litre water thermostat surrounded the test vessel on three sides, and was heated by means of a constantly operating, low energy heater which ran along the entire length of the bath. The temperature was then maintained at 25.00 ± .01°C by means of an intermittently operating heater, identical to the constant heater, controlled by means of a mercury thermoregulator and electronic relay

system. The length of the bath necessitated an effective multiple stirring system in order to maintain a uniform temperature along the bath. This was accomplished by means of three stirrers which ensured rapid circulation of water around the test vessel. In the test vessel itself, four magnetic stirring bars were located which were driven by magnetic stirrers placed under the water thermostat (see Fig. 6). With the system described above, no detectable ($\pm 0.01^{\circ}C$) differences in temperature existed over the entire length of the test vessel.

A reversing motor (windshield wiper motor) was also installed to power the 1 mm. pitch driving screw, and a counter which recorded the number of turns of the shaft required to drive the transducer carriage over a length corresponding to a 360° phase shift in the ultrasonic signals enabled measurements to be made semi-automatically.

The solutions to be studied were made up directly in the test vessel by adding weighed amounts of solute to a known weight of solvent. The concentrations (molalities) were converted to molarities by means of the density data which had been obtained previously in the ϕ_v measurements. Loss of solvent by evaporation was minimised by keeping the long opening along the top of the test vessel covered with a plexiglass lid when the actual measurement was not in progress.

The velocity differences ΔU were obtained with an absolute accuracy of $\pm .02$ m/sec. Test runs were performed on KCl solutions and a value of -45.5×10^{-4} ml (g.mole bar)$^{-1}$ was obtained for the partial molar adiabatic compressibility. This compared favourably with the results of Owen and Kronick, $-44 \pm 1 \times 10^{-4}$ ml (g.mole bar)$^{-1}$ (143) and those of Gucker et al (144), -45.6×10^{-4} ml (g.mole bar)$^{-1}$.

3. Purification of Solvents Used

(i) Water (H_2O)

All water used to make up solutions and rinse the test vessels was doubly distilled, the second distillation being from alkaline permanganate.

(ii) Heavy Water (D_2O)

The heavy water was obtained from Atomic Energy of Canada Ltd. and was 99.75% mole % D_2O. The D_2O was re-used twice after distilling it in a suitably dry apparatus.

4. Preparation and Purification of Solutes Used

All of the salts which were prepared were recrystallised at least twice, while those available commercially were recrystallised once. In all cases the salts were dried for at least two days in vacuo at 50°C prior to use.

(i) Pyridines and Pyridinium Salts

The neutral bases, 2-methylpyridine and 2,6-dimethylpyridine were obtained from Chemical Procurement Laboratories. The pyridine was Analar reagent grade (B.D.H.). These compounds were distilled under a nitrogen atmosphere at reduced pressure before being used either as a reagent for the preparation of the salts, or as a solute.

The HCl gas used to make the hydrochlorides was prepared by dropping concentrated sulphuric acid onto a slurry of analytical grade NH_4Cl and concentrated HCl. The gas was dried by bubbling it through concentrated H_2SO_4. The HBr and HI gas used to make the hydrobromides and hydroiodides was obtained from the Matheson Co.

Pyridinium, 2-methylpyridinium, and 2,6-dimethylpyridinium chlorides were prepared by bubbling the dried HCl gas into a solution of the selected base in ethanol. The reaction mixture was kept in an ice-bath and under a nitrogen atmosphere to prevent excessive heating and oxidation. The hydrochlorides were recrystallised from ethanol. Pyridinium chloride is very hygroscopic, so the salt

was also prepared in solution by titrating the base with standard HCl. The density results obtained with the salt prepared in this way were in agreement with those obtained using solid pyridinium chloride.

The hydrobromide and hydroiodide of 2, 6-dimethyl-pyridine were prepared by bubbling bottled HBr and HI gas into a cold solution of the base in ethanol. These two salts were then re-crystallised from ethanol and their compositions checked by a volumetric halide analysis.

The N-methyl iodides of pyridine, 2-methylpyridine, and 2, 6-dimethylpyridine were prepared by slowly adding methyl iodide to a solution of the base in ethanol. These reactions were very exothermic, so the methyl iodide was added at such a rate as to keep the solution refluxing. When all of the methyl iodide had been added, the reaction mixture was refluxed for three hours. 1-Methylpyridinium iodide was recrystallised from 99% ethanol, 1, 2-dimethylpyridinium iodide was recrystallised from hot water by precipitation with acetone and 1, 2, 6-trimethylpyridinium iodide was recrystallised from a 99% ethanol - 1% water mixture.

1-Ethyl pyridinium iodide was prepared by slowly adding ethyl iodide to a solution of pyridine in ethanol. The reaction mixture was refluxed for three hours and the product was recrystallised from ethanol.

All of the above compounds were kept in subdued light and stored in vacuo prior to use. The melting points of the compounds were checked against the literature values where available.

(ii) Piperidines and Piperidinium Salts

The piperidine was obtained from B. D. H. and the 1-methylpiperidine from Canlab. Both were distilled under a nitrogen atmosphere at reduced pressure prior to use.

Piperidinium and 1-methylpiperidinium chlorides were prepared by bubbling dried HCl gas into a solution of the respective base in ethanol. The reaction mixture was kept in an ice bath and under a nitrogen atmosphere. The products were recrystallised from ethanol and their compositions were checked by means of a Cl^- analysis.

1,1-Dimethylpiperidinium iodide was prepared by slowly adding methyl iodide to a solution of 1-methylpiperidine in ethanol. The resulting compound was recrystallised from ethanol and the purity was verified by a volumetric I^- analysis.

Piperidinium iodide was prepared in solution by titrating piperidine with aqueous HI. The HI had been purified by distillation from red phosphorous. The I^- content of the HI solution was established by a volumetric analysis of the I^-.

(iii) Alkylammonium Chlorides

Diethyl, dipropyl, and dibutyl-ammonium chlorides were prepared by bubbling dry HCl gas into an ethanolic solution of the amine. Diethylamine (B. D. H.), dipropylamine (Matheson-Coleman and Bell), and dibutylamine (tech. grade) were all distilled under a nitrogen atmosphere, the dibutylamine at reduced pressure. The salts were recrystallised from an ethanol (10%) diethylether mixture and the purity was checked by Cl^- analysis.

(iv) Alkylammonium Bromides

Triethylammonium and triethanolammonium bromides were prepared by bubbling HBr gas into a cold solution of the amine in ethanol. Triethanolammonium bromide was recrystallised from a 3:1 alcohol-water mixture , and triethylammonium bromide was recrystallised from ethanol. The melting points of these compounds were checked against the literature values.

(v) Tetra-n-alkylammonium Salts

Tetramethylammonium tetrafluoroborate obtained from Aldrich Chemicals was recrystallised from hot water. The tetra-n-alkylammonium bromide series from tetramethyl to tetra-n-butylammonium bromide were Eastman reagent grade materials. They were recrystallised according to the procedures given in (152).

(vi) Inorganic Salts

KCl, NaCl, NaF, KBr and NaBr were all reagent or analytical grade salts and were used without further puficication. They were dried at 75°C in vacuo for two days prior to use.

(vii) HOD

This compound was prepared in solution by adding a known weight of either H_2O or D_2O to either D_2O or H_2O, respectively, depending on whether a solution of HOD in D_2O or HOD in H_2O was required. The equilibrium constant for the reaction

$$H_2O + D_2O \rightleftharpoons 2HOD$$

is 3.96 (155). The equilibrium concentrations of unreacted D_2O (in excess H_2O) and of H_2O (in excess D_2O) were negligible.

CHAPTER IV

RESULTS

1. Partial Molar Volumes

(i) General

In this chapter the apparent molar volume and partial molar volume results obtained for the various systems studied will be shown in tabular and graphical form. A complete tabulation of the experimental data can be found in the appendices following the last chapter.

(ii) Extrapolation Procedure

The partial molar volume of a component i in solution is equal to the pressure derivative of the partial molar free energy of that component, i.e.

$$\bar{\mu}_i = \bar{\mu}_i^o + RT \ln a_i \qquad \text{IV.1}$$

$$\bar{V}_2 = \left(\frac{\partial \bar{\mu}_i}{\partial P}\right)_T = \bar{V}_2^o + RT \left(\frac{\partial \ln a_i}{\partial P}\right)_T \qquad \text{IV.2}$$

where a_i is the activity of i.

Just as the concentration dependence of the activity coefficient was given by the Debye-Hückel theory, the slope of the relation characterising the dependence of $\bar{V}_2$ on c will be determined by the pressure derivative of the limiting law slope for activity coefficients. For the simplest form of the Debye-Hückel theory, i.e. point charge interactions, Redlich and Rosenfeld (156) showed that,

$$\bar{V}_2 = \bar{V}_2^o + k\, w^{3/2} \sqrt{c} \qquad \text{IV.3}$$

where $w^{3/2} = 1$ for 1:1 electrolytes and k is a constant given by the following equation:

$$k = 2N^2e^3 (2\pi/1000RT)^{1/2} \epsilon^{-3/2} \left(\frac{\partial \ln \epsilon}{\partial P} - \frac{\beta}{3}\right)$$

where N is Avogadro's number, e the electronic charge, ϵ the dielectric constant of the solvent and β the isothermal compressibility of the solvent.

The constant k, which is in fact the limiting slope for 1:1 electrolytes, was evaluated by Redlich and Meyer (157), using the $\frac{\partial \epsilon}{\partial P}$ data of Owen (158), as 1.868 ml.$l^{1/2}$g.mole$^{-3/2}$ for the apparent molar volume. Recent experimental determinations of ϕ_v as a function of $c^{1/2}$ (124, 125, 139) have shown that the theoretical slope is indeed maintained upto reasonably high concentrations, i.e. $\leq$ 0.10 molar for simple 1:1 electrolytes such as NaCl and KCl.

A more complete equation for the partial molar volume of an electrolyte, taking account of the distance of closest approach $\overset{o}{a}$ and its pressure derivative $\partial \ln \overset{o}{a} / \partial P$ is given (159) by:

$$\bar{V}_2 = \bar{V}_2^o + \frac{S_v c^{1/2}}{1 + Ac^{1/2}} + \frac{W_v c}{(1 + Ac^{1/2})^2} + K_v c \qquad \text{IV.4}$$

where $$S_v = k\, W^{3/2} = 2.802 \text{ ml.l}^{1/2}\text{.g.mole}^{3/2} \qquad \text{IV.5}$$

$$W_v = -2.303\, RT.S_a.A \left(\frac{\partial \ln \epsilon}{\partial P} - \frac{2\,\partial \ln \overset{o}{a}}{\partial P} - \beta\right) \qquad \text{IV.6}$$

$$K_v = 2.303\, \upsilon RT.B \left(\frac{\partial \ln B}{\partial P} + \beta\right) \qquad \text{IV.7}$$

$$S_a = \frac{1}{\upsilon} \sum_1^P \upsilon_j z_j^2 \; (\epsilon T)^{-3/2}.1.290 \times 10^6$$

$$A = \overset{o}{a} (\epsilon T)^{-1/2}.35.56$$

and B is an unknown function of c, ϵ, k, T and $\overset{o}{a}$, R the gas constant per mole, T the absolute temperature, υ the sum of the number of ions produced by the dissociation of one molecule of electrolyte, $\overset{o}{a}$ the distance of closest approach in $\overset{o}{A}$, k the Boltzman constant, z the valence and P the pressure.

Since the forms of B and $\frac{\partial \ln B}{\partial P}$ are not known, it is not possible to evaluate the term K_v in eqn. IV.4. The only other unknowns in eqn. IV.4 are $\overset{o}{a}$ and $\frac{\partial \ln \overset{o}{a}}{\partial P}$, the evaluation of which will be discussed in the next chapter.

For extrapolation purposes we have used a simpler equation which is given below (cf. ref. 157):

$$\bar{V}_2 = \bar{V}_2^o + 2.802\ c^{1/2} + hc \qquad \text{IV.8}$$

where

$$h = K_v + W_v - S_v \cdot A \qquad \text{IV.9.}$$

For apparent molar volumes a similar equation is obtained:

$$\phi_v - 1.868\ c^{1/2} = \phi_v^o + j\ c \qquad \text{IV.10}$$

The partial molar volumes of non-electrolytes have been plotted as a function of concentration c.

2. Partial Molar Adiabatic Compressibilities

(i) General

A complete tabulation of the velocity of sound and other associated data used to calculate the compressibility will be found in Appendix II. The $\phi_{K(S)}$ data will be presented in this chapter in tabular and graphical form.

(ii) Extrapolation Procedure

An equation for apparent molar adiabatic compressibility can be obtained by differentiating eqn. IV.10 with respect to pressure and neglecting the hc term*, i.e.

$$-\phi_{K(S)} = \frac{\partial \phi_v}{\partial P} = \frac{\partial \phi_v^o}{\partial P} + \left[\frac{\partial S_v}{\partial P} + \frac{\beta_s S_v}{2}\right] c^{1/2} \qquad \text{IV.11}$$

or

$$\phi_{K(S)} = \phi_{K(S)}^o + S_{K(S)}\, c^{1/2} \qquad \text{IV.12}$$

where

$$S_{K(S)} = -\left[\frac{\partial S_v}{\partial P} + \frac{\beta_s S_v}{2}\right]$$

Since β_s is a function of concentration, the slope $S_{K(S)}$ should not be constant; however, this variation is less than the uncertainty in the slope for the concentration range used in this work, so that eqn. IV.12 can be regarded as linear in $c^{1/2}$.

---

* If the term hc is included and differentiated, an equation similar to IV.11 results but with the additional term:

$$\left(\frac{\partial h}{\partial P} + h\beta\right) c$$

3. Pyridines and Pyridinium Salts

(i) Partial Molar Volumes

In the case of the three neutral pyridine bases studied, hydrolysis corrections were calculated from reported K_B values (160) and found to be negligible. A correction was made, however, to the values of ϕ_v and $\phi_{K(S)}$ for pyridinium and 2-methylpyridinium chlorides. Since the degree of dissociation, α, is given approximately by $(K_A/c)^{1/2}$, the true volume or compressibility is related to the experimental quantity by the following equation:

$$\phi_{SALT} = \frac{\phi_{(EXPT.)} - \alpha(\phi^o_{(BASE)} + \phi^o_{(HCl)})}{1 - \alpha} \qquad \text{IV.13}$$

The correction in ϕ_v ranged from 0.1 ml at c = 0.01 to 0.02 ml at c = 0.20 for pyridinium chloride and was less for 2-methylpyridinium chloride. Similarly, the correction in $\phi_{K(S)}$ ranged from 0.35 ml (g.mole.bar)$^{-1}$ at c = 0.03 to 0.1 ml (g.mole.bar)$^{-1}$ at c = 0.20 for pyridinium chloride, but was negligible for 2-methylpyridinium chloride.

The ϕ_v data for the pyridinium salts (corrected for hydrolysis) were plotted according to eqn. IV.10 and the $\bar{V}_2^o$ values were obtained with the j coefficients. These data are given in Table 1 and some typical plots of $\phi_v - 1.868\ c^{1/2}$ against c are shown in Figs. 7 to 9. The concentration dependence of ϕ_v for 2,6-dimethylpyridinium chloride and bromide is rather unusual. Both of these salts, and to a much lesser extent the I^- salt, exhibit apparent positive deviations from the limiting law. The data for the Cl^- and Br^- salts go through pronounced maxima at ca. 0.05 molar.

The behaviour of the apparent molar volume of 2,6-dimethylpyridinium bromide was further investigated by determining the dependence of the apparent molar volume on temperature. Five temperatures were studied, ranging from 6.20°C to 34.90°C. From the data which is listed in Table 2, it is evident that the concentration dependence of ϕ_v is very sensitive to temperature. At the lowest temperature studied, a slope of +2.35 ml.$l^{1/2}$.g.mole$^{-3/2}$ was observed and the ϕ_v against $c^{1/2}$ curve had the same shape as the curve for 2,6-dimethylpyridinium iodide at 25°C. As the temperature was increased, a slight discontinuity appeared at ca. 0.05 molar, the concentration at which the neutral base showed a maximum in its apparent molar volume. The partial molar volume at infinite dilution also goes through a maximum at ca. 25 - 26°C.

The ϕ_v data for the neutral bases were plotted against concentration and the $\bar{V}_2^o$ and initial slope data are given in Table 3. Typical plots of ϕ_v against c are shown in Fig. 10. The anomalous shape of the relations for 2,6-dimethylpyridinium chloride and bromide is reproduced in the concentration dependence of ϕ_v for 2,6-dimethylpyridine in water. Pyridine exhibits a minimum at about 0.05 molar in water but not in benzene. The minima or maxima reported above seem to be experimentally significant since (a) they were found with several compounds but not with others over the same concentration range; (b) hydrolysis effects could not account for the behaviour since they would lead to opposite effects in the apparent volumes of the 2,6-dimethylpyridinium ion in comparison with that for the neutral molecule; and (c) repetition of points in independent experiments in the region of the maxima served, in fact, to delineate the discontinuity

TABLE 1

Values of $\bar{V}_2^o$ and j in Equation IV.10 (25°C)

Salt	$\bar{V}_2^o$ ml(g.mole)$^{-1}$ ± 0.05 ml(g.mole)$^{-1}$	j ml.l(g.mole)$^{-2}$ ± 8%
Pyridinium chloride	90.96	-1.7
2-Methylpyridinium chloride	108.63	-0.7
2,6-Dimethylpyridinium chloride	125.40	+11.2
2,6-Dimethylpyridinium bromide	133.10	+8.5
2,6-Dimethylpyridinium iodide	144.26	+0.3
1-Methylpyridinium iodide	126.82	+0.3
1,2-Dimethylpyridinium iodide	142.55	+2.6
1,2,6-Trimethylpyridinium iodide	158.23	+0.6
1-Ethylpyridinium iodide	144.03	+0.3

Figure 7. A plot of apparent molar volume minus $1.868\ c^{1/2}$ against concentration, for:
(a) 2-methylpyridinium chloride,
(b) pyridinium chloride, and
(c) 2,6-dimethylpyridinium chloride.

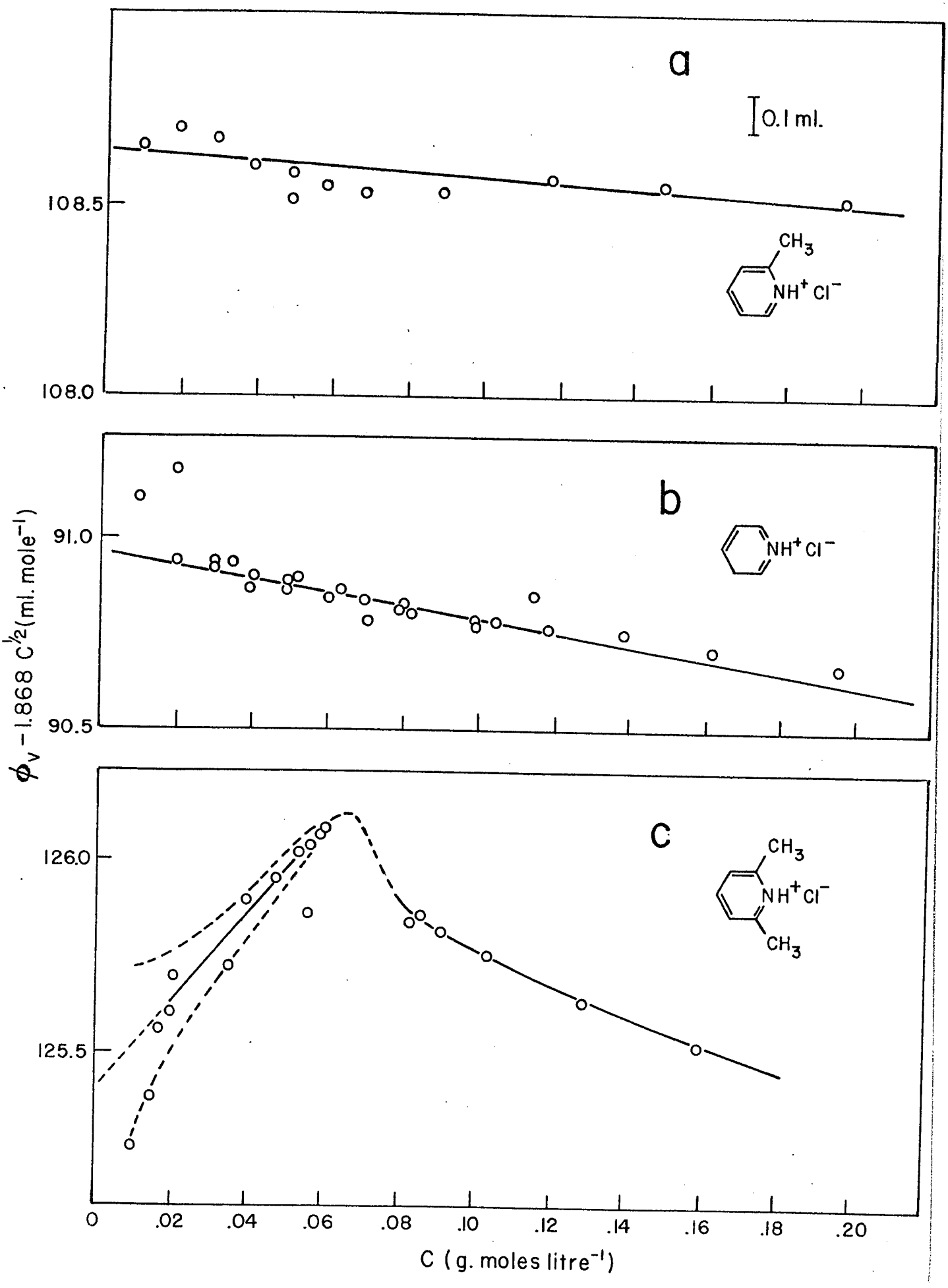
a
0.1 ml.
108.5
108.0
CH3
NH+ Cl−
b
91.0
90.5
NH+ Cl−
c
126.0
125.5
CH3
NH+ Cl−
CH3
0
.02
.04
.06
.08
.10
.12
.14
.16
.18
.20
C (g. moles litre−1)
φv − 1.868 C½ (ml. mole−1)

Figure 8. A plot of apparent molar volume minus $1.868\ c^{1/2}$ against concentration for:
(a) 2, 6-dimethylpyridinium bromide,
(b) 2, 6-dimethylpyridinium iodide,
(c) 1-methylpyridinium iodide.

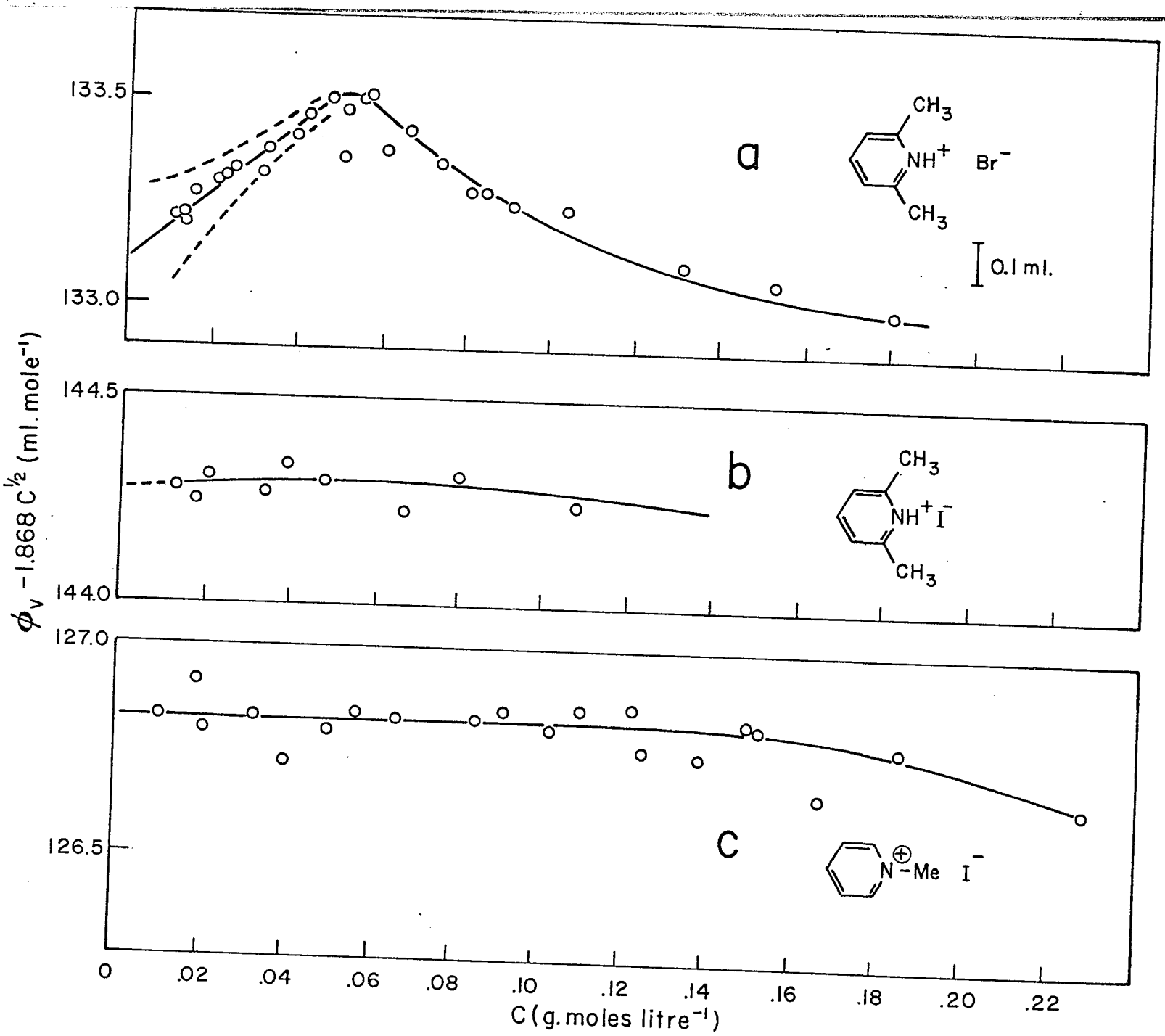
133.5
133.0
a
CH3
NH+
Br−
CH3
0.1 ml.
144.5
144.0
b
CH3
NH+I−
CH3
127.0
126.5
c
N⊕-Me I−
φv − 1.868 C½ (ml. mole−1)
0
.02
.04
.06
.08
.10
.12
.14
.16
.18
.20
.22
C (g. moles litre−1)

Figure 9. A plot of $\phi_v - 1.868\ c^{1/2}$ against concentration for 1,2,6-trimethylpyridinium iodide.

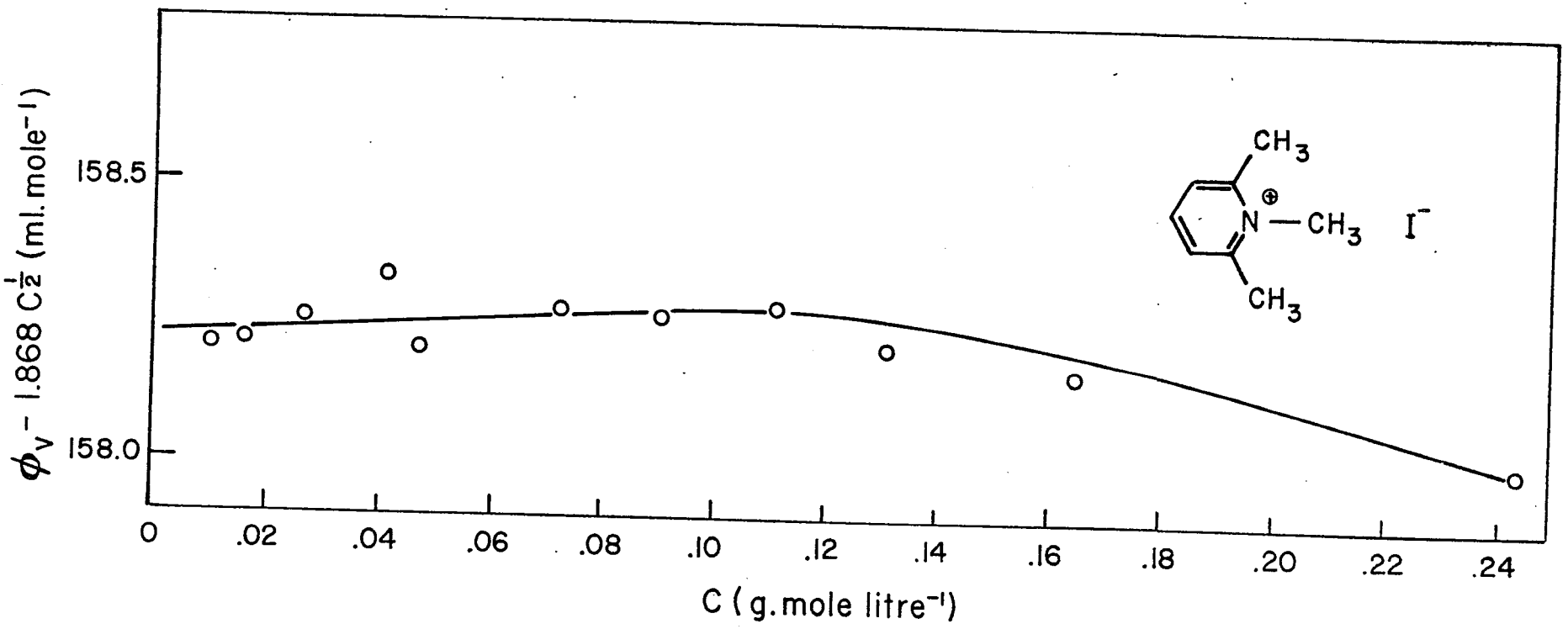
158.5
158.0
$\phi_v - 1.868\, C^{\frac{1}{2}}$ (ml. mole^{-1})
0
.02
.04
.06
.08
.10
.12
.14
.16
.18
.20
.22
.24
C (g. mole litre^{-1})
CH$_3$
N — CH$_3$
I$^-$
CH$_3$

TABLE 2

Values of $\bar{V}_2^o$ and $(\partial \phi_v / \partial c^{1/2})_{c \to o}$ for 2,6-Dimethylpyridinium Bromide as a Function of Temperature

T °C	$\bar{V}_2^o$ ml.(g.mole)$^{-1}$ ± 0.1 ml(g.mole)$^{-1}$	$(\partial \phi_v / \partial c^{1/2})_{c \to o}$ ml.l$^{1/2}$(g.mole)$^{-3/2}$
6.20	131.1_0	+ 2.3
18.20	131.9_3	+ 4.5
25.00	133.00	+ 4.0
29.26	132.7_6	+ 4.8
34.90	132.6_1	+ 7.8

TABLE 3

Values of $\bar{V}_2^o$ and Initial Slopes of ϕ_v vs. c Relations for Neutral Pyridine Bases (25°C)

Compound	$\bar{V}_2^o$ ml(g.mole)$^{-1}$ ± 0.05 ml(g.mole)$^{-1}$	$(\frac{d\phi_v}{dc})_{c \to o}$ ml.l(g.mole)$^{-2}$
Pyridine (in H_2O)	77.70	+ 10.5
Pyridine (in benzene)	80.13	- 1.7
2-Methylpyridine (in H_2O)	93.92	+ 6.0
2,6-Dimethylpyridine (in H_2O)	109.30	- 20.0

Figure 10. A plot of apparent molar volume ϕ_v against concentration for:

(a) pyridine,

(b) pyridine in benzene solution,

(c) 2-methylpyridine, and

(d) 2, 6-dimethylpyridine at 25°C.

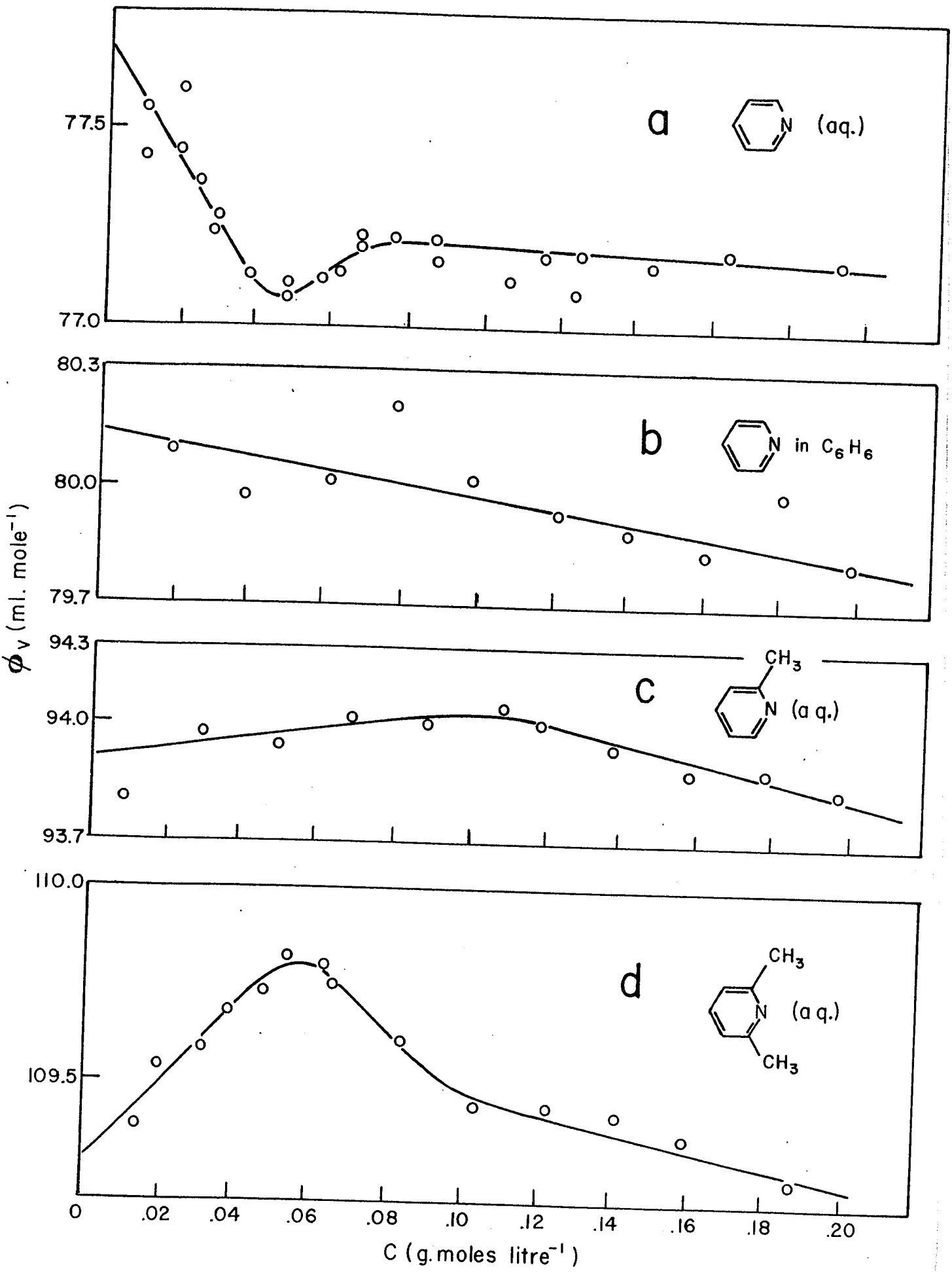
77.5
77.0
a
N (aq.)
80.3
80.0
79.7
b
N in C_6H_6
94.3
94.0
93.7
c
CH_3
N (aq.)
110.0
109.5
d
CH_3
N (aq.)
CH_3
ϕ_v (ml. mole^{-1})
0
.02
.04
.06
.08
.10
.12
.14
.16
.18
.20
C (g. moles litre^{-1})

more clearly. In Figs. 7c and 8a, the dotted lines indicate the uncertainty in ϕ_v associated with an uncertainty of $\pm 3 \times 10^{-6}$ g.ml^{-1} in the density of the solutions. The slopes, j, for any remaining linear concentration dependence of ϕ_v after the Debye-Hückel term in $c^{1/2}$ had been subtracted, varied, both with the coordination of the pyridinium ion and with the counter anion (Table 1) as was found previously for the $R_4N^+X^-$ salts (126, 152). For a number of the salts, however, limiting law behaviour was approached in the concentration range studied (Figs. 7a, 8b, 8c and 9).

(ii) Partial Molar Adiabatic Compressibility

The $\phi_{K(S)}$ data for the pyridinium salts were plotted according to eqn. IV.12 and the $\phi^{\circ}_{K(S)}$ values were obtained together with the slopes $S_{K(S)}$. These data are shown in Table 4 and some typical plots of $\phi_{K(S)}$ against $c^{1/2}$ are shown in Figs. 11 through 14. From Fig. 12 the differences in $\phi^{\circ}_{K(S)}$ between the halide ions for salts having a common cation may be obtained. These differences, together with those obtained by other workers, are listed in Table 6. An estimate of the theoretical limiting slope for 1:1 electrolytes in water has been given for isothermal compressibilities as $6.0 \pm .5$ ml.l$^{1/2}$ (g.mole)$^{-3/2}$bar^{-1}. From Table 1, it can be seen that 2-methylpyridinium chloride and 1-methylpyridinium iodide come closest to the limiting law behaviour in their volumes, i.e. $j \rightarrow 0$, and similarly their $S_{K(S)}$ values from Table 4 are both 6.6 ± 0.5 ml.l$^{1/2}$(g.mole)$^{-3/2}$ bar^{-1}. This indicates that the limiting slopes for the isothermal and adiabatic compressibilities are quite similar in magnitude.

The $\emptyset_{K(S)}$ data for three neutral pyridine bases were plotted as a function of concentration and the $\emptyset^{\circ}_{K(S)}$ values were obtained together with the limiting slopes ($d\emptyset_{K(S)}/dc$). These data are shown in Table 5 and are plotted in Fig. 15.

TABLE 4

Values of $10^4 \phi^o_{K(S)}$ and $S_{K(S)}$ in Equation IV.14

(25°C)

Salt	$10^4 \phi_{K(S)}$ $ml(g.mole.bar)^{-1}$	$S_{K(S)}$ $ml.l^{1/2}(g.mole)^{-3/2}bar^{-1}$
Pyridinium chloride	- 18.6	+ 4.6
2-Methylpyridinium chloride	- 16.4	+ 6.6
2, 6-Dimethylpyridinium chloride	- 15.0	+ 2.6
2, 6-Dimethylpyridinium bromide	- 6.6	+ 2.2
2, 6-Dimethylpyridinium iodide	+ 1.7	+ 7.5
1-Methylpyridinium iodide	+ 1.5	+ 6.6
1, 2-Dimethylpyridinium iodide	+ 0.1	+ 10.8
1, 2, 6-Trimethylpyridinium iodide	- 0.4	+ 12.1
1-Ethylpyridinium iodide	+ 2.0	+ 9.8

Figure 11. A plot of apparent molar adiabatic compressibility $\phi_{K(S)}$ as a function of $c^{1/2}$ for pyridinium chloride and 2-methylpyridinium chloride at 25°C.

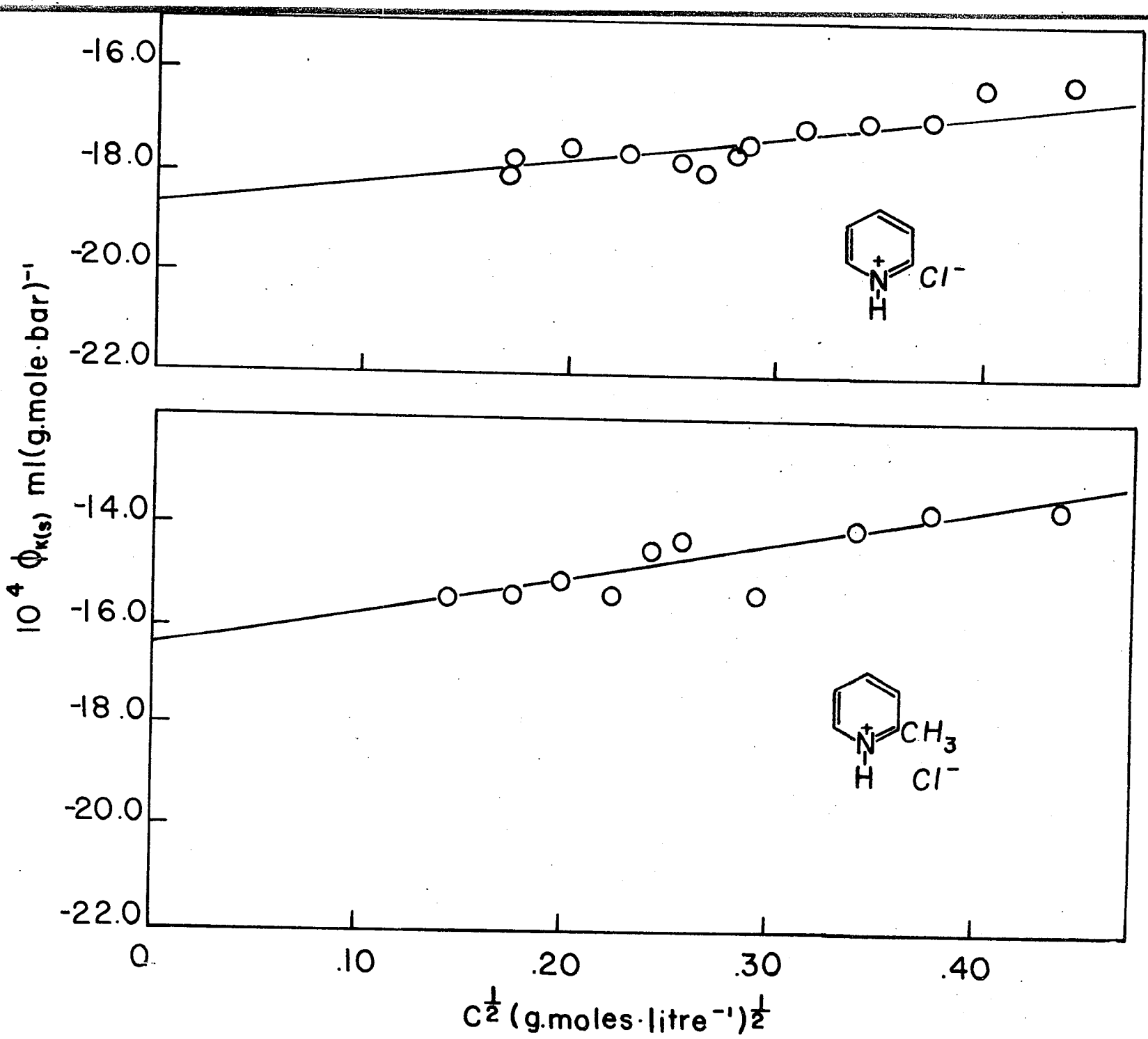
-16.0
-18.0
-20.0
-22.0
-14.0
-16.0
-18.0
-20.0
-22.0
0
.10
.20
.30
.40
$10^4 \phi_{K(s)}$ ml(g.mole·bar)$^{-1}$
$C^{\frac{1}{2}}$ (g.moles·litre^{-1})$^{\frac{1}{2}}$
Cl⁻
CH₃
Cl⁻

Figure 12. A plot of apparent molar adiabatic compressibility $\phi_{K(S)}$ as a function of $c^{1/2}$ for:

(a) 2, 6-dimethylpyridinium iodide;

(b) bromide;

(c) chloride, at 25°C.

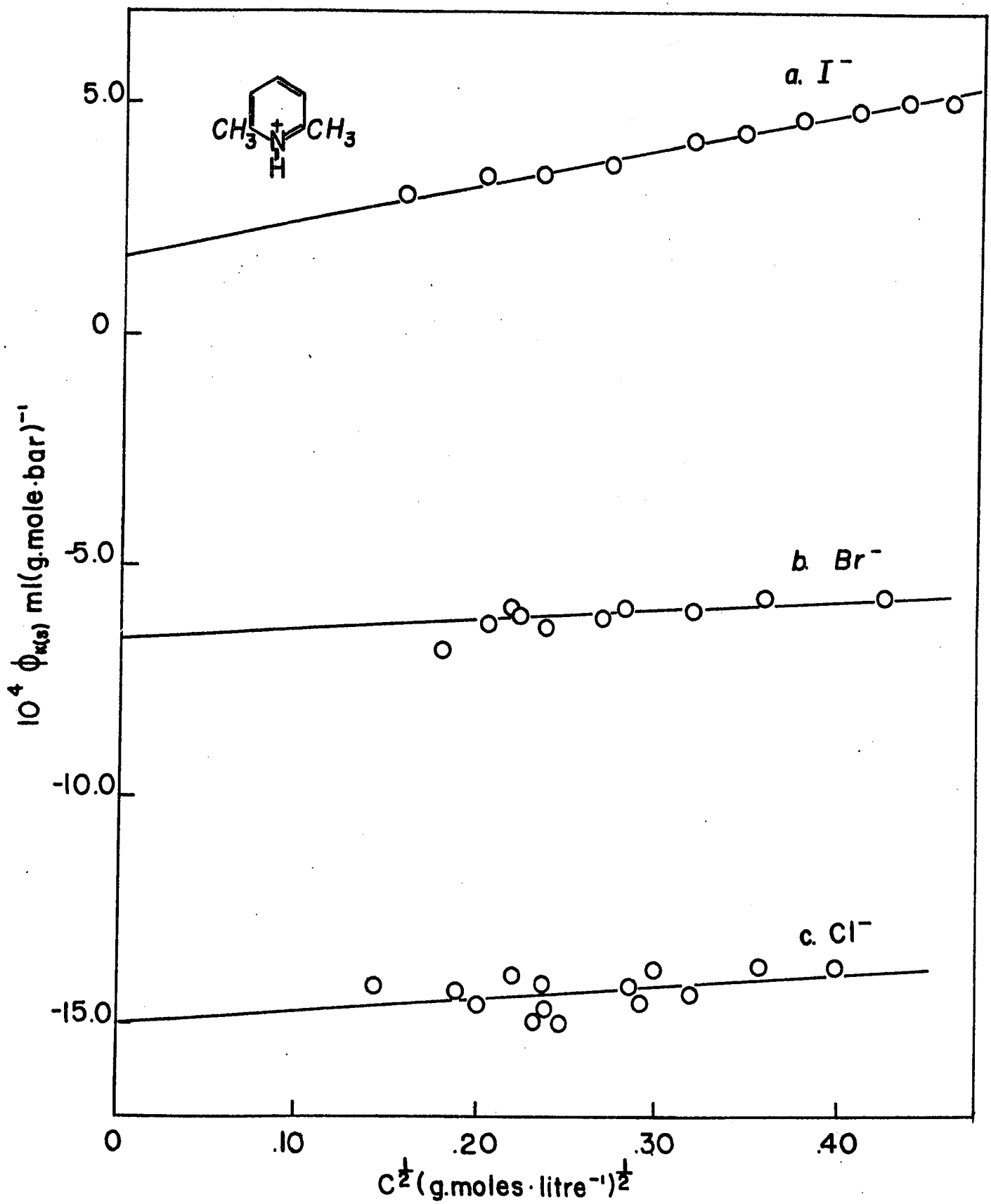
a. I^-
b. Br^-
c. Cl^-
5.0
0
-5.0
-10.0
-15.0
0
.10
.20
.30
.40
$10^4\ \phi_{v(s)}$ ml(g.mole·bar)$^{-1}$
$C^{\frac{1}{2}}$ (g.moles·litre^{-1})$^{\frac{1}{2}}$
CH_3
CH_3
N
H

Figure 13. A plot of apparent molar adiabatic compressibility $\phi_{K(S)}$ as a function of $c^{1/2}$ for 1-methylpyridinium iodide and 1, 2-dimethylpyridinium iodide at 25°C

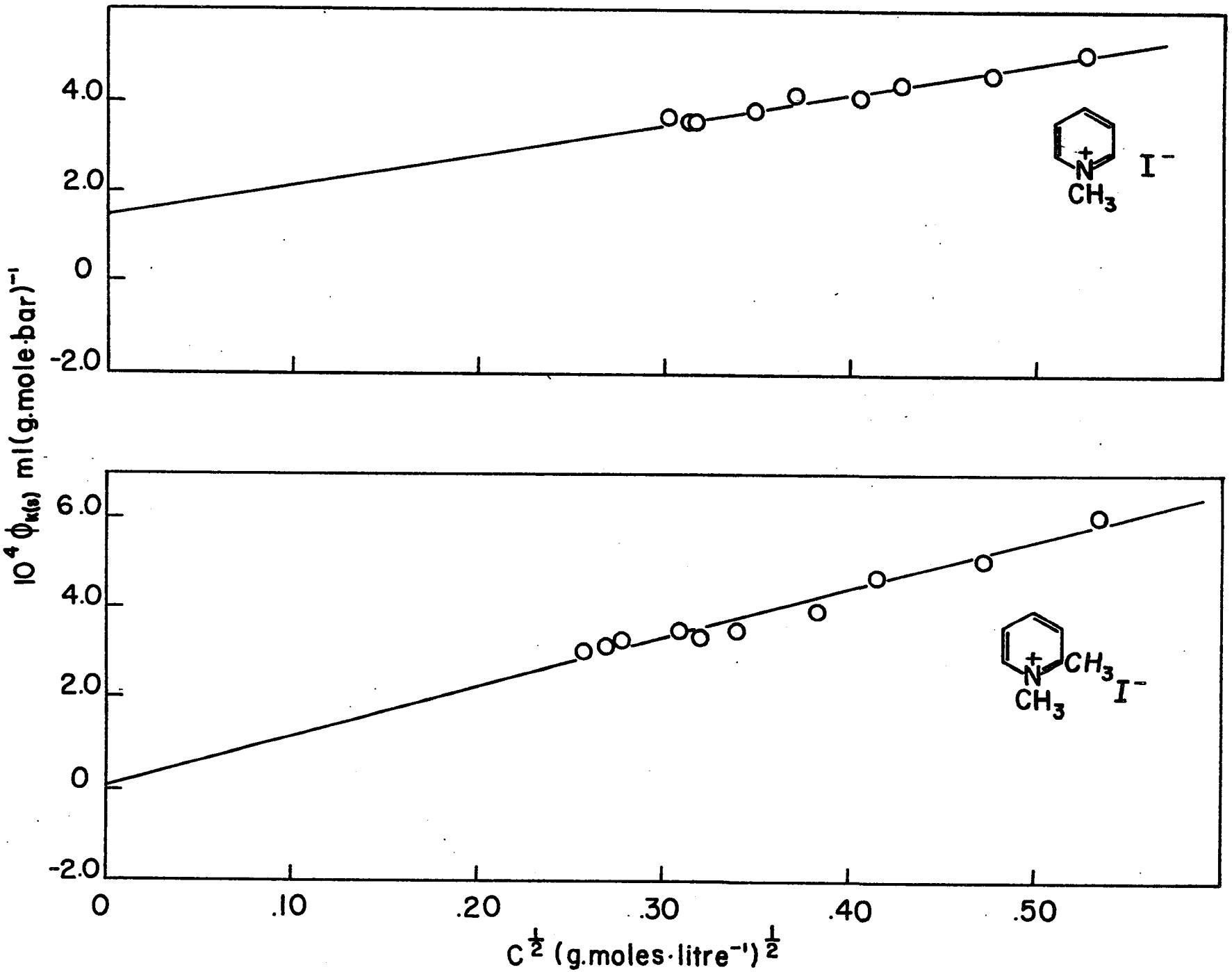
4.0
2.0
0
-2.0
I⁻
CH3
6.0
4.0
2.0
0
-2.0
CH3
CH3
I⁻
0
.10
.20
.30
.40
.50
10⁴ φk(s) ml(g.mole·bar)⁻¹
C½ (g.moles·litre⁻¹)½

Figure 14. A plot of apparent molar adiabatic compressibility $\phi_{K(S)}$ as a function of $c^{1/2}$ for 1, 2, 6-trimethylpyridinium iodide and 1-ethylpyridinium iodide at 25°C.

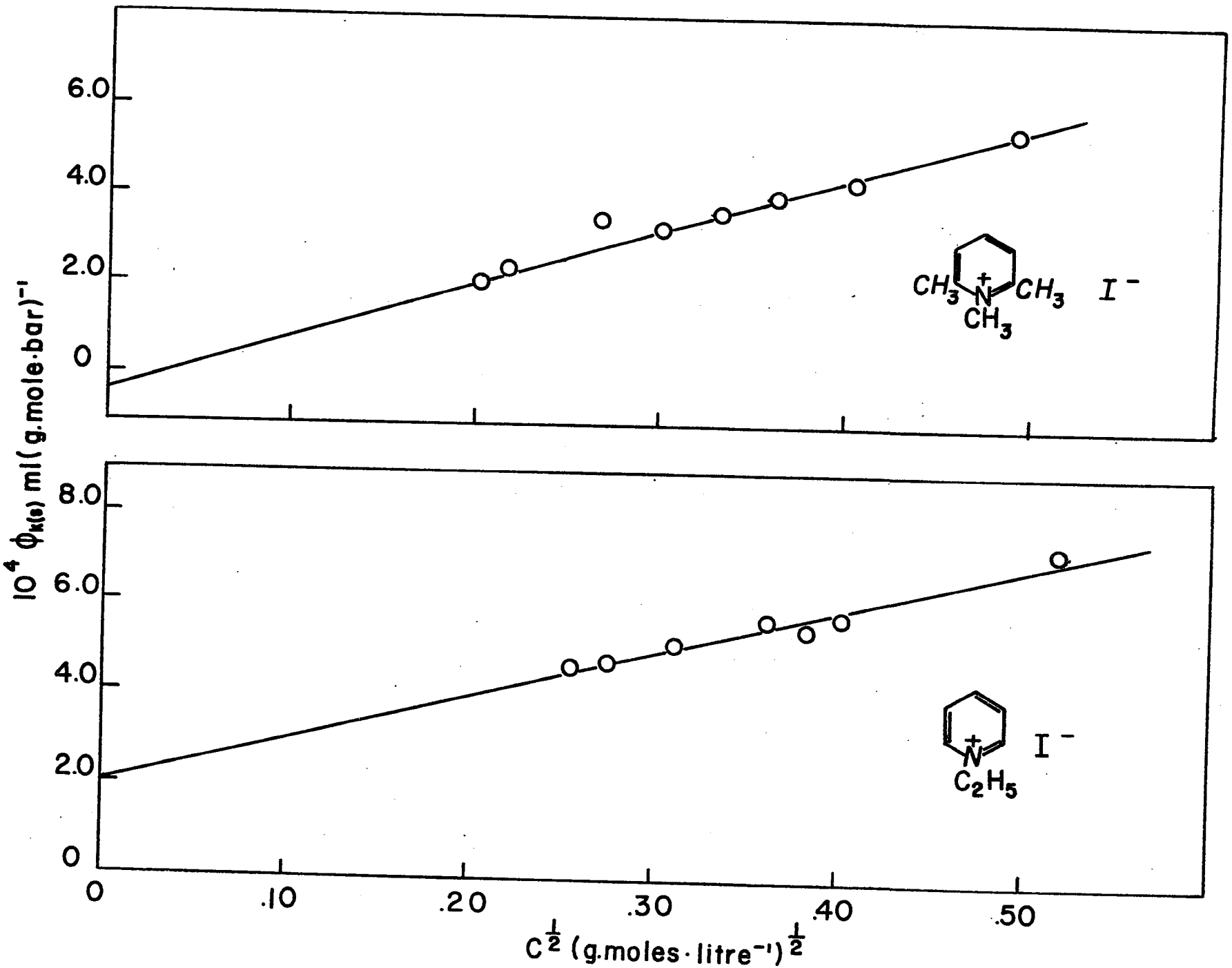
6.0
4.0
2.0
0
CH_3
CH_3
CH_3
I^-
8.0
6.0
4.0
2.0
0
C_2H_5
I^-
$10^4\ \phi_{k(s)}$ ml(g.mole.bar)$^{-1}$
0
.10
.20
.30
.40
.50
$C^{\frac{1}{2}}$ (g.moles·litre^{-1})$^{\frac{1}{2}}$

TABLE 5

Values of $10^4 \phi^o_{K(S)}$ and $(d \phi_{K(S)}/d c)_{c \to 0}$ at 25°C

Compound	$10^4 \phi^o_{K(S)}$ ml.(g.mole.bar)$^{-1}$	$(d\phi_{K(S)}/d c)_{c \to 0}$ ml.l(g.mole^{-2}bar^{-1})
Pyridine	+ 2.2	+ 10.5
2-Methylpyridine	+ 5.3	+ 5.0
2, 6-Dimethylpyridine	+ 7.3	- 20.0

TABLE 6

Values of the Differences in $\phi^{o}_{K(S)}$ between the Halide Ions for Salts having a Common Cation

$10^{-4}\Delta\phi^{o}_{K(S)}$	(a)	(b) $ml(g.mole.bar)^{-1}$	(c)
$Cl^- - Br^-$	8.4	9.5 ± .3	8.6
$Br^- - I^-$	8.3	10.3 ± .8	
$I^- - Cl^-$	16.7	19.8	

(a) Present work

(b) R. E. Verrall (152)

(c) Based on difference between isothermal compressibility of NaCl, KCl, NaBr, and KBr (143).

Figure 15. A plot of apparent molar compressibility $\phi_{K(S)}$ as a function of concentration for pyridine, 2-methylpyridine and 2, 6-dimethylpyridine at 25°C.

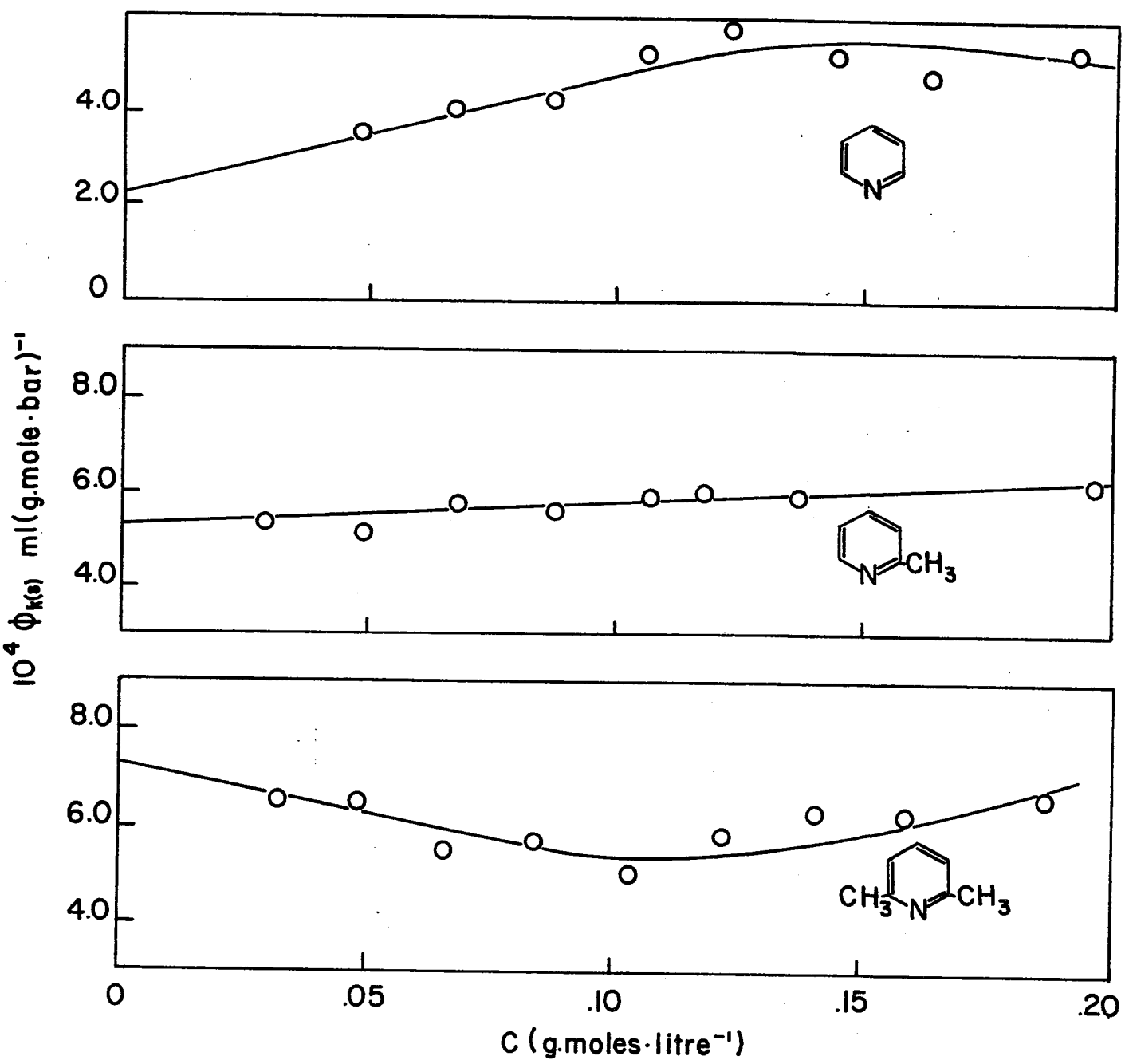
4.0
2.0
0
8.0
6.0
4.0
8.0
6.0
4.0
0
.05
.10
.15
.20
$10^4 \phi_{k(s)}$ ml(g.mole·bar)$^{-1}$
C (g.moles·litre^{-1})
N
N
CH_3
CH_3
N
CH_3

4. Piperidines and Piperidinium Salts

(i) Partial Molar Volumes

Since the piperidines were strong bases, their salts did not hydrolyse (K_a ca. 7×10^{-12}) and no corrections to the volumes and compressibilities were required, as was the case with the pyridinium salts. The neutral bases, on the other hand, would react with water to form significantly the protonated species ($K_B = 1.32 \times 10^{-1}$ for piperidine). If the measurements are done in alkaline solution, it can be shown that the degree of hydrolysis α is given approximately by the following expression:

$$\alpha = \frac{K_B}{C_{OH^-}} \qquad \text{IV.14}$$

where C_{OH^-} is the concentration of KOH in the solvent. For piperidine in 0.1 N KOH, $\alpha = 0.0132$ and since no K_B value was available for 1-methylpiperidine the same α value was assumed to hold. The above considerations led to corrections of 0.1 ml and 0.15 ml in the apparent molar volumes of piperidine and 1-methylpiperidine, respectively.

The ϕ_v data for the piperidinium salts were plotted according to eqn. IV.10 and the $\bar{V}_2^o$ values were obtained with the j coefficients. These data are given in Table 7 and some typical plots are shown in Fig. 16. The slope of the plots of the apparent molar volume vs. $c^{1/2}$ for all three salts approaches the limiting law value in the concentration range studied.

TABLE 7

Values of $\bar{V}_2^o$ and j in Equation IV.10 (25°C)

Salt	$\bar{V}_2^o$ ml (g.mole)$^{-1}$ ± 0.05 ml(g.mole)$^{-1}$	j ml.l.g.mole^{-2}
1,1-Dimethylpiperidium iodide	158.68	0.0 up to c = .040
1-Methylpiperidinium chloride	125.51	0.0 up to c = 0.55
Piperidinium chloride	106.67	0.0 up to c = .075

Compound	$\bar{V}_2^o$ ml.g.mole^{-1}	$(d\phi_v/dc)_{c \to 0}$ ml.l.g.mole^{-2}
Piperidine in 0.1 N KOH	91.10	0.0
1-Methylpiperidine in 0.1 N KOH	109.91	0.0

The ϕ_v data for the neutral piperidine bases are also shown in Table 7 together with their limiting slopes obtained from the ϕ_v against c plots shown in Fig. 17.

(ii) Apparent Molar Adiabatic Compressibility

The $\phi_{K(S)}$ data for the piperidinium salts were plotted in the usual way (Fig. 18) and the $\phi^o_{K(S)}$ and $S_{K(S)}$ values obtained are shown in Table 8. The plot is linear for piperidinium chloride but for 1-methylpiperidinium chloride the linear section extends only to c = 0.10 molar. The $\phi_{K(S)}$ data for the two neutral piperidines in 0.1 N KOH were plotted as a function of concentration (Fig. 19) and the $\phi^o_{K(S)}$, together with the limiting slopes $(d\phi_{K(S)}/dc)$, are shown in Table 8.

Figure 16. A plot of $\phi_v - 1.868\ c^{1/2}$ as a function of concentration for 1,1-dimethylpiperidinium iodide, 1-methylpiperidinium chloride and piperidinium chloride at 25°C

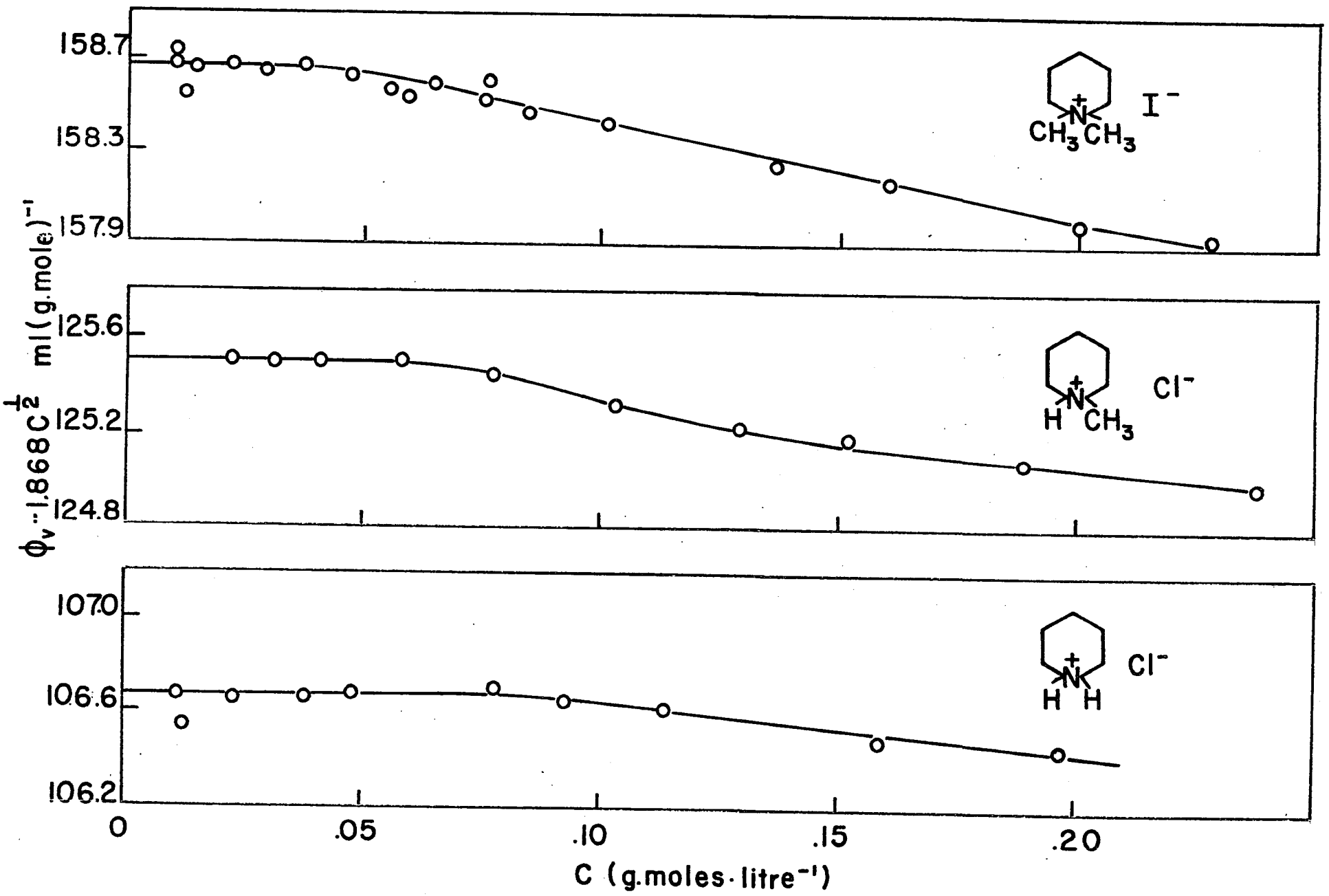
158.7
158.3
157.9
125.6
125.2
124.8
107.0
106.6
106.2
$\phi_v - 1.868C^{\frac{1}{2}}$ ml(g.mole)$^{-1}$
0
.05
.10
.15
.20
C (g.moles·litre^{-1})
CH_3 CH_3
I^-
H CH_3
Cl^-
H H
Cl^-

Figure 17. A plot of apparent molar volume ϕ_V as a function of concentration for piperidine and 1-methylpiperidine in 0.1 N KOH at 25°C

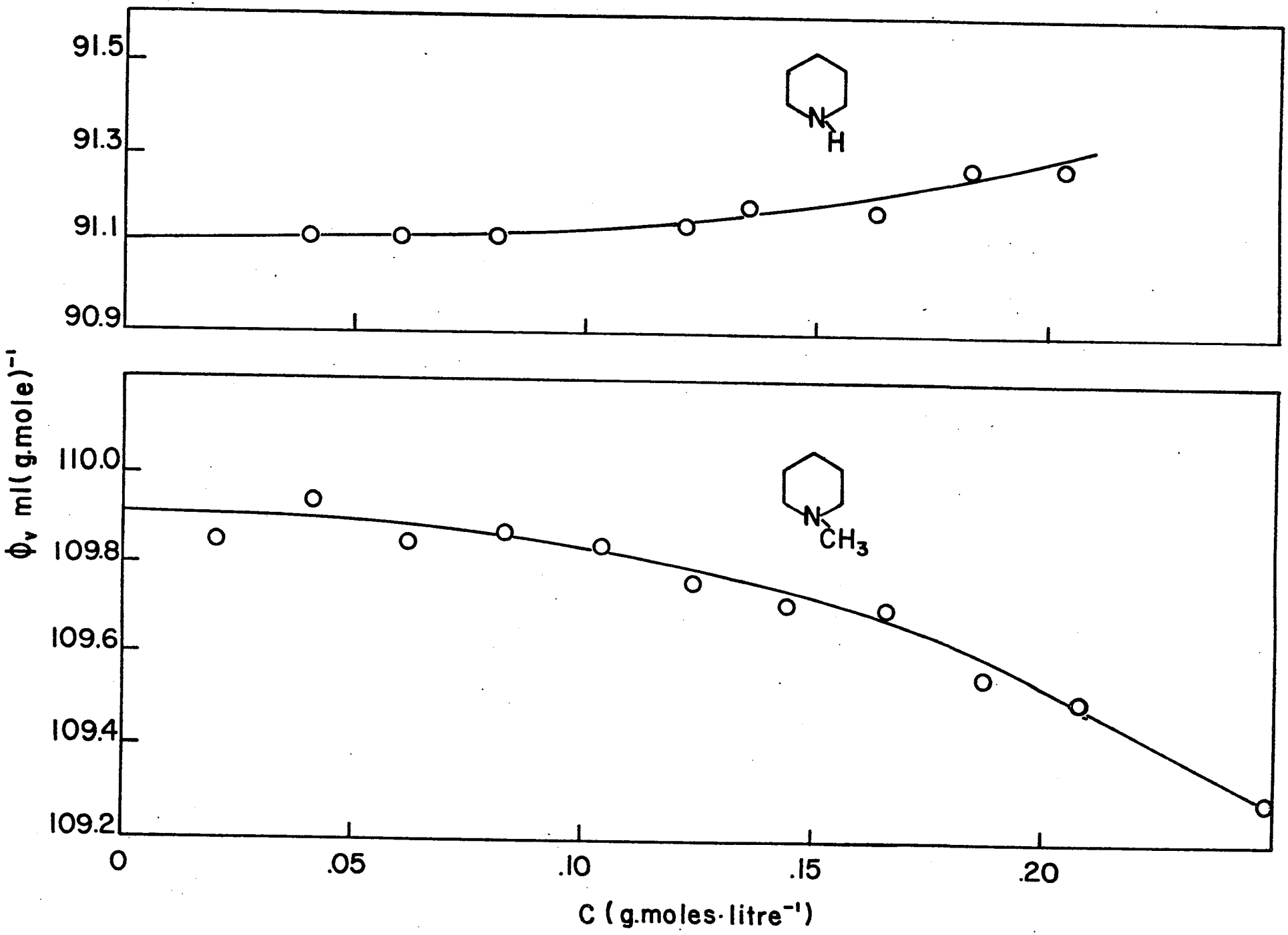
91.5
91.3
91.1
90.9
110.0
109.8
109.6
109.4
109.2
ϕ_v ml(g.mole)$^{-1}$
0
.05
.10
.15
.20
C (g.moles·litre^{-1})
N
H
N
CH$_3$

Figure 18. A plot of apparent molar adiabatic compressibility $\phi_{K(S)}$ as a function of $c^{1/2}$ for piperidinium chloride and 1-methyl-piperidinium chloride at 25°C

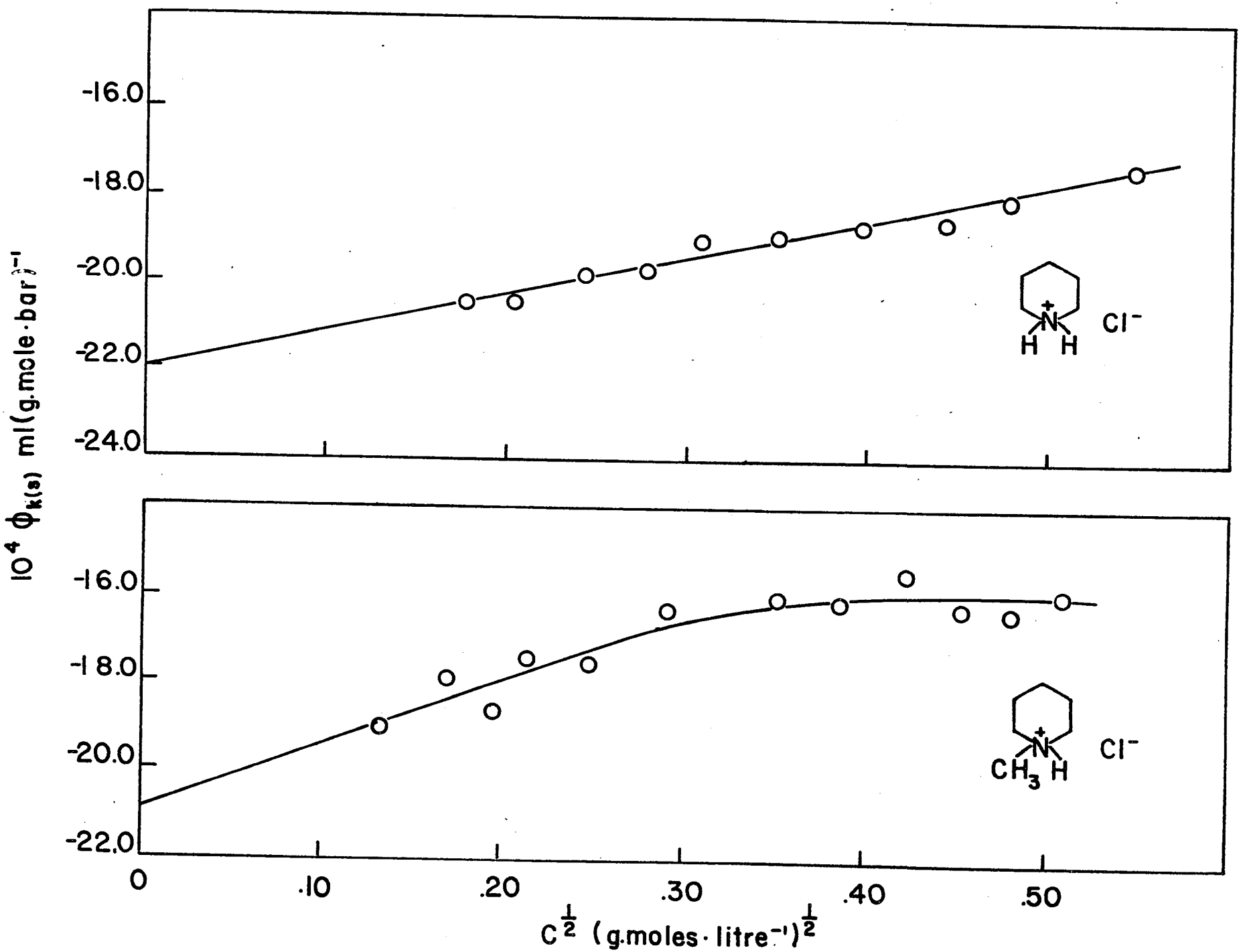
-16.0
-18.0
-20.0
-22.0
-24.0
$10^4 \phi_{k(s)}$ ml(g.mole·bar)$^{-1}$
Cl⁻
-16.0
-18.0
-20.0
-22.0
0
.10
.20
.30
.40
.50
$C^{\frac{1}{2}}$ (g.moles·litre^{-1})$^{\frac{1}{2}}$
Cl⁻

Figure 19. A plot of apparent molar adiabatic compressibility $\phi_{K(S)}$ as a function of concentration for piperidine and 1-methyl-piperidine in 0.1 N KOH at 25°C

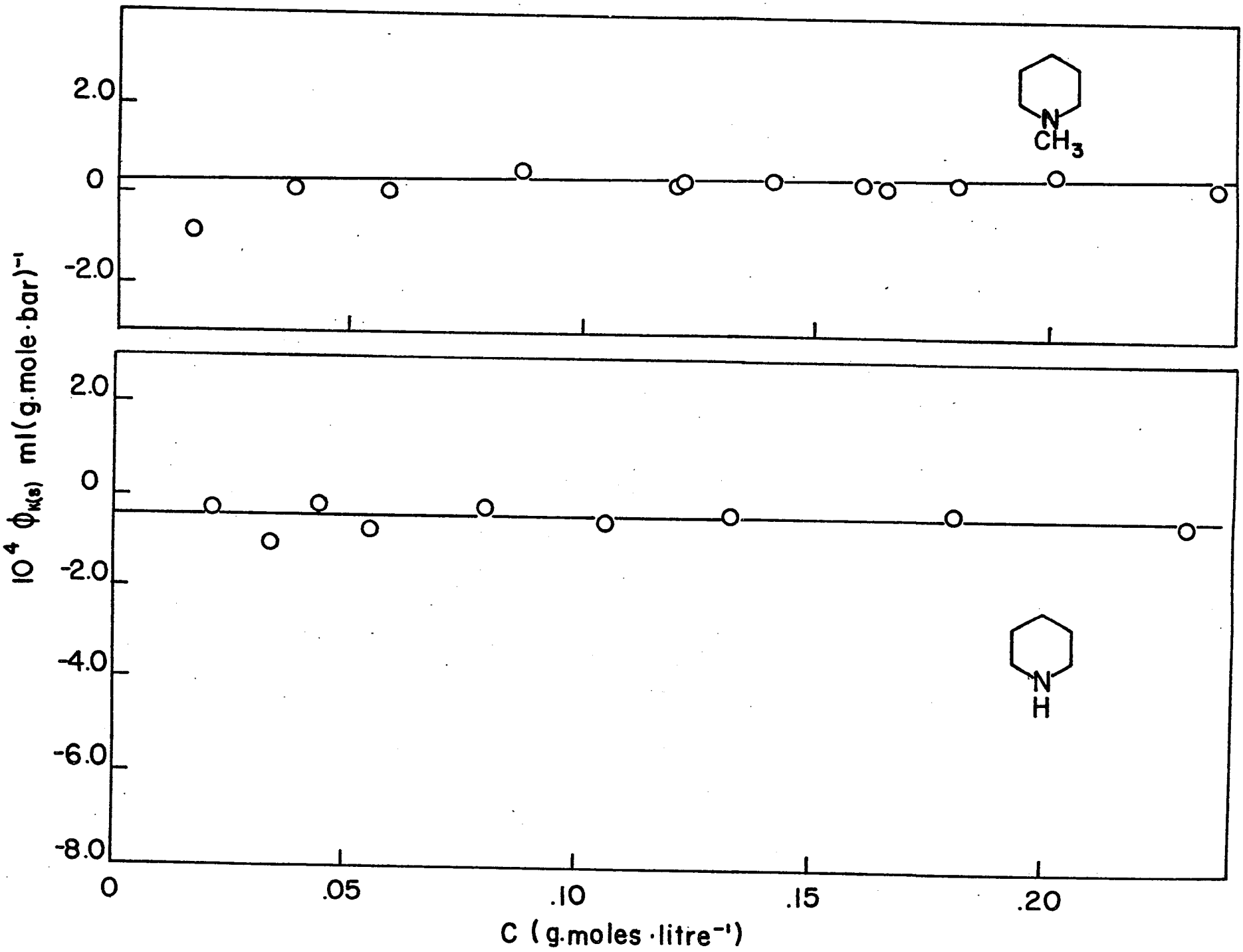
2.0
0
-2.0
2.0
0
-2.0
-4.0
-6.0
-8.0
$10^4\ \phi_{K(s)}$ ml(g.mole·bar)$^{-1}$
0
.05
.10
.15
.20
C (g.moles·litre^{-1})
N
CH$_3$
N
H

TABLE 8

Values of $10^4 \phi^o_{K(S)}$ and $S_{K(S)}$ in Equation IV.14 (25°C)

Salt	$10^4 \phi^o_{K(S)} \pm 0.25$ $ml(g.mole.bar)^{-1}$	$S_{K(S)}$ $ml.l^{1/2}(g.mole)^{3/2}bar^{-1}$
Piperidinium chloride	- 22.0	+ 8.6
1-Methylpiperidinium chloride	- 20.9	+ 15.0

Values of $10^4 \phi^o_{K(S)}$ and $(d\phi_{K(S)}/dc)_{c \to o}$ (25°C)

Compound	$10^4 \phi^o_{K(S)} \pm 0.25$ $ml\,(g.mole.bar)^{-1}$	$(d\phi_{K(S)}/dc)_{c \to o}$ $ml.l\,(g.mole^{-2}.bar^{-1})$
Piperidine in 0.1N KOH	- 0.40	0.0
1-Methylpiperidine in 0.1N KOH	+ 0.30	+ 0.7

5. Alkylammonium Salts

(i) Partial Molar Volumes

The partial molar volumes of selected n-alkylammonium halide salts were examined, partly as an extension of the compressibility studies carried out on these salts and also to complement the volume data already gathered in this laboratory (126) and by others (132). The apparent molar volumes of the salts in the series R_2NH_2Cl, where R = C_2H_5- , C_3H_7- and C_4H_9- , were determined and are shown in Fig. 20. As may be seen from Fig. 20, the deviations from the limiting law slope of 1.868 ml. $l^{1/2}(g.mole)^{-3/2}$ increase with increasing size of the R group. In Fig. 21 the plot of ϕ_v against $c^{1/2}$ for $(HOC_2H_4)_3NH^+Br^-$ shows that the introduction of a polar-OH group into the alkyl section of the molecule causes it to behave like a "normal" 1:1 electrolyte as opposed to the behaviour of $(C_2H_5)_3NHBr$ (Fig. 22) which exhibits a large negative deviation from the Debye-Hückel limiting law. The $\bar{V}_2^o$ and j data for the compounds shown in Figs. 20 - 22 are listed in Table 9. $\bar{V}_2^o$ and j data for Me_4NBF_4 are also included in Table 9.

(ii) Partial Molar Adiabatic Compressibility

The $\phi_{K(S)}$ data for the alkylammonium salts were plotted according to eqn. IV.12 and the $\phi^o_{K(S)}$ values, together with the slopes $S_{K(S)}$, were obtained. These data are shown in Table 10 and are plotted in Figs. 23 and 24. Also included in Table 10 are the $\phi^o_{(KS)}$ data for Me_4NBF_4.

TABLE 9

Values of $\bar{V}_2^o$ and $S_v = (d\phi_v / dc^{1/2})$ for a Series of Alkylammonium Salts.
S_v was taken at c = 0.001 molar

Salt	$\bar{V}_2^o$ ml (g.mole)$^{-1}$ ± 0.05 ml(g.mole)$^{-1}$	S_v ml.l$^{1/2}$.mole$^{-3/2}$ ± 8%
NH_4Cl	36.27	+ 0.6
$(C_2H_5)_2NH_2Cl$	106.73	+ 1.0
$(n\text{-}C_3H_7)_2NH_2Cl$	138.66	+ 0.6
$(n\text{-}C_4H_9)_2NH_2Cl$	170.68	+ 0.3
$(C_2H_5)_3NHBr$	146.17	- 2.2
$(HOC_2H_4)_3NHBr$	147.28	+ 2.1
$(n\text{-}C_3H_7)_3NHBr$ *	193.65	-
$(CH_3)_4NBF_4$	132.60	+ 0.8

* From the data of R.E. Verrall (152) for the Cl^- and I^- salts.

Figure 20. A plot of apparent molar volume ϕ_v against $c^{1/2}$ for $(C_2H_5)_2NH_2Cl$, $(C_3H_7)_2NH_2Cl$, and $(C_4H_9)_2NH_2Cl$ at 25°C.

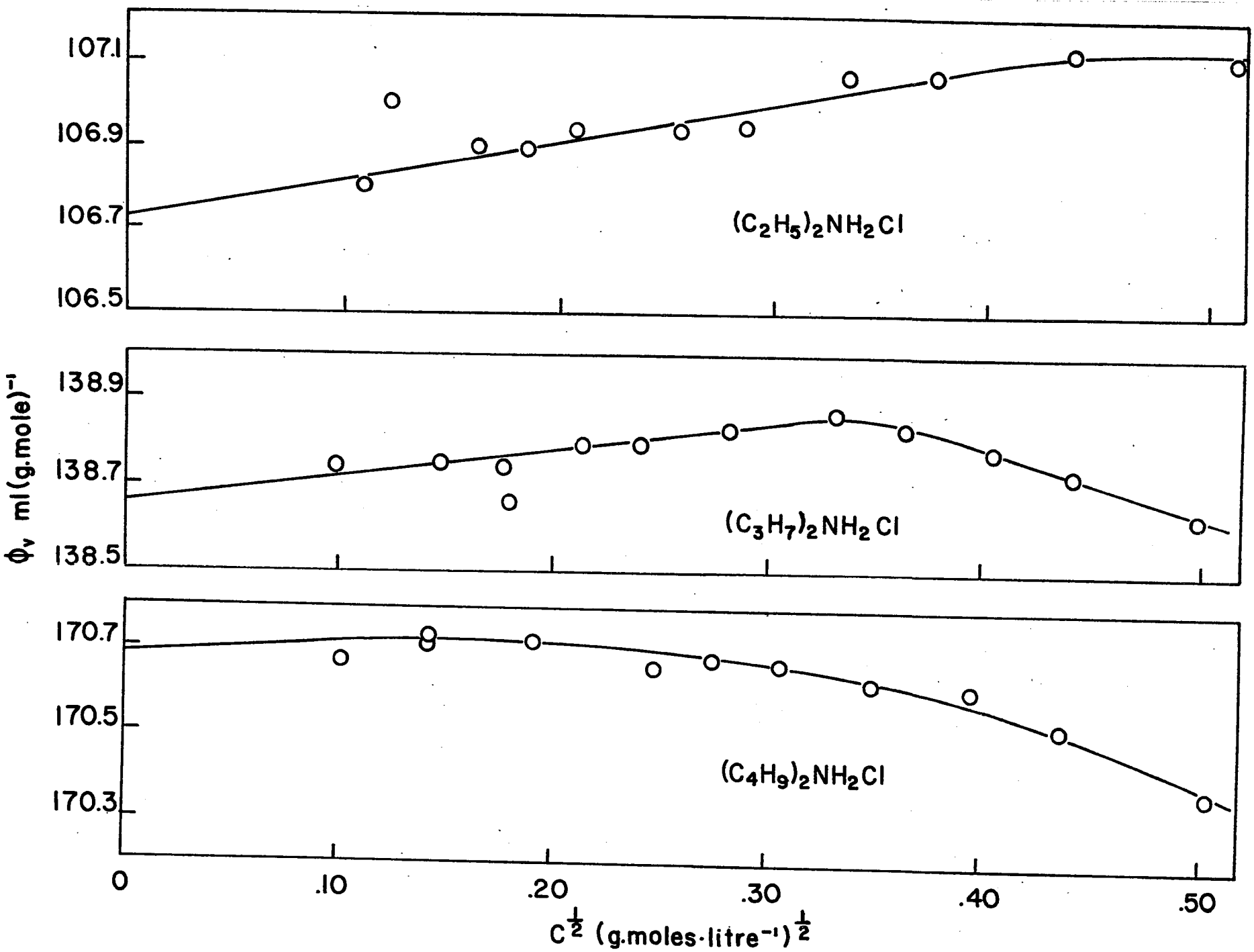
107.1
106.9
106.7
106.5
$(C_2H_5)_2NH_2Cl$
138.9
138.7
138.5
$(C_3H_7)_2NH_2Cl$
170.7
170.5
170.3
$(C_4H_9)_2NH_2Cl$
ϕ_v ml(g.mole)$^{-1}$
0
.10
.20
.30
.40
.50
$C^{\frac{1}{2}}$ (g.moles·litre^{-1})$^{\frac{1}{2}}$

Figure 21. A plot of apparent molar volume ϕ_v against $c^{1/2}$ for triethanolammonium bromide at 25°C.

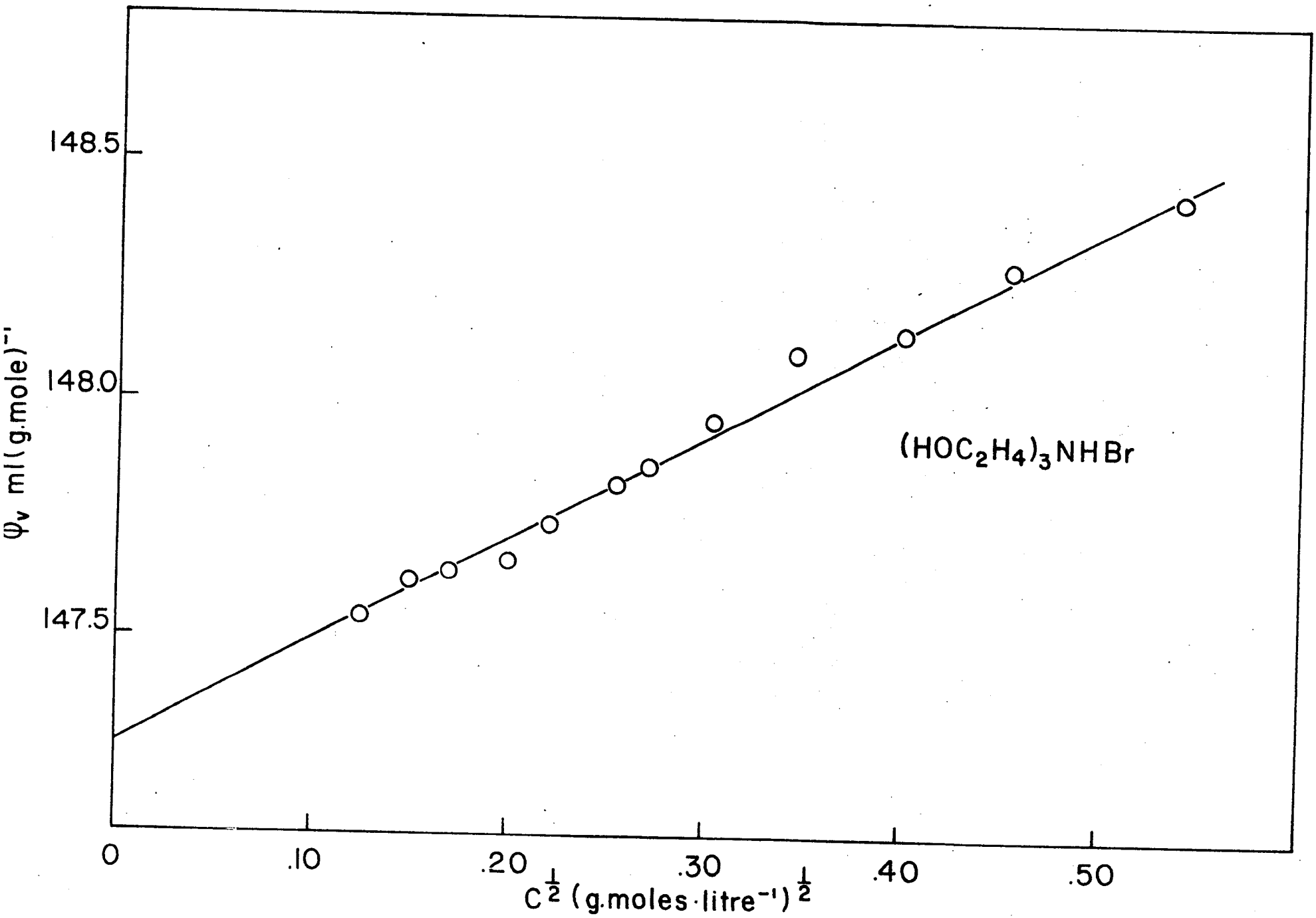
148.5
148.0
147.5
Ψ_v ml(g.mole)$^{-1}$
0
.10
.20
.30
.40
.50
$C^{\frac{1}{2}}$ (g.moles·litre^{-1})$^{\frac{1}{2}}$
$(HOC_2H_4)_3NHBr$

Figure 22. A plot of apparent molar volume ϕ_v against $c^{1/2}$ for triethylammonium bromide at 25°C.

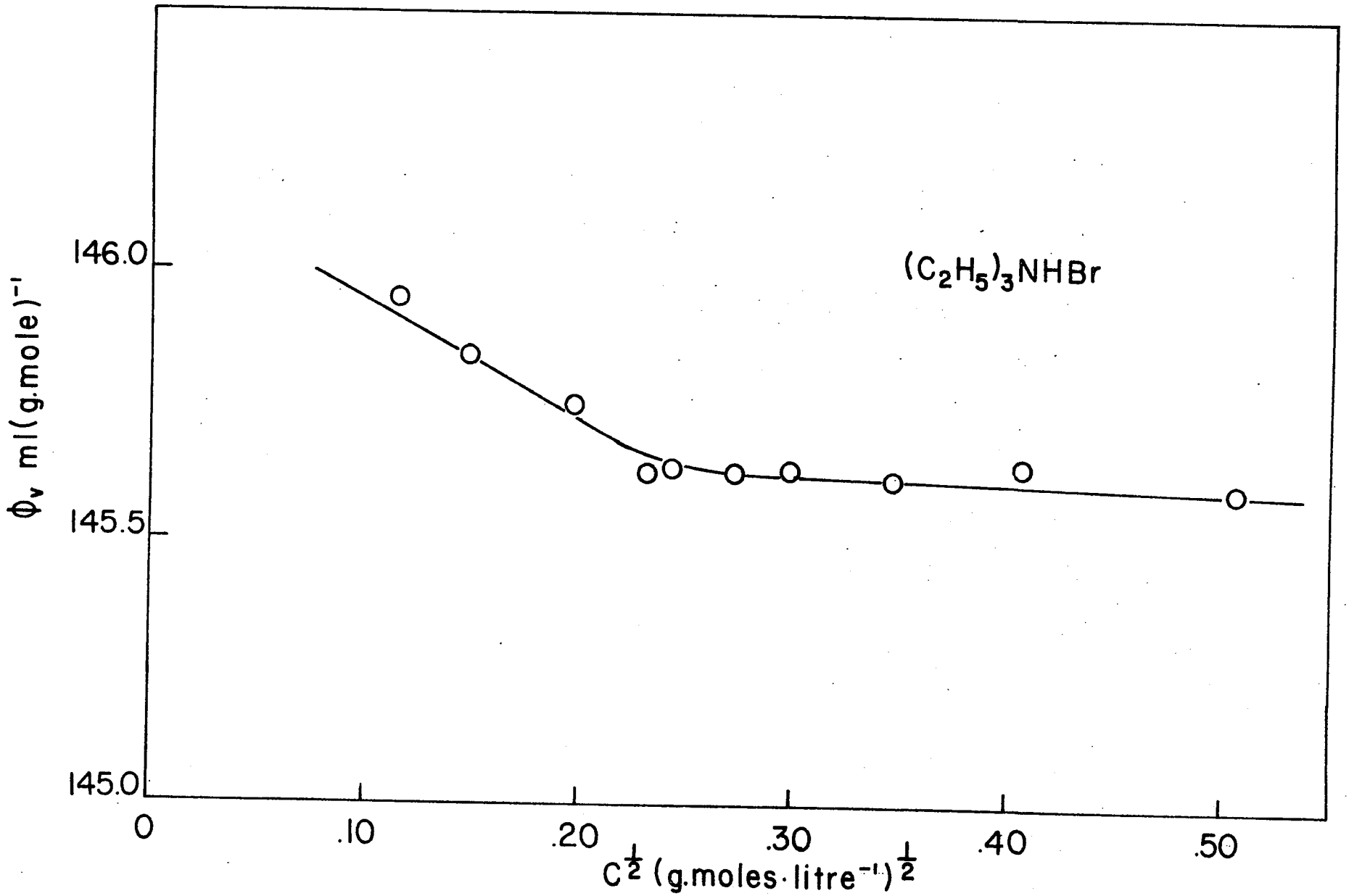
146.0
145.5
145.0
ϕ_v ml(g.mole)$^{-1}$
$(C_2H_5)_3NHBr$
0
.10
.20
.30
.40
.50
$C^{\frac{1}{2}}$ (g.moles·litre^{-1})$^{\frac{1}{2}}$

TABLE 10

Values of $10^4 \phi^{\circ}_{K(S)}$ and $S_{K(S)}$ in eqn. IV.14 for Some Alkylammonium Halides at 25°C

Salt	$10^4 \phi^{\circ}_{K(S)}$ ml(g.mole.bar^{-1}) ± 0.2 ml(g.mole.bar^{-1})	$10^4 S_{K(S)}$ ml.l$^{1/2}$(g.mole)$^{3/2}$bar^{-1}
$(C_2H_5)_2NH_2Cl$	- 25.1	+ 4.0
$(n\text{-}C_3H_7)_2NH_2Cl$	- 17.9	+ 3.8
$(n\text{-}C_4H_9)_2NH_2Cl$	- 25.0	+ 11.0
NH_4Cl	- 25.6	+ 18.0
$(C_2H_5)_3NHBr$	- 5.6	+ 7.4
$(HOC_2H_4)_3NHBr$	- 8.6	+ 9.0
$(CH_3)_4NBF_4$	+ 18.0	+ 7.0
$(CH_3)_4NI$ *	+ 3.3	+ 17.2

* From the data of R.E. Verrall (152)

Figure 23. A plot of apparent molar adiabatic compressibility $\phi_{K(S)}$ against $c^{1/2}$ for $(C_2H_5)_2NH_2Cl$, $(n\text{-}C_3H_7)_2NH_2Cl$, and $(n\text{-}C_4H_9)_2NH_2Cl$ at 25°C.

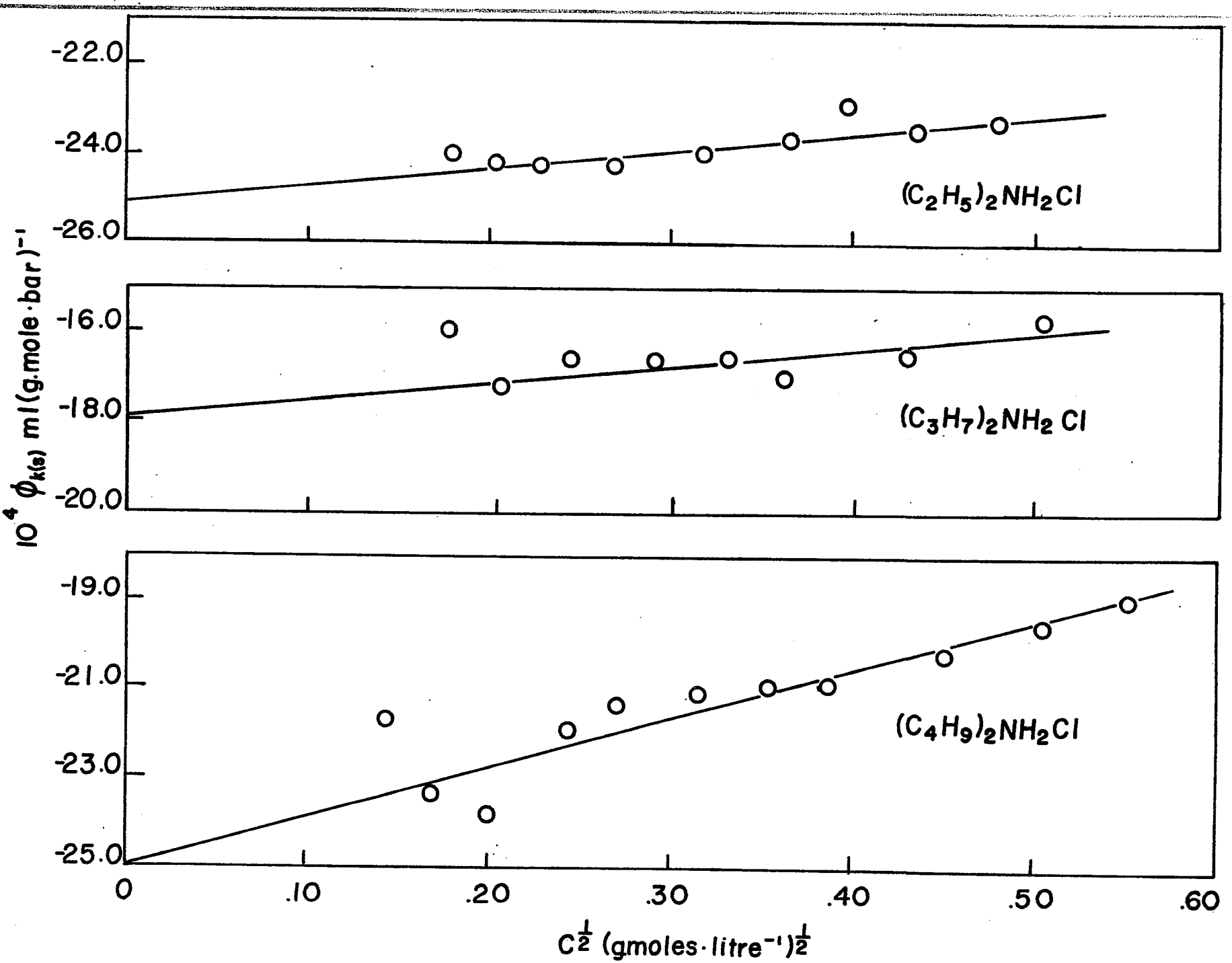
-22.0
-24.0
-26.0
$(C_2H_5)_2NH_2Cl$
-16.0
-18.0
-20.0
$(C_3H_7)_2NH_2Cl$
-19.0
-21.0
-23.0
-25.0
$(C_4H_9)_2NH_2Cl$
$10^4 \phi_{k(s)}$ ml(g.mole·bar)$^{-1}$
0
.10
.20
.30
.40
.50
.60
$C^{\frac{1}{2}}$ (gmoles·litre^{-1})$^{\frac{1}{2}}$

Figure 24. A plot of apparent molar adiabatic compressibility $\phi_{K(S)}$ against $c^{1/2}$ for $(C_2H_5)_3NHBr$ and $(HOC_2H_5)_3NHBr$ at 25°C

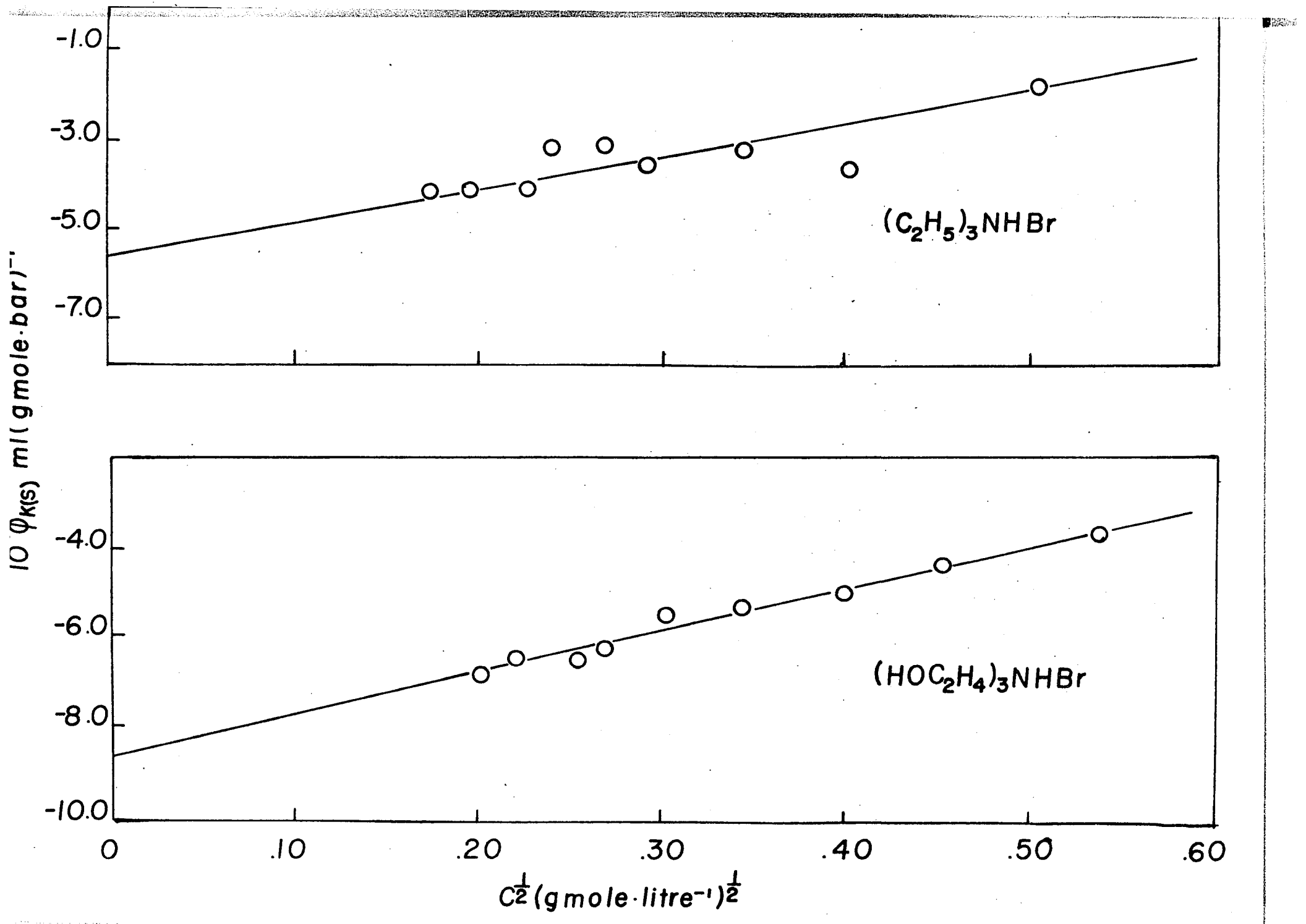
-1.0
-3.0
-5.0
-7.0
$(C_2H_5)_3NHBr$
-4.0
-6.0
-8.0
-10.0
$(HOC_2H_4)_3NHBr$
0
.10
.20
.30
.40
.50
.60
$10\ \phi_{K(S)}\ ml\ (g\,mole \cdot bar)^{-1}$
$C^{\frac{1}{2}}\ (g\,mole \cdot litre^{-1})^{\frac{1}{2}}$

6. Partial Molar Volume of the Tetraalkylammonium Salts

The partial molar volumes of the tetraalkylammonium salts have been studied extensively, both in this laboratory (126) and elsewhere (116, 121-128). Our measurements were primarily confined to the high dilution region, i.e. $0.002 \leq c \leq 0.01$ molar; however, because of the type of dilatometer used, it was also necessary to have accurate ϕ_v data in the region $0.10 \leq c \leq 0.5$ molar. Therefore the existing data in this high concentration region was extended and augmented where needed.

The first member in the series, $(CH_3)_4NBr$, exhibits a positive slope ($d\phi_v/dc^{1/2}$) at quite high (> 0.1 molar) concentrations and has been shown to follow the Debye-Hückel limiting law (124) quite well. Dilatometric measurements were carried out on $(C_2H_5)_4NBr$, $(n\text{-}C_3H_7)_4NBr$ and $(n\text{-}C_4H_9)_4NBr$ in H_2O and in one case in D_2O at 25°C. Figure 25 shows the behaviour of ϕ_v plotted against $c^{1/2}$ for $(C_2H_5)_4NBr$ in H_2O and D_2O at low concentrations. The relation is linear up to c = 0.04 molar and has a slope of 1.65 ± 0.2 ml.$l^{1/2}$ (g.mole)$^{-3/2}$, the ϕ_v plots for D_2O being parallel to those of H_2O in this concentration range. Figure 26 shows the results for the complete range of concentrations studied, both with the dilatometer and with the buoyancy balance. The present results for $(n\text{-}C_3H_7)_4NBr$ have been plotted in Figure 27 together with those of Wen and Saito (123) and Franks and Smith (127). The plot of ϕ_v against $c^{1/2}$ goes through a maximum with $(\partial\phi_v/\partial c^{1/2})$ being positive below ca. 0.015 molar. The limiting law slope is not reached even at the high dilutions used,

Figure 25. A plot of apparent molar volume ϕ_v against $c^{1/2}$ for tetraethylammonium bromide in H_2O and D_2O.

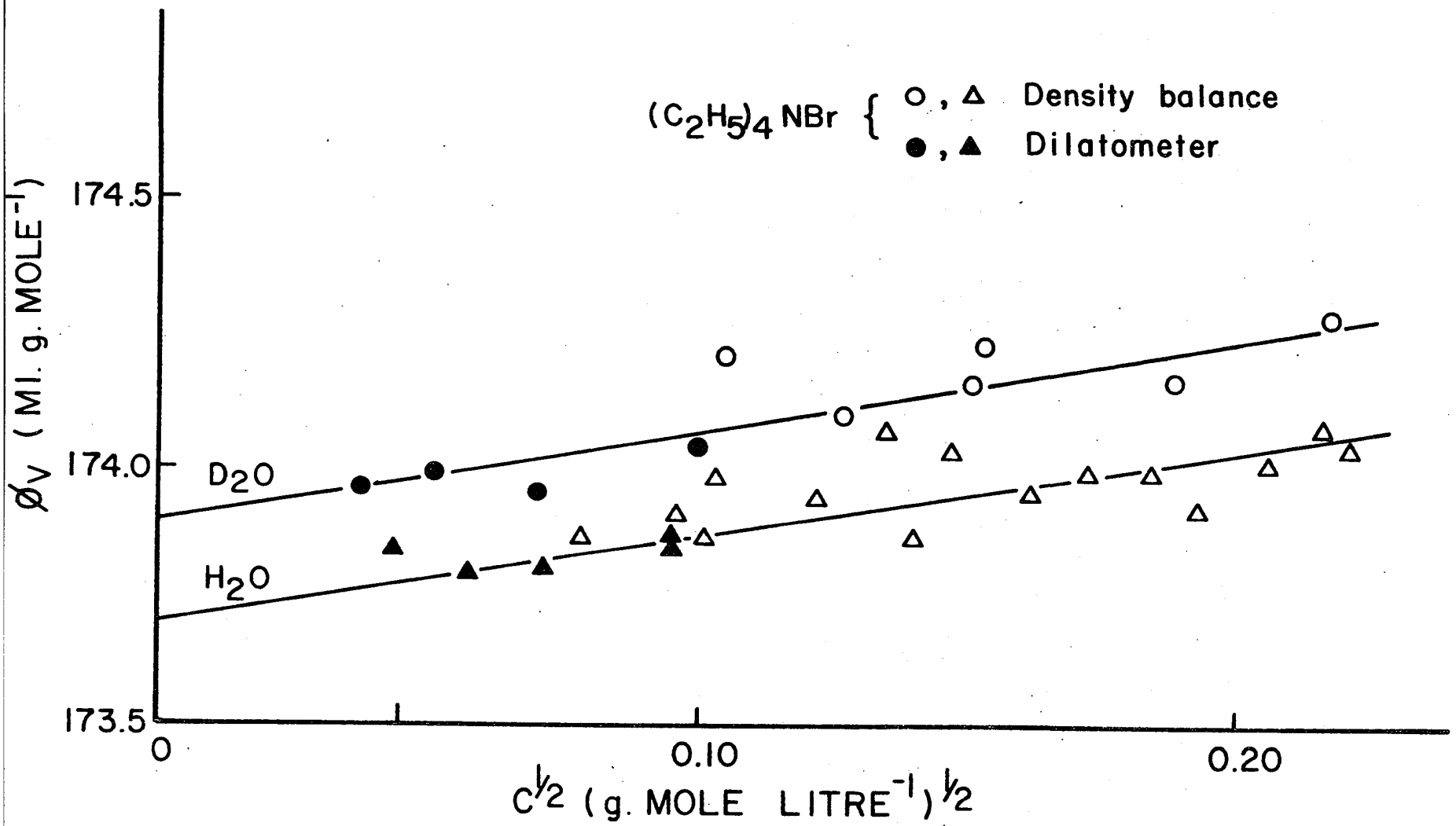
$(C_2H_5)_4NBr$ { ○, △ Density balance
●, ▲ Dilatometer
ϕ_V (Ml. g. MOLE^{-1})
174.5
174.0
173.5
D_2O
H_2O
0
0.10
0.20
$C^{1/2}$ (g. MOLE LITRE^{-1})$^{1/2}$

Figure 26. A plot of apparent molar volume, ϕ_v, against $c^{1/2}$ for tetraethylammonium bromide in H_2O and D_2O

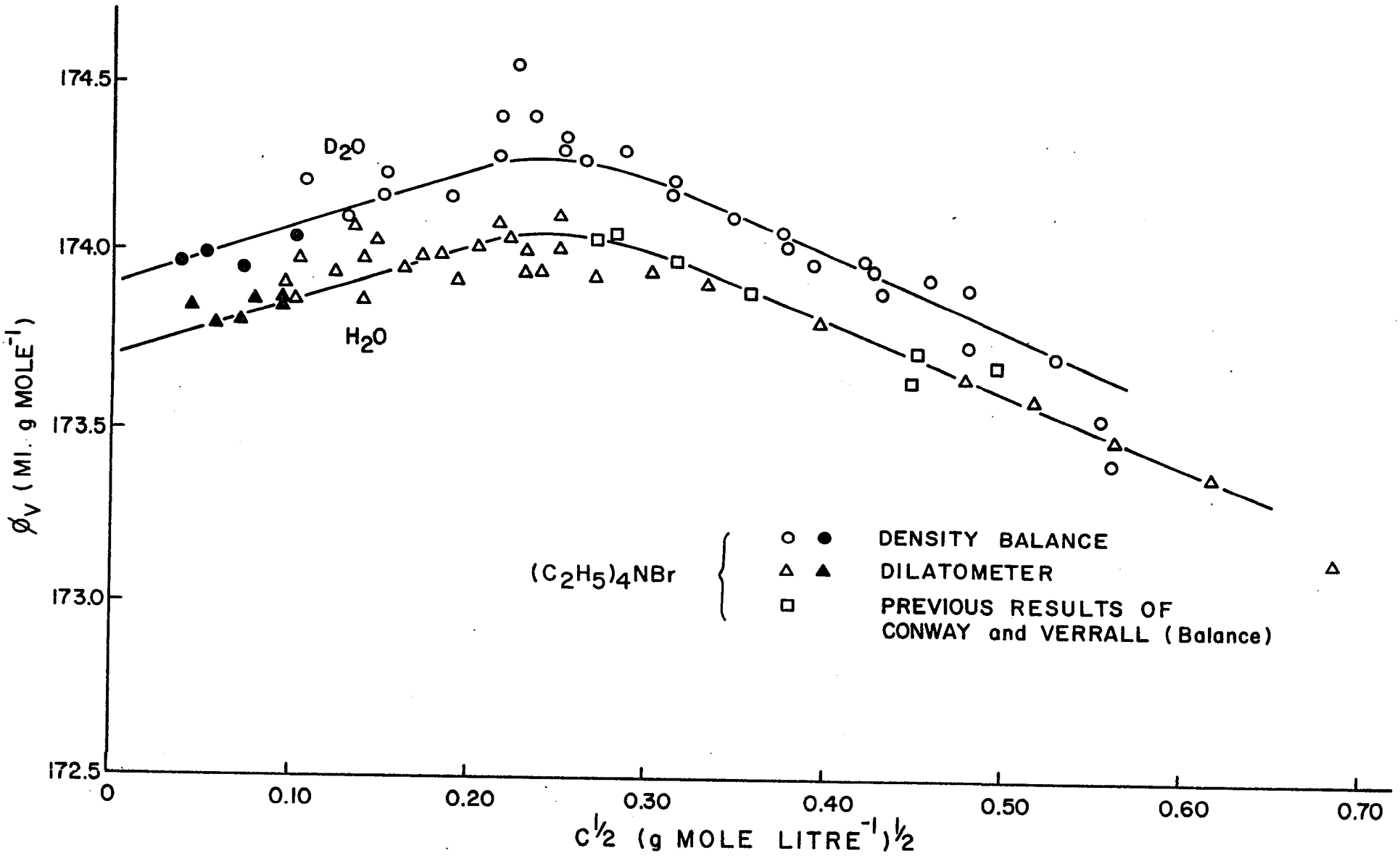
174.5
174.0
173.5
173.0
172.5
ϕ_V (Ml. g MOLE^{-1})
D_2O
H_2O
$(C_2H_5)_4NBr$
DENSITY BALANCE
DILATOMETER
PREVIOUS RESULTS OF CONWAY and VERRALL (Balance)
0
0.10
0.20
0.30
0.40
0.50
0.60
0.70
$C^{1/2}$ (g MOLE LITRE^{-1})$^{1/2}$

Figure 27. A plot of apparent molar volume, ϕ_v, against $c^{1/2}$ for tetra-n-propylammonium bromide in H_2O

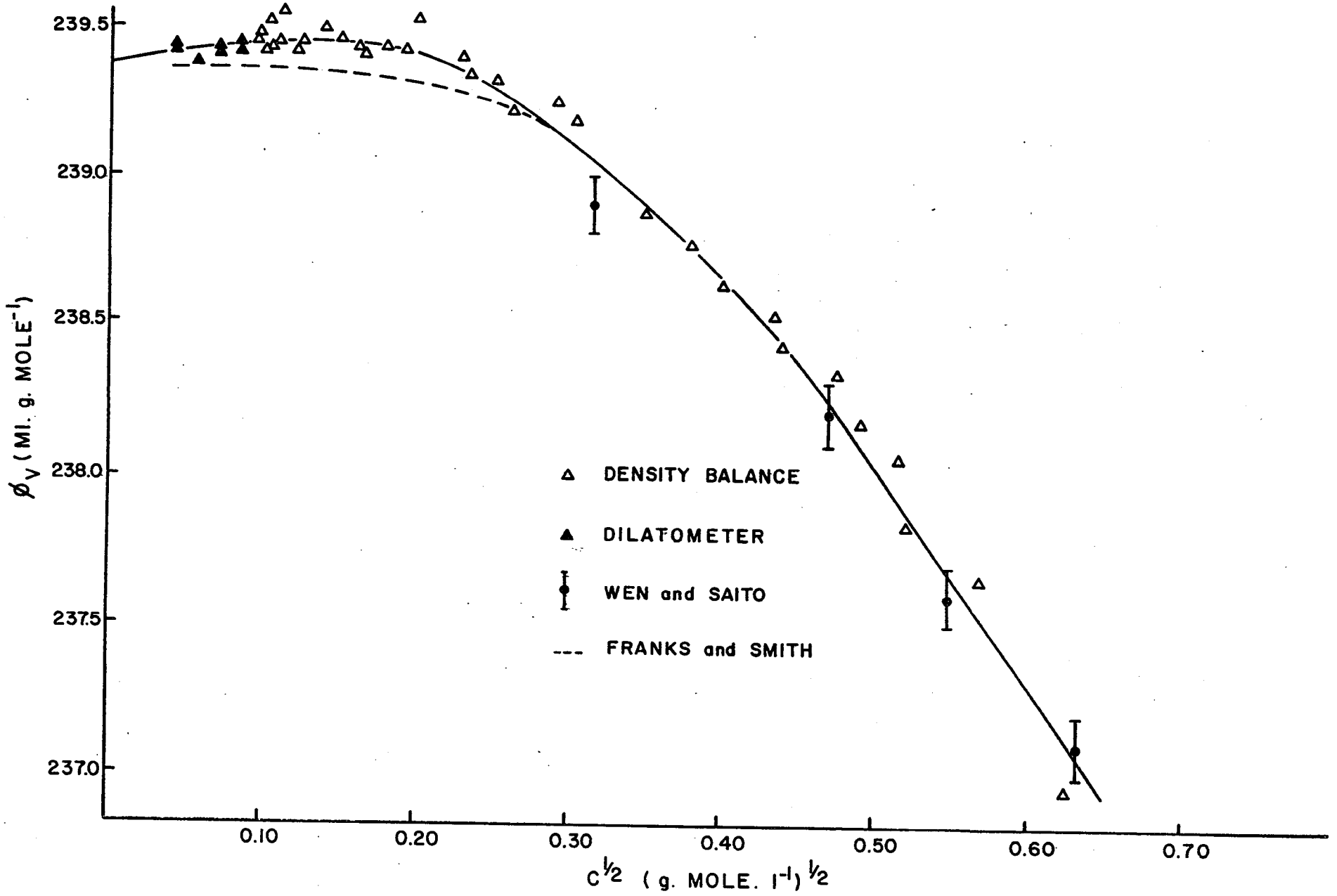
239.5
239.0
238.5
238.0
237.5
237.0
ϕ_V (Ml. g. MOLE^{-1})
0.10
0.20
0.30
0.40
0.50
0.60
0.70
$C^{1/2}$ (g. MOLE. l^{-1}) $^{1/2}$
DENSITY BALANCE
DILATOMETER
WEN and SAITO
FRANKS and SMITH

Figure 28. A plot of apparent molar volume, ϕ_v, against $c^{1/2}$ for tetra-n-butylammonium bromide in H_2O at 25°C.

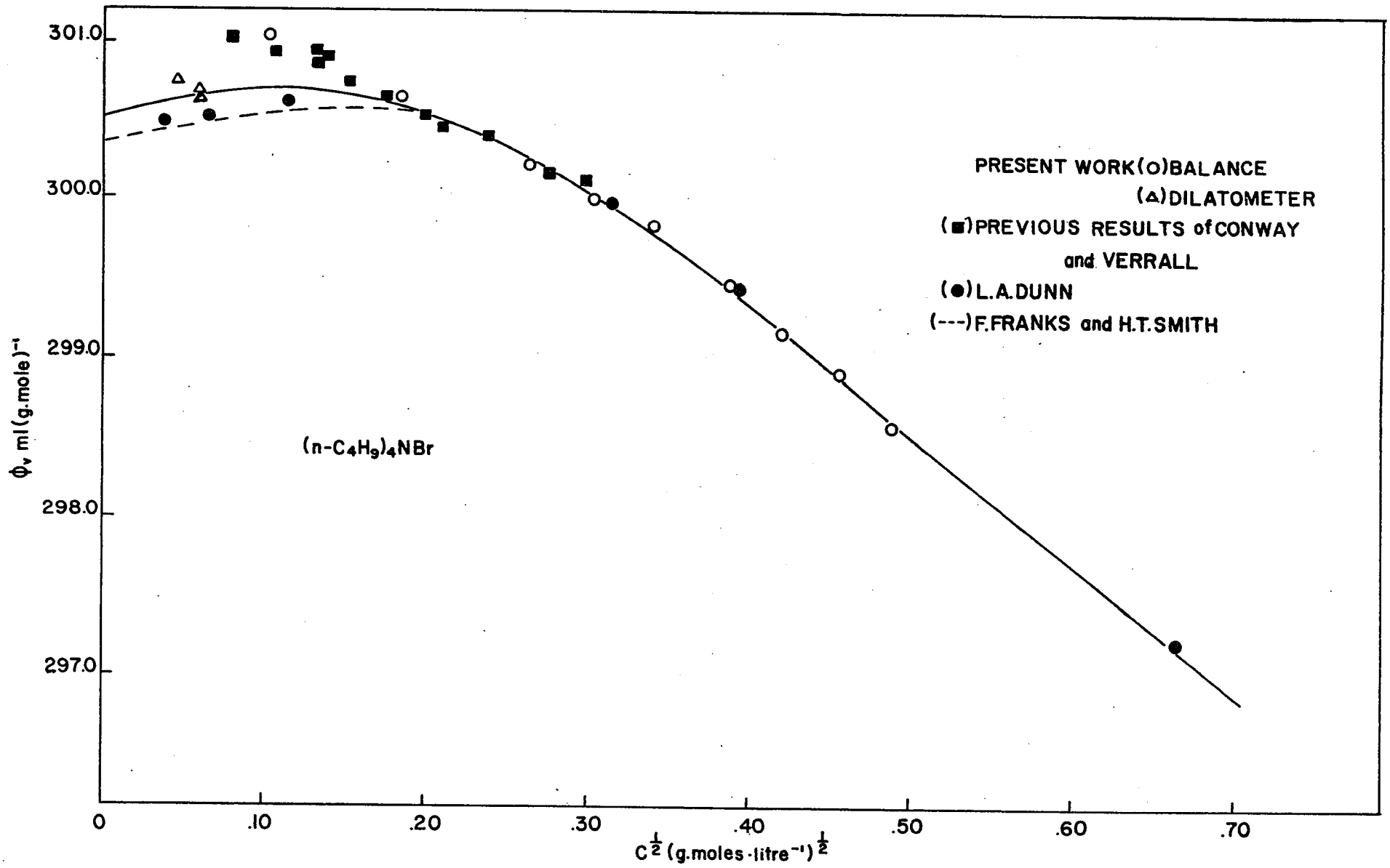
301.0
300.0
299.0
298.0
297.0
ϕ_v ml(g.mole)$^{-1}$
0
.10
.20
.30
.40
.50
.60
.70
$C^{\frac{1}{2}}$ (g.moles·litre^{-1})$^{\frac{1}{2}}$
$(n\text{-}C_4H_9)_4NBr$
PRESENT WORK (○) BALANCE
(△) DILATOMETER
(■) PREVIOUS RESULTS of CONWAY and VERRALL
(●) L.A.DUNN
(---) F.FRANKS and H.T.SMITH

the highest positive slope being ca. $+0.7 \pm 0.2$ ml.$l^{1/2}$(g.mole)$^{-3/2}$. The concentration range over which a positive straight line can be drawn is so small that a scatter of $\pm$ 0.02 ml (g.mole)$^{-1}$ in ϕ_v will introduce a large uncertainty in the value of the slope. Dilatometric measurements on $(n\text{-}C_4H_9)_4NBr$ have recently been reported (125) and are in agreement with the results of the present determinations on this compound (Fig. 28).

The results for $\bar{V}_2^o$ obtained in this study on the TAA bromides have been listed in Table 11 together with the data of other workers, where extrapolations were made from sufficiently high dilutions. As may be seen from Figures 25 to 28 and also from Table 11, there is good agreement between our results and those of other workers. The results obtained dilatometrically are the most precise at high dilutions and thus good agreement is found for $n\text{-}Bu_4NBr$ and Et_4NBr where two dilatometric determinations can be compared.

TABLE 11

Values of $\bar{V}_2^o$ for the Tetra-n-alkylammonium Bromides in H_2O at 25°C

Salt	$\bar{V}_2^o$ ml (g.mole)$^{-1}$ (a)	(b)	(c)
$(CH_3)_4NBr$	*114.26	114.40	114.25
$(C_2H_5)_4NBr$	173.70 ± .05	173.65	173.6 ± .10
$(n\text{-}C_3H_7)_4NBr$	239.38 ± .05	239.15	
$(n\text{-}C_4H_9)_4NBr$	300.41 ± 0.10	300.35	300.40

(a) Present work; ϕ_v data obtained dilatometrically down to c = 0.002.

(b) Franks and Smith (127); ϕ_v data obtained on magnetically operated densitometer down to c = 0.002.
Hepler, Stokes and Stokes (124); ϕ_v data obtained dilatometrically down to c = 0.01 molar.
Dunn (125); ϕ_v data obtained dilatometrically down to c = 0.0015 molar.

* Conway, Verrall and Desnoyers (126); ϕ_v data obtained on a differential buoyancy balance down to c = 0.01 molar.
Wirth (116); ϕ_v data obtained dilatometrically down to c = 0.002 molar.

7. Partial Molar Volumes in H_2O and D_2O at 25°C

The partial molar volumes of a series of alkali halides, tetraalkylammonium bromides and selected neutral compounds have been determined in heavy water solutions at 25°C. The ϕ_v data obtained for D_2O solutions have been plotted on an "aquamolality" (M) scale (164), i.e. moles of salt per 55.51 moles of solvent of either kind. The aquamolality scale becomes, of course, the molality scale when H_2O is the solvent and it ensures that at equal aquamolal concentrations the number of solvent molecules in solution is the same. The concentration scale used will not, of course, affect the $\bar{V}_2^o$ data.

The limiting slope for the apparent molar volume has been assumed to be identical for H_2O and D_2O solutions. The dielectric constants of the two solvents are nearly identical but the pressure derivative of ϵ is not known for D_2O, which precludes any calculation of S_v for that solvent. Experimentally, the slopes of ϕ_v against $c^{1/2}$ for NaCl solutions in H_2O and D_2O are identical and since the limiting slope is approached in H_2O we have assumed that the same limiting slope holds for D_2O solutions.

(i) Inorganic 1:1 Electrolytes

Previous work on the partial molar volume of alkali halides in H_2O and D_2O (134) had shown that $\bar{V}_2^o$ in D_2O was lower than in H_2O. However, the above results (134) were not found to be linear in $c^{1/2}$ although measurements were made at sufficiently low

concentrations for limiting law behaviour to be applicable. Subsequent measurements of ϕ_v in aqueous NaF solutions (137), which were in quantitative agreement with our findings, showed that the value of $\bar{V}_2^o$ for NaF in H_2O found earlier by Robertson (134), was in error by ca. 1 ml $(g.mole)^{-1}$. It was therefore of interest first to repeat the ϕ_v measurements on solutions of NaF in D_2O to see if the previously reported difference in ϕ_v between the two solvents (134) was maintained.

The partial molar volumes of NaF, NaCl, NaBr, KCl and KBr were determined at 25°C in D_2O. The ϕ_v data for NaCl in H_2O was taken from (139), while the ϕ_v data for the other alkali halide salts in H_2O were determined on the differential buoyancy balance. A complete tabulation of the data can be found in Appendix III. The ϕ_v data were plotted according to eqn. IV.10 and are shown in Figures 29 and 30. In all cases the apparent molar volume in D_2O was lower than in H_2O, the difference $\Delta\bar{V}^o_{H_2O-D_2O}$ being inversely proportional to the size of the cation and anion.

(ii) Tetraalkylammonium and Alkylammonium Salts

The ϕ_v data for solutions of the TAA salts in H_2O have been discussed in Section 6 of this Chapter. For comparison with the results obtained in D_2O, the results of Verrall (152) and those obtained in the present work in H_2O have been used. The apparent molar volumes of the salts of the series Me_4NBr to Bu_4NBr were

Figure 29. A plot of ϕ_v - 1.868 $M^{1/2}$ against aquamolality M for NaF, NaBr and NaCl in H_2O (○) and D_2O (●) at 25°C. NaF (----) Millero (137).

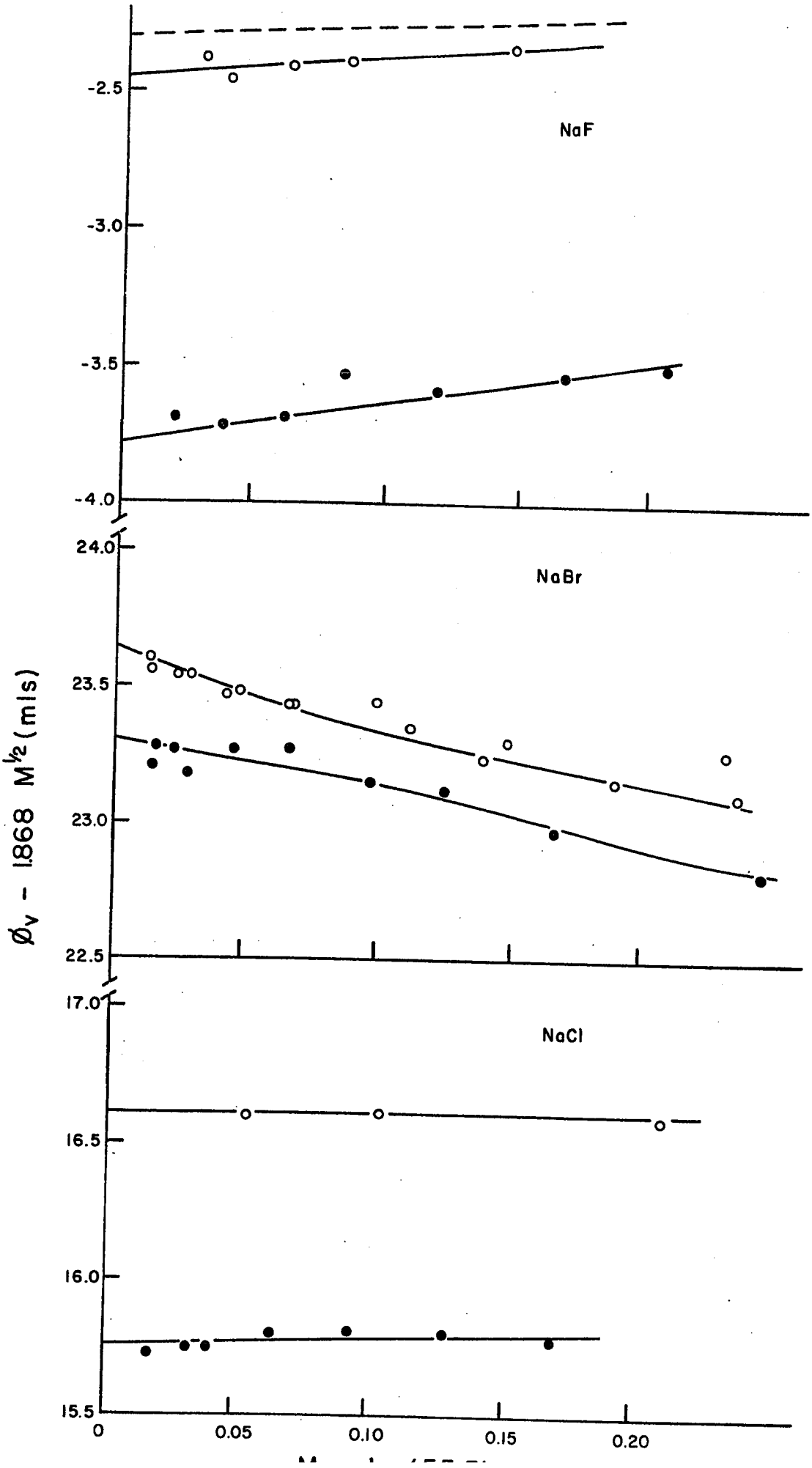
-2.5
-3.0
-3.5
-4.0
NaF
24.0
23.5
23.0
22.5
NaBr
17.0
16.5
16.0
15.5
NaCl
$\phi_v - 1868\ M^{1/2}$ (mls)
0
0.05
0.10
0.15
0.20

Figure 30. A plot of $\phi_v - 1.868\ M^{1/2}$ against aquamolality M for KCl and KBr in H_2O (O) and D_2O (●) at 25°C.

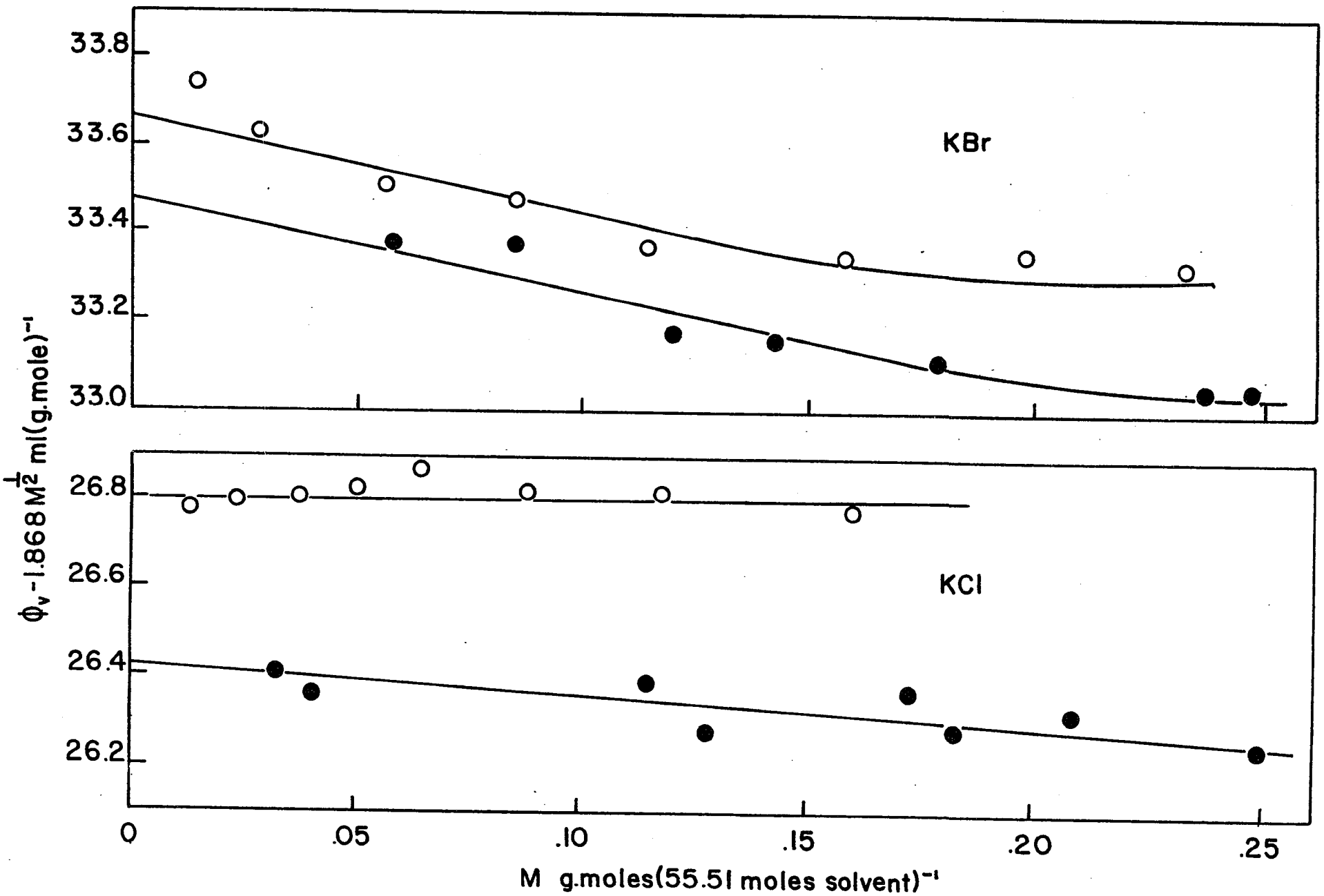
33.8
33.6
33.4
33.2
33.0
KBr
26.8
26.6
26.4
26.2
KCl
$\phi_v - 1.868 M^{\frac{1}{2}}$ ml(g.mole)$^{-1}$
0
.05
.10
.15
.20
.25
M g.moles(55.51 moles solvent)$^{-1}$

determined in D_2O using the differential buoyancy balance technique. In the case of Et_4NBr, dilatometric determinations of ϕ_v in D_2O were carried out down to c = 0.002 molar to verify the persistence of a significant isotopic difference $\Delta\bar{V}_{D_2O-H_2O}$ to high dilutions, from which extrapolations to infinite dilution could be made. The ϕ_v data were plotted according to eqn. IV.10 and are shown for Me_4NBr and Pr_4NBr in Figure 31 while the results for n-Bu_4NBr are shown in Figure 32. Figure 25 shows the dilatometric data for Et_4NBr in D_2O.

The main features evident in the results obtained with the TAA salts were that, with the exception of Me_4NBr, the salts all had a larger apparent molar volume in D_2O than in H_2O. That this positive $\Delta\bar{V}_{D_2O-H_2O}$ was maintained to infinite dilution, was shown by studies at high dilution on Et_4NBr. At low concentrations, the ϕ_v vs. $M^{1/2}$ curve in D_2O became parallel to the ϕ_v vs. $M^{1/2}$ curve in H_2O, while at high concentration some crossing of the curves occurred. Finally, the magnitude of the difference $\Delta\bar{V}_{D_2O-H_2O}$ was proportional to the size of the cations in the TAA bromide series. In Table 12 are listed the values of $\bar{V}_2^o$ and j for the compounds studied in H_2O and D_2O. For comparison between the two solvents, extrapolations were made over the same concentration range for a particular salt.

The apparent molar volumes of solutions of $(DOC_2H_4)_3NDBr$ were determined in D_2O solutions. The salt was prepared in solution by allowing $(HOC_2H_4)_3NHBr$ to exchange with the solvent D_2O. The solvent density was corrected for the formation of HOD as a result of the exchange reaction. The density of HOD/D_2O solutions will be reported in the next section of this chapter. The solvent was not therefore pure D_2O but an HOD/D_2O mixture of varying composition, the highest concentration of HOD being ca. 0.8 molar. The plot of ϕ_v against $c^{1/2}$ is shown in Figure 33.

Figure 31. A plot of $\phi_v - 1.868\ M^{1/2}$ against M for $(CH_3)_4NBr$ and $(n\text{-}C_3H_7)_4NBr$ in H_2O (O) and D_2O (●) at 25°C

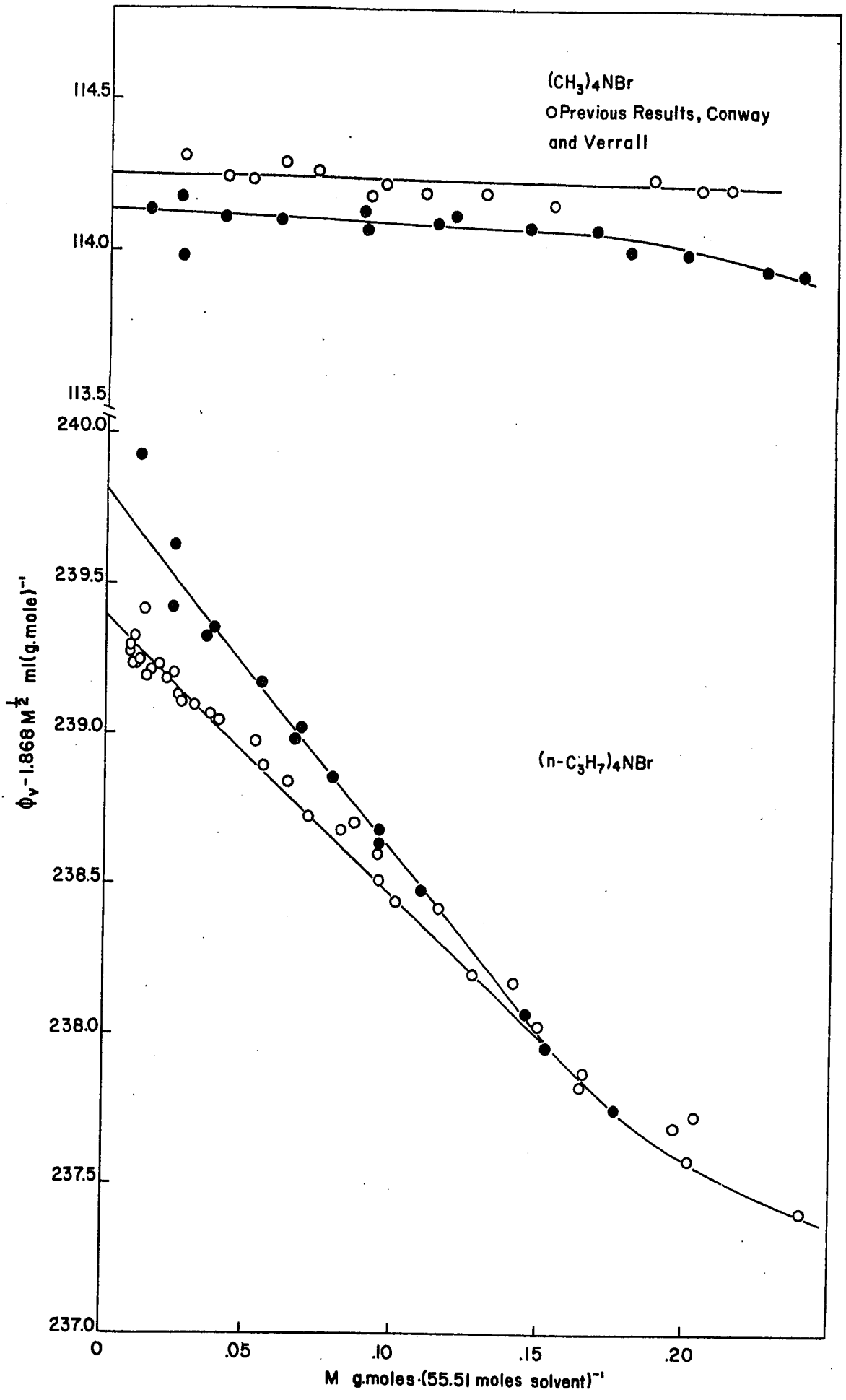
$(CH_3)_4NBr$
○Previous Results, Conway and Verrall
$(n\text{-}C_3H_7)_4NBr$
114.5
114.0
113.5
240.0
239.5
239.0
238.5
238.0
237.5
237.0
$\phi_v - 1.868\,M^{\frac{1}{2}}$ ml(g.mole)$^{-1}$
0
.05
.10
.15
.20
M g.moles·(55.51 moles solvent)$^{-1}$

Figure 32. A plot of $\phi_v - 1.868\ M^{1/2}$ against aquamolality M for $(n\text{-}C_4H_9)_4NBr$ in H_2O (O) and D_2O (●) at 25°C

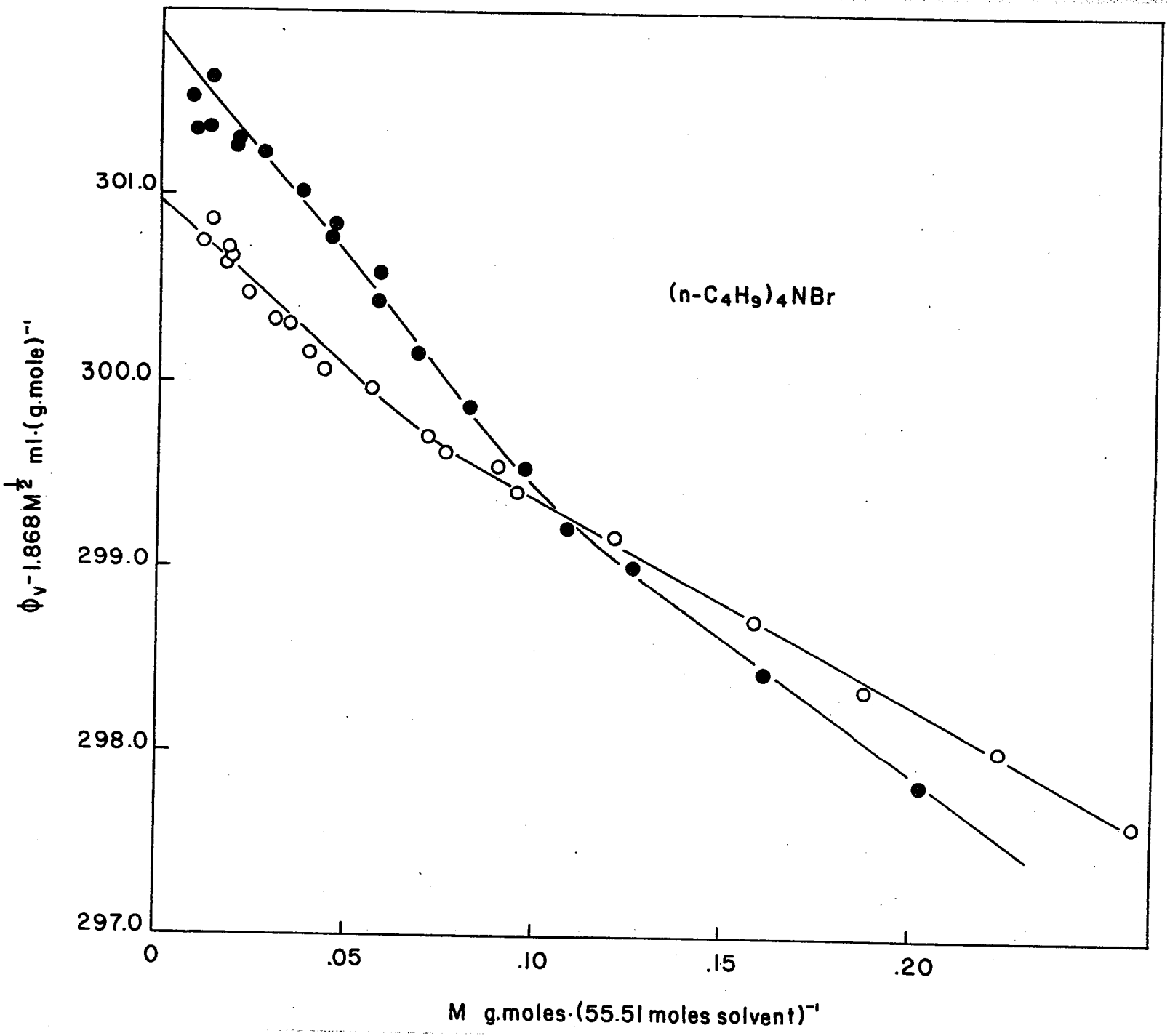
301.0
300.0
299.0
298.0
297.0
0
.05
.10
.15
.20
$\phi_v - 1.868 M^{\frac{1}{2}}$ ml·(g.mole)$^{-1}$
M g.moles·(55.51 moles solvent)$^{-1}$
$(n\text{-}C_4H_9)_4NBr$

TABLE 12

Values of $\bar{V}_2^o$ and j in Equation IV.10 for a Series of Alkali Halide and Tetra-n-alkylammonium Salts in H_2O and D_2O

	H_2O		D_2O		
Solute	$\bar{V}_2^o$ ml(g mole)$^{-1}$	j H_2O ml.l$^{1/2}$(g mole)$^{-3/2}$	$\bar{V}_2^o$ ml(g mole)$^{-1}$	j D_2O ml.l$^{1/2}$(g mole)$^{-3/2}$	$\Delta\bar{V}^o_{D_2O-H_2O}$ ml(g mole)$^{-1}$
NaF	-2.37	+0.46	-3.79	+1.3	-1.42
NaCl	16.61	0	15.76	+.25	-0.86
NaBr	23.64	-3.2	23.30	-1.5	-0.34
KCl	26.80	0	26.43	-0.7	-0.37
KBr	33.67	-2.3	33.48	-2.0	-0.20
$(CH_3)_4NBr$	114.26	-1.5	114.14	-5.0	-.11
$(C_2H_5)_4NBr$	173.70		173.90		+0.20
$(n\text{-}C_3H_7)_4NBr$ *	239.40	-9.4	239.82	-12.1	+0.42
$(n\text{-}C_4H_9)_4NBr$ *	300.96	-18.0	301.90	-24.8	+0.94

*Extrapolated from c $\geqslant$ 0.02 molar

	$\bar{V}_2^o$	j	
$(HOC_2H_4)_3NHBr$ in H_2O	147.28	+0.2	$\Delta\bar{V}_{D_2O-H_2O} = -2.7$
$(DOC_2H_4)_3NDBr$ in D_2O	144.58	+0.6	

(iii) Neutral Solutes in D_2O

The apparent molar volume of HOD in H_2O and D_2O was determined in dilute solution and the ϕ_v data were plotted as a function of m (Figure 34). The apparent molar volume of HOD was 3.1% higher in D_2O than in H_2O. The apparent molar volume of pyridine in D_2O was also determined and is shown as a function of M in Figure 35. For pyridine, the apparent molar volume is greater in D_2O than in H_2O by ca. 0.20 ml. The $\bar{V}_2^o$ and initial slope data have been listed in Table 15.

Figure 33. A plot of apparent molal volume ϕ_v, against $m^{1/2}$ for $(DOC_2H_4)_3NDBr$ in D_2O and $(HOC_2H_4)_3NHBr$ in H_2O at 25°C.

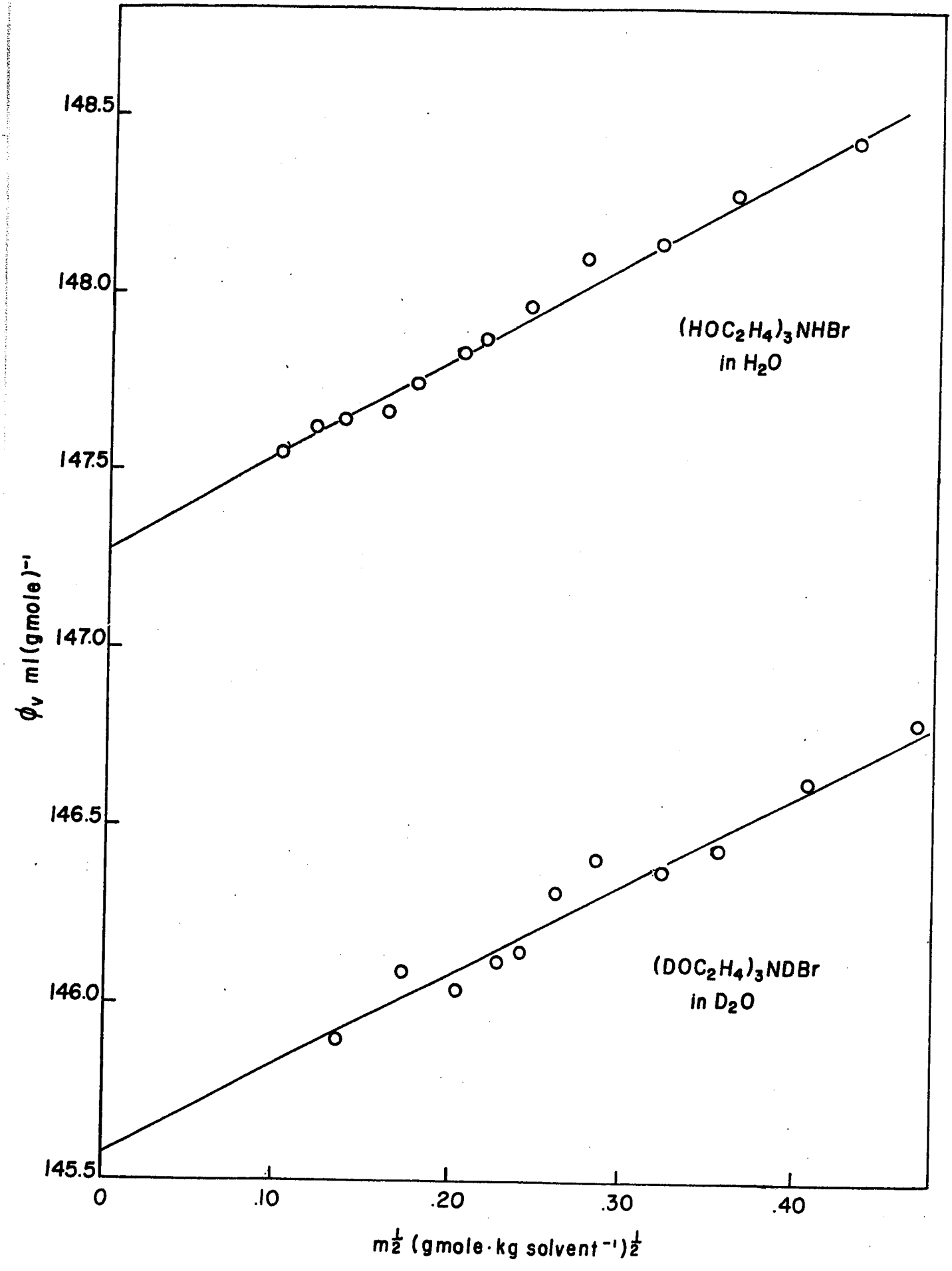
148.5
148.0
147.5
147.0
146.5
146.0
145.5
ϕ_v ml(gmole)$^{-1}$
0
.10
.20
.30
.40
$m^{\frac{1}{2}}$ (gmole·kg solvent^{-1})$^{\frac{1}{2}}$
$(HOC_2H_4)_3NHBr$
in H_2O
$(DOC_2H_4)_3NDBr$
in D_2O

Figure 34. A plot of apparent molal volume ϕ_v against m for HOD in H_2O (O) and D_2O (●) at 25°C

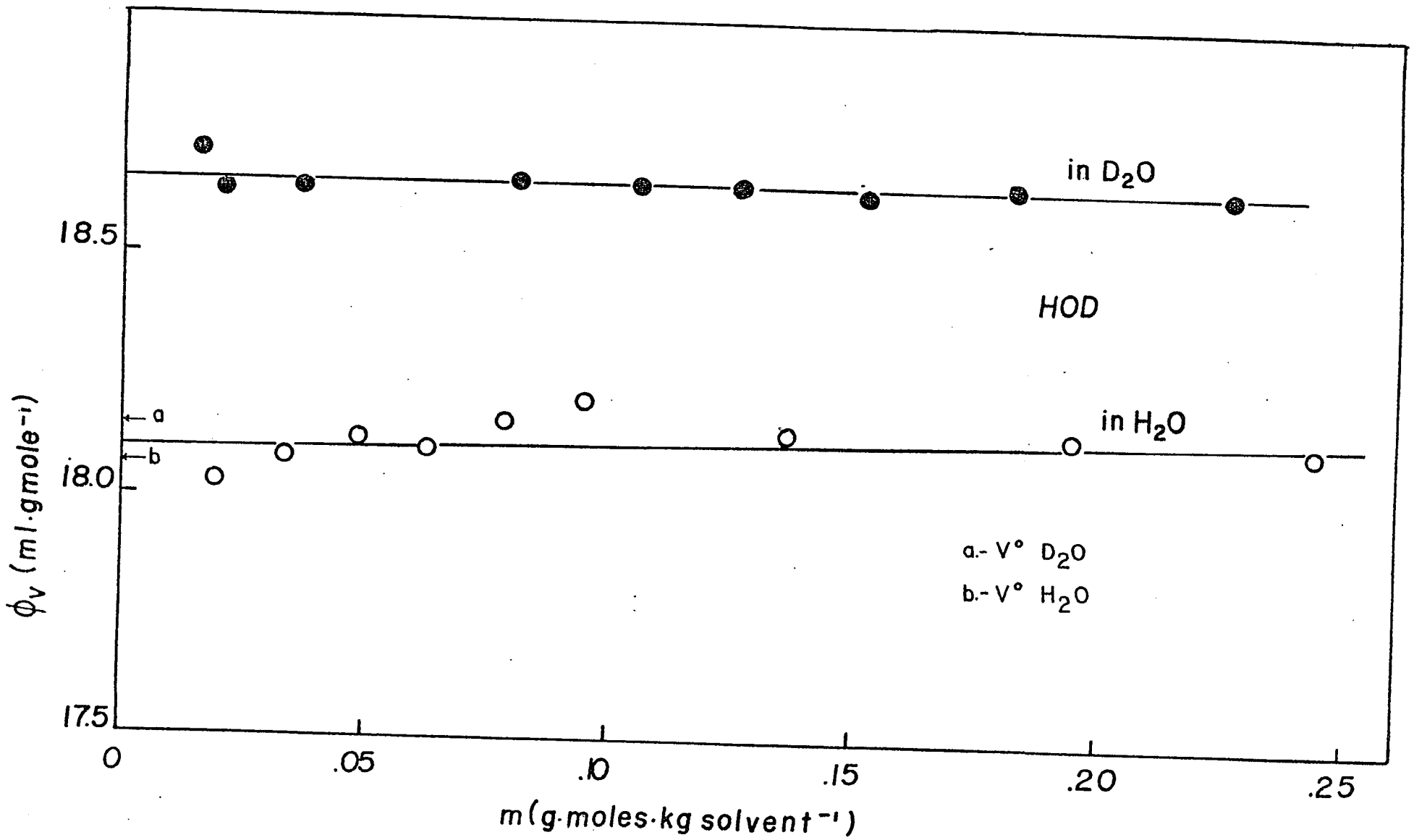
in D_2O
HOD
in H_2O
a
b
a.- V° D_2O
b.- V° H_2O
18.5
18.0
17.5
ϕ_v (ml·gmole^{-1})
0
.05
.10
.15
.20
.25
m(g·moles·kg solvent^{-1})

Figure 35. A plot of apparent molal volume ϕ_v against aquamolality, M, for pyridine in H_2O (O) and D_2O (●) at 25°C.

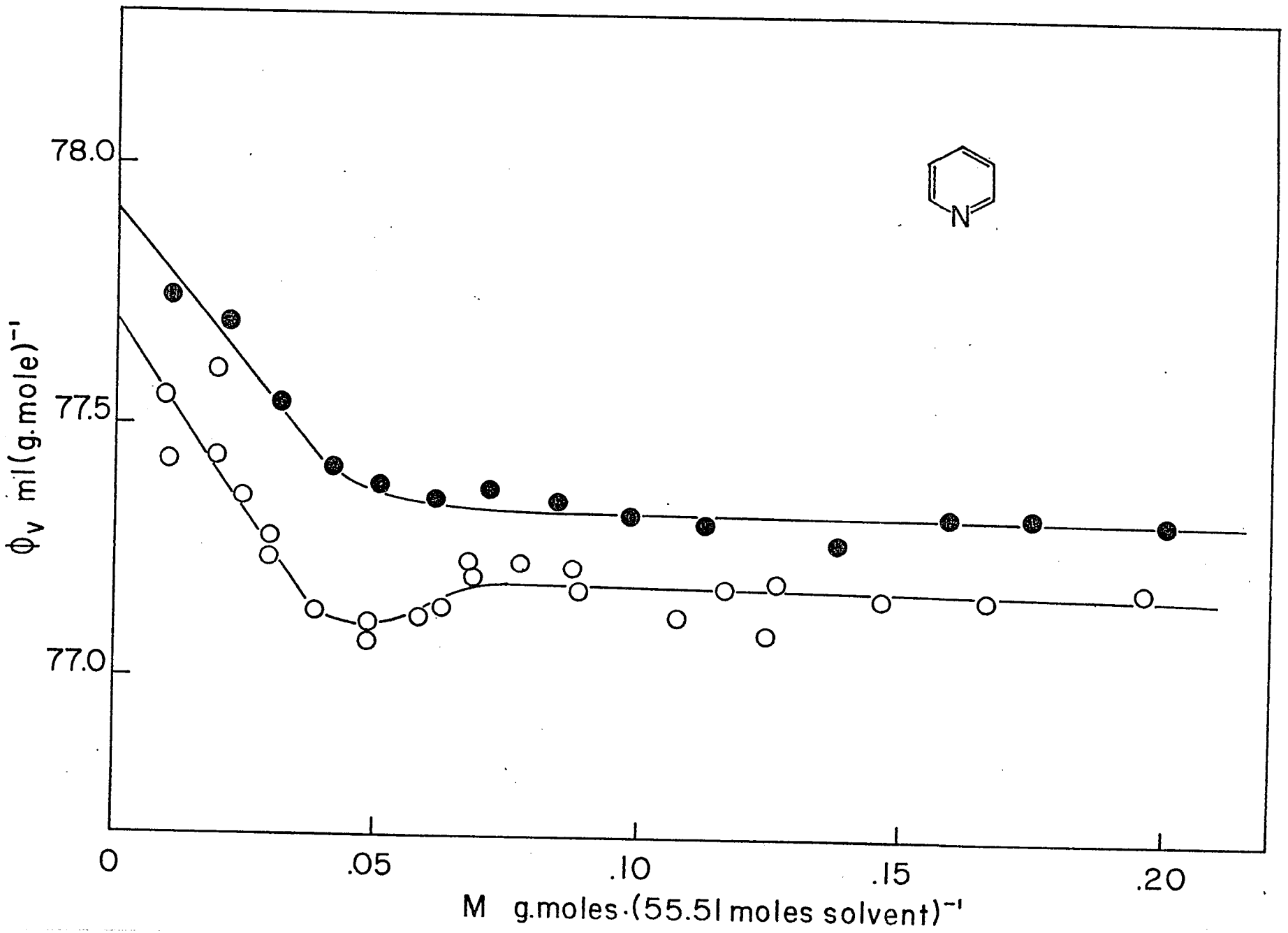
78.0
77.5
77.0
ϕ_v ml(g.mole)$^{-1}$
N
0
.05
.10
.15
.20
M g.moles·(55.51 moles solvent)$^{-1}$

TABLE 13

Values of $\bar{V}_2^o$ and $(d\phi_v/dM)_{M\to o}$ for Neutral Solutes in H_2O and D_2O at 25°C

	H_2O		D_2O		
Solute	$\bar{V}_2^o$ ml (g mole)$^{-1}$	$(\frac{d\phi_v}{dM})_{M\to o}$ *	$\bar{V}_2^o$ ml (g mole)$^{-1}$	$(\frac{d\phi_v}{dM})_{M\to o}$ *	$\Delta\bar{V}^o_{D_2O-H_2O}$
HOD	18.10	+0.10	18.66	0	+ 0.56
Pyridine	77.70	-10.0	77.90	-12.0	+ .20

* Units are ml. · 55.51 moles solvent (g.moles)$^{-2}$

8. Partial Molar Expansibilities in H_2O and D_2O Solutions

(i) Inorganic Salts

The apparent molar volumes of NaCl, NaF and KCl were measured as a function of temperature from 0° to 25°C in H_2O and from 5° to 25°C in D_2O. A single concentration, between 0.08 and 0.10 molal, was studied in each case. The data for ϕ_v as a function of T determined by Dunn (163) were used for NaCl in H_2O. The plots of ϕ_v^o against T for the three inorganic salts in H_2O and D_2O are shown in Figs. 36 - 38. Expansivity measurements made on KCl solutions in H_2O were in good agreement with published data (165, 127). Although only one concentration was used, ϕ_v^o values were calculated from ϕ_v data by subtracting the limiting law term at the various temperatures. The limiting law slope for D_2O was assumed to be identical to that in H_2O at all temperatures. (This is experimentally observed for NaCl solutions at 25°C). Of the three inorganic salts studied, KCl and NaCl had identical partial molar expansibilities in H_2O and D_2O, i.e. the value $\Delta\bar{V}_{(D_2O-H_2O)25^oC}$ was maintained down to 5°C. In the case of NaF, $\Delta\bar{V}_{D_2O-H_2O}$ increased as the temperature decreased, i.e. $\bar{E}^o_{2(D_2O)} > \bar{E}^o_{2(H_2O)}$.

Figure 36. A plot of apparent molal volume at infinite dilution ϕ_v^o against temperature, T, for KCl in H_2O (O) and D_2O (●).

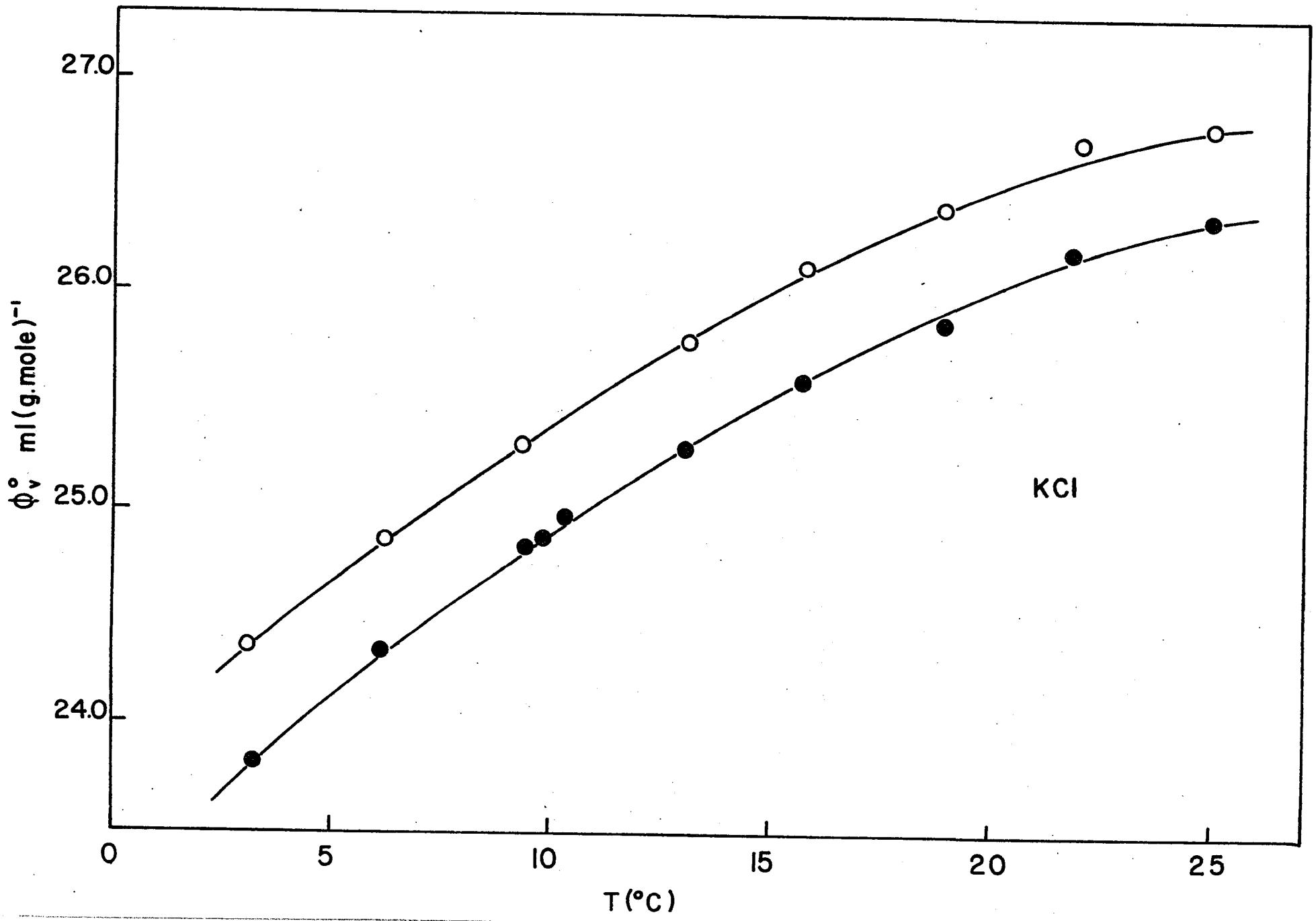
27.0
26.0
25.0
24.0
ϕ_v° ml(g.mole)$^{-1}$
KCl
0
5
10
15
20
25
T(°C)

Figure 37. A plot of apparent molal volume at infinite dilution ϕ_v^o against temperature, T, for NaF in H_2O (O) and D_2O (●).

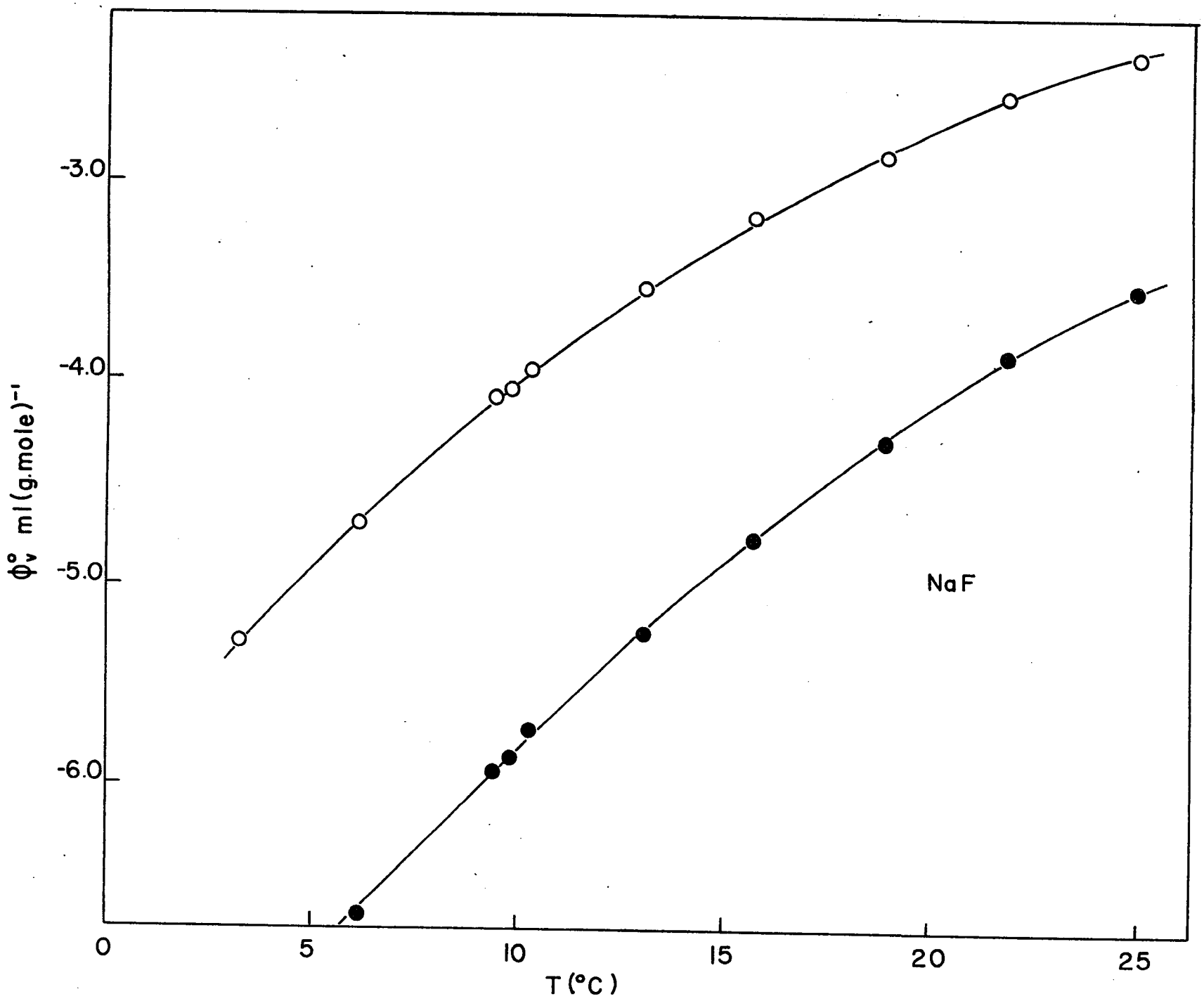
-3.0
-4.0
-5.0
-6.0
ϕ_v° ml(g.mole)$^{-1}$
0
5
10
15
20
25
T (°C)
NaF

Figure 38. A plot of apparent molal volume at infinite dilution ϕ_v^o against T for NaCl in H_2O (O) and D_2O (●).

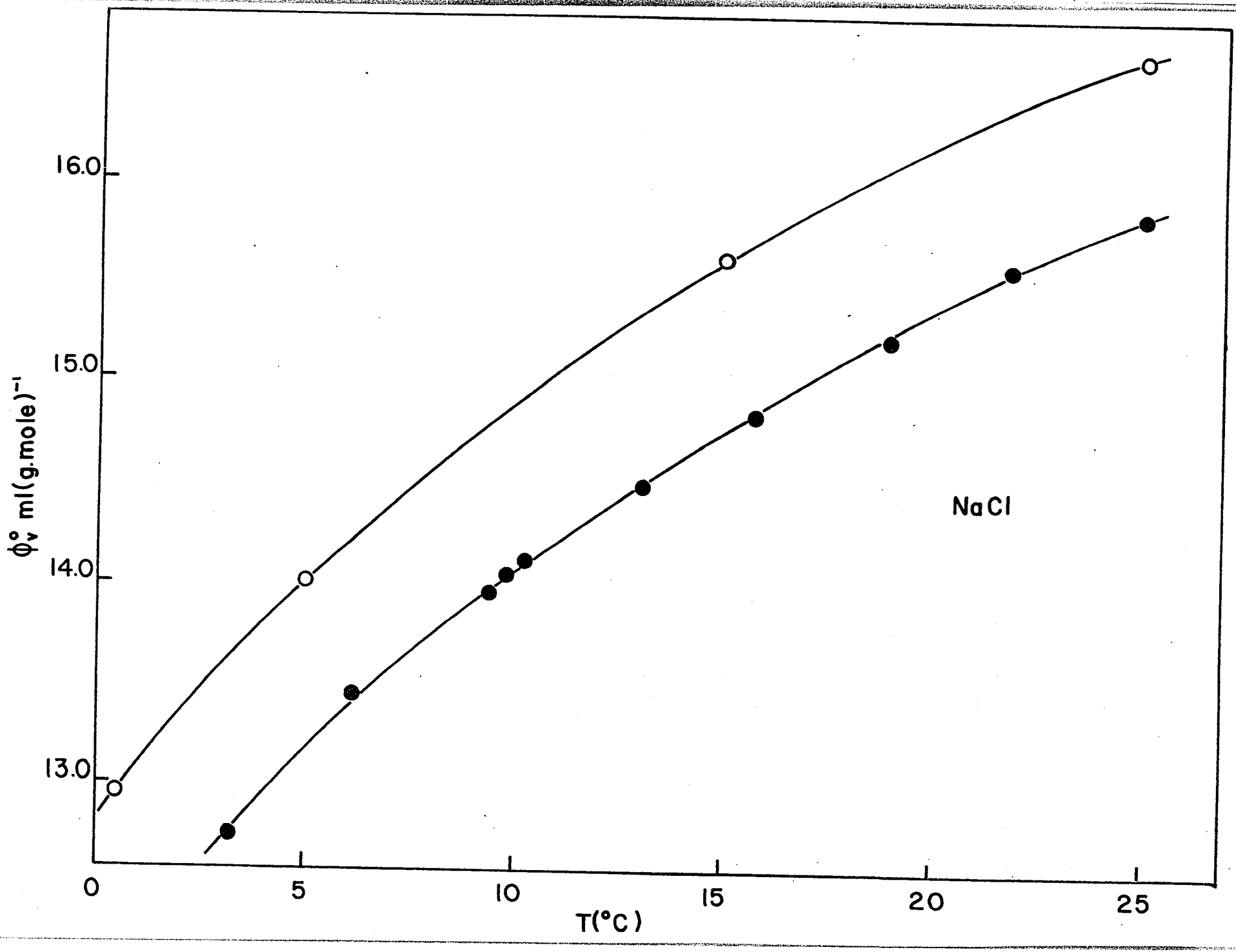
16.0
15.0
14.0
13.0
ϕ_v° ml(g.mole)$^{-1}$
0
5
10
15
20
25
T(°C)
NaCl

(ii) Tetraalkylammonium Salts

The apparent molal volumes of ca. 0.10 molal TAA bromide solutions in H_2O and D_2O were measured as a function of temperature over the same temperature range as that referred to above. Since the concentrations used were not in the limiting law region with this series of compounds, it was not possible to obtain the infinite dilution ϕ_v^o data; hence, the experimental ϕ_v values have been plotted as a function of temperature (Figs. 39 - 42). The values of the partial molar expansibility at 15°C are given in Table 14. The only salt which showed a pronounced difference in behaviour between the two solvents was Me_4NBr, where $\bar{E}_{2(H_2O)} > \bar{E}_{2(D_2O)}$. This difference in expansibilities causes the ϕ_v against T curves to cross at ca. 20°C, so that $\phi_{v(D_2O)}$ for Me_4NBr was greater than ϕ_v in H_2O for the salt below 20°C. For the other three salts in the series, the partial molar expansibilities at 15°C were identical within the experimental measurements.

Figure 39. A plot of apparent molal volume ϕ_v against T for $(CH_3)_4NBr$ in H_2O (O) and D_2O (●).

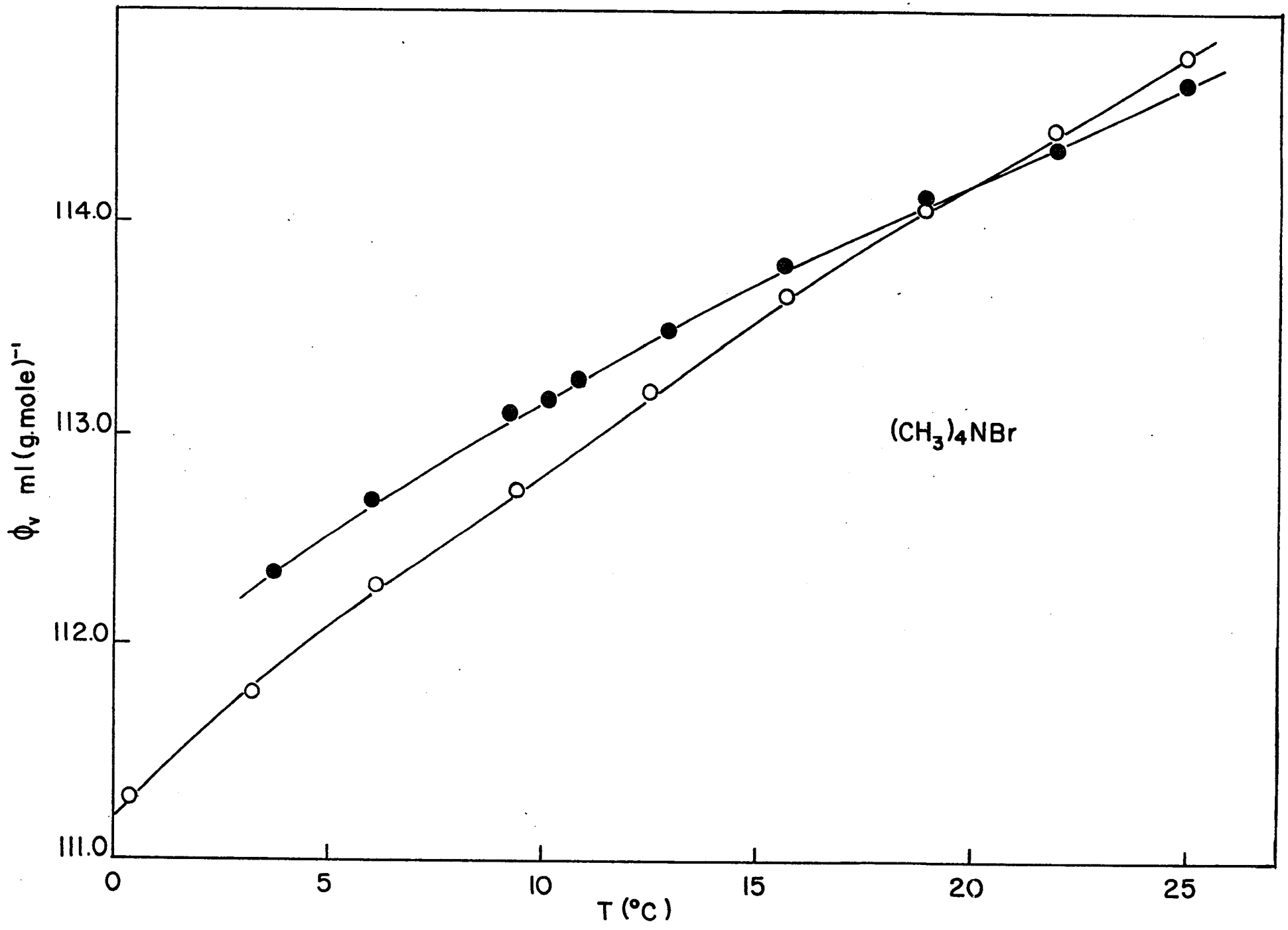
114.0
113.0
112.0
111.0
ϕ_v ml (g.mole)$^{-1}$
0
5
10
15
20
25
T (°C)
$(CH_3)_4NBr$

Figure 40. A plot of apparent molal volume ϕ_v against T for $(C_2H_5)_4NBr$ in H_2O (O) and D_2O (●)

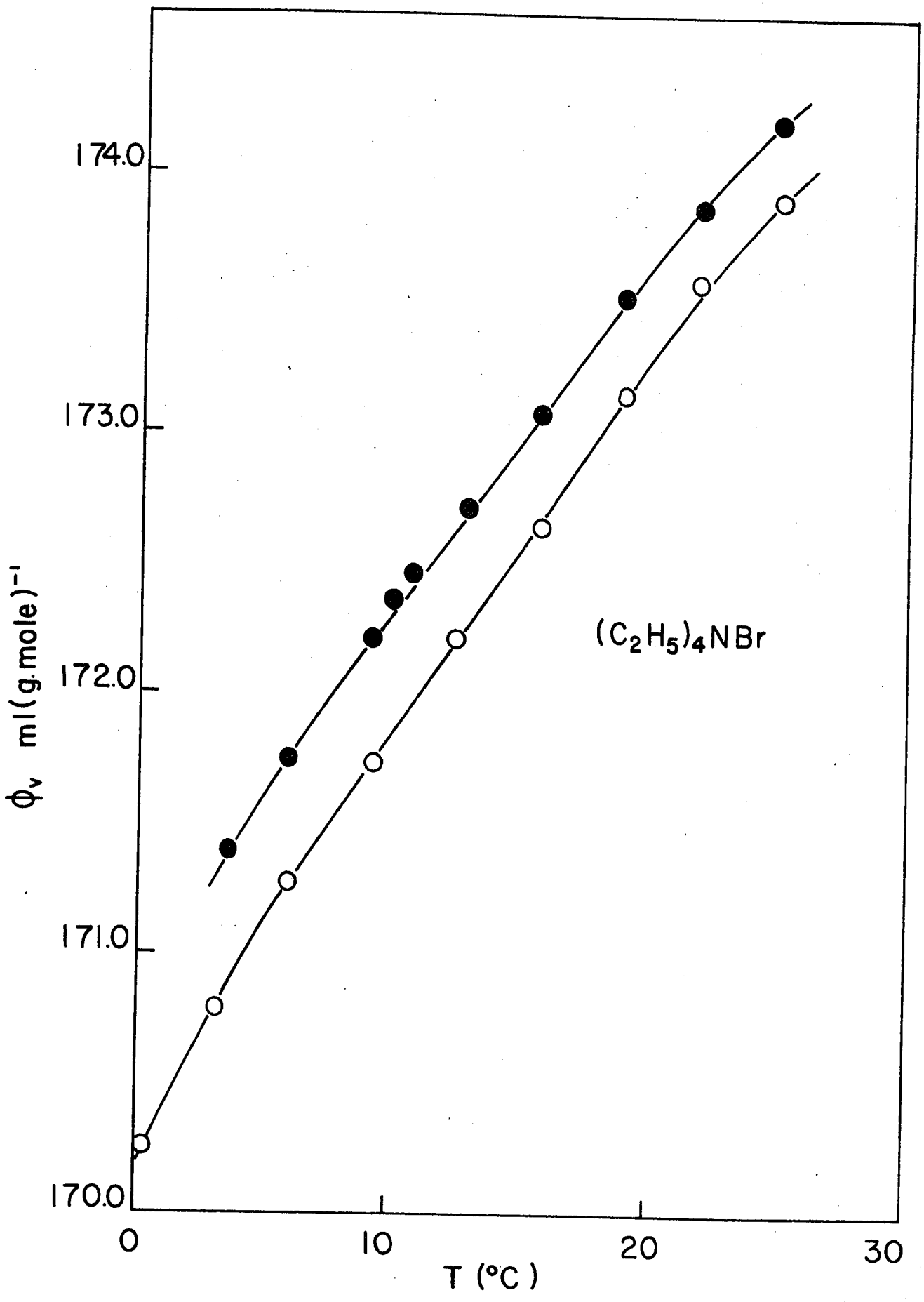
174.0
173.0
172.0
171.0
170.0
ϕ_v ml(g.mole)$^{-1}$
$(C_2H_5)_4NBr$
0
10
20
30
T (°C)

Figure 41. A plot of apparent molal volume ϕ_v against T for $(n\text{-}C_3H_7)_4NBr$ in H_2O (O) and D_2O (●).

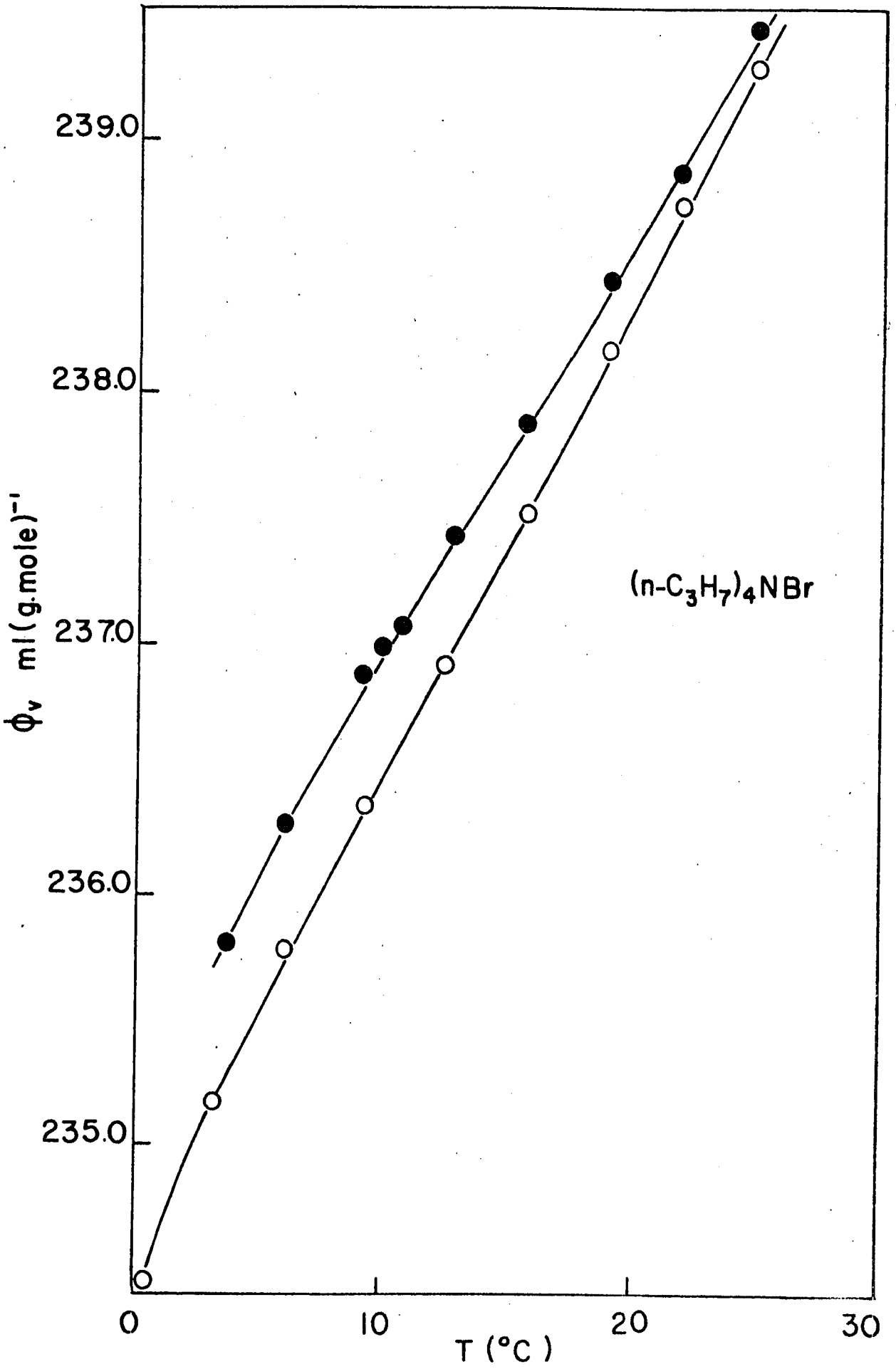
239.0
238.0
237.0
236.0
235.0
ϕ_v ml(g.mole)$^{-1}$
$(n\text{-}C_3H_7)_4NBr$
0
10
20
30
T (°C)

Figure 42. A plot of apparent molal volume ϕ_v against T for $(n\text{-}C_4H_9)_4NBr$ in H_2O (O) and D_2O (●).

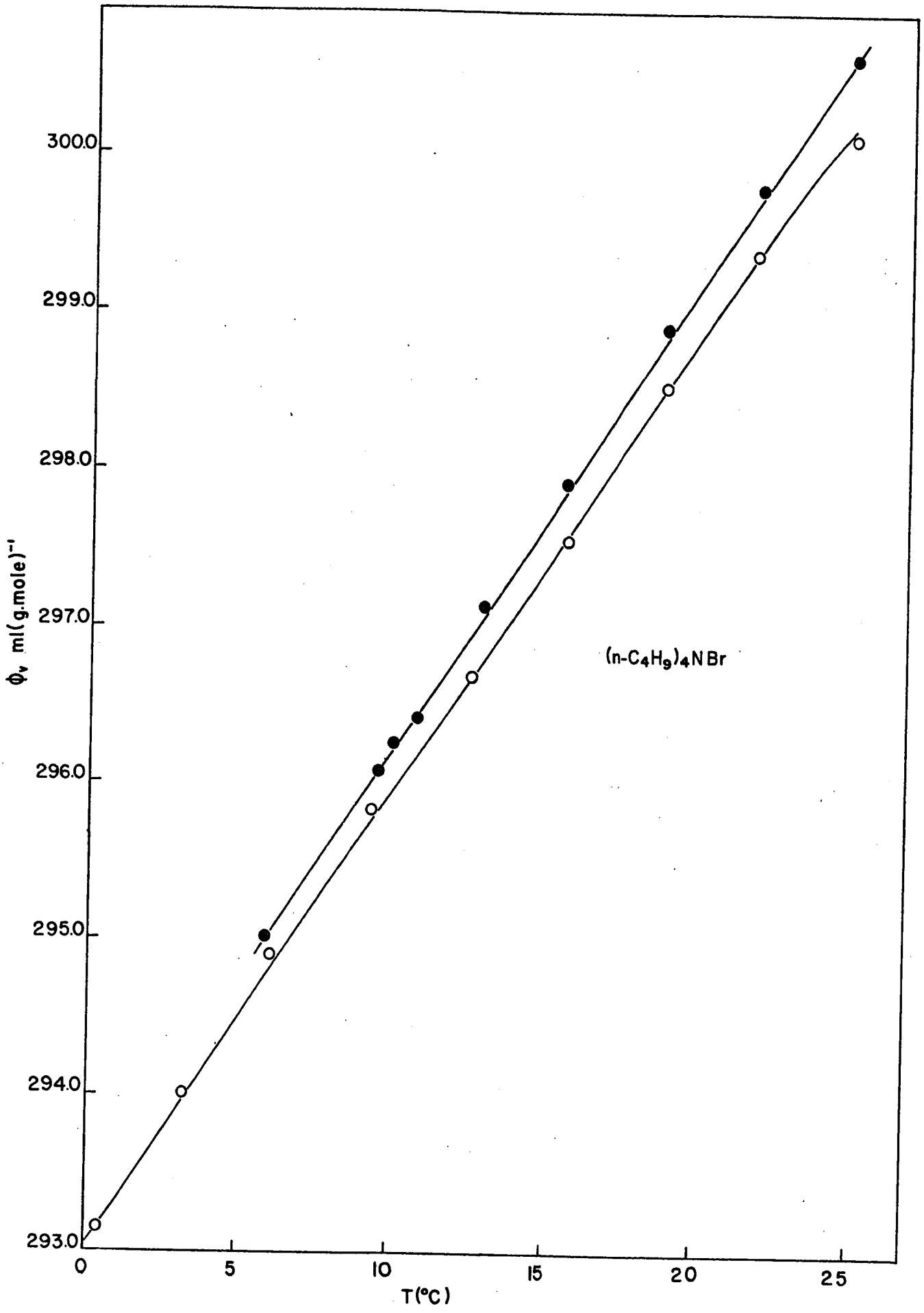
300.0
299.0
298.0
297.0
296.0
295.0
294.0
293.0
ϕ_v ml(g.mole)$^{-1}$
0
5
10
15
20
25
T(°C)
$(n\text{-}C_4H_9)_4NBr$

TABLE 14

Values of the Partial Molal Expansibility at 15°C

Salt	$\bar{E}_2^o$ ml (g.mole.°C)$^{-1}$ ± 0.010 ml (g.mole.°C)$^{-1}$	
	H_2O	D_2O
NaCl	0.131	0.131
NaF	0.120	0.163
KCl	0.107	0.112

	M	$\bar{E}_2$	M	$\bar{E}_2$
$(CH_3)_4NBr$	0.08733	0.144	0.10085	0.108
$(C_2H_5)_4NBr$	0.10250	0.150	0.10597	0.135
$(C_3H_7)_4NBr$	0.08324	0.189	0.09089	0.165
$(C_4H_9)_4NBr$	0.08627	0.289	0.09541	0.295

CHAPTER V

DISCUSSION

1. Introductory Remarks

In considering the ion-solvent interactions determining the behaviour of organic ions, it is necessary to be able to derive values of certain properties such as the partial molar volume pertaining to infinite dilution where secondary ion-ion interactions are absent. With such limiting values for the pair (or more) of ions of the salt, approaches may then be made to the evaluation of the individual ionic contributions to the derived partial molar property. The derivation of the limiting values first requires examination, e.g. with regard to the behaviour of the properties of the salt at high dilution and question of the approach to "Limiting Law" behaviour.

After the limiting values of partial molar volume and compressibility have been considered, the question of additivity of volume contributions is examined in relation to (a) structural effects in hydration and (b) the development of methods for evaluation of individual ionic contributions to the measured properties for the salt. Solvent isotope effects on the partial molar volumes will then be discussed in relation to structural effects and finally relations between the volume and compressibility changes upon ionisation will be discussed in relation to other thermodynamic functions for ionisation processes involving the molecules studied.

2. Limiting Law Behaviour

(i) Tetra-n-alkylammonium Salts

(a) Evaluation of infinite dilution values of the partial molar volume

As was seen in the Introduction, a number of previous studies of the partial molar volume of the TAA salts have been carried out, including those from this laboratory. The evaluation of accurate infinite dilution values of the partial molar volume of these salts has, however, until recently been impossible, because of the lack of ϕ_v data down to sufficiently high dilutions. This problem has arisen since, unlike the simple 1:1 electrolytes such as the alkali halides, the TAA salts exhibit a high degree of non-ideality which persists to very low concentrations. This anomalous behaviour has precluded the use of an extrapolation from high concentration to infinite dilution based on the Debye-Hückel Limiting Law. With the data presented in this thesis, together with other recently published results for Me_4NBr and Bu_4NBr (124, 165), a more complete picture of the concentration dependence of ϕ_v is now available and it is evident that general agreement now exists regarding the values of $\bar{V}_2$ at infinite dilution for the various salts in the TAA series. For n-alkylammonium, pyridinium and piperidinium salts, it was generally possible to approach the limiting law slope at concentrations greater than 0.01 molar.

(b) Structural effects as reflected in ϕ_v

It is now generally accepted that salts such as those in the TAA series affect the structure of the solvent in their vicinity in an unusual way and this is manifested in the characteristic behaviour of the thermodynamic properties of solutions of these salts. The sign and magnitude of the slopes in the plots of ϕ_v against $c^{1/2}$ reflect amongst other factors (see below) the ion-ion interactions which are significant in determining the thermodynamic properties but the details of these interactions, even in a qualitative sense, are not well understood in the case of complex organic ions in water.

The Debye-Hückel theory provides a description of the long-range Coulombic interactions, but in the case of the TAA and other organic salts, large deviations from the limiting law are exhibited which have been variously ascribed, either all or in part to cation-cation pairing (117-119), cation-anion pairing (116), to the solute-solvent size ratio (120) and other aspects of the ion-solvent interaction.

The effect of mutual salting-out, discussed by Conway, Verrall and Desnoyers (120), arises since an ion of finite size forms a cavity in the solution which is less polarizable than the solvent water and this effect was shown to introduce a positive contribution to the concentration dependence of ϕ_v. Another effect known as mutual salting-in (108, 164) will occur with hydrophobic solutes since the presence of some structure enhancing ions will locally order the solvent so that the introduction of subsequent ions will be energetically easier. It is in this

category of interactions that the ion-ion interactions associated with the special behaviour of the water solvent are to be recognised.

Wirth has analysed $\bar{V}_2$ data for the TAA salts in terms of cation-anion association (116) and found significant degrees of association for these salts, although conductance measurements have not revealed any association except in the case of Bu_4NI (96).

Diamond (100) proposed a model based on the idea of "solvent structure enforced" ion pairing. Wen and Nara (117-119) have interpreted their data on volumes of mixing of TAA salts with aqueous alkali halide in terms of Friedman's ionic solution theory. This approach has yielded a quantitative measure of the effect of cation-cation pairing on the volume. It was found that the negative contribution to the volume which was observed decreased with decreasing cation size when the structure of the cation was largely made up of alkyl groups. The introduction of terminal hydroxyl groups into the tetra-n-ethylammonium ion was shown to cause the resulting tetraethanolammonium ion, which is then similar in size to that of $(n\text{-}Pr)_4N^+$, to behave ideally in water due to the more hydrophilic exterior of the ion.

(ii) Neutral Molecules

The variation with concentration of the partial molar volumes of neutral molecules in water-rich solutions is very complex. In the present work, studies have been restricted to the neutral bases in the pyridine and piperidine series and, as was reported in the last chapter, pronounced maxima and minima were observed in the plots

of ϕ_v against c. A similar effect, the presence of a minimum in the plots of ϕ_v against c for the normal alcohols, is well documented (140, 165). In the alcohol series, the minimum shifts to lower alcohol concentration as the hydrophobic portion of the molecule becomes larger. Studies of glycol-water solutions showed the same type of behaviour in the plots of ϕ_v against c.

The excess volume of mixing was calculated for the three pyridines which were studied, and is given by the following equation:

$$\Delta V^E = (x_1 \bar{V}_1 + x_2 \bar{V}_2) - (x_1 V_1^o + x_2 V_2^o) \qquad V.1$$

where x_1 and x_2 are the mole fractions of water and solute, respectively, V_1^o and V_2^o are the molar volumes of the pure components, and $\bar{V}_1$ and $\bar{V}_2$ are the partial molar volumes of water and solute, respectively at the mole fractions x_1 and x_2. The values of ΔV^E are all negative and decrease with concentration as can be seen from the plot shown in Fig. 43. The negative values of ΔV^E observed in the liquid mixtures can be explained in terms of the occupation of cavities in the open solvent structure by the solute and this effect is aided by the hydrophobic nature of the solute which stabilizes the ice-like structure of the solvent in its vicinity. The presence of a maximum or minimum in $\bar{V}_2$ seems to indicate a change in behaviour of the solution which might be due to the total occupation of the most favourable sites in the solution, whereupon a somewhat different configuration could be adopted. The maximum or minimum in the curve relating $\bar{V}_2$ to c will cause a corresponding inflection in

the plots of ΔV^E against x_2 (Fig. 43); for example, the kink in the curve for pyridine in Fig. 43 is significant since a marked minimum is observed experimentally in the curve of ϕ_v vs. c shown in Fig. 10. The behaviour of 2, 6-lutidine is unusual since most "hydrophobic" solutes exhibit a minimum in their partial molar volumes while $\bar{V}_2$ for 2, 6-lutidine goes through a maximum with increasing concentration. One can speculate that the higher basicity of 2, 6-lutidine in comparison with pyridine causes more interaction with the water which destabilizes the hydrophobic interactions associated with the 5 "aromatic" C atoms and the 2 methyl groups. In fact, the partial molar volume of the water decreases at low lutidine concentrations. The hydrophobic effect eventually overcomes this tendency as the volume passes through the maximum.

Figure 43. A plot of the excess volume of mixing ΔV^E against the mole fraction of solute, x_2, for pyridine, 2-methylpyridine and 2, 6-dimethylpyridine in H_2O at 25°C

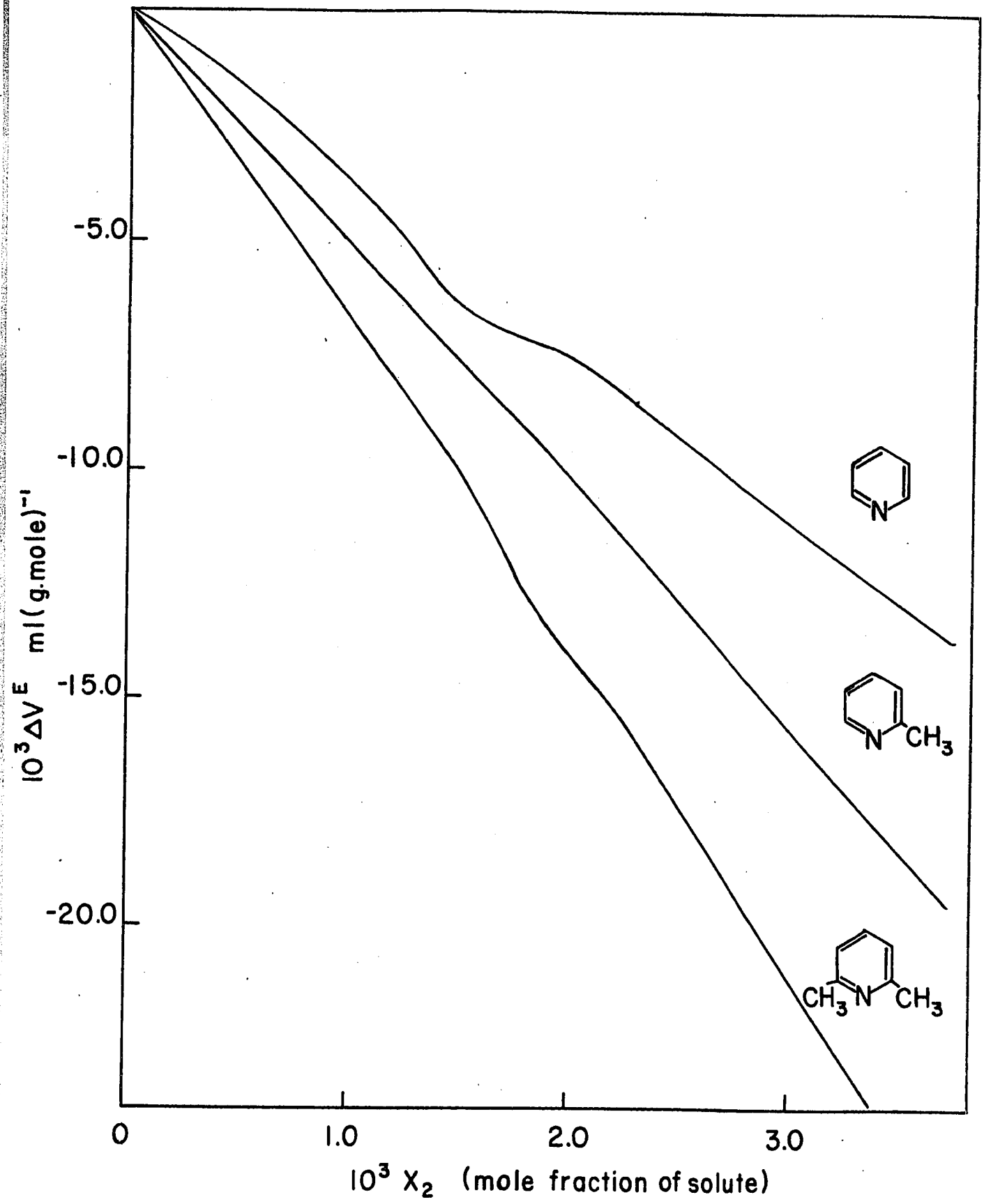
-5.0
-10.0
-15.0
-20.0
$10^3\Delta V^E$ ml(g.mole)$^{-1}$
0
1.0
2.0
3.0
10^3 X_2 (mole fraction of solute)
N
N CH3
CH3 N CH3

3. Linear Additivity Relations

(i) Partial Molar Volumes

It was shown previously (126, 167) for the R_4NX series of salts that values of $\bar{V}_2^o$ were additive in the homologous series of these ions and led, by extrapolation to zero cation molecular weight, to a value for the individual gegen-anion volume in solution. This procedure will be discussed in more detail in the following section. In the different series of salts studied in this work, a similar additivity relation was observed.

Additivity may be expected if (a) the cations in the series are not hydrated or if the extent of hydration of a given type is the same (e.g. electrostriction will be negligible for the TAA cations) for all of the members in the series; this is the case with the R_4NX salts (126); and (b) if the hydration changes progressively due to changes of accessibility of finite sized solvent molecules to the charge centre; this is the case with the pyridinium, piperidinium and alkyl-ammonium ions. In Fig. 44 a plot of $\bar{V}_2^o$ against W_+, the molecular weight of the cation, is shown for the series of salts R_4NI, R_4NCl and $R_xH_{4-x}NCl$ ($R = CH_3$) (126), together with a similar plot based on the data for the series of pyridinium salts.

The values of $\bar{V}_2^o$ for the pyridinium salts fall into two distinct series, those for the N-alkyl substituted salts and those for the pyridine-HCl salts. This distinguishable behaviour illustrates the difference in accessibility of the solvent to the directly (N-alkyl) blocked or indirectly blocked charged centre at the N atom. In Table 15, are listed values of b, the slopes of the linear relations for $\bar{V}_2^o$ against W_+ for the salt series shown in Fig. 44 and also for some other compounds studied. Since the accuracy of most of the individual $\bar{V}_2^o$ is ca. ± 0.05 ml (g.mole)$^{-1}$, differences of better than 0.002 ml.g^{-1} are to be considered significant.

In the symmetrical R_4N^+ series, the coordination at the N^+ centre remains unchanged and the slope b for this series therefore represents the specific volume of added CH_2 groups since electrostriction will be negligible (126). It should be recognized that a structure formation volume related to ionic surface area may, however, be included (168) in this value of b. For the other series of salts referred to in Table 15, the difference of slopes from that for the R_4N^+ series represents the effect of changing extent of hydration due to changes of coordination or steric effects. These differences of b go in the right direction insofar as they are (a) largest for the $R_nH_{4-n}N^+$ series where progressive direct blocking of hydration occurs as $n \rightarrow 4$; (b) less for the pyridine-HCl series where secondary steric effects are involved at C atoms vicinal to the N^+ centre, and (c) least for the N-methylpyridine series where the N^+ centre is somewhat similar to that in R_4N^+ but rather more accessible to solvent molecules due to the geometry associated with the sp^2 hybridation at the N.

Figure 44. A plot of partial molar volume ($\bar{V}_2^o$) against molecular weight of the cation (W_+) for the series of pyridinium chlorides, pyridinium iodides and also for the TAA iodides, chlorides and methyl substituted ammonium chlorides (the latter based on previous work from this laboratory [152]).

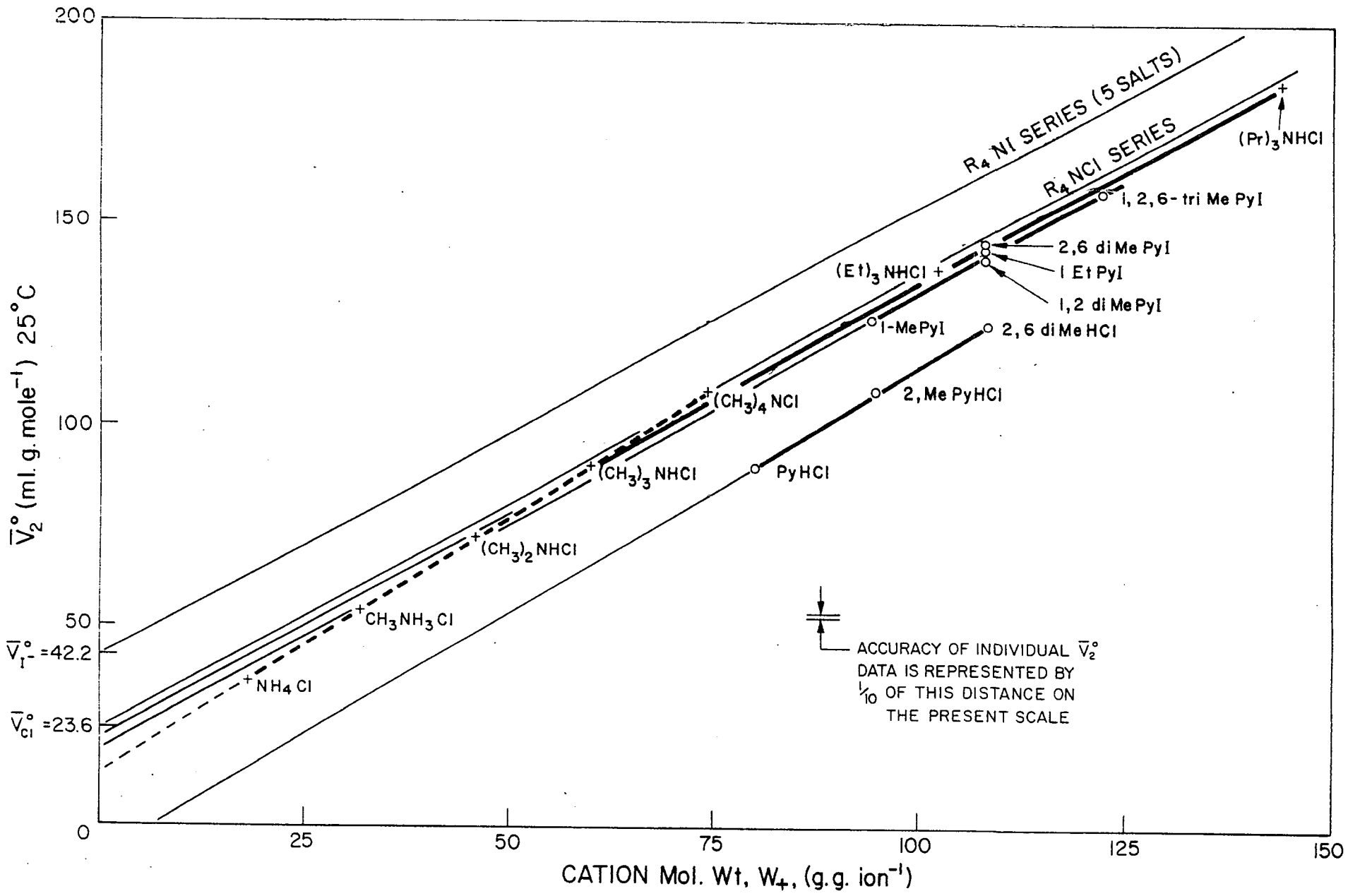
200
150
100
50
0
25
50
75
100
125
150
$\bar{V}_2^\circ$ (ml. g. mole^{-1}) 25°C
CATION Mol. Wt, W_+, (g.g. ion^{-1})
$\bar{V}_{I^-}^\circ$ =42.2
$\bar{V}_{Cl}^\circ$ =23.6
R_4NI SERIES (5 SALTS)
R_4NCl SERIES
$(Pr)_3NHCl$
i, 2, 6- tri Me PyI
2,6 di Me PyI
I Et PyI
1,2 di Me PyI
$(Et)_3NHCl$ +
1-Me PyI
2, 6 di Me HCl
$(CH_3)_4NCl$
2, Me PyHCl
$(CH_3)_3NHCl$
PyHCl
$(CH_3)_2NHCl$
CH_3NH_3Cl
NH_4Cl
ACCURACY OF INDIVIDUAL $\bar{V}_2^\circ$ DATA IS REPRESENTED BY 1/10 OF THIS DISTANCE ON THE PRESENT SCALE

TABLE 15

Values of $d\bar{V}_2^o/dW_+$ Obtained from the Linear Additivity Relations

Series	Slope b ($ml.g^{-1}$)	Accuracy of Slope
$n\text{-}R_4N^+$ (a)	1.115	± .002
$R_xH_{4-x}N^+$ ($R = CH_3$) (a)	1.284	± .002
Pyridine-HCl series (b)	1.227	± .002
N-Me-pyridine series (b)	1.145	± .002
$R_2NH_2^+$ (b) R → Me → Bu	1.155	± .002
RNH_3^+ (c) R → Me → nOCT.	1.150	± .002

(a) Conway and Verrall (126)
(b) Present work
(c) Desnoyers and Arel (132)

The data for the $R_2NH_2^+$ series, where R is varied from methyl to n-butyl, together with that for the RNH_3^+ series studied by Desnoyers and Arel (132), (where R varies from methyl to n-octyl) lead in both cases to b values which are considerably lower than that for the methyl substituted ammonium ion series [$Me_{4-x}NH_x^+$]. This reflects the greater shielding effect (with respect to hydration) of the higher alkyl substituents in these two series.

The RNH_3X and R_2NH_2X series of salts differ from the TAA halides in that there must be a significant electrostriction term in their volumes due to the direct accessibility of the N^+ centre. Assuming that the TAA salts do not themselves cause any electrostriction (126), it is possible to determine the (relative) electrostriction caused by the partially alkyl substituted salts discussed above. This was done by measuring the deviation at a given value of W^+, (i.e. for isomeric ions) of the volume of the salt concerned from the line characterising the linear additivity relation for the TAA salts. The results of these calculations are shown graphically in Fig. 45, where the electrostriction caused by the cation is plotted against its molecular weight. In the series of RNH_3X salts (132), the electrostriction reaches a constant value of -3.5 ml $(g.mole)^{-1}$ after R becomes larger than an n-propyl group. If the substituent is smaller than a propyl group, the influence of the field at the charge centre can evidently still be manifested in the properties of thewater molecule at that coordination position. From the results obtained on the R_2NH_2Cl salt series studied in the present work, it is apparent that when the two R groups are larger than C_2H_5 the electrostriction is completely eliminated. This

Figure 45. A plot of the electrostriction caused by n-alkylammonium cations ($Ve_{(+)}$) against the molecular weight of the cation. (Zero line for ordinate axis, $V_{e(+)} = 0$, corresponds to reference line for the TAA salt series). Data for the $Me_{4-x}NH_x^+$ series are from previous work in this laboratory by Verrall.

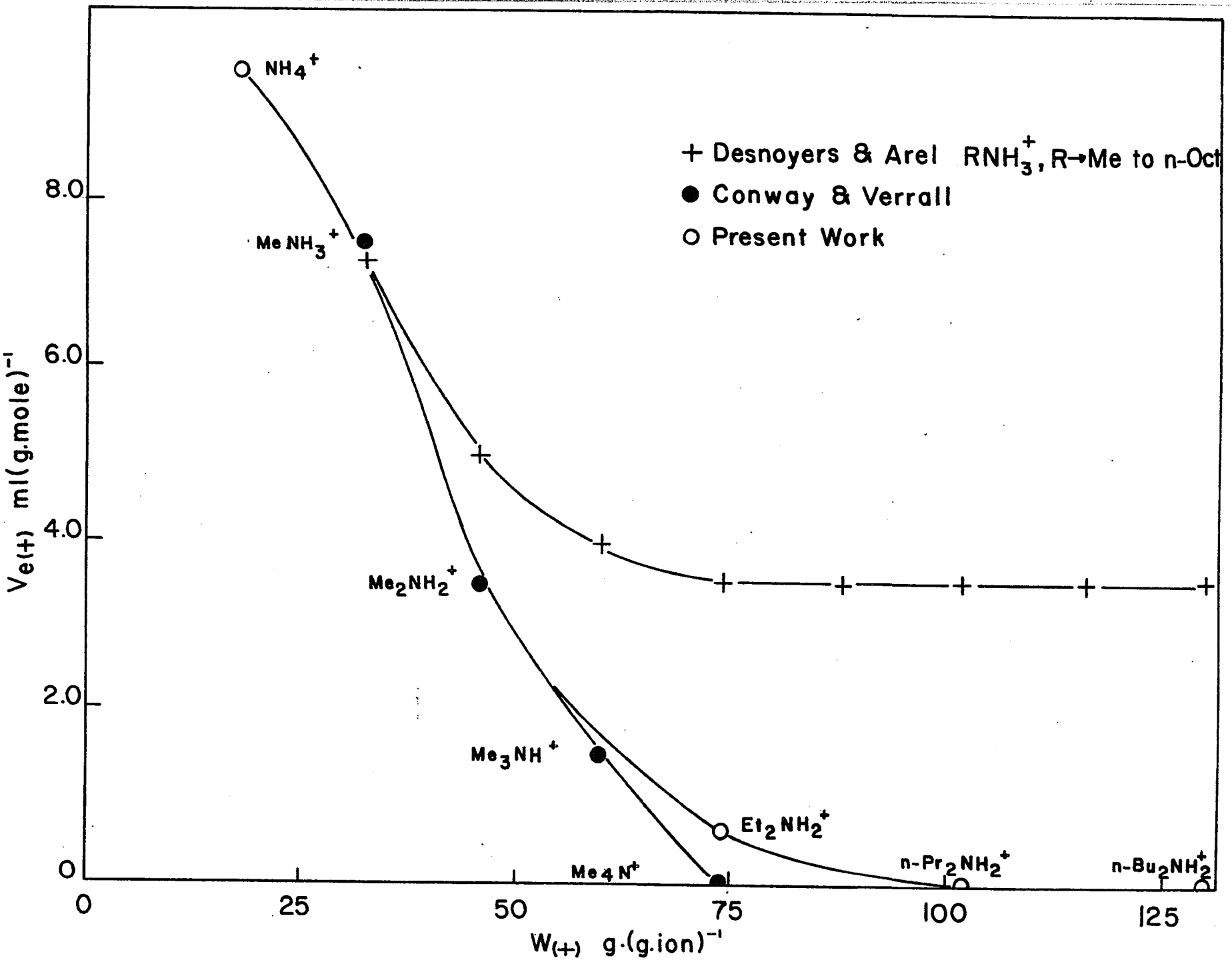
+ Desnoyers & Arel RNH_3^+, R→Me to n-Oct
● Conway & Verrall
○ Present Work
NH_4^+
$MeNH_3^+$
$Me_2NH_2^+$
Me_3NH^+
Me_4N^+
$Et_2NH_2^+$
$n\text{-}Pr_2NH_2^+$
$n\text{-}Bu_2NH_2^+$
$V_{e(+)}$ ml(g.mole)$^{-1}$
$W_{(+)}$ g·(g.ion)$^{-1}$
0
2.0
4.0
6.0
8.0
0
25
50
75
100
125

must be attributed to the ability of the two alkyl groups to shield the positive charge on the nitrogen centre. However, it is of interest to note that when only one alkyl group is present, even when it is a long chain, appreciably more electrostriction remains (Fig. 45). Behaviour similar to that observed with the dialkylammonium salts was found with the trialkylammonium ions Et_3NH^+ and $(n\text{-}Pr)_3NH^+$. The series of methyl substituted ammonium ions studied by Conway and Verrall (126) show, however, the effect of progressive blocking of the charged centre.

The difference in b values in going from the methyl ammonium series to the TAA series suggests that each CH_2 group eliminates a degree of electrostriction of solvent equivalent to 14 X (1.115 - 1.284), i.e. -2.37 ml.mole^{-1}. This is equivalent (cf. the previous calculations, 169, 170) to the effect of a local field of ca. 2.7 x 10^5 e.s.u. which is reasonable for an exposed NH^+ centre (radius ca. 1.05 Å), since 90 per cent of the electrostriction arising at charged centres of small radius can be shown to occur within one H_2O diameter from the centre. Correspondingly, in the methyl ammonium series, it has been estimated (171) that each CH_3 group removed allows an increase of hydration energy of ca. 8 Kcal.mole^{-1}. A similar calculation for the pyridine-HCl salts showed that substitution of methyl groups on the pyridine ring adjacent to the charged nitrogen, eliminated an electrostriction of solvent equivalent to -1.6 ml.mole^{-1}. This lower value of the decrease in the electrostriction reflects the indirect nature of the blocking effect at the charged

centre which arises in the case of the ring substituted pyridinium ions. With the N-methylpyridinium salts, effective primary hydration of the charged nitrogen is prevented; for this case, ring substitution eliminated only -0.42 ml.mole^{-1} of electrostriction. Similarly, in the $R_2NH_2^+$ and RNH_3^+ series, the addition of CH_2 groups is being made at some distance from the charged centre, so that only ca. -0.50 ml.mole^{-1} of net electrostriction is eliminated per CH_2 group added.

(ii) Partial Molar Adiabatic Compressibilities: Additivity and Individual Ionic Contributions

The values of the apparent molar adiabatic compressibilities at infinite dilution for the series of hydrochloride salts of various bases studied were plotted against the molecular weights of the cations and are shown in Fig. 46. Also included in this figure are data for the methyl substituted ammonium ion series from $CH_3NH_3^+$ to $(CH_3)_4N^+$, determined by Conway and Verrall (115). In the ring substituted pyridine-HCl series, $\phi^o_{K(S)}$ also increases in a linear manner with the molecular weight of the cation, W_+, and the same trend was observed with the two piperidine-HCl salts. In the series $Me_2NH_2^+$ to n-$Bu_2NH_2^+$, the behaviour is more complex and illustrates the various effects which determine $\phi^o_{K(S)}$. In going from $Me_2NH_2^+$ to $Et_2NH_2^+$, the hydrophobic nature of the salt has been increased without significantly increasing the shielding of the positive charge and this evidently leads to a decrease in $\phi^o_{K(S)}$. On the other hand, on going from $Et_2NH_2^+$ to n-$Pr_2NH_2^+$, the two n-propyl groups can apparently block the primary hydration of the

Figure 46. A plot of apparent molar adiabatic compressibility at infinite dilution $\emptyset^{o}_{K(S)}$ against the molecular weight of cations in the series of hydrochlorides studied.

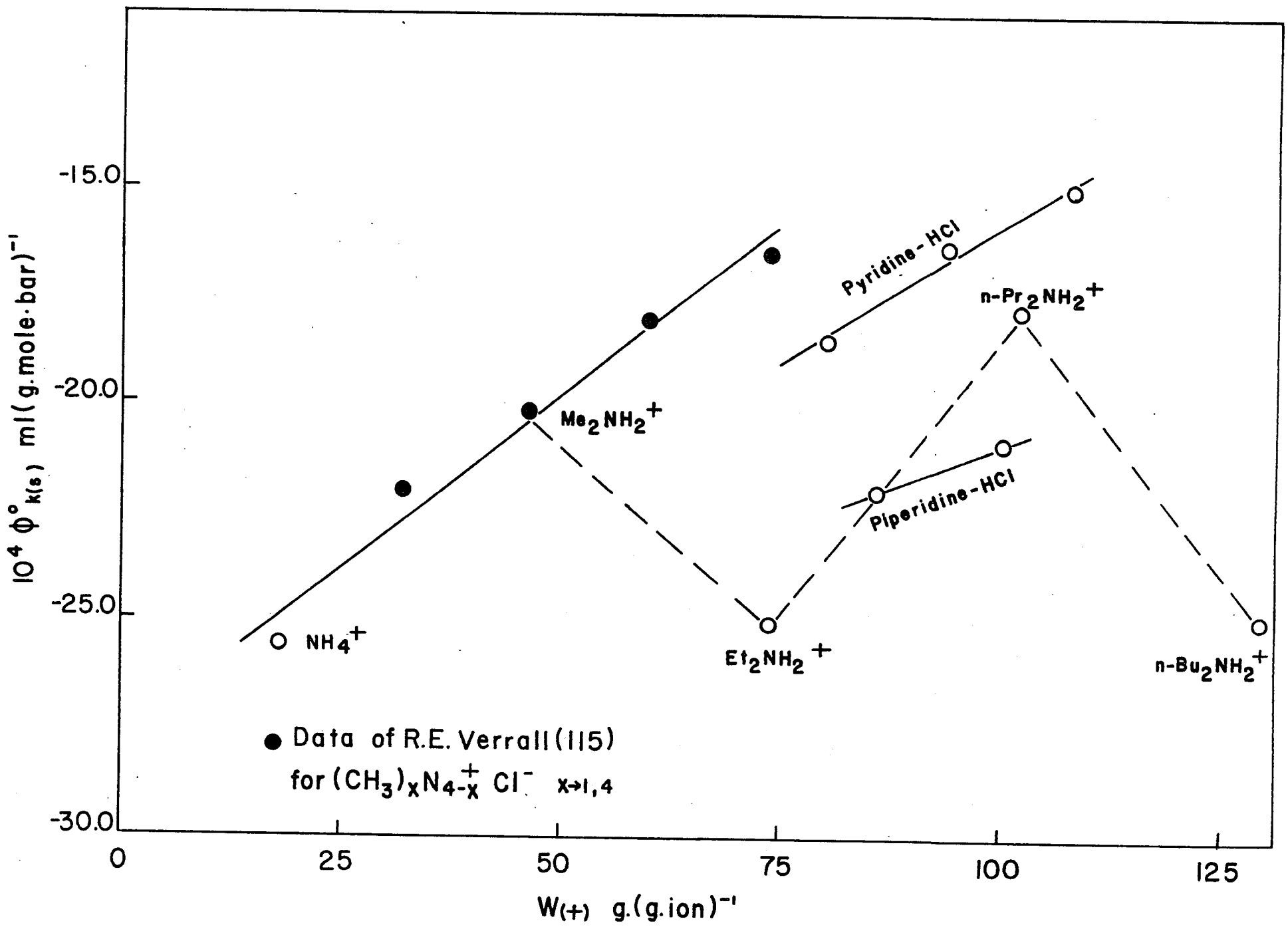
-15.0
-20.0
-25.0
-30.0
$10^4 \phi^\circ_{k(s)}$ ml(g.mole·bar)$^{-1}$
0
25
50
75
100
125
$W_{(+)}$ g.(g.ion)$^{-1}$
NH_4^+
$Me_2NH_2^+$
$Et_2NH_2^+$
$n\text{-}Bu_2NH_2^+$
$n\text{-}Pr_2NH_2^+$
Pyridine-HCl
Piperidine-HCl
● Data of R.E. Verrall (115)
for $(CH_3)_xN_{4-x}^+ Cl^-$ x→1,4

charged centre, thereby diminishing the electrostriction and consequently increasing $\phi^{o}_{K(S)}$. The addition of two further CH_2 groups to the n-propyl salt to give n-$Bu_2NH_2^+$ again increases the hydrophobic character of the ion, leading to a greater volume of less compressible water near the ion and with a resultant further decrease of $\phi^{o}_{K(S)}$. In discussing the trends in the compressibility results, the model proposed by Conway and Verrall (115, 152) has been employed, where electrostricted water and the supposed "ice-like" water surrounding a hydrophobic solute was regarded as essentially incompressible, while "structure broken" water was assumed to be relatively more compressible.

For the pyridinium chloride series investigated, $\phi^{o}_{K(S)}$ changed to more negative values as the coordination by CH_3 groups near to the N^+ centre decreased; N-methylation made only a small further difference (+0.1 to -0.40) to the $10^4\,\phi^{o}_{K(S)}$ value. Using the principle of additivity of ionic contributions to $\phi^{o}_{K(S)}$, $10^4\,\phi^{o}_{K(S)}$ for pyridinium iodide is -1.9, so that N-methylation of pyridinium causes a change in $10^4\,\phi^{o}_{K(S)}$ of $\underline{1.9} + 2.0 = \underline{3.9}$, in comparison with the pyridinium iodide salt, i.e. an effect much larger than that found in the case of 2,6-dimethylpyridinium iodide (Table 16). This is as expected since two vicinal CH_3 groups are evidently almost as effective (in terms of compressibility changes) in blocking access of solvent to the N^+ centre, as direct methylation is at that centre. For comparison, increasing coordination by CH_3 in the series $(CH_3)_xH_{4-x}N^+$ $(x,l \rightarrow 4)$ gives (115) an almost linear incremental change in $10^4\,\phi^{o}_{K(S)}$ of +1.8 ml. $(g.mole.bar)^{-1}$ per CH_3 group (see Table 16).

In all cases, except the addition of the $N\text{-}CH_3$ on the 2,6-pyridinium ion, the changes of $10^4 \phi^o_{K(S)}$ are positive indicating release of previously electrostricted water at the N^+ centre. The volume increment, as well as the $\delta \phi^o_{K(S)}$ for $N\text{-}CH_3$ substitution at the lutidinium ion, is abnormally low presumably because the space between the two CH_3 groups vicinal to the N is relatively inaccessible so there is a smaller volume change than expected in filling this space by another CH_3 group. Correspondingly, release of compressible water, previously electrostricted, is less.

In conclusion, it may be noted that the compressibility variations from one type of ion to another are evidently much more sensitive than are the volume variations to specificities of structure of the molecular ions and to the solvent structure changes which such ions produce in water.

TABLE 16

Values of the Changes, δ , of Partial Molal Compressibility and Volume due to Effects of Neighbouring CH_3 Groups at N^+ Centres

Salt Series		$\delta\ 10^4\ \phi^\circ_{K(S)}$ $ml(g.mole.bar)^{-1}$	$\delta\ \bar{V}^\circ_+$ $ml(g.mole)^{-1}$
Pyridinium	1st CH_3 on ring	+ 2.2	17.6
	2nd CH_3 on ring	+ 3.6	16.76
	N-CH_3 on 2, 6-dimethylpyridinium	- 2.1	13.97
	N-CH_3 on pyridinium	+ 3.9	17.16
Piperidinium	1st CH_3 on N^+	+ 1.1	18.84
	2nd CH_3 on N^+	-	14.50
$R_xH_{4-x}N^+$	1st CH_3	+ 2.0	17.8
	2nd CH_3	+ 1.8	18.6
	3rd CH_3	+ 2.1	18.1
	4th CH_3	+ 1.5	16.7

The changes quoted correspond to addition of 1 CH_3 replacing 1 H (in the ring at the 2 or the 6 position or at the NH^+ centre).

4. Determination of Individual Ionic Properties

(i) General

The measurement of ϕ_v, $\phi_{K(S)}$ and other partial molar properties of salts yields the total value of the property for the salt. Unlike the measurement of kinetic properties, where values of the property associated with each type of ion can be separated, it is not possible by means of any purely thermodynamic principle to separate a partial molar quantity into its ionic components. Various attempts have been made to assign single ion properties, all of which depend on some model for the system under study. Since most theories of ionic solvation are based on electrostatic calculations which are made for individual ions, it is of great importance to establish reliable methods for obtaining the individual ionic contributions from measured experimental data for salts.

The question of the determination of individual ionic properties has been reviewed by Desnoyers and Jolicoeur (23). Most of the methods used rely on an extrapolation based on some function of the radius of the ion in solution and, as such, cannot be considered entirely reliable since there is still some question as to the values of the ionic radii which should be used (172 - 175). Despite these difficulties, there is now fair agreement concerning the individual ionic values for the free energy, entropy, enthalpy and partial molar volume of individual ions. The basis for the assignment of the latter quantity for ions has been the subject of previous work from this laboratory.

In the present work, we have been concerned with developing a satisfactory method for obtaining absolute individual ionic partial molar adiabatic compressibilities. An extrapolation procedure was developed in this laboratory by Conway, Verrall and Desnoyers (126) to determine individual ionic volumes. The values so obtained have been strongly supported by the recent ultrasonic potential measurements of Zana and Yeager (176, 177) which are completely independent of the underlying assumptions made in the extrapolation procedure used above and depend on quite different experimental measurements.

(ii) Extrapolation Procedure

(a) Partial molar volume

The procedure used by Conway, Verrall and Desnoyers (126) to determine individual volumes was based on a plot of the partial molar volume of a series of TAA salts having a common anion, against the molecular weight of the cation. An extrapolation to zero cation molecular weight yielded the partial molar volume of the common co-anion in the series. A review of this procedure, which will be given below, will lead to a better understanding of the limitations involved and allows a related method to be developed for the evaluation of individual $\phi^{o}_{K(S)}$ values.

The total partial molar volume of a salt can be written as:

$$\bar{V}^{o}_{2} = \bar{V}^{o}_{+} + \bar{V}^{o}_{-} \qquad \text{V.2.}$$

where $\bar{V}_+^o$ and $\bar{V}_-^o$ are the individual partial molar volumes at infinite dilution of the cation and anion, respectively. The volume of an ion can further be broken down into various contributions to yield the following expression:

$$\bar{V}_2^o = V_{in(+)} + V_{e(+)} + V_{s(+)} + \bar{V}_-^o \qquad V.3$$

where $V_{in(+)}$ is the intrinsic volume of the ion and is always positive; $V_{e(+)}$ is the electrostriction of the solvent caused by the field of the ion and is always negative, and $V_{s(+)}$ is the structural contribution to the volume due to the inclusion of the ion into a cavity in the solvent (negative effect) and to any increase in "ice-likeness" of the solvent in the vicinity of non-polar groups on the ion (positive effect).

The problem, therefore, is to find a series of ions for which $V_{e(+)}$ and $V_{s(+)}$ are small or zero. The series of tetra-n-alkylammonium salts come closest to the requirement of $V_{e(+)} \rightarrow 0$, since the field at the periphery of these ions will be negligible in terms of electrostrictive effects. There is evidence that the term $V_{s(+)}$ will be negative (129, 178), i.e. the ion may increase the ice-like nature of the solvent in its vicinity, but it will usually be accommodated in the solvent cage so formed with an overall economy of space. The $V_{s(+)}$ term is more difficult to estimate quantitatively, and there is some evidence, to be presented later in this section, that it becomes important only for Bu_4NBr. Assuming, therefore, that $V_{e(+)}$ and $V_{s(+)}$ can be neglected, we are left with only $V_{in(+)}$.

The final assumption made was that the intrinsic volume was proportional to the molecular weight, a supposition well supported by the results previously obtained (126),

$$V_{in(+)} = \frac{W_+}{d_+} \qquad V.4$$

where d_+ is a proportionality constant having the dimensions of density. Equation V.4 implies that the ions in the series have the same density. An alternative method would involve calculating the intrinsic volume of the ion using the ionic radius. For spherically symmetrical ions in water, Conway (126) has given the following relation:

$$V_{in} = 2.52\ r^3 + 3.15\ r^2 \qquad V.5$$

where r is the radius of the ion in Ångstrom units.

By plotting the partial molar volume of the salt against either W_+ or $V_{in(+)}$, the y intercept of the straight line so obtained should be $\bar{V}_-^o$, the partial molar volume of the anion. Since the plots obtained (126) were linear with deviations not exceeding $\pm$ 0.5 ml(g.mole)$^{-1}$ we may conclude that the assumptions made were reasonably valid. Further support for this procedure was provided by Zana and Yeager (176, 177), who obtained a value of $\bar{V}_-^o$ for the Cl^- ion of 23.7 $\pm$ 0.5 ml(g.mole)$^{-1}$, in agreement with the value of 23.6 $\pm$ 0.2 ml(g.mole)$^{-1}$ obtained by Conway and Verrall (126, 152).

We have redeveloped the arguments used to determine the volumes since the same assumptions can be used in part to find the individual ionic $\phi^{o}_{K(S)}$ values.

(b) Partial molar adiabatic compressibility

The partial molar adiabatic compressibility is the pressure derivative of the partial molar volume at constant entropy

$$-\phi^{o}_{K(S)} = \left(\frac{\partial \bar{V}^{o}_{2}}{\partial P}\right)_S = \left(\frac{\partial \bar{V}^{o}_{+}}{\partial P}\right)_S + \left(\frac{\partial \bar{V}^{o}_{-}}{\partial P}\right)_S \qquad V.6$$

This can also be written as:

$$\phi^{o}_{K(S)} = \bar{V}^{o}_{+}\left[-\frac{1}{\bar{V}^{o}_{+}}\left(\frac{\partial \bar{V}^{o}_{+}}{\partial P}\right)_S\right] + \phi^{o}_{K(S)(-)} \qquad V.7$$

where the term $-\frac{1}{\bar{V}^{o}_{+}}\left(\frac{\partial \bar{V}^{o}_{+}}{\partial P}\right)_S$ is similar to a specific compressibility and will be replaced by $\bar{\beta}^{o}_{+}$. For the series of salts, Me_4NI to Pr_4NI, studied by Conway and Verrall (162) and for four N-alkyl substituted pyridinium iodides studied in the present work, $\bar{\beta}^{o}_{2}$ is essentially a constant, where $\bar{\beta}^{o}_{2}$ is equal to the total partial molar compressibility divided by the total partial molar volume. The observation that $\bar{\beta}^{o}_{2}$ is approximately constant implies that the nature and not the extent of hydration remains constant in the series. In fact $10^6\,\bar{\beta}^{o}_{2} = -0.7 \pm 1.0\ \text{bar}^{-1}$ for the series of iodide salts described above.

Equation V.7 can therefore be written as:

$$\phi^{o}_{K(S)} = V_{in(+)} \cdot \bar{\beta}^{o}_{+} + \phi^{o}_{K(S)(-)} \qquad V.8$$

where $V_{e(+)}$ and $V_{s(+)}$ have been assumed to be negligible as in the case of the partial molar volumes. Finally, Equation V.8 can be written with $V_{in(+)}$ in terms of W_+ to yield:

$$\phi^{o}_{K(S)} = W_{+}\left(\frac{\bar{\beta}^{o}_{+}}{d_{+}}\right) + \phi^{o}_{K(S)(-)} \qquad V.9$$

The data were plotted according to Equation V.9 (Fig. 47) and a fairly straight line was obtained up to the W_+ value corresponding to Pr_4NBr. From the $-\partial \bar{V}_2 / \partial P$ intercept, a value of $+6.0 \pm 1.0 \times 10^{-4}$ ml(g.mole.bar)$^{-1}$ was obtained for $\phi^{o}_{K(S),I^-}$. A similar plot using the data of Conway and Verrall (152) for the TAA bromides, yielded a value of -3.8 ± 1.0 for $10^4\,\phi^{o}_{K(S),Br^-}$. These two results agree with the thermodynamically determinable difference in $10^4\,\phi^{o}_{K(S)}$ between an iodide and a bromide salt with a common cation, as listed in Table 6. In the above plot, the datum for Bu_4NBr does not fall on the line and in fact exhibits a large negative compressibility.

A similar analysis of the partial molar compressibilities of the TAA chlorides by Millero and Drost-Hansen (129) also yielded a straight line but with the result for Bu_4NBr displaced from the line and indicating an abnormally high expansibility.

Figure 47. A plot of apparent molar adiabatic compressibility at infinite dilution against the molecular weight of the cations for a series of tetra-n-alkylammonium iodides (based on data of ref. 152) (O) and pyridinium iodides (●).

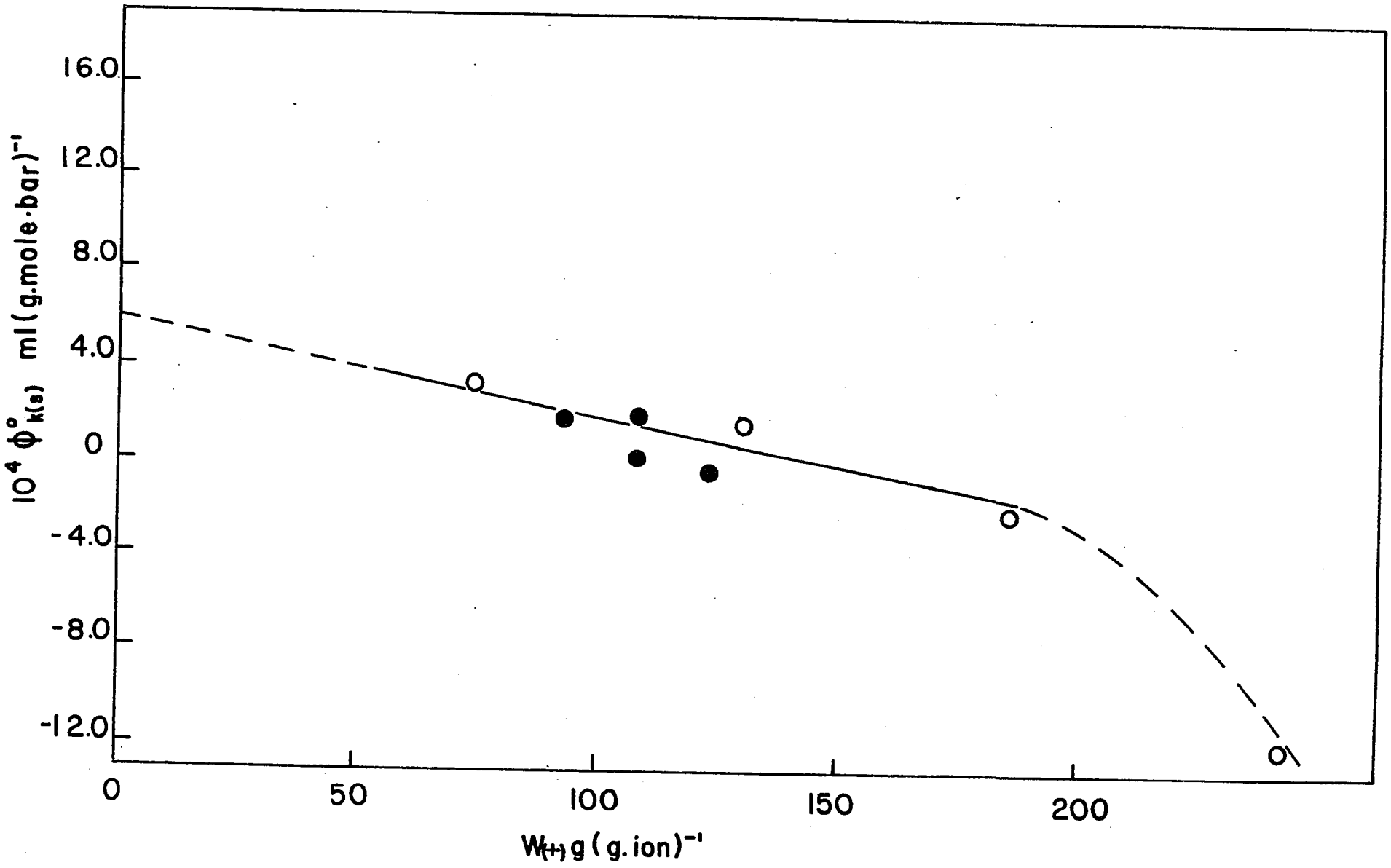
16.0
12.0
8.0
4.0
0
-4.0
-8.0
-12.0
$10^4 \phi^\circ_{k(s)}$ ml(g.mole·bar)$^{-1}$
0
50
100
150
200
$W_{(+)}$ g (g.ion)$^{-1}$

We have remarked above that the partial molar compressibilities reflect more sensitively than do the volumes any specificities in ion-solvent interactions. Hence, in proposing the above method for evaluation of individual ionic compressibilities by extrapolation of the $\phi^{o}_{K(S)}$ values with respect to W_{+}, it must be recognised that the procedure may not be so unambiguous as in the case of the analogous extrapolation of $\bar{V}^{o}_{2}$ data. For example, a progressive structural contribution $V_{s(+)}$ in $\phi^{o}_{K(S)}$, varying with molecular weight of the cation, might still be present in the data plotted in Fig. 47. However, since the data for the pyridinium series as well as for the TAA series, which have rather different molecular structures, seem to fall with reasonable consistency on the same line, it is felt that the extrapolation procedure is justified. Assuming that the conditions outlined above are justified, we estimate that the uncertainty in the $\phi^{o}_{K(S)}$ value for the iodide ion in water at 25°C is $\pm 1.0 \times 10^{-4}$ ml(g.mole.bar)$^{-1}$ as indicated in Table 17.

Using the values of $\phi^{o}_{K(S)(ion)}$ determined above, it is possible to construct an absolute scale of partial molar adiabatic compressibilities. In Table 17 a list of the $\phi^{o}_{K(S)}$ values for individual ions has been given, together with the $\bar{V}^{o}_{(ion)}$ (152) and $\bar{E}^{o}_{(ion)}$ (129) data where available.

TABLE 17

Values of Individual Ionic Partial Molar Volumes, Compressibilities and Expansibilities

Ion	$\bar{V}^{o}_{ion}$ ml(g.mole)$^{-1}$ ± 0.2 ml(g.mole)$^{-1}$ (a)	$10^{2}(\frac{\partial \bar{V}^{o}_{ion}}{\partial T})_{P}$ ml(g.mole.^{o}C)$^{-1}$ (b)	$10^{4}(\frac{\partial \bar{V}^{o}_{ion}}{\partial P})_{s}$ ml(g.mole.bar)$^{-1}$ ± 1.0 ml(g.mole.bar)$^{-1}$ (a)
H^+	- 5.7	- 1.2	- 3.9
NH_4^+	12.8 *	- 3.0	+ 13.4 *
$CH_3NH_3^+$	30.2	-	+ 10.0
$(CH_3)_2NH_2^+$	48.9	-	+ 7.6
$(CH_3)_3NH^+$	67.0	-	+ 5.9
$(CH_3)_4N^+$	83.4 *	+ 3.1	+ 3.8
$(C_2H_5)_4N^+$	142.8 *	+ 5.2	+ 4.4
$(C_3H_7)_4N^+$	208.5 *	+ 9.3	+ 8.3
$(C_4H_9)_4N^+$	270.1 *	+ 17.5	+ 17.9
$(C_2H_5)_2NH_2^+$	83.1 *	-	+ 13.0 *
$(C_3H_7)_2NH_2^+$	115.1 *	-	+ 5.7 *
$(C_4H_9)_2NH_2^+$	147.1 *	-	+ 12.8 *
BF_4^-	49.0 *	-	- 21.8 *
Cl^-	23.6	+ 4.8	+ 12.2 *
Br^-	30.9	+ 3.5	+ 3.8
I^-	42.2	-	- 6.0 *

K^+	3.2 *	+ 3.5	+ 33.3 *
Pyridinium	67.4 *	-	+ 6.4 *
1-Me-pyridinium	84.6 *	-	+ 7.5 *
1,2-di-Me-pyridinium	100.4 *	-	+ 6.1 *
1,2,6-tri-Me-pyridinium	116.0 *	-	+ 5.6 *
1-Et-pyridinium	101.8 *	-	+ 8.0 *
Piperidinium	83.1 *	-	+ 9.8 *
1-Me-piperidinium	101.9 *	-	+ 8.7 *
1,1-Dimethylpiperidinium	116.5	-	-

(a) Conway and Verrall (126, 152)

(b) Millero and Drost-Hansen (129)

* Present results

The quantity $-\left(\frac{\partial \bar{V}^{o}_{ion}}{\partial P}\right)$ is made up of three terms which involve the pressure derivative of V_{in}, V_e and V_s. $\left(\frac{\partial V_{in}}{\partial P}\right)$ will be negative or close to zero since it involves the compressibility of the ion itself and the dead space between the ion and the solvent molecules. For the larger TAA ions, $V_{e(+)}$ will be negligible; therefore, we are left with a large positive value for $\frac{\partial V_{s(+)}}{\partial P}$. This is in accord with current thoughts about the hydration of hydrophobic groups, since the structural volume term, V_s, is thought to be made up of a positive contribution due to the local enhancement of structure in the solvent and a negative contribution due to the inclusion of the ion in cavities formed in the solvent. If, as has been proposed, V_s is negative (129, 178), positive values of $\frac{\partial V_{s(+)}}{\partial P}$ and $\frac{\partial V_{s(+)}}{\partial T}$ (129) would indicate that the enhancement of solvent structure ceases to be significant with increasing temperature and pressure from which it is to be concluded that the ions are less able to influence the formation of the solvent cages. Possibly the average size of the cages is decreasing and thus cooperative effects such as cation-cation pairing (117-119) become less significant and this leads to an overall increase in partial molar volume of the ions; these latter considerations apply, of course, to finite but small concentrations.

5. Solvent Isotope Effect

(i) General

A comparison of the thermodynamic properties of ionic solutions in light and heavy water might be expected to provide information concerning the degree to which these properties are sensitive to the rather subtle differences (20, 32, 53, 179-184) in the properties of the two solvents.

Previous solvent isotope studies on properties of ionic solutions have involved measurements of the heats of dilution of LiCl, NaCl and NaI solutions in D_2O (162). Davies and Benson (185) have also measured heats of solution in H_2O and D_2O. They concluded that salts such as NaF tended to decrease the degree of structure in water and that the structure-breaking effect was greatest in D_2O, in agreement with the observed (186) positive entropies of transfer from H_2O to D_2O. A conductance (99) and a viscosity (94) study of TAA salts in D_2O showed that the ratio of the Walden product in D_2O to that in H_2O was greater than unity in the case of salts which are considered to be hydrophobic structure makers, while a ratio of less than one was observed for structure-breaking salts. Other work of a thermodynamic and spectroscopic kind has been carried out on D_2O solutions (187-188).

(ii) Partial Molar Volumes

The present work was initiated in order to see if a solvent isotope effect was observable in ionic partial molar volumes; in particular, the possibility was envisaged that the structure-forming organic ions might have greater volumes in D_2O than in H_2O, while structure-breaking and electrostricting ions might have a smaller volume in D_2O than in H_2O. Robertson et al.(134) measured the apparent molar volumes of NaF, NaI and $Na\emptyset SO_3$ in H_2O and D_2O and found that the apparent molar volumes were all less in D_2O than in H_2O. The present work shows that an isotope effect $\Delta\bar{V}^o_{D_2O-H_2O}$ is measurable and in fact reaches appreciable values for compounds such as NaF at one end of the scale and $(n\text{-}Bu)_4NBr$ at the other. Of particular interest was the observation of a positive isotope effect (i.e. $\bar{V}^o_{2(D_2O)} > \bar{V}^o_{2(H_2O)}$) for "structure-forming" ions and a negative effect for what are commonly regarded as the "structure-breaking" ions.

Since H_2O and D_2O molecules are approximately the same size, i.e. bond lengths are identical (32) to within 0.001Å, differences in $\bar{V}^o_2$ must reflect the degree to which the solute affects the structure of the solvent. The isotope effect $\Delta\bar{V}^o_{D_2O-H_2O}$ can be regarded therefore as the difference between the electrostriction or structure formation volume in H_2O and D_2O and it might be expected that $\Delta\bar{V}^o_{D_2O-H_2O}$ would be related to the field strength at the ion in the same way as is the electrostricted volume (126). We have estimated the field strength acting on the water in the first hydration layer using the following equation:

$$\bar{E} = \frac{q}{\epsilon(r_{ion} + r_{H_2O})^2} \qquad V.10$$

ϵ was taken as ca. 2 since local dielectric saturation will prevail in the primary solvation region at least with the inorganic ions. The r_{ion} values were taken from Gourary and Adrian (174) for the inorganic ions, and from ref. (152) for the organic ions. It was also assumed that the organic ions were not "electrostatically" hydrated, i.e. no r_{H_2O} term is involved in Equation V.10. The results of these calculations are presented in Table 18 and a plot of $\Delta\bar{V}^o_{D_2O-H_2O}$ against the mean ionic field $\bar{E}$ is shown in Fig. 48. The plot of $\Delta\bar{V}^o_{D_2O-H_2O}$ against $\bar{E}$ shows a reasonable linearity considering the possible errors in $\Delta\bar{V}^o_{D_2O-H_2O}$ and the assumptions made in the calculcation of $\bar{E}$. The values of $\bar{E}$ obtained using Equation V.10 and used in this plot are only intended to illustrate the trend in the results for various salts and no special significance should be attached to the absolute values of $\bar{E}$. For example, a similar trend results if the data are plotted in terms of the field in the primary hydration layer of the cation itself

TABLE 18

Values of the Mean Field $\bar{E}$ in the First Solvent Coordination Layer and Values of the Solvent Isotope Effect on the Partial Molar Volume $\Delta\bar{V}^{o}_{D_2O-H_2O}$ for a Series of Inorganic and Tetra-n-alkylammonium Ions

Solute	$\Delta\bar{V}^{o}_{D_2O-H_2O}$ ml(g.mole)	$\bar{E}$ (10^5 e.s.u.)
NaF	- 1.42	3.70
NaCl	- 0.86	3.15
NaBr	- 0.34	3.05
KCl	- 0.37	2.77
KBr	- 0.20	2.64
$(CH_3)_4NBr$	- 0.11	2.66
$(C_2H_5)_4NBr$	+ 0.20	2.18
$(n\text{-}C_3H_7)_4NBr$	+ 0.42	1.95
$(n\text{-}C_4H_9)_4NBr$	+ 0.94	1.82

Figure 48. A plot of $\Delta \bar{V}^{o}_{D_2O\text{-}H_2O}$ against the mean field strength $\bar{E}$ in the first solvent hydration layer for a series of alkali halides and tetra-n-alkylammonium bromides

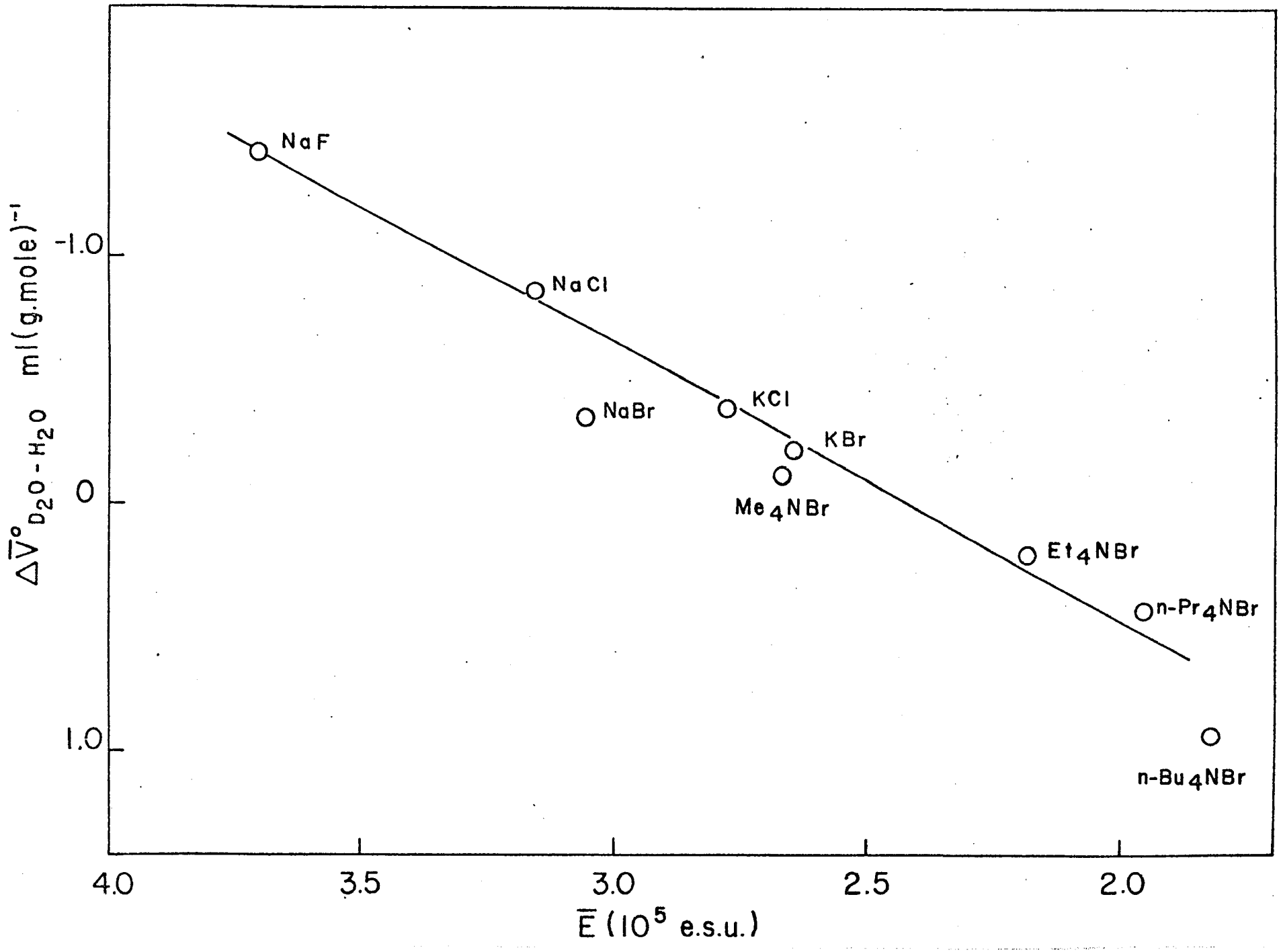
NaF
NaCl
NaBr
KCl
KBr
Me4NBr
Et4NBr
n-Pr4NBr
n-Bu4NBr
-1.0
0
1.0
4.0
3.5
3.0
2.5
2.0
ΔV̄°D2O - H2O ml(g.mole)⁻¹
Ē (10⁵ e.s.u.)

(iii) Individual Ionic Volumes in D_2O

In the previous section, the extrapolation procedure used by Conway and Verrall (126) to determine the partial molar volume of a halide ion in H_2O was reviewed. It was shown that

$$\bar{V}^o_{2(H_2O)} = \bar{V}^o_{-(H_2O)} + b_{(H_2O)}W_+ \qquad V.11$$

where the subscript (H_2O) refers to the partial molar volume in H_2O, while $\bar{V}_{2(D_2O)}$ will refer to the quantities in D_2O, i.e.

$$\bar{V}^o_{2(D_2O)} = \bar{V}^o_{-(D_2O)} + b_{D_2O}W_+ \qquad V.12$$

Subtraction of V.12 from V.11 gives:

$$\bar{V}^o_{2(D_2O)} - \bar{V}^o_{2(H_2O)} = \Delta\bar{V}^o_{D_2O-H_2O} = (\bar{V}^o_{-(D_2O)} - \bar{V}^o_{-(H_2O)}) + W_+(b_{D_2O} - b_{H_2O}) \qquad V.13$$

Therefore a plot of $\Delta\bar{V}^o_{D_2O-H_2O}$ against W_+ should also give a straight line but with a slope of $(b_{D_2O} - b_{H_2O})$ and an intercept $\Delta\bar{V}^o_{(-)(D_2O-H_2O)}$, where $\Delta\bar{V}^o_{(-)(D_2O-H_2O)}$ is the difference in partial molar volume between, in the present case, a bromide ion in D_2O and in H_2O. Since $\bar{V}^o_{H_2O(Br^-)}$ is known, then a scale of absolute volumes can also be obtained in D_2O. Using the data from Table 12,

the plot shown in Fig. 49 was obtained. From Fig. 49 a value of -0.53 was obtained for $\Delta\bar{V}^{o}_{D_2O\text{-}H_2O(Br^-)}$. In Fig. 49 the uncertainty associated with $\Delta\bar{V}^{o}_{D_2O\text{-}H_2O}$ for each of the four TAA bromides is indicated by the error bars. The uncertainty in the values of $\Delta\bar{V}^{o}_{D_2O\text{-}H_2O}$ for $(n\text{-}Pr)_4NBr$ and $(n\text{-}Bu)_4NBr$ is larger than for the first two members of the series, since the extrapolations to infinite dilution were made from a higher concentration.

The least squares uncertainty in the intercept, $\Delta\bar{V}^{o}_{D_2O\text{-}H_2O}$, of the plot shown in Fig. 49 is estimated as ± 0.05 ml $(g.mole)^{-1}$. The value of $\Delta\bar{V}^{o}_{D_2O\text{-}H_2O,(Br^-)}$ together with $\bar{V}^{o}_{H_2O(Br^-)}$ yields a value of 30.4 ml $(g.mole)^{-1}$ for the partial molar volume of the bromide ion in D_2O. Using the above value for $\Delta\bar{V}^{o}_{D_2O\text{-}H_2O(Br^-)}$, the differences in the partial molar volume of the ions studied in D_2O and H_2O were calculated and are listed in Table 19. Although the uncertainty in $\Delta\bar{V}^{o}_{D_2O\text{-}H_2O}$ for individual ions is of the order of ± 0.05 $ml(g.mole)^{-1}$, the uncertainty associated with the total value of the individual ionic partial molar volume depends on the plot of $\Delta\bar{V}^{o}_{2}$ vs. W_+ for the TAA bromides (126, 152). This was estimated by Conway and Verrall (126) as ± 0.2 $ml(g.mole)^{-1}$ and therefore the uncertainty associated with the $\bar{V}^{o}_{ion}$ values listed in Table 19 is ca. 0.2 $ml(g.mole)^{-1}$.

Figure 49. A plot of $\Delta \bar{V}^{o}_{D_2O\text{-}H_2O}$ against W_+ for a series of tetra-n-alkylammonium bromides.

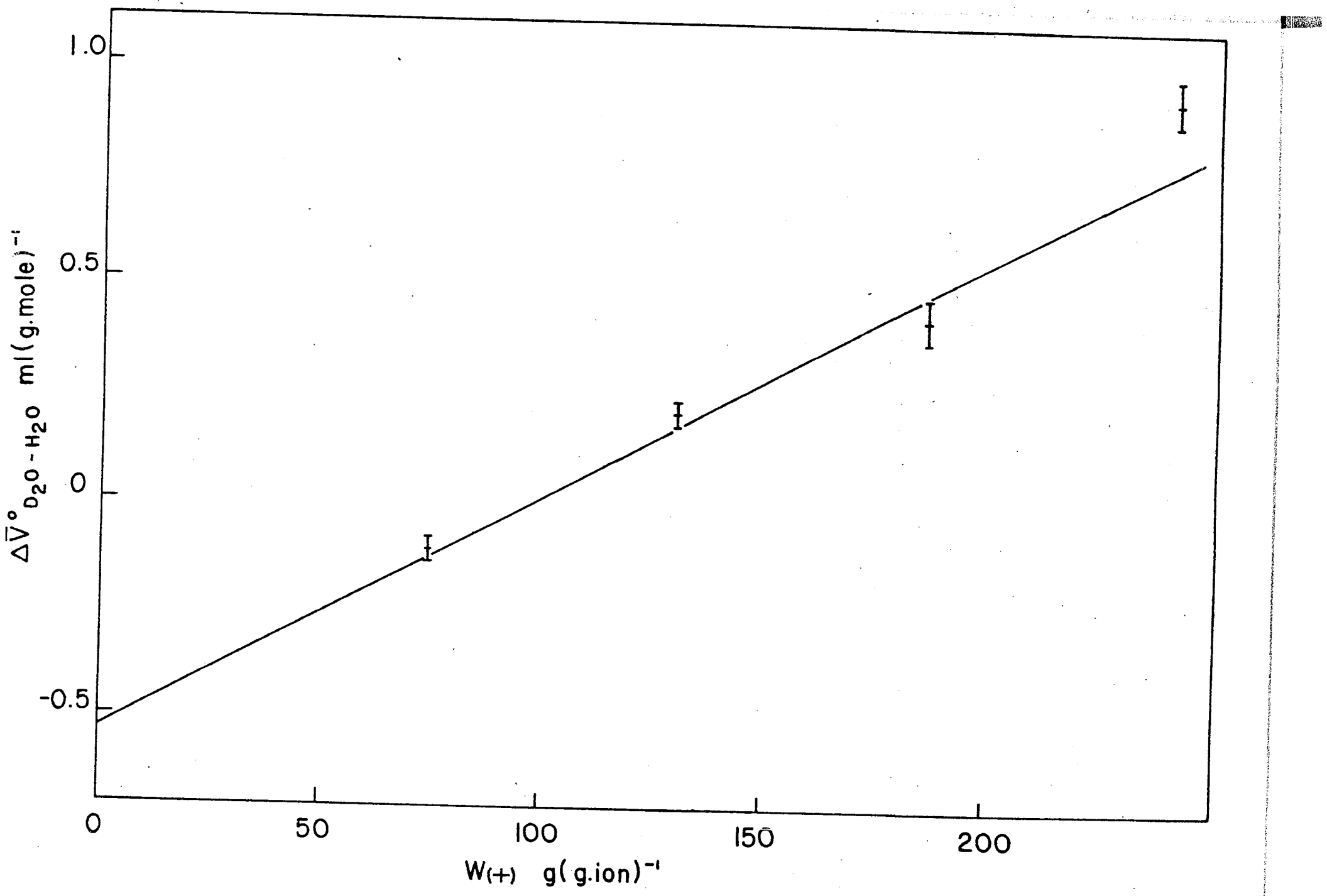
1.0
0.5
0
-0.5
$\Delta\bar{V}^{\circ}_{D_2O-H_2O}$ ml(g.mole)$^{-1}$
0
50
100
150
200
W(+) g(g.ion)$^{-1}$

TABLE 19

Values of the Individual Ionic Partial Molar Volume of a Series of Ions in H_2O (126,152) and in D_2O

Ion	$\bar{V}^o_{ion(H_2O)}$ ml(g.mole)$^{-1}$ ± 0.2 ml(g.mole)$^{-1}$	$\bar{V}^o_{ion(D_2O)}$ ml(g.mole)$^{-1}$ ± 0.2 ml(g.mole)$^{-1}$
F^-	4.6	3.3
Cl^-	23.6	22.9
Br^-	30.9	30.4
Na^+	-7.0	-7.1
K^+	+3.2	3.5
Me_4N^+	83.4	83.8
Et_4N^+	142.8	143.5
$n\text{-}Pr_4N^+$	208.5	209.4
$n\text{-}Bu_4N^+$	270.1	271.5

(iv) Discussion of the Isotope Effect

Although the model for the structure of liquid D_2O presented by Némethy and Scheraga (32) has been criticised (35) in regard to some of its quantitative predictions, it is felt that the general conclusions regarding the structure of D_2O are still to be regarded as valid. The trend in the isotope effect can be rationalised on the basis of current models and particularly on the basis of the differences between the structure and "hydrogen" bonding in the two solvents. Although the cluster size (32, 182) at low temperature is considerably higher in D_2O compared with that in H_2O, it falls much faster with increasing temperature and both solvents appear to have nearly the same degree of "order" at high temperatures. This can also be seen by examining the melting points which differ by $3.8^{o}C$ while the boiling points differ only by $1.4^{o}C$. The fact that D_2O has a higher heat capacity than H_2O (152) could be interpreted as being due to its having structured regions which are more susceptible to "melting". The higher compressibility (181) would also support these conclusions.

The results of this part of the work lead to the conclusion that both structure-making and structure-breaking effects are greater in magnitude in D_2O than in H_2O. For the structure-breaking and hydrophilic alkali halides, this is immediately evident since the lower values of $\bar{V}_2^o$ in D_2O could only be due to a larger value of the electrostriction term (V_e) brought about by the destruction of structure in the more structured solvent. In the case of the hydrophobic structure forming ions, we have argued, as have others (129, 178), that the structural volume

term (V_s) is negative in H_2O. Since the volume of a TAA ion is greater in D_2O than in H_2O, $|V_s(D_2O)| < |V_s(H_2O)|$, but is still negative.

Solutes such as the ones used here can cause a shift in the structural temperature of the solvent. Worley and Klotz (60), by means of infra-red measurements, have measured the structural temperature of solutions of structure-making and structure-breaking ions and found, for example, that a 0.641 molar $(n\text{-}Bu)_4NBr$ solution in H_2O causes a shift of -3^oC in the structural temperature, i.e. the hydrophobic salt affects the structure of the solvent in a manner which is analogous to lowering the temperature of the pure solvent. As we have seen, one of the results obtained by Némethy and Scheraga (182) in their calculations on D_2O was that the average size of the hydrogen bonded clusters was greater in D_2O than in H_2O. It was also shown that the rate of cluster breakdown was higher in D_2O than in H_2O as the temperature was increased. Therefore a solute which has the effect of lowering the structural temperature of water will bring about an increase in the average cluster size. The cluster size will thus increase faster in D_2O than in H_2O and consequently will lead to a higher partial molar volume for the salt in D_2O.

Only a brief mention will be made of the concentration dependence of $\Delta\bar{V}_{D_2O\text{-}H_2O}$, since the cross-over seen with $n\text{-}Pr_4NBr$ and $n\text{-}Bu_4NBr$ in the plots of ϕ_v vs. concentration in H_2O and D_2O (Figs. 31, 32) is the result of rather complex ion-ion and ion-solvent interactions at the higher concentrations. The large negative slopes of the plots of ϕ_v against $c^{1/2}$ observed for the higher TAA salts in H_2O

have been ascribed to various effects (116-119). Since D_2O can be considered as a more highly structured form of H_2O, it is not surprising that an even larger negative slope should be observed in this solvent.

The behaviour of the partial molar volume of $(DOC_2H_4)_3NDBr$ in D_2O (Fig. 33) demonstrates the fact that the positive isotope effect associated with hydrophobic ions is due to the alkyl groups. This large but non-hydrophobic solute behaves like a "normal" 1:1 electrolyte.

(v) Neutral Solutes in D_2O

As discussed earlier in this chapter, an examination of the behaviour of a few selected neutral compounds was also carried out in D_2O.

A study of the partial molar volume of HOD in H_2O and D_2O showed that the volume of HOD in D_2O was greater than in H_2O. Since a deuterium bond is more "stable" than a hydrogen bond (183), a D_2O molecule in the vicinity of HOD will preferentially "hydrogen" bond to another D_2O-solvent molecule rather than with the H on the HOD. Thus HOD in D_2O will act as a structure maker although it can hardly be called hydrophobic. In the case of HOD in H_2O, the converse of the above effect would apply, i.e. preferential bonding will occur between the D on HOD and the H_2O solvent, making the properties of HOD in H_2O similar to those of a "structure breaker".

The other neutral molecule studied was pyridine, which can be considered as a hydrophobic structure maker. Its volume in D_2O is found to be larger than in H_2O and the curious concentration dependence observed in H_2O for this solute is reproduced in D_2O.

6. Volume and Compressibility Changes Resulting from Ionisation

The volume and compressibility changes upon acid ionisation, i.e. in processes of the type $BH^+ + H_2O \rightleftharpoons B + H_3O^+$, were calculated from the ϕ_v^o and $\phi_{K(S)}^o$ data for molecules in the pyridine and piperidine series. The individual ionic volumes quoted are based on the scale $\bar{V}_{I^-}^o = 42.2$ ml(g.mole)$^{-1}$ (126). The results for the pyridine series are shown in Table 20, together with the data for ΔH_i^o, ΔG_i^o and ΔS_i^o obtained by Laidler and co-workers (189-190). Also shown in Table 20 are the $\Delta \bar{V}_i^o$ and $\Delta \phi_{K(S)i}^o$ data for the piperidine series.

Systematic relations between $\Delta \phi_{K(S)i}^o$ and $\Delta \bar{V}_i^o$ and the other thermodynamic functions were found only in the case of ΔG_i^o (Fig. 50). In the case of 2, 6-dimethylpyridinium chloride, the curiously shaped concentration dependence of the sum of the ϕ_v's for the neutral base and the free acid runs specifically parallel to the variation of ϕ_v with concentration for the salt, so that the difference $\Delta \bar{V}_i$ is largely independent of concentration (Fig. 51).

TABLE 20

Values of $\Delta\bar{V}_i^o$ and Other Thermodynamic Data for the Ionisation Process in the Pyridine and Piperidine Series

B	$\bar{V}^o$ (B)	$\bar{V}^o$ BH^+	$\Delta\bar{V}_i^o$ ± 0.2 ml	ΔG_i^o	ΔH_i^o	ΔS^o (e.u.)
	ml $(g.mole)^{-1}$		$(g.mole)^{-1}$	Kcals $(g.mole)^{-1}$		
Pyridine (Cl^-)	77.70	67.5	+ 4.5	+ 7.12	+ 5.7	- 4.76
2-Methylpyridine (Cl^-)	93.92	85.1	+ 3.1	+ 8.13	+ 6.9	- 3.95
2,6-Dimethylpyridine (Cl^-)	109.30	101.8	+ 1.8	+ 9.17	+ 6.15	- 10.11
2,6-Dimethylpyridine (Br^-)	109.30	102.1	+ 1.5	+ 9.17	+ 6.15	- 10.11
2,6-Dimethylpyridine (I^-)	109.30	102.0	+ 1.6	+ 9.17	+ 6.15	- 10.11
Piperidine (Cl^-)	91.1	83.1	+ 2.3			
1-Methylpiperidine (Cl^-)	109.9	101.9	+ 2.3			

Values of $\Delta\phi_{K(S)i}^o$ for the Ionisation Process in the Pyridine and Piperidine Series

Base	$10^4\,\phi_{K(S)}^o$ (B) ml.$(g.mole.bar)^{-1}$	$10^4\,\phi_{K(S)}^o$ (BH^+Cl^-) ml$(g.mole.bar)^{-1}$	$10^4\,\Delta\phi_{K(S)i}^o$ ml$(g.mole.bar)^{-1}$ ± 0.5 ml$(g.mole.bar)^{-1}$
Pyridine	+ 2.2	- 18.6	+ 12.5
2-Methylpyridine	+ 5.3	- 16.4	+ 13.4
2,6-Dimethylpyridine	+ 7.3	- 15.0	+ 14.0
Piperidine	- 0.40	- 22.0	+ 13.3
1-Methylpiperidine	+ 0.30	- 20.9	+ 12.9

$10^4\,\phi_K^o$ (HCl) = -8.3 ml$(g.mole.bar)^{-1}$ (only an isothermal compressibility was available here) (159).

Figure 50. A plot of volume change ($\Delta\bar{V}_i^o$) and compressibility change on ionisation ($\Delta\phi_{K(S)i}^o$) against the standard free energy change on ionization (ΔG_i^o) for the three homologous pyridines studied.
(Temperature = 25°C)

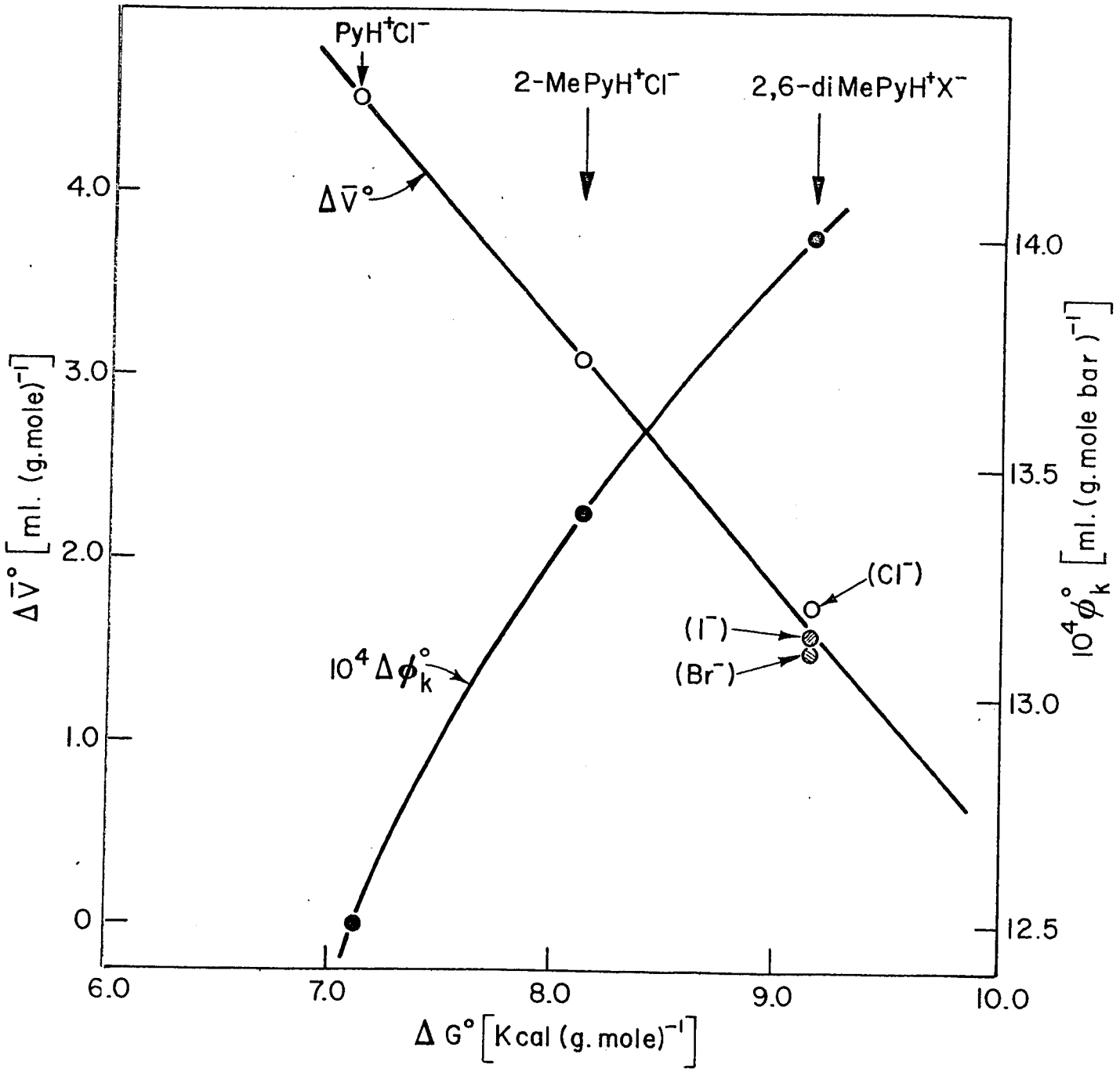
PyH⁺Cl⁻
2-MePyH⁺Cl⁻
2,6-diMePyH⁺X⁻
ΔV̄°
10⁴Δφ°k
(Cl⁻)
(I⁻)
(Br⁻)
4.0
3.0
2.0
1.0
0
14.0
13.5
13.0
12.5
6.0
7.0
8.0
9.0
10.0
ΔV̄° [ml. (g.mole)⁻¹]
10⁴φ°k [ml. (g.mole bar)⁻¹]
Δ G° [Kcal (g. mole)⁻¹]

For all of the reactions studied, the sign of the volume and compressibility changes on ionisation indicates that there is, as expected, a release of previously electrostricted water. As discussed in Section 3 of this chapter, substitution of the ring in the 2 and/or 6 position in the pyridinium salts decreases the amount of electrostriction that can be relieved when the charge is removed from the nitrogen. This accounts for the trend toward lower values of $\Delta\bar{V}_i^o$ as the "coordination" increases in ring positions adjacent to the nitrogen.

The smooth trends in the relation between $\Delta\bar{V}_i^o$ or $\Delta\phi_{K(S)i}^o$ with ΔG_i^o in the pyridine series can lead to an underestimation of the complexity of the problem, since examination of the relations of $\Delta\bar{V}_i^o$ or $\Delta\phi_{K(S)i}^o$ to entropy and enthalpy changes reveals that the situation is not at all simple.

The entropy change in the reaction will reflect primarily the change in the state of the water surrounding the products and reactants. A large negative entropy change can be due to the presence of electrostricted water or water undergoing hydrophobic hydration and the presence of competing trends within a series of ions and neutral molecules make the interpretation of the entropy changes, at the moment, rather uncertain. The more systematic relations of such properties as $\Delta\bar{V}_i^o$ to ΔG_i^o and of ΔS_i^o to structural changes in ionisable molecules usually results from well known "compensation" effects operating between the ΔH_i^o and the ΔS_i^o functions, i.e. when

Figure 51. A plot of apparent molar volume ϕ_v against $c^{1/2}$ for 2, 6-dimethylpyridine + H^+Cl^- and 2, 6-dimethylpyridinium chloride at 25°C

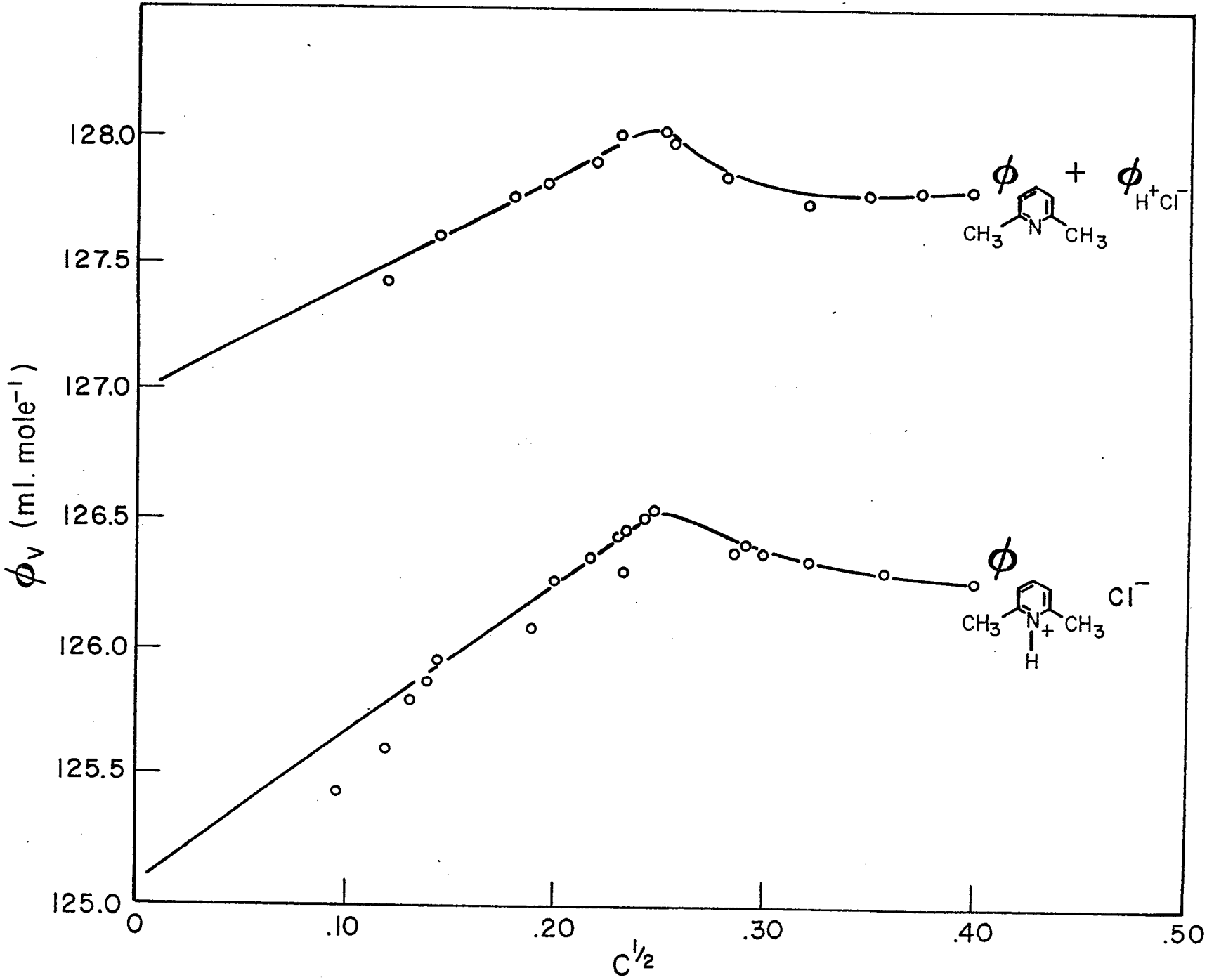
128.0
127.5
127.0
126.5
126.0
125.5
125.0
ϕ_v (ml. mole^{-1})
0
.10
.20
.30
.40
.50
$C^{1/2}$
ϕ + $\phi_{H^+Cl^-}$
CH_3
N
CH_3
ϕ
Cl^-
CH_3
N^+
CH_3
H

ΔH_i^o is increasingly negative in a series of molecules, the ΔS_i^o also usually becomes more negative so that $-T\Delta S_i^o$ compensates for the changesin ΔH_i^o . Such effects are also operative in respect to the enthalpies and entropies of solvation of simple ions and are therefore of significance in ionisation processes such as those referred to above.

7. Partial Molar Expansibilities in H_2O and D_2O

(i) Inorganic Salts

Of the three inorganic salts studied over a range of temperatures, only NaF showed any difference in its expansibility in H_2O and D_2O. For NaCl and KCl, the difference between the partial molar volumes in H_2O and D_2O at 25°C was maintained, within the experimental uncertainty, down to the freezing point of the solvents. In the case of NaF, which exhibits the largest negative solvent isotope effect in $\tilde{V}^o_{ion}$ at 25°C, the difference $\Delta\tilde{V}^o_{D_2O-H_2O}$ increases with decreasing temperature. This behaviour is presumably due to the small radius and highly hydrophilic nature of the F^- ion which can electrostrict much more effectively than can the structure-breaking Cl^- and K^+ ions. The behaviour of NaF is consistent with the model of D_2O discussed above in this chapter where it was pointed out that the extent of formation of structure in D_2O increases faster with decreasing temperature than in the case of H_2O; as a result, electrostriction of the structure in D_2O by the ions will be possible at the lower temperatures and will hence cause the partial molar volume to become relatively smaller at the lower temperatures.

(ii) Tetra-n-alkylammonium Salts

In the case of the four TAA salts studied over a range of temperatures, only Me_4NBr exhibited a behaviour in H_2O different from that in D_2O. Within the experimental uncertainty in the results, Et_4NBr, n-Pr_4NBr and n-Bu_4NBr all gave plots of ϕ_v against T which were parallel in H_2O and D_2O. On the basis of the criterion of the sign of the isotope effect, Me_4NBr is a structure-breaker at 25°C; however, a cross-over in the results for ϕ_v occurs between 15 and 20°C which corresponds to Me_4NBr having a higher volume in D_2O than in H_2O at low temperature. Since D_2O is more structured than H_2O at low temperature than it is at 25°C, and since structure-making is a phenomenon which is due to the structured nature of the solvent, then a salt such as Me_4NBr which is barely a structure-breaker at 25°C becomes a structure-maker at the lower temperatures.

(iii) Temperature of Maximum Density

It was also possible to obtain the temperature of maximum density from the data required to determine the ϕ_v against T curves. Only one concentration of each salt was, however, used; therefore the Despretz constants, D, (defined in Table 21) (191) quoted can be based only on two points. The effect of the TAA salts on the temperature of maximum density of H_2O was studied by Darnell and Greyson (71, 72). The value of D which they obtained for Et_4NBr in H_2O (the only TAA bromide which they studied) agrees with the result of the present

determinations on this salt. In Table 21 are listed the Despretz constants obtained for the TAA bromides in H_2O and D_2O. As in the investigations of Darnell and Greyson (71, 72) on the temperature of maximum density of TAA solutions in water, it was found in the present work that the Despretz constant increased with increasing cation size. Here it was found, however, that each of the salts at a given concentration lowered the T_m of H_2O to a greater extent than they did the T_m of D_2O. This is consistent with the other evidence which has been gathered in the present work regarding the greater structure-forming ability of the TAA salts in D_2O than in H_2O. If the temperature of maximum density of the solvent reflects the equilibrium ratio of structured and unstructured water (18), then the shift in T_m should reflect the way in which certain ions affect the proportion of structured and unstructured forms of water. Indeed, for simple univalent ions such as the halide ions, I^- depresses the T_m more than does Cl^-, indicating that it is a stronger structure-breaker. On the other hand, the depression of T_m is proportional to cation size for the TAA salts. This result was interpreted by Darnell and Greyson (71) as indicating that structure-formation, which arises at 25°C because of the ordering of the supposed "unbound" water by the hydrophobic groups, does not occur at the T_m because of the fewer unbound water molecules available for cluster formation. In fact, the large ions would disrupt the highly structured solvent and thus lead to the observed dependence of depression in the T_m upon cation size.

TABLE 21

Values of the Despretz Constants for the Tetra-n-alkylammonium Bromides in H_2O and D_2O

SALT	$D = \frac{T_m^o - T_m^M(b)}{M}$ °C (g.mole)$^{-2}$. 55.51 moles solvent	
	H_2O	D_2O
$(CH_3)_4NBr$	- 8.8 (8.4)[a]	- 6.9
$(C_2H_5)_4NBr$	- 10.6	- 7.6
$(C_3H_7)_4NBr$	- 12.6	- 8.8
$(C_4H_9)_4NBr$	- 16.0	- 14.7

(a) Darnell and Greyson (71)

(b) T_m^o temperature of maximum density of pure solvent, 3.98°C (H_2O) and 11.2°C (D_2O)

T_m^M temperature of maximum density of a solution of aquamolality M.

It is felt that the present results on the temperature dependence of the apparent molar volume in H_2O and D_2O indicate that structure formation is still occurring at temperatures near the temperature of maximum density and further T_m data obtained for the TAA bromides in D_2O indicate that structure-formation is still occurring to a greater degree in D_2O than in H_2O. The study of the temperature dependence of the apparent molar volume of the TAA bromides in H_2O carried out by Franks and Smith (127) showed, from the concentration dependence of ϕ_v at the low temperature, that the non-ideal behaviour observed at room temperature was accentuated at 5°C.

The observed behaviour of the temperature of maximum density does demonstrate the dangers of extending hydration models developed for 25°C to higher or lower temperatures.

APPENDIX I

Experimental results for the apparent molar volume and density of solutions of salts and neutral solutes studied in H_2O at $25^{\circ}C$ are presented in tabular form in this section.

Apparent Molar Volumes and Densities, for Aqueous Solutions of Pyridinium Chloride, 2-Methylpyridinium Chloride, 2,6-Dimethylpyridinium Chloride, Bromide, Iodide, 1-Methylpyridinium Iodide, 1-Ethylpyridinium Iodide, 1,2-Dimethylpyridinium Iodide and 1,2,6-Trimethylpyridinium Iodide at 25°C

Salt	c mole litre^{-1}	ϕ_2 ml.g.mole^{-1}	d $\pm 3 \times 10^{-6}$ g.ml.$^{-1}$
pyridinium chloride	0.00987	91.30	0.997315
	0.01974	91.44	0.997554
	0.02000	91.21	0.997565
	0.02904	91.25	0.997786
	0.02962	91.26	0.997800
	0.03500	91.29	0.997931
	0.03949	91.24	0.998043
	0.04065	91.28	0.998070
	0.04936	91.31	0.998282
	0.04936	91.29	0.998283
	0.05226	91.33	0.998352
	0.05923	91.31	0.998525
	0.06000	91.35	0.998541
	0.06388	91.33	0.998637
	0.06968	91.29	0.998782
	0.07020	91.35	0.998790
	0.07898	91.36	0.999004
	0.07977	91.32	0.999027
	0.08130	91.35	0.999062
	0.09872	91.38	0.999485
	0.09872	91.37	0.999486
	0.10453	91.40	0.999624
	0.11850	91.42	0.999963
	0.13820	91.46	1.000440
	0.16110	91.47	1.000995
	0.19550	91.51	1.001824

continued from previous page:

2-methylpyridinium chloride	0.009822	108.84	0.997280
	0.01965	108.95	0.997484
	0.02947	108.99	0.997688
	0.03930	108.97	0.997894
	0.04912	109.00	0.998097
	0.04912	108.93	0.998101
	0.05895	109.01	0.998505
	0.06877	109.02	0.998908
	0.08841	109.09	0.998301
	0.11726	109.21	0.999492
	0.14734	109.27	1.000105
	0.19544	109.34	1.001078
2,6-dimethyl-pyridinium chloride	0.009272	125.43	0.997246
	0.01414	125.60	0.997334
	0.01687	125.79	0.997381
	0.01903	125.86	0.997419
	0.02041	125.96	0.997442
	0.03549	126.07	0.997710
	0.03998	126.26	0.997783
	0.04780	126.35	0.997917
	0.05368	126.44	0.998016
	0.05688	126.30	0.998080
	0.05903	126.51	0.998106
	0.05654	126.46	0.998065
	0.06098	126.54	0.998138
	0.08247	126.37	0.998527
	0.08548	126.40	0.998577
	0.09039	126.37	0.998667
	0.10355	126.35	0.998900
	0.12849	126.30	0.999346
	0.15961	126.26	0.999903

continued from previous page:

2,6-dimethyl-pyridinium bromide	0.01090	133.41	0.997674
	0.01314	133.44	0.997797
	0.01381	133.42	0.997834
	0.01545	133.50	0.997923
	0.02194	133.58	0.998278
	0.02245	133.59	0.998306
	0.02418	133.62	0.998400
	0.03130	133.65	0.998790
	0.03252	133.72	0.998854
	0.03960	133.78	0.999240
	0.04218	133.84	0.999378
	0.04774	133.91	0.999678
	0.05035	133.78	0.999827
	0.05047	133.89	0.999829
	0.05403	133.93	1.000020
	0.05626	133.95	1.000141
	0.06020	133.84	1.000362
	0.06594	133.91	1.000671
	0.07298	133.86	1.001059
	0.08028	133.81	1.001461
	0.08424	133.80	1.001680
	0.10329	133.84	1.002716
	0.09062	133.81	1.002027
	0.13070	133.79	1.004219
	0.15239	133.80	1.005405
	0.18094	133.80	1.006964
	0.27224	133.80	1.001957
2,6-dimethyl-pyridinium iodide	0.01212	144.49	0.998177
	0.01352	144.47	0.999305
	0.01701	144.49	0.998622
	0.02025	144.58	0.998915
	0.02976	144.57	0.999780
	0.03803	144.70	1.000527
	0,04740	144.71	1.001377
	0.05836	144.78	1.002368
	0.06623	144.71	1.003087

continued from previous page:

	0.07902	144.83	1.004238
	0.09426	144.86	1.005618
	0.10700	144.86	1.006772
	0.13054	144.87	1.008905
	0.16214	144.81	1.011777
	0.18542	144.81	1.013889
	0.23444	144.80	1.018339
	0.32898	144.78	1.026919
1-methylpyridinium iodide	0.01018	127.01	0.998035
	0.01899	127.17	0.998863
	0.02056	127.07	0.999013
	0.03217	127.17	1.000105
	0.04051	127.10	1.000894
	0.04996	127.22	1.001779
	0.05675	127.29	1.002415
	0.06660	127.31	1.003340
	0.08508	127.38	1.005074
	0.09150	127.42	1.005673
	0.10264	127.41	1.006723
	0.10925	127.48	1.007334
	0.12468	127.42	1.008792
	0.13719	127.44	1.009967
	0.12164	127.51	1.008496
	0.14864	127.55	0.011023
	0.15160	127.55	1.011302
	0.16508	127.42	1.012592
	0.18363	127.58	1.014305
	0.22758	127.54	1.018437
	0.27883	127.34	1.023305

continued from previous page:

1-ethylpyridinium iodide	0.009299	144.20	0.997923
	0.01518	144.26	0.998459
	0.01935	144.33	0.998838
	0.03090	144.36	0.999891
	0.05313	144.49	1.001909
	0.06528	144.53	1.003012
	0.07558	144.55	1.003948
	0.09786	144.64	1.005965
	0.13087	144.73	1.008955
	0.14776	144.76	1.010484
	0.16208	144.67	1.011797
	0.27031	144.87	1.021570
1, 2, 6-trimethyl-pyridiniumiodide	0.01004	142.76	0.998005
	0.02207	142.88	0.999118
	0.02910	142.85	0.999770
	0.03750	142.98	1.000543
	0.04563	142.99	1.001295
	0.06622	143.06	1.003195
	0.07252	143.16	1.003770
	0.07746	143.18	1.004224
	0.09562	143.26	1.005893
	0.10312	143.27	1.006584
	0.14727	143.45	1.010629
	0.11678	143.34	1.007836
	0.17316	143.41	1.013019
	0.22357	143.35	1.017652
	0.28654	143.46	1.023444
1, 2, 6-trimethyl-pyridinium iodide	0.01099	158.40	0.998076
	0.01642	158.46	0.998570
	0.02671	158.56	0.999505
	0.04133	158.72	1.000829
	0.04733	158.62	1.001379
	0.07223	158.78	1.003632
	0.09050	158.83	1.005287
	0.11165	158.91	1.007197
	0.13161	158.89	1.009009
	0.16497	158.93	1.012028
	0.24298	158.93	1.019098

Apparent Molar Volumes and Densities, for Aqueous Solutions of 2,6-Dimethylpyridinium Bromide at Four Temperatures

2,6-dimethyl-pyridinium bromide	m g.moles $(KgH_2O)^{-1}$	ϕ_v ml (g.mole)	d $g.ml^{-1}$
T = 34.90°C	0.01480	133.61	0.994906
	0.02304	133.71	0.995354
	0.02572	133 95	0.995493
	0.04118	134.16	0.996320
	0.05166	134.40	0.996869
	0.05808	134.32	0.997215
	0.11711	134.48	1.000317
	0.15671	134.56	1.002347
	0.28336	134.78	1.008775
T = 29.26°C	0.01128	133.36	0.996525
	0.001480	133.50	0.996716
	0.02304	133.64	0.997163
	0.02572	133.62	0.997309
	0.04118	133.86	0.998139
	0.05166	134.08	0.998692
	0.05808	133.90	0.999046
	0.11711	134.01	1.002177
	0.15671	134.24	1.004219
	0.28336	134.12	1.010724
T = 18.82°C	0.01553	132.44	0.999340
	0.02258	132.59	0.999728
	0.03152	132.72	1.000218
	0.03993	132.83	1.000675
	0.05096	132.92	1.001274
	0.06081	132.86	1.001817
	0.08545	132.92	1.003146
	0.09200	132.98	1.003494
	0.15602	133.04	1.006906
	0,28336	133.07	1.013527

continued from previous page:

T = 6.20°C	0.01320	131.36	1.000071
	0.01553	131.36	1.000842
	0.02258	131.45	1.001238
	0.03152	131.51	1.001739
	0.03993	131.55	1.002208
	0.05096	131.56	1.002824
	0.06081	131.57	1.003375
	0.08545	131.60	1.004736
	0.09200	131.55	1.005101
	0.15602	131.56	1.008602
	0.28336	131.51	1.015409

Apparent Molar Volumes and Densities, for Aqueous Solutions of 1,1-Dimethylpiperidinium Iodide, 1-Methylpiperidinium Chloride, Piperidinium Chloride and Piperidinium Iodide at 25°C

	c	ϕ_v	d
	moles.l^{-1}	ml(g.mole)$^{-1}$	g.ml^{-1}
1,1-dimethylpiperidinium iodide	0.01014	158.87	0.997913
	0.01033	158.93	0.997928
	0.01282	158.76	0.998136
	0.01426	158.88	0.998253
	0.02225	158.96	0.998912
	0.02904	158.97	0.999473
	0.03794	159.03	1.000206
	0.04712	159.04	1.000963
	0.05540	159.01	1.001648
	0.05951	159.00	1.001988
	0.06409	159.07	1.002362
	0.07525	159.04	1.003285
	0.07648	159.13	1.003380
	0.08496	159.01	1.004090
	0.10289	159.03	1.005569
	0.13685	158.93	1.008386
	0.16084	158.92	1.010370
	0.20012	158.86	1.013630
	0.22824	158.83	1.015962
1-methylpiperidinium chloride	0.01162	125.85	0.997192
	0.02296	125.79	0.997309
	0.03187	125.84	0.997398
	0.04171	125.89	0.997496
	0.05858	125.96	0.997663
	0.07765	125.97	0.997853
	0.10311	125.93	0.998114
	0.12944	125.91	0.998381
	0.15251	125.92	0.998613
	0.18987	125.90	0.998994
	0.23798	125.90	0.999479

continued from previous page:

piperidinium chloride	0.01190	106.88	0.997253
	0.01298	106.75	0.997271
	0.02376	106.94	0.997430
	0.03806	107.03	0.997641
	0.04867	107.09	0.997796
	0.07853	107.22	0.998228
	0.09335	107.22	0.998447
	0.11431	107.25	0.998751
	0.15930	107.23	0.999415
	0.19726	107.28	0.999962
	0.25590	107.32	1.000810
piperidinium iodide	0.01757	126.35	0.998604
	0.02636	126.37	0.999369
	0.03514	126.58	1.000126
	0.04393	126.64	1.000887
	0.06150	126.78	1.002403
	0.07907	126.80	1.003924
	0.11421	126.83	1.006965
	0.13178	126.89	1.008479
	0.15813	126.89	1.010759
	0.19327	126.91	1.013797
	0.21963	126.93	1.016073

Apparent Molar Volumes and Densities, for Aqueous Solutions of Diethylammonium Chloride, Di-n-propylammonium Chloride, Di-n-butylammonium Chloride, Triethylammonium Bromide, Triethanolammonium Bromide, Tetramethylammonium Tetrafluoroborate and Ammonium Chloride at 25°C

	c moles.l^{-1}	ϕ_v ml(g.mole)$^{-1}$	d g.ml^{-1}
diethylammonium chloride	0.01215	106.80	0.997112
	0.01497	107.00	0.997118
	0.02680	106.90	0.997155
	0.03402	106.89	0.997177
	0.04386	106.94	0.997205
	0.06641	106.94	0.997272
	0.08369	106.95	0.997322
	0.1130	107.07	0.997397
	0.14205	107.07	0.997480
	0.19573	107.12	0.997623
	0.26765	107.10	0.997832
	0.32528	107.12	0.997986
di-n-propylammonium chloride	0.009813	138.74	0.997068
	0.02192	138.75	0.997059
	0.03138	138.74	0.997053
	0.03245	138.66	0.997055
	0.04532	138.79	0.997041
	0.05769	138.79	0.997032
	0.07965	138.83	0.997013
	0.10888	138.87	0.996986
	0.13107	138.83	0.996974
	0.16072	138.78	0.996960
	0.19075	138.73	0.996947
	0.24207	138.63	0.996936

continued from previous page:

di-n-butylammonium chloride	0.01052	170.67	0.997027
	0.02000	170.71	0.996984
	0.02032	170.73	0.996986
	0.03654	170.72	0.996909
	0.04215	170.50	0.996894
	0.06081	170.66	0.996783
	0.07491	170.68	0.996739
	0.09280	170.67	0.996659
	0.12088	170.62	0.996542
	0.14665	170.61	0.996427
	0.18645	170.52	0.996269
	0.24502	170.37	0.996055
triethylammonium bromide	0.01295	145.94	0.997548
	0.02199	145.84	0.997881
	0.03911	145.75	0.998513
	0.05356	145.63	0.999051
	0.05883	145.64	0.999245
	0.07391	145.63	0.999802
	0.08722	145.64	1.000293
	0.12057	145.62	1.001525
	0.16519	145.65	1.003168
	0.25861	145.60	1.006628
triethanolammonium bromide	0.01583	147.54	0.998388
	0.02249	147.62	0.998939
	0.02889	147.64	0.999469
	0.04073	147.66	1.000450
	0.04891	147.74	1.001124
	0.06538	147.83	1.002482
	0.07355	147.87	1.003155
	0.09206	147.96	1.004677
	0.11904	148.10	1.006888
	0.16019	148.14	1.010276
	0.20715	148.28	1.014116
	0.29130	148.43	1.020995

	m g.moles $(KgH_2O)^{-1}$	ϕ_v $ml(g.mole)^{-1}$	d $g.ml^{-1}$
tetramethylammonium tetrafluoroborate	0.009578	133.24	0.997342
	0.02151	133.00	0.997680
	0.03541	133.08	0.998067
	0.04923	133.23	0.998445
	0.06563	133.27	0.998894
	0.08223	133.37	0.999343
	0.10546	133.46	0.999963
	0.12659 (insoluble)	133.28	1.000557
ammonium chloride	0.03430	36.51	0.997658
	0.05548	36.39	0.998025
	0.06843	36.41	0.998244
	0.08331	36.44	0.998496
	0.10875	36.43	0.998930
	0.12712	36.49	0.999233
	0.16099	36.46	0.999811
	0.17591	36.50	1.000055
	0.20171	36.50	1.000489
	0.24209	36.55	1.001156
	0.31066	36.61	1.002280

Apparent Molar Volumes and Densities for Solutions of Pyridine, 2-Methylpyridine, 2, 6-Dimethylpyridine and HOD in Water: Piperidine and 1-Methylpiperidine in 0.1 N KOH and Pyridine in Benzene, all at 25°C

	c moles.l^{-1}	ϕ_v ml(g.mole)$^{-1}$	d g.ml^{-1}
pyridine in H_2O	0.009616	77.55	0.997091
	0.01008	77.43	0.997093
	0.01923	77.60	0.997107
	0.01923	77.44	0.997110
	0.02404	77.36	0.997121
	0.02885	77.24	0.997134
	0.02908	77.28	0.997133
	0.03846	77.13	0.997158
	0.04808	77.11	0.997180
	0.04816	77.07	0.997182
	0.05769	77.12	0.997201
	0.06250	77.14	0.997210
	0.06731	77.23	0.997214
	0.06762	77.20	0.997217
	0.07692	77.23	0.997234
	0.08654	77.22	0.997255
	0.08717	77.17	0.997261
	0.10632	77.12	0.997307
	0.11540	77.18	0.997320
	0.12305	77.09	0.997347
	0.12500	77.19	0.997340
	0.14463	77.16	0.997385
	0.16362	77.20	0.997420
	0.19325	77.18	0.997486

continued from previous page:

pyridine in benzene	0		0.873545
	0.009854	80.09	0.873635
	0.01971	79.98	0.0873727
	0.03097	80.02	0.873830
	0.03942	80.21	0.0873901
	0.04927	80.02	0.873998
	0.06053	79.94	0.874106
	0.07038	79.89	0.874200
	0.08024	79.84	0.874294
	0.09009	79.99	0.874376
	0.09854	79.92	0.874460
2-methylpyridine in H_2O	0.009811	93.81	0.997070
	0.02943	93.98	0.997057
	0.04906	93.95	0.997047
	0.06868	94.02	0.997031
	0.08830	94.01	0.997020
	0.10792	94.05	0.997004
	0.1182	94.01	0.997002
	0.1378	93.95	0.996999
	0.1575	93.89	0.996997
	0.1771	93.89	0.996988
	0.1969	93.85	0.996986
2,6-dimethylpyridine in H_2O	0.01016	109.71	0.997051
	0.01072	109.53	0.997052
	0.01450	109.40	0.997046
	0.02058	109.55	0.997031
	0.02085	109.54	0.997031
	0.03246	109.59	0.997005
	0.03589	109.71	0.996994
	0.03665	109.69	0.996993
	0.03829	109.69	0.996989
	0.04704	109.83	0.996963
	0.04833	109.74	0.996964
	0.05377	109.83	0.996947

continued from previous page:

	0.06430	109.81	0.996923
	0.06629	109.76	0.996922
	0.06664	109.80	0.996920
	0.07944	109.68	0.996900
	0.08492	109.62	0.996891
	0.09414	109.66	0.996871
	0.10382	109.45	0.996868
	0.12252	109.45	0.996831
	0.13680	109.41	0.996813
	0.14115	109.42	0.996798
	0.15928	109.37	0.996770
	0.18756	109.26	0.996738
	0.21745	109.11	0.996727
	0.25735	109.00	0.996692
	0.29589	108.90	0.996664
	0.33561	108.77	0.996653
	0.040990	108.72	0.996586
piperidine in 0.1N KOH	0.04012	91.11	0.996849
	0.06018	91.11	0.996737
	0.08024	91.11	0.996626
	0.12034	91.14	0.996396
	0.13374	91.18	0.996315
	0.16049	9117	0.996165
	0.18055	91.27	0.996034
	0.20061	91.27	0.995918
1-methylpiperidine in 0.1N KOH	0.02082	109.85	0.996860
	0.04164	109.94	0.996643
	0.06246	109.85	0.996432
	0.08328	109.87	0.996212
	0.10409	109.84	0.996005
	0.12492	109.76	0.995801
	0.14574	109.71	0.995596
	0.16656	109.70	0.995387
	0.18738	109.55	0.995204
	0.20820	109.50	0.995005
	0.24984	109.29	0.994643

	m g.moles $(KgH_2O)^{-1}$	ϕ_v $ml(g.mole)^{-1}$	d $g.ml^{-1}$
HOD in H_2O	0.01909	18.03	0.997094
	0.03336	18.08	0.997107
	0.04820	18.12	0.997119
	0.06230	18.10	0.997135
	0.07842	18.16	0.997146
	0.09480	18.20	0.997157
	0.13636	18.14	0.997202
	0.19497	18.14	0.997254
	0.24485	18.12	0.997306

APPENDIX II

Experimental results for the apparent molar adiabatic compressibility and the associated data used in its calculation are presented in this section in tabular form.

Values of the Apparent Molal Adiabatic Compressibility $\phi_{K(S)}$ and the Associated Data Used in its Calculation, for Aqueous Solutions of $(CH_3)_4NBF_4$, NH_4Cl, $(C_2H_5)_3NHBr$ and $(HOC_2H_4)_3NHBr$ at 25°C

Salt	c g.mole l^{-1}	u m.sec^{-1}	d g.ml^{-1}	ϕ_v ml(g.mole)$^{-1}$	$10^6\beta_{(S)}$ bar^{-1}	$10^4\,\phi_{K(S)}$ ml(g.mole.bar)$^{-1}$
$(CH_3)_4NBF_4$	0.02105	1498.06	0.997670	132.99	44.64	+ 18.46
	0.02880	1498.41	0.997888	133.05	44.633	18.91
	0.03642	1498.71	0.998101	133.12	44.606	19.92
	0.04603	1499.18	0.998370	133.17	44.566	19.53
	0.05500	1499.55	0.998620	133.23	44.533	20.07
	0.06528	1500.08	0.998905	133.29	44.488	19.56
	0.07721	1500.61	0.999235	133.35	44.442	19.80
	0.09256	1501.26	0.999658	133.42	44.385	20.27
	0.11389	1502.27	1.000241	133.50	44.300	20.19
	Insoluble					
NH_4Cl	0.02622	1498.45	0.997514	36.36	44.647	- 22.90
	0.04076	1499.21	0.997767	36.38	44.591	- 22.73
	0.05511	1499.84	0.998016	36.40	44.542	- 21.42
	0.07178	1500.53	0.998304	36.41	44.489	- 20.15
	0.08957	1501.38	0.998611	36.43	44.425	- 20.05
	0.12031	1502.74	0.999140	36.45	44.321	- 19.39
	0.14566	1503.90	0.999573	36.47	44.234	- 19.12
	0.20288	1506.51	1.000546	36.51	44.037	- 18.80
	0.24092	1508.19	1.001186	36.54	43.911	- 18.48
	0.31143	1511.36	1.002361	36.61	43.676	- 18.09
	0.43786	1516.92	1.00431	36.70	43.267	- 17.47

Continued from previous page:

$(C_2H_5)_3NHBr$	0.03182	1499.90	0.998244	145.77	44.529	- 4.15
	0.03911	1500.54	0.998513	145.75	44.479	- 4.06
	0.05356	1501.82	0.999051	145.63	44.379	- 4.09
	0.05883	1502.20	0.999245	145.64	44.348	- 3.16
	0.07391	1503.51	0.999802	145.63	44.246	- 3.02
	0.08722	1504.75	1.000293	145.64	44.151	- 3.50
	0.12057	1507.65	1.001525	145.62	43.920	- 3.18
	0.16519	1511.82	1.003168	145.65	43.614	- 3.59
	0.25861	1519.62	1.006628	145.60	43.019	- 1.78
$(HOC_2H_4)_3NHBr$	0.04073	1499.51	1.000450	147.66	44.453	- 6.84
	0.04891	1499.99	1.001124	147.74	44.395	- 6.47
	0.06538	1501.00	1.002482	147.83	44.275	- 6.50
	0.07355	1501.48	1.003155	147.87	44.217	- 6.29
	0.09206	1502.50	1.004677	147.96	44.090	- 5.48
	0.11904	1504.14	1.006888	148.10	43.898	- 5.30
	0.16019	1506.59	1.010276	148.14	43.608	- 5.00
	0.20715	1509.34	1.014116	148.28	43.285	- 4.36
	0.29130	1514.34	1.020995	148.43	42.710	- 3.61

Values of the Apparent Molar Adiabatic Compressibility $\phi_{K(S)}$ and the Associated Data Used in its Calculation, for Aqueous Solutions of pyridinium chloride, 2-methylpyridinium chloride, 2,6-dimethylpyridinium chloride, bromide, iodide, 1-methylpyridinium iodide, 1,2-dimethylpyridinium iodide, 1,2,6-trimethylpyridinium iodide and 1-ethylpyridinium iodide at 25°C

Salt	c g.mole l^{-1}	u m.sec^{-1}	d g.ml^{-1}	ϕ_v ml(g.mole)$^{-1}$	$10^6\beta_{(S)}$ bar^{-1}	$10^4\phi_{K(S)}$ ml (g.mole)$^{-1}$
pyridinium chloride	0.02904	1499.31	0.997786	91.25	44.584	- 18.03
	0.02920	1499.37	0.997790	91.25	44.580	- 17.70
	0.04065	1500.28	0.998070	91.28	44.514	- 17.48
	0.05226	1501.21	0.998352	91.33	44.446	- 17.54
	0.06388	1502.16	0.998637	91.33	44.377	- 17.74
	0.07020	1502.70	0.998790	91.35	44.339	- 17.96
	0.07861	1503.33	0.998996	91.36	44.292	- 17.58
	0.08130	1503.52	0.999062	91.35	44.278	- 17.37
	0.09760	1504.79	0.999455	91.37	44.186	- 17.06
	0.11850	1506.47	0.999963	91.42	44.065	- 16.91
	0.1382	1508.15	1.000440	91.46	43.944	- 16.88
	0.1611	1509.71	1.000995	91.47	43.831	- 16.24
	0.1955	1512.45	1.001824	91.51	43.636	- 16.15
2-methyl-pyridinium chloride	0.01965	1498.86	0.997484	108.95	44.624	- 15.36
	0.02947	1499.77	0.997688	108.99	44.561	- 15.36
	0.03930	1500.66	0.997894	108.97	44.499	- 15.10
	0.04912	1501.58	0.998097	109.00	44.435	- 15.35
	0.05895	1502.41	0.998505	109.01	44.377	- 14.49
	0.06877	1503.29	0.998908	109.02	44.316	- 14.32
	0.08841	1505.26	0.998301	109.09	44.183	- 15.31
	0.11726	1507.74	0.999492	109.21	44.012	- 14.06
	0.14734	1510.41	1.000105	109.27	43.829	- 13.61
	0.19544	1514.99	1.001078	109.34	43.526	- 13.69

continued from previous page:

2,6-dimethyl-	0.02041	1499.20	0.997442	125.96	44.606	- 14.19
pyridinium	0.03549	1500.80	0.997710	126.07	44.499	- 14.30
chloride	0.03998	1501.29	0.997783	126.26	44.466	- 14.53
	0.04780	1502.09	0.997917	126.35	44.413	- 13.96
	0.05368	1502.82	0.998016	126.44	44.366	- 14.95
	0.05654	1503.04	0.998065	126.46	44.350	- 14.16
	0.05688	1503.12	0.998080	126.30	44.345	- 14.68
	0.06098	1503.63	0.998138	126.54	44.313	- 15.03
	0.08247	1505.80	0.998527	126.37	44.167	- 14.14
	0.08548	1506.20	0.998577	126.40	44.142	- 14.56
	0.09039	1506.61	0.998667	126.37	44.114	- 13.81
	0.10355	1508.12	0.998900	126.35	44.016	- 14.34
	0.12849	1510.68	0.999346	126.30	43.847	- 13.76
	0.15961	1514.03	0.999903	126.26	43.629	- 13.73
2,6-dimethyl-	0.03252	1499.36	0.998854	133.72	44.533	- 6.89
pyridinium	0.04218	1500.01	0.999378	133.84	44.471	- 6.25
bromide	0.04774	1500.37	0.999678	133.91	44.436	- 5.85
	0.05035	1500.56	0.999827	133.78	44.418	- 6.07
	0.05626	1501.04	1.000141	133.95	44.377	- 6.36
	0.07298	1502.19	1.001059	133.86	44.268	- 6.14
	0.08028	1502.66	1.001461	133.81	44.222	- 5.89
	0.10329	1504.31	1.002716	133.84	44.070	- 5.94
	0.13070	1506.21	1.004219	133.79	43.894	- 5.62
	0.18094	1509.84	1.006964	133.80	43.564	- 5.67

continued from previous page:

2,6-dimethyl-	0.02510	1497.95	0.999347	144.57	44.595	+ 3.03
pyridinium	0.04066	1498.48	1.000758	144.67	44.501	3.45
iodide	0.05498	1498.99	1.002058	144.74	44.413	3.46
	0.07494	1499.68	1.003868	144.82	44.292	3.69
	0.10207	1500.57	1.006330	144.84	44.131	4.19
	0.11998	1501.17	1.007956	144.86	44.025	4.39
	0.14362	1501.95	1.010101	144.84	43.886	4.64
	0.16720	1502.73	1.012242	144.82	43.748	4.85
	0.18938	1503.45	1.014254	144.81	43.619	5.07
	0.21225	1504.27	1.016330	144.80	43.482	5.07
1-methyl-	0.09150	1498.84	1.005673	127.42	44.262	+ 3.69
pyridinium	0.09819	1499.00	1.006299	127.44	44.225	3.56
iodide	0.10078	1499.06	1.006542	127.45	44.211	3.55
	0.12164	1499.45	1.008496	127.51	44.102	3.79
	0.13719	1499.69	1.009967	127.44	44.024	4.11
	0.16508	1500.28	1.012592	127.42	43.875	4.01
	0.18363	1500.61	1.014305	127.58	43.782	4.38
	0.22758	1501.47	1.018437	127.54	43.555	4.56
	0.27883	1502.25	1.023305	127.34	43.302	5.05
1,2-dimethyl-	0.06622	1499.26	1.003195	143.06	44.346	+ 3.01
pyridinium	0.07252	1499.47	1.003770	143.16	44.308	3.11
iodide	0.07746	1499.63	1.004224	143.18	44.279	3.26
	0.09562	1500.24	1.005893	143.26	44.170	3.45
	0.10312	1500.53	1.006584	143.27	44.123	3.31
	0.11678	1500.98	1.007836	143.34	44.041	3.43
	0.14727	1501.96	1.010629	143.45	43.862	3.90
	0.17316	1502.63	1.013019	143.41	43.720	4.69
	0.22357	1504.23	1.017652	143.45	43.428	5.06
	0.28654	1505.93	1.023444	143.46	43.085	6.01

continued from previous page:

1,2,6-trimethyl-	0.04133	1499.03	1.000829	158.72	44.465	+ 2.07
pyridinium	0.04733	1499.29	1.001379	158.62	44.425	2.32
iodide	0.07223	1500.35	1.003632	158.78	44.262	3.49
	0.09050	1501.26	1.005287	158.83	44.136	3.23
	0.11165	1502.19	1.007197	158.91	43.998	3.76
	0.13161	1503.09	1.009009	158.89	43.867	4.01
	0.16497	1504.58	1.012028	158.93	43.649	4.38
	0.24298	1507.89	1.019098	158.93	43.156	5.52
1-ethyl-	0.06528	1499.20	1.003012	144.53	44.358	4.62
pyridinium	0.07558	1499.53	1.003948	144.55	44.297	4.75
iodide	0.09786	1500.23	1.005965	144.64	44.167	5.15
	0.13087	1501.24	1.008955	144.73	43.977	5.70
	0.14776	1501.86	1.010484	144.76	43.874	5.49
	0.16208	1502.25	1.011797	144.67	43.794	5.75
	0.27031	1505.39	1.021570	144.87	43.195	7.30

Values of the Apparent Molal Adiabatic Compressibility $\phi_{K(S)}$ and the Associated Data Used in its Calculation, for Aqueous Solutions of Piperidinium Chloride and 1-Methylpiperidinium Chloride at 25°C

Salt	c g.mole l^{-1}	u m.sec^{-1}	d g.ml^{-1}	ϕ_v ml(g mole)$^{-1}$	$10^6\beta_{(S)}$ bar^{-1}	$10^4\phi_{K(S)}$ ml (g.mole)$^{-1}$
piperidinium chloride	0.03170	1500.35	0.997542	107.00	44.533	- 20.57
	0.04295	1501.53	0.997709	107.06	44.456	- 20.54
	0.05946	1503.19	0.997953	107.12	44.347	- 19.84
	0.07753	1505.05	0.998222	107.19	44.225	- 19.75
	0.09500	1506.77	0.998476	107.22	44.113	- 19.07
	0.12402	1509.76	0.998901	107.26	43.920	- 18.93
	0.15876	1513.34	0.999407	107.29	43.690	- 18.76
	0.19765	1517.38	0.999970	107.31	43.433	- 18.61
	0.23124	1520.74	1.000453	107.31	43.221	- 18.10
	0.30285	1527.93	1.001472	107.31	42.771	- 17.33
1-methyl-piperidinium chloride	0.01779	1499.18	0.997.249	125.76	44.616	- 19.05
	0.02896	1500.45	0.997363	125.82	44.535	- 17.94
	0.03812	1501.58	0.997457	125.87	44.464	- 18.70
	0.04605	1502.44	0.997538	125.91	44.410	- 17.49
	0.06165	1504.27	0.997697	125.94	44.294	- 17.61
	0.08555	1506.92	0.997941	125.94	44.128	- 16.35
	0.12402	1511.36	0.998331	125.93	43.852	- 16.05
	0.15028	1514.48	0.998596	125.92	43.660	- 16.18
	0.17929	1517.70	0.998888	125.92	43.462	- 15.49
	0.20580	1521.13	0.999154	125.91	43.255	- 16.30
	0.23189	1524.31	0.999414	125.89	43.063	- 16.41
	0.26131	1527.68	0.999707	125.88	42.861	- 15.96

Values of the Apparent Molal Adiabatic Compressibility $\phi_{K(S)}$ and the Associated Data Used in its Calculation, for Aqueous Solutions of $(C_2H_5)_2NH_2Cl$, $(n\text{-}C_3H_7)_2NH_2Cl$ and $(n\text{-}C_4H_9)_2NH_2Cl$ at 25°C

Salt	c g.mole.l^{-1}	u m.sec^{-1}	d g.ml^{-1}	ϕ_v ml (g.mole)$^{-1}$	$10^6\beta_{(S)}$ bar^{-1}	$10^4\phi_{K(S)}$ ml (g.mole bar)$^{-1}$
$(C_2H_5)_2NH_2Cl$	0.03259	1500.31	0.997983	106.89	44.516	- 23.97
	0.04193	1501.26	0.998243	106.91	44.448	- 24.18
	0.05175	1502.25	0.998516	106.93	44.377	- 24.23
	0.07253	1504.37	0.999094	106.97	44.227	- 24.24
	0.10106	1507.22	0.999891	107.02	44.024	- 23.95
	0.13258	1510.40	1.000776	107.07	43.801	- 23.66
	0.15632	1512.62	1.001445	107.09	43.643	- 22.89
	0.18934	1516.15	1.002380	107.12	43.399	- 23.42
	0.23294	1520.63	1.003621	107.13	43.091	- 23.28
$(C_3H_7)_2NH_2Cl$	0.01042	1498.41	0.997073	138.72	44.670	- 14.70
	0.02000	1499,61	0.997063	138.74	44.599	- 13.41
	0.03189	1501.27	0.997051	138.77	44.501	- 15.98
	0.04246	1502.75	0.997041	138.78	44.413	- 17.27
	0.05957	1505.00	0.997026	138.81	44.281	- 16.61
	0.08440	1508.37	0.997006	138.84	44.085	- 16.66
	0.11137	1512.02	0.996986	138.86	43.873	- 16.61
	0.13143	1514.86	0.996974	138.84	43.709	- 17.08
	0.18577	1522.23	0.996948	138.74	43.288	- 16.61
	0.25617	1531.65	0.996933	138.61	42.758	- 15.73

continued from previous page:

$(C_4H_9)_2NH_2Cl$	0.02068	1500.55	0.996977	170.72	44.547	- 21.77
	0.02866	1501.97	0.996942	170.72	44.464	- 23.39
	0.03992	1503.93	0.996891	170.71	44.350	- 23.81
	0.05897	1507.06	0.996804	170.70	44.170	- 21.97
	0.07396	1509.55	0.996738	170.68	44.027	- 21.38
	0.10123	1514.20	0.996619	170.65	43.763	- 21.14
	0.12611	1518.44	0.996514	170.62	43.523	- 20.95
	0.15105	1522.76	0.996411	170.58	43.281	- 20.92
	0.20354	1531.72	0.996206	170.47	42.785	- 20.25
	0.25612	1540.70	0.996014	170.33	42.296	- 19.59
	0.030697	1549.36	0.995844	170.14	41.832	- 18.92

Values of the Apparent Molar Adiabatic Compressibility $\phi_{K(S)}$ and the Associated Data Used in its Calculation, for Aqueous Solutions of Piperidine, 1-Methylpiperidine, Pyridine, 2-Methylpyridine and 2,6-Dimethylpyridine at 25°C

Solute	c g.mole.l^{-1}	u m.sec^{-1}	d g.ml^{-1}	ϕ_v ml.(g.mole)$^{-1}$	$10^6\beta_{(S)}$ bar^{-1}	$10^4\phi_{K(S)}$ ml(g.mole bar)$^{-1}$
piperidine in 0.1N KOH	0.02163	1498.64	0.996951	91.06	44.661	- 0.30
	0.04468	1500.32	0.996823	91.09	44.567	- 0.20
	0.05584	1501.20	0.996761	91.11	44.518	- 0.87
	0.08030	1502.94	0.996623	91.14	44.421	- 0.23
	0.10608	1504.90	0.996476	91.17	44.317	- 0.54
	0.13305	1506.88	0.996319	91.20	44.202	- 0.37
	0.18092	1510.45	0.996037	91.24	44.006	- 0.30
	0.23056	1514.29	0.995738	91.32	43.796	- 0.50
	0.28583	1518.43	0.995395	91.40	43.573	- 0.29
1-methyl-piperidine in 0.1N KOH	0.01680	1498.60	0.996899	109.95	44.666	- 0.86
	0.03824	1500.51	0.996675	109.93	44.562	+ 0.10
	0.05895	1502.39	0.996461	109.89	44.461	+ 0.05
	0.08702	1504.86	0.996176	109.84	44.327	+ 0.56
	0.12276	1508.13	0.995822	109.78	44.151	+ 0.33
	0.16571	1512.06	0.995407	109.69	43.940	+ 0.21

continued from previous page:

pyridine	0.04816	1499.48	0.997182	77.07	44.601	+ 3.55
	0.06762	1500.42	0.997217	77.20	44.544	4.08
	0.08717	1501.36	0.997261	77.17	44.486	4.25
	0.10632	1502.12	0.997307	77.12	44.439	5.26
	0.12305	1502.79	0.997347	77.09	44.397	5.81
	0.16362	1504.08	0.997420	77.20	44.320	4.80
	0.19325	1504.86	0.997486	77.18	44.272	5.33
	0.14463	1506.32	0.997385	77.16	44.183	5.20
2-methyl-pyridine	0.02943	1498.88	0.997057	93.98	44.642	+ 5.36
	0.04906	1500.12	0.997047	93.95	44.569	5.15
	0.06868	1501.27	0.997031	94.02	44.501	5.81
	0.08830	1502.51	0.997020	94.01	44.428	5.60
	0.10792	1503.66	0.997004	94.05	44.361	5.95
	0.1182	1504.29	0.997002	94.01	44.324	6.03
	0.1378	1505.50	0.996999	93.95	44.253	5.98
	0.1575	1506.18	0.996997	93.89	44.213	7.92
	0.1771	1507.40	0.996988	93.89	44.142	7.68
	0.1969	1509.08	0.996986	93.85	44.044	6.14
2,6-dimethyl-pyridine	0.03246	1499.42	0.997005	109.59	44.612	+ 6.53
	0.04833	1500.60	0.996964	109.74	44.544	6.49
	0.06629	1502.04	0.996922	109.76	44.461	5.52
	0.08492	1503.40	0.996891	109.62	44.382	5.72
	0.10382	1504.91	0.996868	109.45	44.294	5.06
	0.12252	1506.16	0.996831	109.45	44.222	5.88
	0.14115	1507.44	0.996798	109.42	44.148	6.32
	0.15928	1508.79	0.996770	109.37	44.071	6.31
	0.18756	1510.75	0.996738	109.26	43.958	6.68

APPENDIX III

Experimental results for the apparent molar volume and density of tetra-n-alkylammonium and alkali halide salts in H_2O and D_2O at 25°C are tabulated in this section.

The density of 99.75% D_2O was determined on the differential buoyancy balance as $1.104526 \pm 3 \times 10^{-6}$ g.ml^{-1} at 25.00°C.

Apparent Molal Volumes, Partial Molal Volumes and Densities of a Series of Tetra-n-alkylammonium Bromides in D_2O at 25°C

Salt	m g.mole(1000 g D_2O)$^{-1}$	ϕ_v ml(g.mole)$^{-1}$	d g.ml^{-1}
$(CH_3)_4NBr$	0.01306	114.35	1.104926
	0.02283	114.48	1.105221
	0.02372	114.29	1.105252
	0.03668	114.49	1.105640
	0.05395	114.56	1.106156
	0.07931	114.70	1.106901
	0.08033	114.63	1.106938
	0.09973	114.72	1.107503
	0.10589	114.76	1.107680
	0.12999	114.79	1.108382
	0.15066	114.84	1.108973
	0.17879	114.83	1.109787
	0.16194	114.80	1.109309
	0.20289	114.83	1.110478
	0.21332	114.85	1.110773
	0.32214	114.87	1.113828
$(C_2H_5)_4NBr$	0.01044	174.21	1.104730
	0.01570	174.10	1.104834
	0.02140	174.23	1.104943
	0.02074	174.16	1.104932
	0.03241	174.16	1.105159
	0.04307	174.40	1.105353
	0.04316	174.28	1.105361
	0.04702	174.55	1.105419
	0.05153	174.40	1.105515
	0.05896	174.30	1.105662
	0.05930	174.34	1.105666
	0.06465	174.27	1.105772
	0.07606	174.30	1.105987
	0.09056	174.17	1.106276
	0.09162	174.21	1.106290
	0.11261	174.10	1.006701

continued from previous page:

	0.13163	174.06	1.107066
	0.13308	174.02	1.107098
	0.14338	173.97	1.107300
	0.14747	173.98	1.107378
	0.16584	174.05	1.107707
	0.16994	173.95	1.107803
	0.17427	173.89	1.107895
	0.19587	173.93	1.108290
	0.21716	173.90	1.108690
	0.22687	173.74	1.108912
	0.25412	173.71	1.109425
	0.29273	173.54	1.110183
	0.29957	173.42	1.110350
$(C_3H_7)_4NBr$	0.01137	240.13	1.104537
	0.02186	239.71	1.104560
	0.02240	239.93	1.104555
	0.03265	239.68	1.104579
	0.04986	239.61	1.104612
	0.06007	239.47	1.104640
	0.06185	239.51	1.104640
	0.07148	239.38	1.104669
	0.08559	239.21	1.104714
	0.08562	239.26	1.104709
	0.09815	239.10	1.104755
	0.13132	238.79	1.104879
	0.13675	238.69	1.104908
	0.15834	238.54	1.104994
	0.03490	239.72	1.104581

continued from previous page:

$(C_4H_9)_4NBr$	0.008352	301.72	1.104426
	0.009943	301.55	1.104409
	0.01333	301.87	1.104364
	0.01345	301.60	1.104367
	0.02004	301.54	1.104291
	0.02077	301.57	1.104282
	0.02738	301.54	1.104206
	0.03760	301.37	1.104096
	0.04471	301.16	1.104027
	0.04636	301.24	1.104004
	0.05705	300.87	1.103911
	0.05801	301.03	1.103890
	0.06865	300.64	1.103809
	0.08274	300.41	1.103574
	0.09763	300.13	1.103574
	0.10887	299.86	1.103501
	0.12678	299.68	1.103368
	0.16099	299.19	1.103161
	0.20635	298.68	1.102922
	0.27432	297.98	1.102647

Apparent Molar Volume and Density of $(DOC_2H_4)_3NDBr$ in D_2O at 25°C

$(DOC_2H_4)_3NDBr$	m g.moles$(KgD_2O)^{-1}$	ϕ_v ml $(g.mole)^{-1}$	d $g.ml^{-1}$
	0.01871	145.90	1.106030
	0.02991	146.09	1.106919
	0.04127	146.04	1.107824
	0.05172	146.12	1.108647
	0.05824	146.15	1.109160
	0.06811	146.32	1.109923
	0.08162	146.41	1.110970
	0.10495	146.38	1.112786
	0.12726	146.44	1.114497
	0.16522	146.63	1.117356
	0.21970	146.80	1.121394

Apparent Molal Volumes and Densities of a Series of Tetra-n-alkylammonium Bromides in H_2O at 25°C

Salt	c g.mole.l^{-1}	m g.mole(KgH_2O)$^{-1}$	ϕ_v ml(g.mole)$^{-1}$	d g.ml^{-1}
$(C_2H_5)_4NBr$	0.009278	0.009320	173.91	0.997415
	0.01021	0.01026	173.86	0.997450
	0.01066	0.01071	173.98	0.997465
	0.01540	0.01549	173.94	0.997639
	0.01825	0.01836	174.07	0.997742
	0.01971	0.01984	173.86	0.997800
	0.02175	0.02190	174.03	0.997871
	0.02642	0.02662	173.95	0.998044
	0.02996	0.03021	173.99	0.998173
	0.03372	0.03402	173.99	0.998311
	0.03429	0.03460	174.14	0.998327
	0.03735	0.03771	173.92	0.998447
	0.04221	0.04265	174.01	0.998622
	0.04659	0.04711	174.08	0.998779
	0.04949	0.05007	174.04	0.998887
	0.05325	0.05391	173.94	0.999030
	0.05361	0.05427	174.00	0.999040
	0.05770	0.05845	173.94	0.999193
	0.06283	0.06371	174.01	0.999377
	0.07303	0.07419	173.93	0.999757
	0.09130	0.09304	173.94	1.000427
	0.11186	0.11441	173.91	1.001185
	0.15716	0.16205	173.80	1.002868
	0.22931	0.23952	173.65	1.005563
	0.26817	0.28209	173.59	1.007017
	0.31248	0.33136	173.48	1.008696
	0.37724	0.40483	173.38	1.011140
	0.46826	0.51106	173.13	1.014651

continued from previous page:

$(C_3H_7)_4NBr$	0.009678	0.009729	239.48	0.997342
	0.009274	0.009322	239.45	0.997329
	0.01044	0.01050	239.42	0.997362
	0.01082	0.01088	239.52	0.997371
	0.01133	0.01139	239.43	0.997386
	0.01218	0.01225	239.45	0.997408
	0.01265	0.01273	239.23	0.997425
	0.01408	0.01417	239.63	0.997459
	0.01514	0.01524	239.42	0.997491
	0.01608	0.01619	239.45	0.997515
	0.01980	0.01995	239.49	0.997618
	0.02261	0.02280	239.46	0.997696
	0.02647	0.02672	239.43	0.997803
	0.02769	0.02796	239.41	0.997837
	0.02431	0.02452	239.49	0.997742
	0.03253	0,03288	239.43	0.997970
	0.03739	0.03784	239.42	0.998104
	0.04044	0.04096	239.52	0.998184
	0.05304	0.05388	239.40	0.998536
	0.05580	0.05672	239.34	0.998616
	0.06342	0.06459	239.32	0.98828
	0.06973	0.07112	239.22	0.999010
	0.08032	0.08213	239.22	0.999309
	0.08528	0.08731	239.25	0.999438
	0.09296	0.09535	239.19	0.999659
	0.09325	0.09566	239.09	0.999673
	0.09858	0.10126	239.03	0.999828
	0.11244	0.11589	239.06	1.000212
	0.12370	0.12784	238.87	1.000550
	0.13636	0.14137	238.88	1.000896
	0.14511	0.15080	238.76	1.001168
	0.15989	0.1667	238.62	1.001606
	0.15886	0.16560	238.59	1.001582
	0.19300	0.2029	238.42	1.002584
	0.18771	0.1971	238.52	1.002414
	0.19413	0.20416	238.58	1.002583
	0.22780	0.24159	238.33	1.003595
	0.24093	0.24159	238.17	1.004013
	0.26589	0.2564	238.06	1.004760
	0.27082	0.2847	237.84	1.004956
	0.32453	0.3527	237.66	1.006586
	0.39274	0.4344	237.06	1.008820

continued from previous page:

$(C_4H_9)_4NBr$	0.01033	0.01039	301.04	0.997303
	0.03449	0.03496	300.65	0.997854
	0.06984	0.07154	300.21	0.998684
	0.09253	0.09545	299.99	0.999227
	0.11665	0.12123	299.82	0.999807
	0.15073	0.15832	299.45	1.000663
	0.17708	0.18754	299.15	1.001343
	0.20794	0.22237	298.91	1.002136
	0.23958	0.25880	298.58	1.002986

Apparent Molar Volumes of Et_4NBr, n-Pr_4NBr and n-Bu_4NBr Solutions at High Dilutions Obtained with a Dilution Dilatometer

Salt	moles of solute in capsule	$\Delta\phi_v$ ml(g.mole)$^{-1}$	final conc. (moles l^{-1})	ϕ_v ml (mole)$^{-1}$
Et_4NBr in H_2O	0.0009256	- 0.10	0.001903	173.84
	0.001591	0.00	0.003272	173.79
	0.002479	+ 0.20	0.005098	173.80
	0.003002	+ 0.36	0.006173	173.86
	0.004409	+ 0.64	0.009066	173.84
	0.004409	+ 0.66	0.009066	173.86
Et_4NBr in D_2O	0.0006748	- 0.32	0.001388	173.96
	0.001265	- 0.07	0.002602	173.99
	0.002531	+ 0.25	0.005204	173.95
	0.005061	+ 1.07	0.01041	174.04
n-Pr_4NBr in H_2O	0.0008850	+ 0.36	0.001820	239.42
	0.0008850	+ 0.31	0.001820	239.47
	0.001585	+ 0.75	0.003259	239.38
	0.002539	+ 1.48	0.005221	239.41
	0.002539	+ 1.49	0.005221	239.42
	0.003610	+ 2.32	0.007423	239.43
	0.003610	+ 2.28	0.007423	239.47
n-Bu_4NBr in H_2O	0.001029	+ 0.90	0.002116	300.76
	0.001751	+ 1.55	0.003601	300.68
	0.001751	+ 1.53	0.003601	300.64

Apparent Molal Volumes and Densities of a Series of Alkali Halides in H_2O and D_2O at 25°C

Salt and Solvent	m g.mole(1000 g. solvent)$^{-1}$	ϕ_v ml (g.mole)$^{-1}$	d g.ml^{-1} ± 3 x 10^{-6} g.ml^{-1}
KCl/ (H_2O)	0.01337	26.99	0.997709
	0.02332	27.08	0.998179
	0.03784	27.17	0.998863
	0.05078	27.25	0.999470
	0.06491	27.34	1.000130
	0.08832	27.37	1.001227
	0.11837	27.46	1.002624
	0.16014	27.53	1.004564
	0.23538	27.58	1.008048
NaF/ (H_2O)	0.03077	- 2.05	0.998425
	0.04000	- 2.09	0.998832
	0.06333	- 1.94	0.999848
	0.08441	- 1.87	1.000767
	0.14575	- 1.63	1.003414
KBr/ (H_2O)	0.01446	33.96	0.998301
	0.02836	33.94	0.999480
	0.05629	33.94	1.001845
	0.08587	34.02	1.004338
	0.11421	34.09	1.006719
	0.15830	34.08	1.010422
	0.19751	34.18	1.013686
	0.23363	34.22	1.016693
	0.26523	34.20	1.019325

continued from previous page:

NaBr/ (H_2O)	0.01228	23.81	0.998043
	0.01377	23.78	0.998161
	0.02316	23.82	0.998901
	0.02869	23.86	0.999335
	0.04289	23.86	1.000454
	0.04725	23.89	1.000796
	0.06673	23.91	1.002327
	0.06837	23.92	1.002455
	0.09887	24.03	1.004839
	0.11125	23.97	1.005815
	0.13872	23.94	1.007970
	0.14689	24.02	1.008597
	0.18910	23.96	1.011906
	0.23139	24.16	1.015156
	0.23526	24.01	1.015494
	0.32315	24.07	1.022303
KCl/ (D_2O)	0.02933	26.75	1.105983
	0.03623	26.73	1.106326
	0.10314	27.02	1.109603
	0.11519	26.94	1.110207
	0.15462	27.15	1.112102
	0.16403	27.08	1.112574
	0.18678	27.17	1.113665
	0.23043	27.20	1.115778
	0.25757	27.31	1.117057
NaCl/ (D_2O)	0.01518	15.97	1.105209
	0.02845	16.08	1.105804
	0.03567	16.12	1.106126
	0.05704	16.27	1.107074
	0.08333	16.38	1.108235
	0.11469	16.47	1.109613
	0.15183	16.55	1.111242

continued from previous page:

NaF/ (D_2O)	0.01887	- 3.42	1.105480
	0.03517	- 3.35	1.1060301
	0.05658	- 3.22	1.107373
	0.07580	- 2.99	1.108319
	0.10625	- 2.95	1.109837
	0.15027	- 2.77	1.112006
	0.18563	- 2.65	1.113740
	0.23896	- 2.53	1.116353
	0.33599	- 2.28	1.121056
KBr/ (D_2O)	0.05245	33.82	1.109247
	0.07664	33.92	1.111409
	0.10875	33.84	1.114291
	0.12897	33.86	1.116096
	0.16178	33.90	1.119014
	0.21424	33.96	1.123658
	0.22368	33.99	1.124482
NaBr/ (D_2O)	0.01230	23.43	1.105571
	0.01375	23.51	1.105694
	0.02038	23.55	1.106256
	0.02464	23.49	1.106619
	0.04058	23.67	1.107963
	0.05977	23.75	1.109581
	0.08708	23.73	1.111887
	0.11105	23.77	1.113901
	0.14965	23.73	1.117155
	0.22041	23.74	1.123090
	0.29194	23.78	1.129053

Apparent Molal Volume and Density Data for Pyridine in D_2O

m g.moles(Kg.D_2O)$^{-1}$	ϕ_v ml.(g.mole)	d g.ml^{-1}
0.009648	77.74	1.104453
0.01891	77.69	1.104385
0.02816	77.54	1.104322
0.03726	77.42	1.104262
0.04574	77.39	1.104204
0.05502	77.36	1.104141
0.06460	77.38	1.104073
0.07601	77.36	1.103996
0.08871	77.33	1.103912
0.10084	77.31	1.103831
0.12382	77.27	1.103681
0.14321	77.33	1.103539
0.15778	77.33	1.103443
0.18128	77.32	1.103284

CONTRIBUTIONS TO ORIGINAL RESEARCH

1) The apparent molar volumes, ϕ_V, of a series of tetra-n-alkylammonium bromides have been measured down to high dilutions in H_2O at 25°C in order to approach the limiting law region and correctly evaluate the true partial molar volume at infinite dilution. In this work, a specially designed new type of dilution dilatometer and a differential buoyancy balance were employed.

2) The apparent molar volumes of a series of pyridinium, piperidinium and n-alkylammonium salts, together with the volumes of some neutral pyridine and piperidine bases have been measured in water at 25°C as a function of concentration in order to investigate steric effects in the ionisation and solvation of these molecules.

3) The partial molar adiabatic compressibility, $\phi_{K(S)}$, of a series of pyridinium, piperidinium and n-alkylammonium salts, together with a series of neutral pyridine and piperidine bases has been measured in water at 25°C as a function of concentration.

4) The effect of direct and indirect coordination at the nitrogen charged centre has been investigated in relation to the partial molar volumes and partial molar adiabatic compressibilities of a series of molecules of related structure.

5) An extrapolation procedure has been proposed for obtaining individual ionic $\phi^{o}_{K(S)}$ values.

6) The partial molar volumes of a series of inorganic 1:1 electrolytes and tetra-n-alkylammonium salts were measured in D_2O at 25°C as a function of concentration.

7) The sign of the solvent isotope effect in partial molar volumes $\Delta\bar{V}^{o}_{D_2O\text{-}H_2O}$, determined in (6), was interpreted in terms of the structure-making and structure-breaking ability of the ions on water.

8) The individual ionic partial molar volume of the bromide ion was determined in D_2O, thus establishing an absolute scale of ionic partial molar volumes in D_2O.

9) The temperature dependence of the partial molar volumes for a series of inorganic and tetra-n-alkylammonium salts was determined in H_2O and D_2O from 25°C to the freezing point of the two solvents and related to structural changes in the solvent.

10) The temperature of maximum density for a series of tetra-n-alkylammonium salts was determined in H_2O and D_2O.

11) The partial molar volume and adiabatic compressibility changes have been derived for the acid ionisation of a series of pyridinium and piperidinium salts. The observed changes have been interpreted in terms of the effect of coordination of the charged nitrogen centre and related to the standard free energies, heats and entropies of ionisation.

REFERENCES

1. R.K. Nigham and P.P. Singh, Trans.Faraday Soc., 65, 950 (1969).
2. M. Born, Z.Physik., 1, 45 (1920).
3. J.D. Bernal and R.H. Fowler, J.Chem.Phys., 1, 515 (1933).
4. D.D. Eley and M.G. Evans, Trans.Faraday Soc., 34, 1093 (1938).
5. A.D. Buckingham, Discussions Faraday Soc., 24, 151 (1957); J.S. Muirhead-Gould and K.J. Laidler, Chemical Physics of Ionic Solutions, Eds. B.E. Conway and R.G. Barradas, John Wiley and Sons, Inc., New York, 1966, p. 75; see also Trans.Faraday Soc., 63, 944, 953, 958 (1967).
6. H.S. Frank, Chemical Physics of Ionic Solutions, Eds. B.E. Conway and R.G. Barradas, John Wiley and Sons Inc., New York, 1966.
7. H.S. Frank and M.W. Evans, J.Chem.Phys., 13, 507 (1945).
8. W.F.K. Wynne-Jones, Proc.Roy.Soc., A140, 440 (1933).
9. D.H. Everett and W.F.K. Wynne-Jones, Trans.Faraday Soc., 35, 1380 (1938 b).
10. P.G. Owston, Adv. in Phys., 7, 172 (1958).
11. S.W. Peterson and H.A. Levy, Acta.cryst., 10, 70 (1957).
12. W.F. Giauque and M.F. Ashley, Phys.Rev., 43, 81 (1933).

13. Stewart, Phys.Rev., 37, 9 (1931).

14. J. Morgan and B.E. Warren, J.Chem.Phys., 6, 666 (1938).

15. A.H. Narten, M.D. Danford and H.A. Levy, Disc.Faraday Soc., 43, 97 (1967).

16. L. Pauling, Hydrogen Bonding, Pergamon Press, London, 1959.

17. D.J.G. Ives, Inaugural Lecture at Birkbeck College, 1963, J.W. Ruddock, London, 1963.

18. J.L. Kavanau, Water and Solute-Water Interactions, Holden-Day, San Francisco, 1964.

19. O.Ya. Samoilov, Structure of Electrolyte Solutions and the Hydration of Ions, Engl.Transl., Consultants Bureau Enterprises Inc., New York, 1965.

20. B.E. Conway, Ann.Rev.Phys.Chem., 17, 481 (1966).

21. H.S. Frank, Federation Proc., 24 Pt. III (1965) S-1.

22. D.J.G. Ives and T.H. Lemon, R.I.C. Review, 1, 62 (1968).

23. J.E. Desnoyers and C. Jolicoeur, Modern Aspects of Electrochemistry, Eds. J.O'M. Bockris and B.E. Conway, Vol.V., Butterworths Scientific Publications, London (1969).

24. E. Forslind, Acta.Polytechnica. 115, 9 (1952) and Proc.Second Internat.Congr.Rheology, Butterworths, London 1953.

25. O.Ya. Samoilov, Zhur.Fiz.Khim., 20, 12 (1946).

26. Yu.V. Gurikov, Zhur.strukt.Khim., 7, 8 (1966).

27. V.M. Volovenko, Yu.V. Gurikov and E.K. Legin, Zhur. strukt.Khim., 8, 403 (1967).

28. V.M. Volovenko, Yu.V. Gurikov and E.K. Legin, Zhur. strukt.Khim., 8, 600 (1967).

29. Yu. V. Gurikov, Zhur. strukt. Khim., 9, 771 (1968).

30. H.S. Frank and W.-Y. Wen, Disc. Faraday Soc., 24, 133 (1957).

31. G.H. Haggis, J.B. Hasted and T.J. Buchanan, J. Chem. Phys., 20, 1452 (1952).

32. G. Nemethy and H.A. Scheraga, J. Chem. Phys., 36, 3382 (1962); ibid. 36, 3401 (1962).

33. R. P. Marchi and H. Eyring, J. Phys. Chem., 68, 221 (1964).

34. V. Vand and W.A. Senior, J. Chem. Phys., 43, 1873 (1965); ibid. 43, 1878 (1965); ibid. 43, 1869 (1965).

35. S. Levine and J.W. Perram, Hydrogen Bonded Solvent Systems, Eds. A.K. Covington and P. Jones, Taylor Francis Ltd., London, 1968, p. 115.

36. M. Orentlicher and P.O. Vogelhut, J. Chem. Phys., 45, 4719 (1966).

37. M.J. Sparnay, J. Colloid and Interf. Sci., 22, 23 (1966).

38. M.S. Jhon, J. Grosh, T. Ree and H. Eyring, J. Chem. Phys., 44, 1465 (1966); T.A. Litovitz and C.M. Davis, J. Chem. Phys., 42, 2563 (1965).

39. W.H. Baur, Acta. Cryst., 19, 901 (1965).

40. J.A. Pople, Proc. Roy. Soc., A205, 163 (1951).

41. H.S. Frank, Disc. Faraday Soc., 43, 137 (1967).

42. K. Buijs and G.R. Choppin, J. Chem. Phys., 39, 2035 (1963).

43. D.F. Hornig, J. Chem. Phys., 40, 3119 (1964).

44. G.E. Walrafen, J. Chem. Phys., 40, 3219 (1964).

45. W.A.P. Luck, Ber. Bunsenges. Phys. Chem., 69, 626 (1965); ibid. 66, 766 (1962); 67, 186 (1963); 68, 895 (1964).

46. W.A.P. Luck, Fortschr. Chem. Forsch., Bd. 4, 653 (1964).

47. W.A.P. Luck, Naturwiss., 52, 25; 49 (1965).

48. D.P. Stevenson, J.Phys.Chem., 69, 2149 (1965).

49. M. Falk and T.A. Ford, Can.J.Chem., 44, 1699 (1966).

50. J.J. Fox and A.E. Martin, Proc.Roy.Soc.London, Ser. A., 174, 234 (1940).

51. G. Boettger, H. Harders and W.A.P. Luck, J.Phys.Chem., 71, 459 (1966).

52. R. Goldstein and S.S. Penner, J.Quant.Spectry., 4, 441 (1964).

53. M.R. Thomas, H.A. Scheraga and E.E. Shrier, J.Phys.Chem., 69, 3722 (1965).

54. T.T. Wall and D.F. Hornig, J.Chem.Phys., 43, 2079 (1965).

55. E.U. Franck and K. Roth, Disc.Faraday Soc., 43, 108 (1967).

56. G.E. Walrafen, J.Chem.Phys., 44, 1546 (1966).

57. K.A. Hartman, J.Phys.Chem., 70, 270 (1966).

58. G.E. Walrafen, J.Chem.Phys., 47, 114 (1967).

59. E. Fishman and P. Saumagne, J.Phys.Chem., 69, 3671 (1965).

60. J.D. Worley and I.M. Klotz, J.Chem.Phys., 45, 2868 (1966).

61. G.E. Walrafen, Hydrogen Bonded Solvent Systems, Eds. A.K. Covington and P. Jones, Taylor Francis Ltd., London, 1968, p. 9.

62. T.A. Ford and M. Falk, Can.J.Chem., 46, 3579 (1968).

63. W.A.P. Luck, Disc.Faraday Soc., 43, 132 (1967).

64. B.V. Deryaguin, N.V. Shuraev, N.V. Fedyakin, N.N. Talaev and I.G. Ershova, Izvest.Akad.Nauk.S.S.S.R., Ser.Khim., 10, 2178 (1967).

65. B.V. Deryaguin, N.N. Fedyakin and M.V. Talaev, Dokl.Akad. Nauk.S.S.S.R., 167, 376 (1966).

66. B.V. Deryaguin, D.S. Lychikov, K.M. Merzhanov, Ya.I. Rabinovich and N.V. Shuraev, Dokl. Akad. Nauk. S.S.S.R., 181, 823 (1968).

67. B.V. Deryaguin, Peroda, 4, 16 (1968).

68. English Summary of Results available from Joint Publications Research Service, Transl. 45989, U.S. Department of Commerce, Washington, D.C.

69. R.W. Bolander, J.L. Kassner and J.T. Zung, Nature, 221, 1233 (1969).

70. E.R. Nightingale, Chemical Physics of Ionic Solutions, Eds. B.E. Conway and R.G. Barradas, John Wiley and Sons Inc., New York, 1966, p. 87.

71. A.J. Darnell and J. Greyson, J. Phys. Chem. 72, 3021 (1968).

72. A.J. Darnell and J. Greyson, J. Phys. Chem., 72,3032 (1968).

73. G. Wada and S. Umeda, Bull. Chem. Soc. Jap., 35, 646 (1962); ibid. 35, 1797 (1962).

74. F. Franks and B. Watson, Trans. Faraday Soc., 63, 329 (1967).

75. D.W. McCall and D.C. Douglass, J. Phys. Chem., 69, 2001 (1965).

76. M.C.R. Symons, M.J. Blandamer, Hydrogen Bonded Solvent Systems, Eds. A.K. Covington and P. Jones, Taylor Francis Ltd, London, 1968, p. 211.

77. K.W. Bunzl, J. Phys. Chem., 71, 1358 (1967).

78. G.E. Walrafen, J. Chem. Phys., 36, 1035 (1962).

79. J.C. Hindman, J. Chem. Phys., 44, 4582 (1966).

80. J.C. Hindman, J. Chem. Phys., 36, 1000 (1962).

81. M.S. Bergqvist and E. Forslind, Acta. Chem. Scand., 16, 2069 (1962).

82. R.E. Glick and T.C. Tewari, J.Chem.Phys., 45, 4049 (1966).

83. J. Clifford and B.A. Pethica, Trans.Faraday Soc., 60, 1483 (1964).

84. H.G. Hertz and W. Spalthoff, Z.Electrochem., 63, 1096 (1959).

85. H.H. Ruterjans and H.A. Scheraga, J.Chem.Phys., 45, 3296 (1966).

86. G. Engel and H.G. Hertz, Ber.Bunsenges.physik.Chem., 72, 808 (1968).

87. E. Wicke, Angew.Chem.Intern.Ed. Engl., 5, 106 (1966).

88. W.M. Cox and J.H. Wolfenden, Proc.Roy.Soc.(London), 145A, 475 (1934).

89. E.R. Nightingale, J.Phys.Chem., 63, 1381 (1959).

90. M.R. Thomas and H.A. Scheraga, J.Phys.Chem., 69, 3722 (1965).

91. R.W. Gurney, Ionic Processes in Solution, Chap. 9, 16, McGraw-Hill Book Company, New York, 1954.

92. R.A. Horne and J.D. Birkett, Elect.Acta., 12, 1153 (1967).

93. H.G. Hertz and M.D. Zeidler, Ber.Bunsenges.Phys.Chem., 68, 821 (1964).

94. R.L. Kay, T. Vituccio, C. Zawoyski and D.F. Evans, J.Phys.Chem., 70, 2336 (1966).

95. R.L. Kay, G.P. Cunningham and D.F. Evans, Hydrogen Bonded Solvent Systems, Eds. A.K. Covington and P. Jones, Taylor Francis Ltd., London, 1968, p. 249.

96. D.F. Evans and R.L. Kay, J.Phys.Chem., 70, 366 (1966).

97. B.J. Levien, Australian J.Chem., 18, 1161 (1965).

98. R.L. Kay and D.F. Evans, J.Phys.Chem., 70, 2325 (1966).

99. R.L. Kay and D.F. Evans, J. Phys. Chem., 69, 4216 (1965).

100. R.N. Diamond, J. Phys. Chem., 67, 2513 (1963).

101. D.F. Evans, G.P. Cunningham and R.L. Kay, J. Phys. Chem., 70, 2974 (1966).

102. D.F. Evans and T.L. Broadwater, J. Phys. Chem., 72, 1037 (1968).

103. R.A. Horne and R.P. Young, J. Phys. Chem., 72, 1763 (1968).

104. W.-Y. Wen, S. Saito and M. Lee, J. Phys. Chem., 70, 1244 (1966).

105. S. Lindenbaum and G.E. Boyd, J. Phys. Chem., 68, 911 (1964).

106. J.E. Prue, A.J. Read and G. Romeo. Hydrogen Bonded Solvent Systems, Eds. A.K. Covington and P. Jones, Taylor Francis Ltd., London, 1968, p. 155.

107. H.S. Frank, Chemical Physics of Ionic Solutions, Eds. B.E. Conway, and R.G. Barradas, John Wiley and Sons Inc., New York, 1966, p. 53.

108. H.S. Frank, J. Phys. Chem., 68, 1554 (1963).

109. G. Atkinson, R. Garnsey and M.J. Tait, Hydrogen Bonded Solvent Systems, Eds. A.K. Covington and P. Jones, Taylor Francis Ltd., London, 1968, p. 161.

110. W.-Y. Wen and S. Saito, J. Phys. Chem., 69, 3569 (1965).

111. G.E. Boyd, A. Schwartz and S. Lindenbaum, J. Phys. Chem., 70, 821 (1966).

112. S. Lindenbaum, J. Phys. Chem., 70, 814 (1966).

113. G.E. Boyd, J.W. Chase and F. Vaslow, J. Phys. Chem., 71, 573 (1967).

114. R.H. Wood, H.L. Anderson, J.D. Beck, J.R. France, W.E. de Vry and L.J. Saltzberg, J. Phys. Chem., 71, 2149 (1967).

115. B.E. Conway and R.E. Verrall, J. Phys. Chem., 70, 3952 (1966).

116. H.E. Wirth, J. Phys. Chem., 71, 2922 (1967).

117. W.-Y. Wen and K. Nara, J. Phys. Chem., 71, 3907 (1967).

118. W.-Y. Wen and K. Nara, J. Phys. Chem., 72, 1137 (1968).

119. W.-Y. Wen, K. Nara and R.H. Wood, J. Phys. Chem., 72, 3048 (1968).

120. B.E. Conway and R.E. Verrall, J. Phys. Chem., 70, 1473 (1966); B.E. Conway, R.E. Verrall and J.E. Desnoyers, Trans. Faraday Soc., 62, 2738 (1966).

121. R. Gopal and A.K. Rastogi, J. Ind. Chem. Soc., 43, 269 (1966).

122. W.R. Gilkerson and J.L. Stewart, J. Phys. Chem., 65, 146 (1961).

123. W.-Y. Wen and S. Saito, J. Phys. Chem., 68, 2639 (1964).

124. L.G. Hepler, J.M. Stokes and R.H. Stokes, Trans. Faraday Soc., 61, 20 (1965).

125. L.A. Dunn, Trans. Faraday Soc., 64, 1898 (1968).

126. B.E. Conway and R.E. Verrall, J. Phys. Chem. 70, 3961 (1966); B.E. Conway, R.E. Verrall and J.E. Desnoyers, Zeitschr. phys. Chem., 230, 157 (1965).

127. F. Franks and H.T. Smith, Trans. Faraday Soc., 63, 2586 (1967).

128. R. Gopal and M.A. Siddiqi, J. Phys. Chem., 72, 1814 (1968).

129. F.J. Millero and W. Drost-Hansen, J. Phys. Chem., 72, 1758 (1968).

130. J. Padova and I. Abrahamer, J. Phys. Chem., 71, 2112 (1967).

131. I. Lee and J.B. Hyne, Can. J. Chem., 46, 2333 (1968).

132. J.E. Desnoyers and M. Arel, Can.J.Chem., 45, 359 (1967).

133. T.L. Broadwater and D.F. Evans, J.Phys.Chem., 73, 164 (1969).

134. R.E. Robertson, S.E. Sagamori, R. Tse and C.Y. Wu, Can.J.Chem., 44, 487 (1966).

135. A.J. Ellis, J.Chem.Soc.(A), 660 (1967); ibid. 1579 (1966).

136. A.J. Ellis and I.M. McFadden, Chem.Comm., 516 (1968).

137. F.J. Millero, J.Phys.Chem., 4589 (1968); ibid. 71, 4567 (1967).

138. F.J. Millero and W. Drost-Hansen, J.Chem. and Eng. Data, 13, 330 (1968).

139. F. Vaslow, J.Phys.Chem., 70, 2286 (1966); ibid. 71, 4585 (1967).

140. F. Franks and D.J.G. Ives, Quarterly Reviews, 20, 1 (1966).

141. F. Franks and H.T. Smith, Trans.Faraday Soc., 64, 2962 (1968); also J.Chem. and Eng.Data, 13, 538 (1968).

142. D.S. Allam and W.H. Lee, J.Chem.Soc.A, 6049 (1964); ibid. A 426 (1966); ibid A1, 5 (1966).

143. B.B. Owen and P.L. Kronick, J.Phys.Chem., 65, 84 (1961).

144. F.T. Gucker, C.L. Chernick and P. Roy-Chowdhury, Proc.Nat.Acad.of Sciences, 55, 12 (1966).

145. T.F. Hueter and R.H. Bolt, Sonics, John Wiley and Sons Inc., New York, 1955, p. 30.

146. N. Bauer and S.Z. Lewin, Physical Methods of Organic Chemistry, Ed. Weissberger, Interscience, N.Y. p. 131 (1960).

147. A.B. Lamb and R.E. Lee, J.Am.Chem.Soc., 35, 1666 (1913).

148. W. Geffcken and D. Price, Z.physik.Chem., 26B, 81 (1934).

149. D.A. MacInnes, M.O. Dayhoff and D.R. Ray, Rev.Sci.Inst., 22, 642 (1951).

150. F. Kohlrausch and W. Hallwachs, Weid. Ann. d. Phys., 50, 118 (1893).

151. H.E. Wirth, J. Am. Chem. Soc., 59, 2549 (1937).

152. R.E. Verrall, Ph.D. Thesis, University of Ottawa (1966).

153. G.S. Kell, J. Chem. Eng. Data, 12, 66 (1967).

154. E.L. Carstensen, J. Acoust. Soc. of Am., 26, 858 (1954).

155. J. Bigeleisen, J. Chem. Phys., 23, 2264 (1955).

156. O. Redlich and P. Rosenfeld, Zeit. für phys. Chem., A155, 65 (1931).

157. O. Redlich and D.M. Meyer, Chem. Rev., 64, 221 (1964).

158. B. B. Owen, R. C. Miller, C.E. Milner and H. L. Cogan, J. Phys. Chem., 65, 2065 (1961).

159. H.S. Harned and B. B. Owen, The Physical Chemistry of Electrolytic Solutions, Reinhold, New York, 3rd Ed., p. 79 (1958).

160. R.L.J. Andon, J.D. Cox and E.F.G. Herrington, Trans. Faraday Soc., 50, 918 (1954).

161. F.T. Gucker jun., Chem. Rev., 13, 117 (1933).

162. Y.C. Wu and H. L. Friedman, J. Phys. Chem., 70, 166 (1966).

163. L.A. Dunn, Trans. Faraday Soc., 64, 2951 (1968).

164. J.E. Desnoyers, G.E. Pelletier and C. Jolicoeur, Can. J. Chem., 43, 3232 (1965).

165. K. Nakanishi, Bull. Chem. Soc. Japan, 33, 793 (1960).

166. K. Nakanishi, N. Kato and M. Maruyama, J. Phys. Chem., 71, 814 (1967).

167. B.E. Conway, R.E. Verrall and J.E. Desnoyers, Trans. Faraday Soc., 62, 2738 (1966).

168. S. Schiavo, B. Scrasati and A. Tommasini, Ricerca Sci., 37, 211 (1965).

169. J.E. Desnoyers, R.E. Verrall and B.E. Conway, J. Chem. Phys., 43, 243 (1965).

170. A.G. Passyniskii, Acta Physicochim. U.R.S.S., 8, 385 (1938).

171. R.G. Pearson and D.C. Vogelsong, J. Am. Chem. Soc., 80, 1038 (1958).

172. L. Pauling, The Nature of the Chemical Bond, 3rd Ed., Cornell University Press, Ithaca, N.Y. 1960.

173. V.M. Goldschmidt, Skrifter Norske Videnskaps-Acad., Oslaw, 1, Mat. Natur. v.kl., 1926.

174. B.S. Gourary and F.J. Adrian, Solid State Phys., 10, 127 (1960).

175. T.C. Waddington, Trans. Faraday Soc., 62, 1482 (1966).

176. R. Zana and E. Yeager, J. Phys. Chem., 71, 521 (1967).

177. R. Zana and E. Yeager, J. Phys. Chem., 70, 954 (1966).

178. M.E. Friedman and H.A. Scheraga, J. Phys. Chem., 69, 3795 (1965).

179. G.A. Vidulich, D.F. Evans, R.L. Kay, J. Phys. Chem., 71, 656 (1967).

180. A.A. Maryott, E.R. Smith, National Bureau of Standards, Circular 514, U.S. Government Printing Office, Washington, D.C. 1951.

181. A. Eucken and M. Eigen, Z. Elektrochem. 55, 343 (1951).

182. G. Némethy and H.A. Scheraga, J. Chem. Phys., 41, 680 (1964).

183. A. Eucken, Nachr. Akad. Wiss. Gottingen, Math.-Phys. Biol. physiol. abt., 1 (1949); cf. E. Whalley, Trans. Faraday Soc., 51, 1578 (1957).

184. B.E. Conway, Can.J.Chem., 37, 178 (1959).

185. D.H. Davies and G.C. Benson, Can.J.Chem., 43, 3100 (1965).

186. J. Greyson, J. Phys.Chem., 71, 2210 (1967).

187. A. Ben-Naim, J.Chem.Phys., 42, 1512 (1965).

188. G.C. Swain and R.F.W. Bader, Tetrahedron, 10, 182 (1960).

189. K.J. Laidler, Trans.Faraday Soc., 55, 1725 (1959).

190. K.J. Laidler, H.M. Papée and T. Zawidzky, Trans.Faraday Soc., 55, 1734 (1959).

191. M.C. Despretz, Ann.Chim.Phys., 70, 49 (1839); 73, 296 (1840).